

Dissertation zur Erlangung des Doktorgrades  
der Fakultät für Chemie und Pharmazie  
der Ludwig-Maximilians-Universität München

# **Theoretical Studies in Nucleophilic Organocatalysis**

Von

**Yin Wei**

Aus

Xinxiang, China

München 2008

## **Erklärung**

Diese Dissertation wurde im Sinne von § 13 Abs. 3 der Promotionsordnung vom 29. Januar 1998 von Herrn Prof. Dr. Hendrik Zipse betreut.

## **Ehrenwörtliche Versicherung**

Diese Dissertation wurde selbständig, ohne unerlaubte Hilfe erarbeitet.

München, am 02. 12. 2008

Yin Wei

Dissertation eingereicht am 02. 12. 2008

1. Gutachter: Prof. Dr. Hendrik Zipse
2. Gutachter: Prof. Dr. Herbert Mayr

Mündliche Prüfung am 08.01.2009

This work was carried out from April 2005 to October 2008 under the supervision of Professor Dr. Hendrik Zipse at the Department Chemie und Pharmazie of the Ludwig-Maximilians-Universität, München.



The work for this thesis was encouraged and supported by a number of people to whom I would like to express my gratitude at this point.

First of all, I would like to appreciate my supervisor Prof. Dr. Hendrik Zipse for giving me the opportunity to do my Ph. D. in his group and his guidance in the course of scientific research presented here. He at all times had an open ear for any questions regarding the work. His critical comments on manuscripts and on this thesis were always instructive, stimulating, and motivating.

I thank Prof. Dr. Herbert Mayr for agreeing to be my “Zweitgutachter”, as well as Prof. Dr. Regina de-Vivie Riedle, Prof. Dr. Manfred Heuschmann, Prof. Dr. Rudolf Knorr and Prof. Dr. Wolfgang Steglich for the interest shown in the present manuscript by accepting to be referees.

I am especially indebted to Dr. G. N. Sastry for giving some “weird” but inspired suggestions and for being a great host during my two months stay in ICT, Hyderabad, India.

I would especially like to thank my great colleague Dr. Ingmar Held who I spent the whole Ph. D. time with, for his helps, interesting discussions and helpful suggestions.

Furthermore, I would like to thank my colleagues Boris Maryasin and Florian Achrainger for careful corrections of the present manuscript, and other staff, post-docs and Ph. D. students that went through my Ph. D., especially for Ms. Anna Katharina Probst, Dr. Christian Fischer, Yinghao Liu, Evgeny Larionov for their helps and lasting friendships, which have made my time in Germany a pleasant and worthwhile experience.

I thank DFG and Ludwig-Maximilians-Universität, München for financial support and Leibniz-Rechenzentrum München for providing some computation facilities.

Words of special gratitude are addressed to my family, especially my parents, my brother for their love and persistent support.

Finally, I sincerely thank my husband Xiaoyin Yang for his love, encouragement and supporting throughout these years.—Thank you very much!

Parts of this Ph. D. Thesis have been published:

1. Estimating the Stereoinductive Potential of Cinchona Alkaloids with a Prochiral Probe Approach

**Yin Wei**, G. N. Sastry, Hendrik Zipse, *Org. Lett.* **2008**, *23*, 5413-5416.

2. Tautomeric Equilibria in 3-Amino-1-(2-aminoimidazol-4-yl)-prop-1-ene, a Central Building Block of Marine Alkaloids

**Yin Wei**, Hendrik Zipse, *Eur. J. Org. Chem.* **2008**, 3811-3816.

3. Methyl Cation Affinities of Commonly Used Organocatalysts

**Yin Wei**, G. N. Sastry, Hendrik Zipse, *J. Am. Chem. Soc.* **2008**, *130*, 3473-3477.

4. Assessment of Theoretical Methods for the Calculation of Methyl Cation Affinities

**Yin Wei**, Thomas Singer, Herbert Mayr, G. N. Sastry, Hendrik Zipse,

*J. Comput. Chem.* **2008**, *29*, 291-297.

5. Stacking Interactions as the Principal Design Element in Acyl-Transfer Catalysts

**Yin Wei**, Ingmar Held, Hendrik Zipse, *Org. Biomol. Chem.* **2006**, *4*, 4223-4230.

6. The Performance of Computational Techniques in Locating the Charge Separated Intermediates in Organocatalytic Transformations

**Yin Wei**, B. Sateesh, Boris Maryasin, G. N. Sastry, Hendrik Zipse,

*J. Comput. Chem.* submitted.

# Table of Contents

<b>1. GENERAL INTRODUCTION .....</b>	<b>1</b>
1.1 ACYLATION REACTIONS CATALYZED BY DMAP DERIVATIVES .....	1
1.2 MORITA-BAYLIS-HILLMAN REACTION.....	4
1.3 OBJECTIVE AND SYNOPSIS.....	6
<b>2. METHYL CATION AFFINITY – A GENERAL DESCRIPTOR OF ORGANOCATALYTIC REACTIVITY.....</b>	<b>8</b>
2.1 INTRODUCTION.....	8
2.2 ASSESSMENT OF THEORETICAL METHODS FOR CALCULATIONS OF METHYL CATION AFFINITIES .....	9
2.2.1 Using NH <sub>3</sub> and PH <sub>3</sub> as Model Systems .....	9
2.2.2 Using Small Neutral and Anionic Nucleophiles as Model Systems .....	14
2.2.3 Using Small Nitrogen- and Phosphorous-Containing Bases as Model Systems.....	17
2.2.4 Conclusions.....	19
2.3 METHYL CATION AFFINITIES (MCAs) OF COMMONLY USED ORGANOCATALYSTS .....	20
2.3.1 MCA Values of Commonly Used Organocatalysts .....	20
2.3.2 Correlation of MCA and PA Values.....	24
2.3.3 Correlation of MCA and Experimental Catalytic Rates .....	25
2.3.4 Conclusions.....	28
<b>3. ESTIMATING THE STEREOINDUCTIVE POTENTIAL OF CINCHONA ALKALOIDS WITH A PROCHIRAL PROBE APPROACH.....</b>	<b>29</b>
3.1 INTRODUCTION.....	29
3.2 MOSHER'S CATION AFFINITY (MOSCA) VALUES AND MCA VALUES .....	31
3.3 CONFORMATIONAL PROPERTIES OF CINCHONA ALKALOIDS, THEIR METHYL CATION ADDUCTS AND MOSC ADDUCTS .....	35
3.4 CORRELATION OF MOSCA VALUES WITH OTHER PROPERTIES .....	45
3.5 CONCLUSIONS .....	47
<b>4. THE PERFORMANCE OF COMPUTATIONAL METHODS IN LOCATING THE CHARGE-SEPARATED INTERMEDIATES IN ORGANOCATALYTIC TRANSFORMATIONS .....</b>	<b>48</b>
4.1 INTRODUCTION.....	48
4.2 GEOMETRIES AND ENERGIES OF ZWITTERIONIC ADDUCTS.....	49
4.3 THEORETICAL BENCHMARKING OF REACTION ENERGIES.....	53
4.4 EXTENSION TO LARGER SYSTEMS .....	57
4.5 CONCLUSIONS .....	59
<b>5. CRITICAL DESIGN ELEMENTS FOR ACYL-TRANSFER CATALYSTS.....</b>	<b>60</b>
5.1 INTRODUCTION.....	60
5.2 FORCE FIELD DEVELOPMENT AND SELECTION OF METHODS .....	62
5.2.1 Development of OPLS All-Atom Force Field and Conformational Search .....	62
5.2.2 Selection of Methods.....	64
5.3 CONFORMATIONAL PROPERTIES OF ACYLPYRIDINIUM-CATIONS .....	67
5.4 REACTION ENTHALPIES FOR ACETYL GROUP TRANSFER .....	73
5.5 CONCLUSIONS .....	76
<b>6. OPTIMAL SELECTIVITY OF CHIRAL ANALOGUES OF 4-(DIMETHYLAMINO)PYRIDINE FOR NONENZYMATIC ENANTIOSELECTIVE ACYLATIONS: A THEORETICAL INVESTIGATION.....</b>	<b>77</b>
6.1 INTRODUCTION.....	77
6.2 NUCLEOPHILIC CATALYSIS VS. BASE CATALYSIS .....	79
6.3 REACTION BARRIERS AND CONFORMATIONAL SPACE OF TSS.....	82
6.4 THEORETICAL PREDICTION OF SELECTIVITY AND A MODIFICATION OF CATALYST .....	88
6.5 CONCLUSIONS .....	93

<b>7. TAUTOMERIC EQUILIBRIA IN 3-AMINO-1-(2-AMINOIMIDAZOL-4-YL)-PROP-1-ENE, A CENTRAL BUILDING BLOCK OF MARINE ALKALOIDS .....</b>	<b>94</b>
7.1 INTRODUCTION .....	94
7.2 STABILITIES OF NEUTRAL TAUTOMERS .....	95
7.2.1 <i>Tautomeric Equilibria in Gas Phase</i> .....	95
7.2.2 <i>Tautomeric Equilibria in Water</i> .....	98
7.3 STABILITIES OF PROTONATED FORMS .....	100
7.4 CONCLUSIONS .....	103
<b>8. SUMMARY AND GENERAL CONCLUSIONS .....</b>	<b>104</b>
<b>9. APPENDIX .....</b>	<b>109</b>
9.1 COMPUTATIONAL DETAILS FOR MCA .....	109
9.2 CORRELATION OF $pK_a$ , $pA$ , AND MCA VALUES WITH AVAILABLE EXPERIMENTAL RATE DATA OF ORGANOCATALYTIC PROCESSES .....	110
9.3 COMPUTATIONAL DETAILS FOR MOSCA .....	115
9.4 COMPUTATIONAL DETAILS FOR THE STABILITY OF ZWITTERIONIC ADDUCTS .....	116
9.5 COMPUTATIONAL DETAILS FOR CHAPTER 5 .....	117
9.5.1 <i>Theoretical Methods</i> .....	117
9.5.2 <i>Force Field Parameters and Conformational Search</i> .....	118
9.6 COMPUTATIONAL DETAILS FOR CHAPTER 6 .....	123
9.7 COMPUTATIONAL DETAILS FOR CHAPTER 7 .....	125
9.8 ENERGIES OF ALL COMPOUNDS .....	127
<b>BIBLIOGRAPHY .....</b>	<b>191</b>
<b>CURRICULUM VITAE .....</b>	<b>197</b>

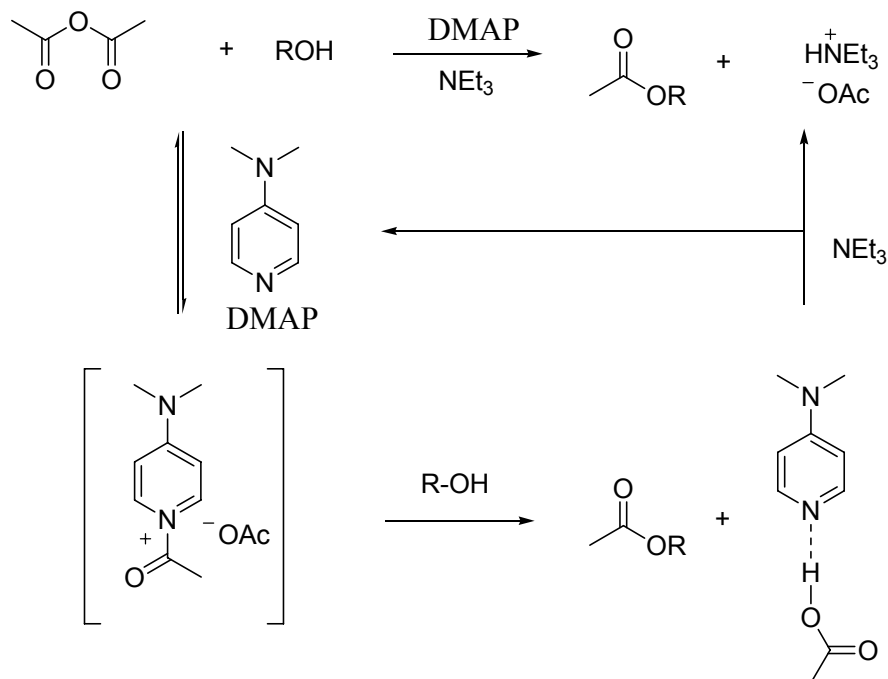
## 1. General Introduction

During the past decades, organocatalysis has drawn remarkable attention and become a highly dynamic chemical research area due to its wide applicability in organic synthesis.<sup>1</sup> One dominating class of organocatalysis is Lewis base catalysis, which is a catalytic process accelerated by Lewis bases. Nucleophilic catalysis is also a commonly used term in organocatalysis, and it is defined as catalysis by a Lewis base, involving formation of a Lewis adduct as a reaction intermediate by IUPAC.<sup>2</sup> Among nucleophilic catalysts, donor-substituted pyridines such as 4-(dimethylamino)pyridine (DMAP), cinchona alkaloids, as well as some other simple nitrogen or phosphorous bases are proven to be particular versatile and have seen extensive applications in organic synthesis.<sup>1,3</sup> At the beginning of this thesis, two types of common transformations catalyzed by nitrogen-containing and phosphorus-containing organocatalysts will be briefly reviewed, and the motives and scope of this thesis are introduced as follows.

### 1.1 Acylation Reactions Catalyzed By DMAP Derivatives

The acylation of alcohols and amines is a common transformation that can be promoted by a variety of catalysts. The utility of DMAP as active catalyst in acylation reactions was described in two pioneering reports almost simultaneously by Litvinenko and Kirichenko,<sup>4</sup> and by Steglich and Höfle<sup>5</sup> in the 1960s. Since then it has been applied extensively as catalyst in many acylation reactions. Recently, the attention has focused on the development of more active achiral catalysts or chiral catalysts for the kinetic resolution of alcohols and related enantioselective transformations, which have been the subject of a number of reviews.<sup>6-8</sup>

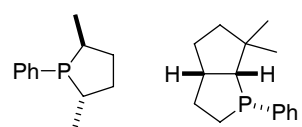
For the development of new active catalysts, the insights into the mechanism of the acylation reaction are helpful, and mechanistic studies have therefore been conducted recently by Zipse *et al.*<sup>9,10</sup> The currently accepted consensus mechanism involves the preequilibrium formation of an acylpyridinium cation through reaction of DMAP with an acyl donor (Scheme 1.1). The alcohol then reacts with the acylated catalyst in the rate-determining second step to form the ester product together with the deactivated catalyst. Regeneration of the latter requires an auxiliary base such as triethylamine.



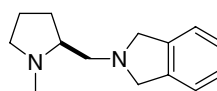
**Scheme 1.1.** Proposed Mechanism for DMAP-Catalyzed Acylation Reaction.

The importance of the stability of the N-acylpyridinium ion **I** and the effect on the overall reaction rate have been shown in recent work by the Zipse group.<sup>9,10</sup> It has also been shown that the design of these catalysts can be guided by the stability of their acetyl intermediate as obtained from theoretical calculations.<sup>11</sup>

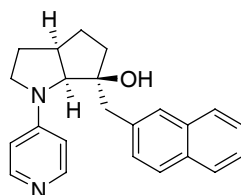
Chiral variants of DMAP (selected examples are summarized in Scheme 1.2) have been developed extensively to apply for a catalytic, enantioselective process such as the kinetic resolution of racemic alcohols. The first process achieving high selectivity was reported by Vedejs *et al.* in 1996 using C<sub>2</sub>-symmetric phosphines,<sup>12</sup> and later more complex bicyclic systems.<sup>13,14</sup> Other centrally chiral amine catalysts reported for kinetic resolution of alcohols include the (S)-prolinol-derived dihydroisoindolines developed by Oriyama,<sup>15</sup> the chiral DMAP analogs developed by Fuji and Kawabata,<sup>16,17</sup> by Campbell,<sup>18</sup> by Yamada,<sup>19,20</sup> and by Connon.<sup>21</sup> The nucleophilic catalyst with axial chirality developed by Spivey<sup>22,23</sup> and those with planar chirality developed by Fu<sup>24</sup> are also quite efficient in the kinetic resolution of racemic alcohols. A recent addition to the field concerns the class of sulfur-containing heterocycles developed by Birman *et al.*<sup>25</sup> The development of new chiral DMAP catalysts is still one of the hot topics in organocatalysis. The strategy used in the development of new catalysts in most cases involves a series of preparation, characterization and analysis of new compounds and the development procedure is by trial and error.



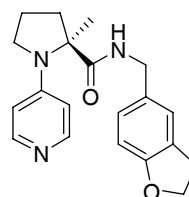
Vedejs *et al.*



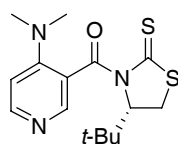
Oriyama *et al.*



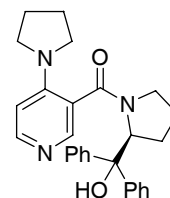
Kawabata-Fuji *et al.*



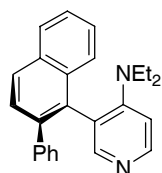
Campbell *et al.*



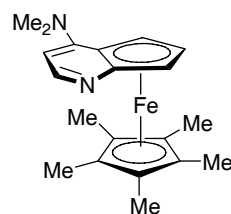
Yamada *et al.*



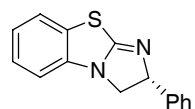
Connon *et al.*



Spivey *et al.*



Fu *et al.*

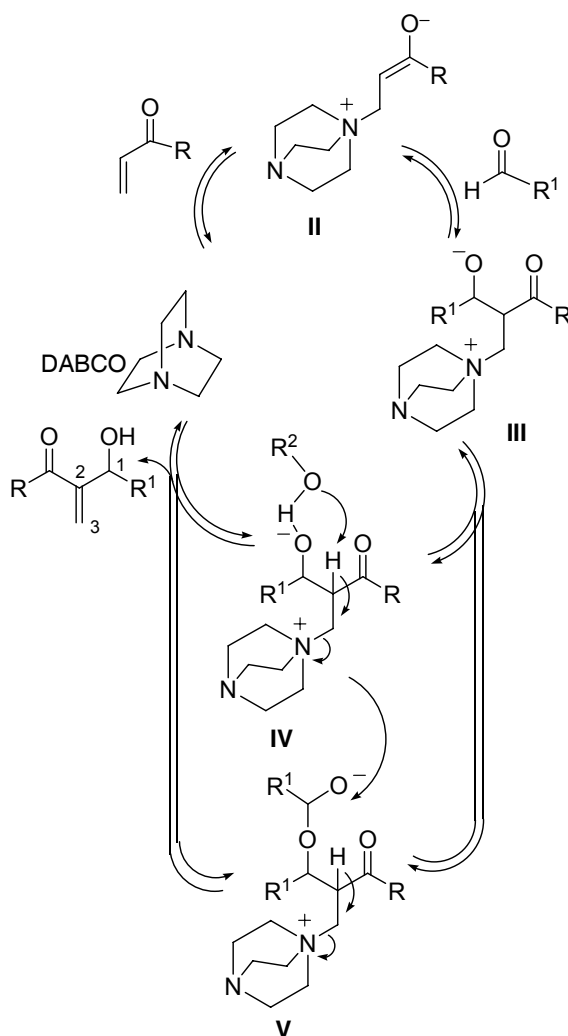


Birman *et al.*

**Scheme 1.2.** Selected Chiral DMAP Derivatives and Related Chiral Acylation Catalysts.

## 1.2 Morita-Baylis-Hillman Reaction

The Morita–Baylis–Hillman (MBH) reaction can be broadly defined as a condensation of an electron-deficient alkene and an aldehyde using highly Lewis basic tertiary phosphines or amines, such as  $\text{PPh}_3$  and 1,4-diazabicyclo[2.2.2]octane (DABCO), as catalysts.<sup>26</sup> Nevertheless, these reactions are notoriously slow, often requiring days to reach useful levels of conversion. Numerous mechanistic studies have attempted to rationalize the low catalytic efficiencies observed.<sup>27-29</sup> The Morita–Baylis–Hillman reaction involves a sequence of Michael addition, aldol reaction, and  $\beta$ -elimination. A commonly accepted mechanism is displayed in Scheme 1.3.



**Scheme 1.3.** Proposed Mechanism for the MBH Reaction.

The catalytic cycle is initiated by the conjugate addition of a Lewis basic catalyst, such as DABCO, to an  $\alpha,\beta$ -unsaturated carbonyl compound (Scheme 1.3). This reaction leads to the formation of a zwitterionic enolate **II**, which possesses enhanced nucleophilic character at C2

through the action of the Lewis base. This species then attacks the aldehyde, leading to formation of the zwitterionic alkoxide **III**. The involvement of both of these species has been supported by the isolation of key reaction intermediates<sup>27</sup> related to **II** and **III** as well as recent NMR<sup>28</sup> and ESI-MS<sup>29</sup> studies. At this point, the mechanism diverges and two distinct pathways lead to the observed products. In the first pathway, proton transfer in **IV** followed by elimination of the Lewis basic catalyst completes the catalytic cycle. The second pathway involves attack of the alkoxide **III** on a second molecule of aldehyde which leads to the formation of the zwitterionic hemiacetal **V**. This intermediate facilitates proton transfer and subsequent elimination of the catalyst.<sup>30</sup> Recently, the theoretical studies of mechanisms of MBH reactions have shown that the proton transfer step is the rate-determining step.<sup>31-33</sup>

Even though a number of mechanistic studies have been reported theoretically and experimentally, the good design of efficient catalysts for the MBH reaction is still a challenge due to its mechanistic complexity. Most of the efficient catalysts developed for the MBH reaction are often directly taken from the simple nitrogen or phosphorus bases, or from the chiral pool such as cinchona alkaloids.<sup>34</sup>

### 1.3 Objective and Synopsis

As mentioned above, organocatalysts are currently developed via a sequence of steps involving preparation, characterization and analysis. Fast development of new highly selective and active organocatalysts is difficult due to the mechanistic complexity of organocatalytic transformations and a dearth of appropriate quantitative studies. An important aim of research in organocatalysis is to accelerate this process. Theoretical studies are becoming an important means for the studies of many issues in organocatalysis besides conventionally experimental measures because the development of theories and computational methods in quantum mechanics (QM), density functional theory (DFT) and molecular mechanics (MM), and the fast increase in computer power have opened up a new avenue for solving various vital chemical problems. The task of this thesis is to study the organocatalytic transformation and investigate factors influencing the activity and selectivity of nucleophilic organocatalysts by theoretical methods.

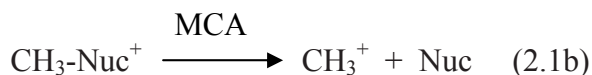
This thesis is organized as follows. In Chapter 2, the concept of methyl cation affinity (MCA) is introduced and the methodology is discussed about how to calculate the MCA values accurately. The use of MCA values as a general descriptor for organocatalytic reactivity is discussed. In Chapter 3, the energy difference between the adducts formed by *re* and *si* face attack to Mosher's cation (MOSCA*re-si*) is proposed as a measure of stereoinductive potential, by taking the example of cinchona alkaloids. In many organocatalytic transformations neutral electrophiles react with neutral nucleophiles to give zwitterionic adducts at some stage of the catalytic cycle such as in the MBH reaction. In order to identify theoretical methods suitable for the reliable description of the formation of zwitterionic adducts, a series of theoretical methods have been investigated in Chapter 4. Then, the issues concerning the reactivities and selectivities of organocatalysts in acylation reactions are explored. In Chapter 5, the critical design element for acyl-transfer catalysts is discussed, meanwhile, the OPLS-AA force field for DMAP derivatives is developed, which is helpful to solve conformational search problems during practical calculations. Theoretical predictions of the stereochemical outcome of enantioselective acylation reactions are discussed in Chapter 6. The factors affecting the selectivity of chiral analogs of 4-(dimethylamino)pyridine in nonenzymatic enantioselective acylations are discussed and a new catalyst with potential high selectivity is suggested. From the perspective of catalysis research, 3-amino-1-(2-aminoimidazol-4-yl)-prop-1-ene, a common intermediate in natural product synthesis, may be used as an ideal starting point for the development of new organocatalysts due to the existence of its potentially four different active sites, based on the

assumption of the comparable stability of its various tautomeric forms. The tautomeric equilibria in 3-amino-1-(2-aminoimidazol-4-yl)-prop-1-ene have thus been studied quantitatively in Chapter 7.

## 2. Methyl Cation Affinity – a General Descriptor of Organocatalytic Reactivity

### 2.1 Introduction

A multitude of N- and P-centered bases have recently been tested in their ability to act as catalysts in organocatalytic transformations.<sup>1</sup> These include secondary and tertiary aliphatic amines, pyridines, imidazoles, and tertiary aliphatic and aromatic phosphines, as well as combinations thereof as in the quinuclidine bases. Variations in the observed catalytic activities have often been rationalized on the basis of variable basicities of the respective catalysts. The proton basicities represented by proton affinity (PA) data or  $pK_a$  data used in this process undoubtedly reflect the affinity of basic compounds towards electrophilic species in general,<sup>35</sup> however, most organocatalytic transformations involve initial nucleophilic attack of the catalyst at electrophilic carbon. This type of nucleophilic reactivity may better be described by affinity data towards a carbon-based electrophile such as the methyl cation,<sup>36,37,38</sup> which is termed as methyl cation affinity (MCA). MCA and PA data are defined in this context as the reaction enthalpies at 298 K for the transformations shown in equations 2.1a and 2.1b.



That MCA has received little attention in the past is simply due to the lack of reliable experimental or theoretical data of this kind. Therefore, in this chapter the performance of various theoretical methods for the accurate prediction of methyl cation affinities (MCA) of organic bases are first explored and discussed. Then, the theoretical procedure identified to provide accurate MCA values is used to calculate MCA values for a wide variety of N- and P-based organocatalysts. Correlations between MCA and PA have then been used to identify factors leading to the potentially poor predictive value of PA or  $pK_a$  data.

## 2.2 Assessment of Theoretical Methods for Calculations of Methyl Cation Affinities

### 2.2.1 Using NH<sub>3</sub> and PH<sub>3</sub> as Model Systems

A rigorous comparison of various theoretical methods to model the MCAs of nitrogen and phosphorous bases was carried out by first taking small molecules NH<sub>3</sub> and PH<sub>3</sub>. The theoretical methods tested here include the compound model chemistries G2,<sup>39</sup> G3B3,<sup>40</sup> G3,<sup>41</sup> and W1;<sup>42,43</sup> and four different density functional theory (DFT) methods, PBE/PBE,<sup>44</sup> MPWB95,<sup>45,46</sup> B3LYP,<sup>47,48,49</sup> B98,<sup>50,51,52</sup> as well as CCSD(T) and MP2 calculations with the frozen-core (FC) approximation or with all electrons correlated (full). DFT and MP2 calculations have been performed using a variety of basis sets developed by Pople and coworkers<sup>53,54</sup> and by Dunning and coworkers.<sup>55,56,57</sup> The experimental MCA values<sup>58,59</sup> for these two systems are incidentally almost identical with +441 and +440 kJ/mol, respectively. The deviations between experimentally measured and theoretically calculated MCA values  $\Delta\text{MCA} = \text{MCA}(\text{calc.}) - \text{MCA}(\text{exp.})$  for a variety of methods have been collected in Table 2.1, positive values indicating  $\text{MCA}(\text{calc.}) > \text{MCA}(\text{exp.})$ .

Good results are obtained using the compound methods G2, G3B3, G3, and W1, the largest deviation for NH<sub>3</sub> being obtained at G2 level (-5 kJ/mol) and for PH<sub>3</sub> at the W1 level (+7 kJ/mol). Our apprehension that the latter is due to differences between the implementation of the W1 method in Gaussian03 (H decontracted in the MTsmall basis set) and the original description (H contracted in the MTsmall basis set) was found to be incorrect as both approaches produce practically identical results. Whether or not f functions are used on phosphorous also is of little relevance for the results obtained for PH<sub>3</sub>. The results obtained at G2, G3B3, and G3 level are in good agreement with those obtained at the more rigorous CCSD(T)/aug-cc-pVTZ level, indicating little problems with the additivity assumptions or the geometries used in these compound methods.

**Table 2.1.** MCA Values (kJ/mol) for NH<sub>3</sub> and PH<sub>3</sub> Obtained at Various Levels of Theory, Compared with Experimental Values.

	NH <sub>3</sub>	PH <sub>3</sub>
Exp. <sup>a</sup>	+441	+440
$\Delta$ MCA(kJ/mol) <sup>b</sup>		
G2	-5.0	0.0
G3B3	-3.0	-1.0
G3	-2.5	+0.2
W1 (H decontracted)	0.0	+7.0
W1 (H contracted)	-0.4	+6.7
W1 (H contracted, without f on P)	-0.4	+7.2
CCSD(T)/aug-cc-pVQZ <sup>c</sup>	-1.1	+2.9
PBEPBE/6-31++G(d,p)	+30.0	+21.0
MPWB95/6-31++G(d,p)	+22.0	+11.0
B3LYP/6-31G(d)	+21.0	-11.0
B3LYP/6-31++G(d,p)	-5.0	-13.0
B3LYP/6-311++G(d,p)	-9.0	-13.0
B3LYP/aug-cc-pVDZ+2df//B3LYP/6-31G(d)	-8.0	-8.0
B3LYP/6-31++G(2df,p)//B3LYP/6-31G(d)	-8.0	-8.0
B3LYP/cc-pVTZ+d <sup>d</sup>	-1.8	-4.0
B98/6-31G(d)	+27.9	-5.4
B98/6-31++G(d, p)	+3.5	-7.0
B98/6-31++G(2df,p)//B98/6-31G(d)	+1.0	-1.4
B98/6-31++G(2df,p)	+1.0	-0.7
B98/6-311++G(2df,p)	-1.2	+2.0
B98/cc-pVTZ+d	+6.2	+2.4
MP2(FULL)/6-31G(d) <sup>c</sup>	+30.6	+10.9
MP2(FC)/6-31G(d, p)	+22.0	+8.0
MP2(FC)/6-31++G(d,p)	+0.5	+7.0
MP2(FULL)/6-31++G(d,p)	+2.5	+10.0
MP2(FC)/aug-cc-pVDZ	-4.4	-2.1
MP2(FC)/aug-cc-pVTZ	+2.3	+17.2
MP2(FULL)/aug-cc-pVTZ	+9.7	+28.0
MP2(FC)/6-311G(d, p)//MP2(FULL)/6-31G(d)	+16.4	+11.0
MP2(FC)/6-311+G(d,p)//MP2(FULL)/6-31G(d)	+1.2	+20.3
MP2(FC)/6-311G(2df,p)//MP2(FULL)/6-31G(d)	+19.3	+18.7
MP2(FC)/6-311+G(3df,2p)//MP2(FULL)/6-31G(d)	+3.3	+18.6
MP2(FC)/AVDZ+2df//B3LYP/cc-pVTZ+d	-5.2	+6.6
MP2(FC)/AVTZ+2df//B3LYP/cc-pVTZ+d	+2.2	+21.3
MP2(FC)/AVQZ+2df//B3LYP/cc-pVTZ+d	+4.6	+25.3

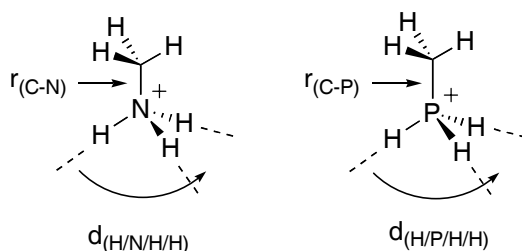
<b>Table 2.1.</b> Continued		
	NH <sub>3</sub>	PH <sub>3</sub>
SCS-MP2(FC)/AVDZ+2df//B3LYP/cc-pVTZ+d	-19.7	-12.2
SCS-MP2(FC)/AVTZ+2df//B3LYP/cc-pVTZ+d	-14.4	+1.1
SCS-MP2(FC)/AVQZ+2df//B3LYP/cc-pVTZ+d	-12.3	+5.0
MP2(FC)/6-31++G(d,p)//B98/6-31G(d)	+0.6	+7.0
MP2(FC)/6-31++G(2d,p)//B98/6-31G(d)	-4.8	+8.4
MP2(FC)/6-31+G(2d,p)//B98/6-31G(d)	-4.5	+8.5

<sup>a</sup> Experimental values from the NIST chemistry webbook; <sup>b</sup>  $\Delta\text{MCA} = \text{MCA}_{\text{calc.}} - \text{MCA}_{\text{exp.}}$ ; <sup>c</sup> Thermal corrections have been taken from G3 theory; <sup>d</sup> Following the notation of Martin *et al.*,<sup>42,43</sup> the “cc-pVTZ+d” indicates the addition of a high-exponent d-type function to the cc-pVTZ basis set for second-row elements, the exponent having been set equal to the highest d exponent in the corresponding cc-pV5Z basis set.

The predictive power of the two GGA functionals (PBEPBE and MPWB95) chosen here is rather moderate, while much better results are obtained with the two hybrid functionals (B98 and B3LYP). B98 performs better than B3LYP that has larger errors for PH<sub>3</sub>. In how far the hybrid DFT methods respond sensitively to the basis set choice was subsequently tested for B98 and B3LYP. In line with earlier systematic studies of basis set effects in PA calculations,<sup>60,61,62</sup> poor results are obtained with basis sets lacking diffuse basis functions. Addition of further polarization functions improve the B98/6-31++G(d,p) results especially for PH<sub>3</sub>, and very good results are thus obtained at the B98/6-31++G(2df,p) level for both systems with  $\Delta\text{MCA} = +1.0$  (NH<sub>3</sub>) and  $-0.7$  (PH<sub>3</sub>). Despite the pronounced effect of diffuse and polarization basis functions on the reaction energetics, geometries optimized with much smaller basis sets appear to be perfectly suitable for the calculation of accurate MCA values. This is exemplified by the similarity of the B98/6-31++G(2df,p) and B98/6-31++G(2df,p)//B98/6-31G(d) results. Going from a double to a triple zeta basis set such as 6-311++G(2df,p) has a comparatively minor effect, leading to a slightly lower MCA value for NH<sub>3</sub> and a slightly higher value for PH<sub>3</sub>. Similar observations can be made for the results obtained at MP2 level, where the best MCA values are obtained with the aug-cc-pVDZ and 6-31++G(d,p) basis sets. That this is, to some extent, the result of fortuitous error cancellation can be seen from the MCAs calculated with the AVxZ+2df basis sets used in the framework of W1 theory. Increasing basis set size with  $x = 2, 3,$  and  $4$  leads for both systems to increasingly large MCA values, overshooting the experimental values in particular for PH<sub>3</sub>. That error cancellation can also be perturbed through including all electrons in the correlation calculation is seen by comparing the MP2(FC)/6-31++G(d,p) and MP2(FULL)/6-31++G(d,p) results. For both systems the MCA values become more positive on inclusion of

all electrons in the correlation calculation, leading to larger deviations at MP2(FULL) than at MP2(FC) level. The same trend can be noted in MP2 calculations with the aug-cc-pVTZ basis set with somewhat larger absolute deviations. Application of the spin-component-scaled (SCS) scaling procedure<sup>63</sup> does, for these two cases, not lead to drastically improved results. The good results obtained with MP2(FC)/6-31++G(d,p) persist when using B98/6-31G(d) instead of MP2 geometries. Addition of a second d function or elimination of diffuse functions on hydrogen lead to slightly higher deviations as compared to MP2(FC)/6-31++G(d,p)//B98/6-31G(d). For NH<sub>3</sub> and PH<sub>3</sub> we can thus conclude that kJ/mol accuracy is obtained either at the G3 level or using the B98 hybrid functional in combination with the 6-31++G(2df,p) basis set.

Structural parameters calculated for the methyl cation adducts of NH<sub>3</sub> and PH<sub>3</sub> show little variation with the employed level of theory. The experimentally determined structure for NH<sub>3</sub> ( $r_{(\text{N-H})} = 101.2$  pm,  $a_{(\text{H-N-H})} = 106.67^\circ$ )<sup>64</sup> is practically identical to that calculated at CCSD(T)/aug-cc-pVQZ level ( $r_{(\text{N-H})} = 101.3$  pm,  $a_{(\text{H-N-H})} = 106.55^\circ$ ). A similarly good agreement is found for PH<sub>3</sub> (exp.:  $r_{(\text{P-H})} = 141.6$  pm,  $a_{(\text{H-P-H})} = 93.56^\circ$ ; calc.:  $r_{(\text{P-H})} = 142.1$  pm,  $a_{(\text{H-P-H})} = 93.56^\circ$ ).<sup>64</sup> It should be noted that the calculated geometries refer to a motionless state at the minimum of the potential energy surface, while the experimental structures refer to ground-state geometries including zero-point motion. Considering the largely similar structural data obtained at CCSD(T)/aug-cc-pVQZ and all other levels listed in Table 2.2 it appears that the methodological choice for geometry optimizations is indeed not critical for the evaluation of exact thermochemical values. The key structural elements related to the formation of methyl cation adducts of organic bases are (a) the length of the newly formed X-CH<sub>3</sub> bond  $r_{(\text{C-X})}$  (X = N, P) and (b) the pyramidalization of the nitrogen/phosphorous center as indicated by the dihedral angle  $d(\text{H/X/H/H})$  (Scheme 2.1).



**Scheme 2.1.**

**Table 2.2.** Structural Parameters  $r_{(C-X)}$  [pm],  $d_{(H/X/H/H)}$  for  $\text{CH}_3\text{XH}_3^+$  and  $\Delta d_{(H/X/H/H)}$  for  $\text{NH}_3$  (X=N) and  $\text{PH}_3$  (X=P) Calculated at MP2, B3LYP, B98, and CCSD(T) Levels of Theory.

level of theory	$r_{(C-X)}$ [pm]	$d_{(H/X/H/H)}$ [ $\text{CH}_3\text{XH}_3^+$ ]	$\Delta d_{(H/X/H/H)}$
<b>NH<sub>3</sub></b>			
MP2(FULL)/6-31G(d)	150.8	115.0	+2.0
MP2(FC)/6-31++G(d,p)	150.6	115.1	-1.6
MP2(FC)/aug-cc-pVDZ	150.4	115.6	+2.2
MP2(FC)/aug-cc-pVTZ	150.4	115.6	+1.7
B3LYP/6-31G(d)	151.7	115.0	+3.1
B3LYP/6-31++G(d,p)	151.6	115.2	-1.5
B3LYP/cc-pVTZ+d	151.3	115.4	+2.0
B98/6-31G(d)	151.5	115.0	+2.9
B98/6-31++G(d,p)	151.4	115.2	-1.2
B98/6-31++G(2df,p)	151.2	115.4	+0.6
B98/6-311++G(2df,p)	151.0	115.3	+0.3
B98/cc-pVTZ+d	151.0	115.4	+2.5
CCSD(T)/aug-cc-pVQZ	150.7	115.6	+2.1
<b>PH<sub>3</sub></b>			
MP2(FULL)/6-31G(d)	180.0	114.7	19.7
MP2(FC)/6-31++G(d,p)	179.8	114.7	19.5
MP2(FC)/aug-cc-pVDZ	181.2	114.4	20.5
MP2(FC)/aug-cc-pVTZ	179.2	114.3	20.4
B3LYP/6-31G(d)	181.4	113.7	20.1
B3LYP/6-31++G(d,p)	181.4	113.7	19.8
B3LYP/cc-pVTZ+d	179.5	113.9	20.3
B98/6-31G(d)	181.3	113.8	20.0
B98/6-31++G(d,p)	181.2	114.0	20.0
B98/6-31++G(2df,p)	180.2	113.9	20.3
B98/6-311++G(2df,p)	179.8	114.1	20.5
B98/cc-pVTZ+d	179.5	113.9	20.3
CCSD(T)/aug-cc-pVQZ	179.4	114.3	20.6

This latter parameter is expected to change significantly on going from the neutral nucleophile to the corresponding methyl cation adduct. The magnitude of this dihedral angle change  $\Delta d(X)$  as defined by eq. (2.2) is a quantitative measure of the structural reorganization of the nucleophile on reaction with the methyl cation.

$$\Delta d(X) = d_{(H/X/H/H)}(\text{CH}_3\text{XH}_3^+) - d_{(H/X/H/H)}(\text{XH}_3) \quad (2.2)$$

According to this definition negative values indicate enhanced pyramidalization of the nucleophile during electrophilic addition. As already indicated by the insensitivity of the MCA values as a function of the underlying geometry there are little differences between the geometrical parameters collected in Table 2.2 calculated at different levels of theory. Thus,

the C-N bond length in  $\text{CH}_3\text{NH}_3^+$  is predicted to be around 151 pm, while the C-P bond length varies around 181 pm in  $\text{CH}_3\text{PH}_3^+$ . The pyramidalization angles  $d_{(\text{H}/\text{X}/\text{H}/\text{H})}$  are predicted to be rather similar in  $\text{CH}_3\text{NH}_3^+$  and  $\text{CH}_3\text{PH}_3^+$ , but the  $\Delta d_{(\text{H}/\text{X}/\text{H}/\text{H})}$  are not: while rather small differences exist in the pyramidalization of  $\text{NH}_3$  and  $\text{CH}_3\text{NH}_3^+$  (leading to small  $\Delta d_{(\text{H}/\text{N}/\text{H}/\text{H})}$  values),  $\text{PH}_3$  is significantly more pyramidalized (with  $d_{(\text{H}/\text{P}/\text{H}/\text{H})}$  values around  $95^\circ$ ) than  $\text{CH}_3\text{PH}_3^+$  (with  $d_{(\text{H}/\text{P}/\text{H}/\text{H})}$  values around  $114^\circ$ ), leading to large positive values for  $\Delta d_{(\text{H}/\text{P}/\text{H}/\text{H})}$ . This indicates that phosphorous nucleophiles may generally show a much larger structural reorganization than comparable nitrogen nucleophiles on reaction with electrophiles. Reorganization energies (calculated as the energy difference between the base in its optimized gas phase structure and in its structure assumed in the methyl cation adduct) are indeed much larger for  $\text{PH}_3$  (+34.3 kJ/mol) than for  $\text{NH}_3$  (+1.7 kJ/mol) at the G3 level of theory.

### 2.2.2 Using Small Neutral and Anionic Nucleophiles as Model Systems

A larger data set including small neutral and anionic nucleophiles shown in Table 2.3 was used to test whether the conclusions reached for  $\text{NH}_3$  and  $\text{PH}_3$  are consistent. These small model systems include strong, anionic nucleophiles such as  $\text{NH}_2^-$  and  $\text{OH}^-$  as well as weakly nucleophilic neutral systems such as HF and HCl. As a consequence the experimentally measured MCA values for these systems span a range of more than 1100 kJ/mol. The performance of a selection of methods was in this case tested by the mean absolute deviation (MAD) values over the complete data set and by selecting certain subsets such as neutral or anionic nucleophiles (MAD(n) and MAD(a)) or systems containing first- or second-row elements (MAD(1) and MAD(2)). Generally, the compound methods such as G2, G3B3, G3, and W1 make very good predictions for the complete data set. The predictive quality is usually somewhat better for first-row than for second-row elements. This trend is most clearly seen for the W1 method, giving excellent results for the first-row systems, but less accurate results for systems containing second-row elements. As a consequence, the results obtained at W1 level are not better than those obtained at G3 level, despite the significantly larger computational effort. Less accurate results are obtained at B3LYP or MP2 level, much in line with the observations made already for  $\text{NH}_3$  and  $\text{PH}_3$ . For both methods the predictions can be drastically improved through combination with basis sets including diffuse basis functions. Comparison of MAD values for the respective subsets of the bases shows that this is mainly due to the poor results obtained for anionic bases, the effect being particularly large for systems containing first-row elements only. For calculations at MP2

level the use of B98/6-31G(d) (instead of MP2) geometries leads to a difference of only 0.4 kJ/mol in the overall MAD value. The computationally most economical method B98/6-31++G(2df,p)//B98/6-31G(d) gives surprisingly good results for the complete data set with MAD values only slightly higher than G3.

**Table 2.3.** MCA Values (in kJ/mol) for Neutral and Anionic Bases Obtained at Various Levels of Theory.

	Exp. <sup>a</sup>	G2	G3B3	G3	W1	B3LYP-1 <sup>b</sup>	B3LYP-2 <sup>b</sup>	B98 <sup>b</sup>	MP2-1 <sup>b</sup>	MP2-2 <sup>b</sup>	MP2-3 <sup>b</sup>	MP2-4 <sup>b</sup>	MP2-5 <sup>b</sup>
NH <sub>3</sub>	441	436	438	438.5	440.9	439.2	432	442	463	441.5	441.6	436.2	436.5
H <sub>2</sub> O	279	276	275	276	278.3	287.9	274	282.6	301	273.7	273.8	267.4	267.7
HF	125	124	121	122.6	125.2	141.9	122	129.5	152	114.3	113.3	114.0	114.1
PH <sub>3</sub>	440	440	439	440.2	447	436.0	427	438.6	448	447	447	448.4	448.5
H <sub>2</sub> S	340	336	337	337.0	343.5	338.1	327	342.2	338	338.1	337.5	340.5	340.3
HCl	204	200	197	197.5	200.6	199.9	187	204.9	188	187.4	186.7	191.0	190.8
NH <sub>2</sub> <sup>-</sup>	1234	1225	1232	1231.1	1230.6	1306.7	1223	1235.9	1489	1231.1	1231.6	1225.0	1227.0
OH <sup>-</sup>	1159	1153	1159	1158.4	1158.6	1254.4	1149	1166.9	1314	1142.9	1141	1138.4	1139.4
F <sup>-</sup>	1080	1078	1080	1082.2	1082.8	1178.5	1065	1085.7	1263	1051.5	1050	1051.2	1052.7
PH <sub>2</sub> <sup>-</sup>	1116	1124	1121	1121.3	1127.7	1149.6	1109	1118.6	1180	1133.7	1132.6	1129.8	1130.9
SH <sup>-</sup>	1033	1034	1032	1031.7	1036.7	1057.3	1016	1029.4	1083	1039.7	1039.1	1031.6	1031.7
Cl <sup>-</sup>	952	950	946	947.9	949.6	967.3	925	943	985	941.3	940.2	934.8	935.0
MAD <sup>c</sup>	-	3.2	3.0	2.8	3.3	31.5	12.3	3.7	69.8	10.4	10.8	11.7	11.3
MAD(n)	-	2.8	3.7	2.9	2.5	6.3	10.0	2.3	16.2	7.0	7.4	8.2	8.1
MAD(a)	-	4.7	2.3	2.7	4.1	56.6	14.5	5.1	123.3	13.8	14.2	15.1	14.5
MAD(1)	-	4.3	2.2	2.3	1.3	49.0	8.8	4.1	110.7	10.7	11.3	14.3	13.4
MAD(2)	-	3.2	3.8	3.4	5.3	13.9	15.7	3.3	28.8	10.1	10.2	9.1	9.2

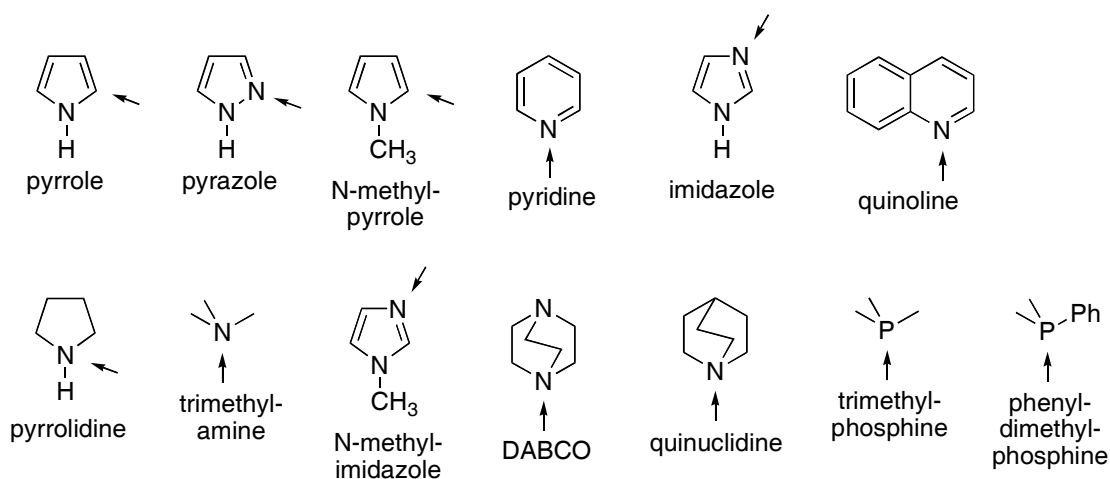
<sup>a</sup> Experimental values from the NIST chemistry webbook;<sup>58</sup> <sup>b</sup> "B3LYP-1 = B3LYP/cc-pVTZ+d; "B3LYP-2" = B3LYP/6-311++G(d,p); "B98" = B98/6-31++G(2df,p)//B98/6-31G(d); "MP2-1" = MP2/6-31G(d,p); "MP2-2" = MP2/6-31++G(d,p); "MP2-3" = MP2/6-31++G(d,p)//B98/6-31G(d); "MP2-4" = MP2/6-31++G(2d,p)//B98/6-31G(d);

"MP2-5" = MP2/6-31+G(2d,p)//B98/6-31G(d); <sup>c</sup> "MAD" = mean absolute deviation from experiment over the complete data set, calculated as  $\sum_{i=1}^n |MCA_{\text{cal.}} - MCA_{\text{exp.}}|_i / n$ ;

"MAD(n)" = mean absolute deviation from experiment for all neutrals; "MAD(a)" = mean absolute deviation from experiment for all anions; "MAD(1)" = mean absolute deviation from experiment for first-row systems; "MAD(2)" = mean absolute deviation from experiment for second-row systems.

### 2.2.3 Using Small Nitrogen- and Phosphorous-Containing Bases as Model Systems

In order to test the performance of the methods described in Table 2.3 for the MCAs of larger systems, we have selected a small group of nitrogen- and phosphorous-containing compounds representing frequently occurring substructures of organocatalysts (Table 2.4, Scheme 2.2). In addition, a number of structurally related cyclic nitrogen compounds such as pyrrole have also been studied for comparison. Some of these bases offer more than one basic center and only methyl cation addition to the most reactive center has been included in this study (as indicated by the arrows in Scheme 2.2). Experimentally measured MCA values are not available for these systems and the G3 values are therefore used as the reference in this case. The MAD values collected in Table 2.4 thus have to be compared to the difference between the MADs in Tables 2.1 and 2.3 and those obtained for the G3 method.



Scheme 2.2.

**Table 2.4.** MCA Values (in kJ/mol) for Selected Larger Neutral Bases Obtained at Various Levels of Theory.

Systems	G3	B98-1 <sup>a</sup>	B98-2 <sup>a</sup>	MP2-3 <sup>a</sup>	MP2-4 <sup>a</sup>	MP2-5 <sup>a</sup>	MP2-6 <sup>a</sup>
Pyrrole (C2)	477.3	477.0	499.1	467.3	466.8	466.7	467.0
Pyrazole (N2)	492.2	495.9	509.6	481.7	484.4	484.7	488.2
N-methylpyrrole (C2)	503.6	499.0	519.9	493.4	492.6	492.6	492.7
Pyridine	519.2	520.7	533.3	517.2	518.4	518.7	521.1
Imidazole (N3)	534.6	535.9	552.4	531.4	531.3	531.7	535.0
Quinoline	535.4	536.2	549.9	528.3	531.7	531.8	534.8
Pyrrolidine	538.2	533.1	550.3	542.2	541.1	541.4	541.4
NMe <sub>3</sub>	540.7	521.6	535.5	540.4	542.1	542.6	542.7
N-methylimidazole (N3)	552.5	553.4	568.7	549.1	549.7	550.0	553.0
DABCO	560.0	546.0	558.8	562.4	562.0	562.2	563.5
Quinuclidine	578.1	560.9	572.8	579.8	580.4	580.6	581.7
PMe <sub>3</sub>	604.7	593.6	591.2	594.6	603.3	604.2	605.9
PMe <sub>2</sub> Ph	611.3	600.1	600.4	597.3	608.0	608.5	610.7
MAD <sup>b</sup>	-	7.0	12.8	6.1	4.1	4.0	3.3

<sup>a</sup> "B98-1" = B98/6-31++G(2df,p)/B98/6-31G(d); "B98-2" = B98/6-31G(d); "MP2-3" = MP2/6-31++G(d,p)/B98/6-31G(d); "MP2-4" = MP2/6-31++G(2d,p)/B98/6-31G(d); "MP2-5" = MP2/6-31+G(2d,p)/B98/6-31G(d); "MP2-6" = MP2/6-311+G(2d,p)/B98/6-31G(d); <sup>b</sup> "MAD" = mean absolute

deviation from G3 results over the complete data set, calculated as  $\sum_{i=1}^n |MCA_{\text{cal.}} - MCA_{\text{cal.}}(\text{G3})|_i / n$ .

The smallest MCA value in this list of compounds has been calculated for pyrrole. Addition to the C2 position is significantly more favorable in this case than addition to N1 or C3 (MCAs are 376.4 kJ/mol for N1 and 436.7 kJ/mol at C3 at MP2-5 level). This selectivity is in line with the relative proton affinities of these three positions.<sup>65</sup> A methyl group at N1 as in N-methylpyrrole leads to slightly higher absolute MCA values, but has little influence on the regioselectivity of methylation. Higher MCA values are found for heterocycles containing formally sp<sup>2</sup> hybridized nitrogen (imidazole, pyridine, N-methylimidazol) and simple aliphatic amines. The highest MCAs are found for the bicyclic amines DABCO and quinuclidine, and for trimethylphosphine. It is noteworthy that PH<sub>3</sub> and PMe<sub>3</sub> differ much more in their MCA values (440.2 vs. 604.7 kJ/mol) than NH<sub>3</sub> and NMe<sub>3</sub> (438.5 vs. 540.7 kJ/mol, all at G3 level). This trend can also be observed in theoretically calculated<sup>66,67</sup> or

experimentally measured<sup>58</sup> proton affinities of these species ( $\text{PH}_3$  vs.  $\text{PMe}_3 = 785.0$  vs.  $958.8$  kJ/mol, but  $\text{NH}_3$  vs.  $\text{NMe}_3 = 853.6$  vs.  $948.9$  kJ/mol) and appears to reflect the higher polarizability of phosphines compared to amines.<sup>66,67</sup> In contrast to the results obtained for the smaller model systems (Table 2.1 and 2.3) we find for the larger systems in Table 2.4 that the results obtained at G3 and B98 level deviate significantly. Moreover, the deviation from the G3 results is significantly larger for all systems containing  $\text{sp}^3$  hybridized nitrogen or phosphorous, indicating a systematic origin of this behaviour.

In contrast, the performance of the MP2 level is somewhat better now with MAD values of around 4 kJ/mol, while a difference of around 8 kJ/mol to the G3 results was obtained for the smaller model systems. Best results are obtained at the MP2 level using the 6-311+G(2d,p) basis set, closely followed by those obtained with the more economical 6-31+G(2d,p) basis set. The MP2(FC)/6-31+G(2d,p)//B98/6-31G(d) level thus appears to be the most promising approach for the treatment of the large, flexible structures common to the field of organocatalysis.

#### 2.2.4 Conclusions

MCAs for a large variety of neutral and anionic bases can be predicted accurately with compound methods such as G2, G3 or W1. The predictive ability of MP2 calculations is slightly lower, but still practically useful. The calculated MCAs depend little on the methods used for structure optimization and the MP2(FC)/6-31+G(2d,p)//B98/6-31G(d) method may thus offer an affordable option for the characterization of even the largest currently used organocatalysts. The performance of the B98 hybrid functional depends strongly on the size of systems at hand. The present study reveals that even when DFT methods work spectacularly well for small model systems, they fail to carry on their good performance to larger systems, a trend noticed recently in several other studies.<sup>68,69</sup> In contrast, the conventional ab initio methods do not show a major weakness as the size of the system increases. This makes the use of hybrid DFT methods for the characterization of organocatalysts unsuitable.

### 2.3 Methyl Cation Affinities (MCAs) of Commonly Used Organocatalysts

Using a theoretical procedure identified to provide accurate methyl cation affinities even for large molecular systems in section 2.2, a set of computed MCA values for a wide variety of N- and P-based organocatalysts are presented here.

#### 2.3.1 MCA Values of Commonly Used Organocatalysts

Figure 2.1 compiles the MCA values for nitrogen and phosphorous nucleophiles listed in Table 2.5 in a graphical manner. The MCA of pyridine (**1**) is rather low at 518.7 kJ/mol but can be enhanced considerably by donor substituents at the C4-position as in 4-(dimethylamino)pyridine (4-DMAP, **27**), 4-pyrrolidinopyridine (PPY, **29**), 4-(tetramethylguanidyl) pyridine (**25**), annulated pyridine derivative **32**, and the 3,4-diaminopyridine **33**. The MCA differences between pyridines **1**, **25**, **27**, **29** and **32** are slightly smaller than those found earlier for reaction with the acetyl cation.<sup>70,71</sup> The absolute MCA values of **1**, **27** and **29** are much larger than the affinities of these pyridines towards the benzhydrylium cation,<sup>72</sup> but the affinity differences are rather comparable. Enlargement of the  $\pi$ -system through benzoanellation as in quinoline (**4**) also leads to higher MCA values, as does substitution of **4** with methyl and methoxy substituents (as in **10** and **16**). The MCA value for **10** of 542.7 kJ/mol is significantly smaller than that for methyl cation addition to the quinoline nitrogen in the cinchona alkaloids cinchonidine (**12**) and cinchonine (**13**).

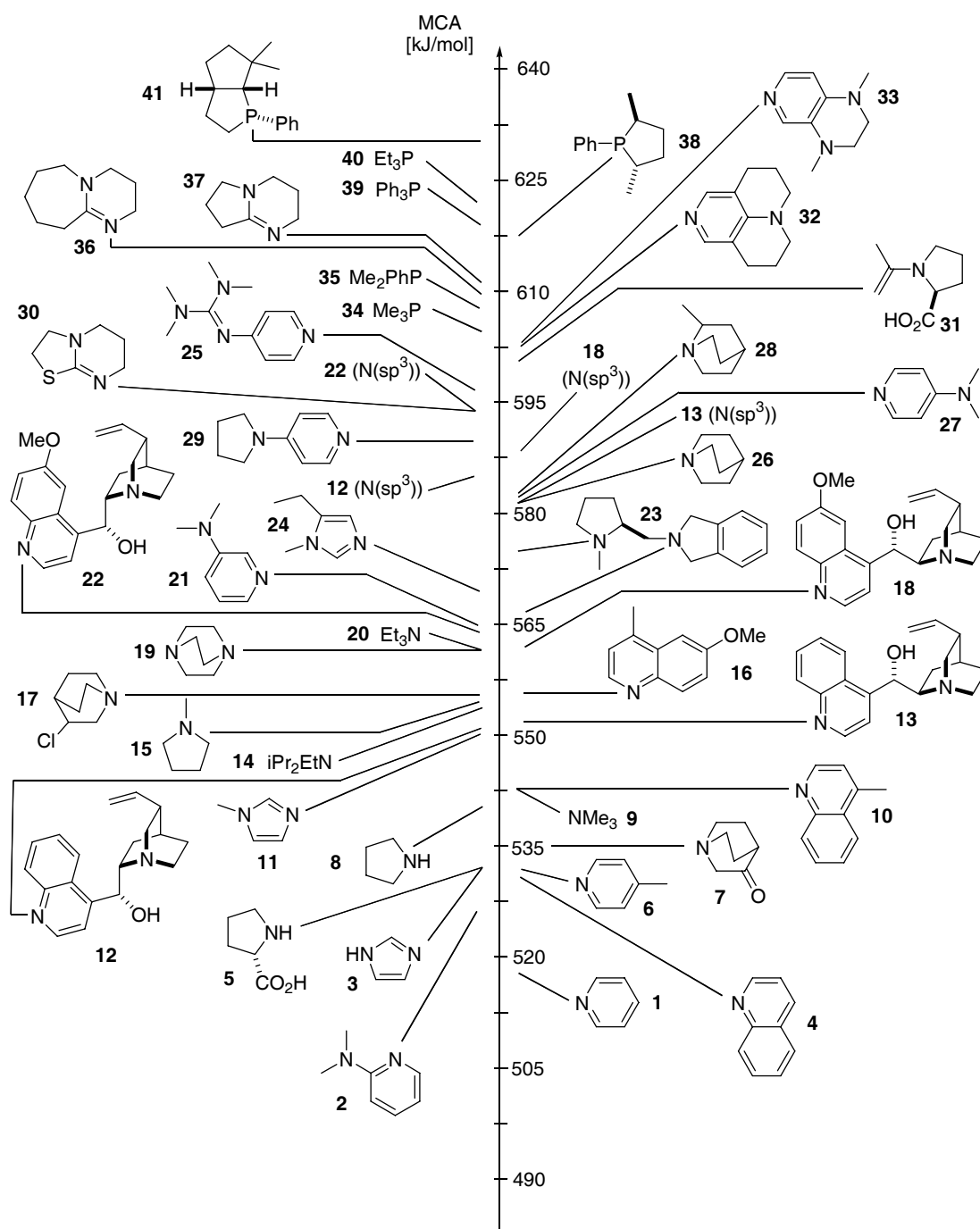


**Figure 2.1.** Structures of N- and P-Centered Organocatalysts Ordered by Their MCA Values.

In the absence of any specific interactions between the methyl group attached to the quinoline nitrogen and the chiral substituent located at C4, this difference of around 10 kJ/mol reflects differences in the polarizability of **10** and **12/13**. The very similar values obtained for **12** and **13** (552.1 vs. 552.4 kJ/mol) indicate that the stereochemistry at the C8/C9 chiral centers has little influence on the stability of methyl cation adducts. This observation can also be made

for the MCA values for the quinoline nitrogen atoms in quinidine (**18**) and quinine (**22**) at 561.8 and 563.9 kJ/mol. The absolute values are now much larger than those for **12** and **13** due to the methoxy substituent at C6 position of the quinoline ring. The MCAs of imidazoles are intrinsically somewhat higher than those of pyridines. Addition of alkyl substituents to the parent system **3** as in *N*-methylimidazole (**11**) and in 1-methyl-5-ethylimidazole (**24**) enhance the methyl cation affinity quite significantly, leading to a MCA of 569.1 kJ/mol for **24**.<sup>73</sup> The methyl cation affinities of tertiary aliphatic amines are mainly guided by the structure of the alkyl groups and their potential to stabilize positive charge through inductive effects. The lowest MCA is therefore obtained for trimethylamine (**9**), the values for triethylamine (**20**) and quinuclidine (**26**) being larger by 19.7 and 38.0 kJ/mol, respectively. The MCA of Huenig's base (**14**) is actually lower than that for **20**, due to steric repulsion between the methyl cation and the isopropyl substituents. The cation stabilizing effects of alkyl substituents can be reduced through introduction of electron-withdrawing substituents as in DABCO (**19**), 3-chloroquinuclidine (**17**), and 3-quinuclidinone (**7**). The MCA values for the quinuclidine nitrogen centers in the cinchona alkaloids **12** and **13** are both very similar to that of quinuclidine (**26**) itself, again indicating little influence of the stereochemistry at the C8 and C9 positions on adduct formation. Addition of a methoxy substituent to the quinoline ring has a surprisingly large influence on the methyl cation affinities of the quinuclidine nitrogen atom in cinchona alkaloids. This enhancement amounts to 8 kJ/mol in **13/18** and to 10 kJ/mol in **12/22**. The quinuclidine nitrogen atom in quinine (**22**) thus represents the center of highest MCA at 594.7 kJ/mol in the cinchona alkaloid systems considered here. A similar observation has been made in binding affinity measurements of cinchona alkaloids toward OsO<sub>4</sub>.<sup>74</sup> The much higher MCA values of the quinuclidine nitrogen atoms in cinchona alkaloids as compared to the respective quinoline nitrogen atoms are, of course, in agreement with the outcome of alkylation reactions, which exclusively favor alkylation of the N(sp<sup>3</sup>) nitrogen atom.

The largest MCA values calculated here are those for the amidine bases such as 1,8-diazabicyclo [5.4.0]undec-7-ene (DBU, **36**) and 1,5-diazabicyclo[4.3.0]non-5-ene (DBN, **37**), the sulfursubstituted derivative **30**,<sup>75</sup> and tertiary phosphanes. A very large difference in MCA values exists between phosphanes and amines of identical substitution pattern, the difference between trimethylamine (**9**) and trimethylphosphane (**34**) amounting to 61.6 kJ/mol. The MCA of phosphanes can be enlarged further through introduction of appropriate aromatic and aliphatic substituents. How these motifs can be combined into the design of chiral catalysts has recently been demonstrated with phosphanes **38** and **41**.<sup>14,76</sup>

**Table 2.5** Methyl Cation Affinity (MCA) and Proton Affinity (PA) Data (in kJ/mol).

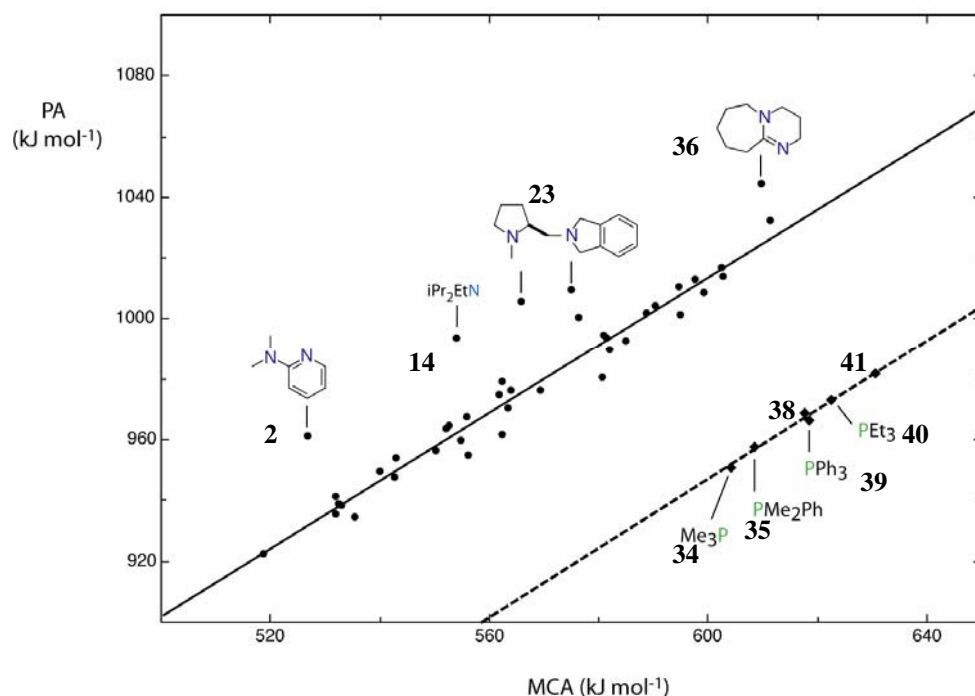
	MCA <sup>a</sup>	PA <sup>a</sup>	MCA/PA <sup>a</sup>	Exp. <sup>b</sup>	MCA <sup>f</sup>
<b>1</b>	518.7	922.6	0.562	930.0, 924.0 <sup>c</sup>	519.2
<b>2</b> (pyridyl N)	526.7	961.3	0.548	-	-
<b>3</b> (N3)	531.7	935.8	0.568	942.8	534.6
<b>4</b>	531.8	941.7	0.565	953.2, 948.0 <sup>c</sup>	535.4
<b>5</b> (N)	532.4	939.2	0.567	920.5, 947.0 <sup>d</sup>	-
<b>6</b>	532.8	938.7	0.567	-	-
<b>7</b>	535.2	934.7	0.573	936.0	-
<b>8</b>	539.8	949.8	0.568	948.3	538.2
<b>9</b>	542.6	948.0	0.572	948.9	540.7
<b>10</b>	542.7	954.2	0.569	-	-
<b>11</b> (N3)	550.0	956.5	0.575	959.6	552.7
<b>12</b> (N(sp <sup>2</sup> ))	552.1	964.1	0.573	-	-
<b>13</b> (N(sp <sup>2</sup> ))	552.4	964.8	0.573	-	-
<b>14</b>	553.8	994.1	0.557	994.3	-
<b>15</b>	554.6	959.9	0.578	965.6	-
<b>16</b>	555.7	967.9	0.574	-	-
<b>17</b>	555.9	955.0	0.588	954.0	-
<b>18</b> (N(sp <sup>2</sup> ))	561.8	974.9	0.576	-	-
<b>19</b>	562.2	962.1	0.584	963.4	560.0
<b>20</b>	562.3	979.2	0.574	981.8	-
<b>21</b> (pyridyl N)	563.4	970.8	0.580	-	-
<b>22</b> (N(sp <sup>2</sup> ))	563.9	976.5	0.577	-	-
<b>23</b> (isoindolyl N)	565.6	1006.0	0.562	-	-
<b>24</b>	569.1	976.5	0.583	-	-
<b>23</b> (pyrrolidyl N)	574.8	1009.7	0.569	-	-
<b>25</b> (guanidyl N)	576.2	1000.9	0.576	-	-
<b>26</b>	580.6	980.8	0.592	983.3	578.1
<b>13</b> (N(sp <sup>3</sup> ))	580.8	995.0	0.584	-	-
<b>27</b> (pyridyl N)	581.2	994.1	0.585	997.6	585.4
<b>28</b>	582.0	989.9	0.588	986.9	-
<b>12</b> (N(sp <sup>3</sup> ))	584.8	993.0	0.589	-	-
<b>18</b> (N(sp <sup>3</sup> ))	588.6	1002.3	0.587	-	-
<b>29</b> (pyridyl N)	590.1	1004.4	0.588	-	594.4
<b>30</b> (N(sp <sup>2</sup> ))	594.4	1010.9	0.588	-	-
<b>22</b> (N(sp <sup>3</sup> ))	594.7	1001.8	0.594	-	-
<b>25</b> (pyridyl N)	597.5	1013.5	0.590	-	-
<b>31</b> (C(sp <sup>2</sup> ))	599.2	1008.9	0.594	-	-
<b>32</b> (pyridyl N)	602.4	1017.0	0.592	-	-
<b>33</b>	602.5	1014.5	0.594	-	-
<b>34</b>	604.2	950.9	0.635	958.8, 950.0 <sup>c</sup>	604.7
<b>35</b>	608.5	957.8	0.635	969.2, 961.0 <sup>c</sup>	611.3
<b>36</b> (N(sp <sup>2</sup> ))	609.6	1044.8	0.583	1047.9, 1035.4 <sup>e</sup>	-
<b>37</b> (N(sp <sup>2</sup> ))	611.3	1032.5	0.592	1038.3, 1025.7 <sup>e</sup>	614.1
<b>38</b>	617.8	968.8	0.638	-	-

Table 2.5. Continued					
	MCA <sup>a</sup>	PA <sup>a</sup>	MCA/PA <sup>a</sup>	Exp. <sup>b</sup>	MCA <sup>f</sup>
<b>39</b>	618.4	966.4	0.640	972.8	-
<b>40</b>	622.4	972.9	0.640	-	-
<b>41</b>	630.7	981.7	0.642	-	-

<sup>a</sup> MP2(FC)/6-31+G(2d,p)//B98/6-31G(d); <sup>b</sup> Experimental values taken from NIST webbook, if not mentioned otherwise; <sup>c</sup> Ref.; <sup>d</sup> Ref.; <sup>e</sup> Ref.; <sup>f</sup> MP2(FC)/6-31+G(2d,p)//MP2(FC)/6-31G(d).

### 2.3.2 Correlation of MCA and PA Values

How do these MCA values compare to the respective proton affinities? The correlation of MCA and PA values in Figure 2.2 shows that there is a good qualitative correlation of both measures of electrophilic affinity. However, two factors appear to lead to deviations from this correlation. The first of these factors concerns steric effects, which are larger for the addition of methyl cations than for protons. As indicated in Figure 2.2 for **2**, **14**, **23**, and **36** these effects lead to MCA values smaller than would be expected on the basis of their PA. For all nitrogen-based compounds (but excluding the sterically most congested systems **2**, **14**, **23**, and **36**) the following correlation exists:  $PA = 343.33 + 1.1175 \times MCA$  (kJ/mol). This is the solid correlation line shown in Figure 2.2.



**Figure 2.2.** Correlation of MCA and PA Values for the Systems Shown in Figure 2.1.

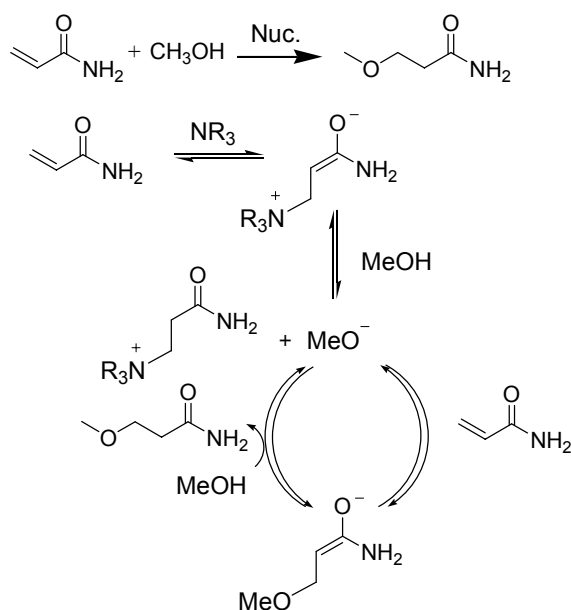
The regression line shifts upward by 13 kJ/mol on consideration of all nitrogen-containing compounds:  $PA = 357.19 + 1.0989 \times MCA$  (kJ/mol). This is hardly surprising for Huenig base **14**, whose design implies its use as a sterically hindered, nonnucleophilic base.

Compounds **23** and **36**, however, are frequently used in organocatalytic processes, and the steric effects visible in Figure 2.2 may thus affect the reaction rates.

Most carbon electrophiles used in organocatalytic transformations are certainly larger than the methyl cation, and one must anticipate that steric effects will be even larger in synthetically relevant transformations than calculated here. The second factor concerns electronic effects when comparing nitrogen and phosphorus bases. The latter are located on a different correlation line shifted to lower PA values by approximately 70 kJ/mol. For phosphanes **34**, **35**, **38**, **39**, **40**, and **41**, the following correlation exists:  $PA = 264.64 + 1.1374 \times MCA$  (kJ/mol). This implies that tertiary phosphanes such as  $PPh_3$  (**39**) or  $PEt_3$  (**40**) will have much higher affinities towards carbon electrophiles as compared to amine bases of comparable proton basicity. The much higher affinity of tertiary phosphanes for carbon electrophiles than for protons is also reflected in reaction rates measured recently for the addition to benzhydrylium cations in apolar solvents.<sup>72</sup>

### 2.3.3 Correlation of MCA and Experimental Catalytic Rates

In how far the MCA values shown in Figure 2.1 correlate with catalytic rate measurements involving nucleophilic organocatalysts has subsequently been explored for all currently available experimental data.<sup>7,11,80-83</sup> The nucleophile-induced addition of methanol to acrylamide was studied by Connon *et al.* (see Scheme 2.3)<sup>80</sup> and represents one of the examples in which rate data cannot be readily correlated with aqueous  $pK_a$  values of the involved nucleophiles ( $R^2 = 0.39$ , Figure 2.3).



**Scheme 2.3.**

**Table 2.6.** Correlation of Observed Rate Constants  $k_{\text{obs}}$  for the Nucleophile-Induced Addition of Methanol to Acrylamide<sup>80</sup> with the Corresponding  $pK_a$ , PA, and MCA Values.

	$k_{\text{obs}}^a$	$\log(k_{\text{obs}})$	$pK_a^a$	PA (kJ/mol) <sup>b</sup>	MCA (kJ/mol) <sup>b</sup>
DABCO ( <b>19</b> )	0.00018	-3.74	8.8	962.1	562.2
4-DMAP ( <b>27</b> )	0.0099	-2	9.7	994.1	581.2
quinuclidine ( <b>26</b> )	0.00595	-2.23	11.3	980.8	580.6
DBU ( <b>36</b> )	0.087	-1.06	12.4	1044.8	609.6
PBu <sub>3</sub> (PEt <sub>3</sub> ) ( <b>40</b> )	0.061	-1.21	8.4	972.9	622.4

<sup>a</sup> Ref. 80; <sup>b</sup> Calculated at MP2(FC)/6-31+G(2d,p)/B98/6-31G(d) level.

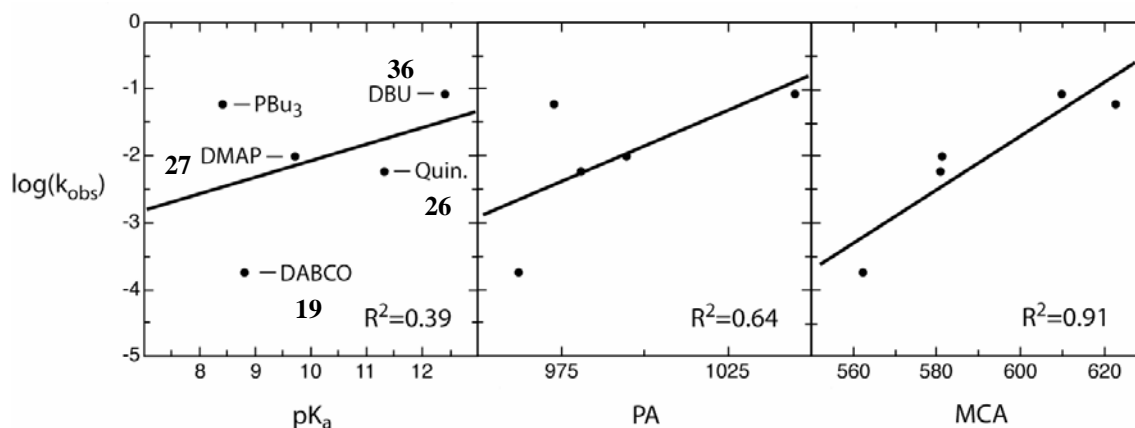


**Figure 2.3.** Correlation of observed rate constants  $k_{\text{obs}}$  for the nucleophile-induced addition of methanol to acrylamide<sup>80</sup> with the corresponding  $pK_a$ , PA (kJ/mol), and MCA (kJ/mol) values. The PA and MCA values of PEt<sub>3</sub> (**40**) have been used for PBu<sub>3</sub>.

Already using gas-phase PA data yields a much better correlation ( $R^2 = 0.64$ ) with experimental rate constants, implying that the polarity of solvent-free or high-concentration reaction conditions may not be described well by aqueous phase data. By far the best correlation ( $R^2 = 0.91$ ) is obtained when using MCA data, which is due to the results for trialkylphosphanes and DABCO. The organocatalytic activity of both compounds correlates much better with their affinity towards carbon than with their affinity towards protons. The transformation shown in Figure 2.3 has also been studied in the presence of triethylamine (**20**) and Huenig's base (**14**), but no rate acceleration has been observed for these two compounds. This likely implies that for many substrates employed under organocatalytic conditions steric effects will be larger than reflected in the MCA values presented here. Similar observations have also been made for the mechanistically more complex Baylis-Hillman reaction. Comparing the activities of quinuclidine derivatives **7**, **17**, **26**, and DABCO

(**19**) in the Baylis-Hillman reaction with acrylate esters as substrates, Aggarwal *et al.* noted that DABCO is a much better catalyst than would be expected on the basis of its aqueous  $pK_a$  value.<sup>81,82</sup> This was ultimately traced back to a reordering of  $pK_a$  values in apolar solvents, but we note that the observed catalytic efficiency is again fully in line with the relative MCA values of these compounds presented here (see Appendix 9.2). That tertiary phosphanes such as  $\text{PMe}_3$  (**34**) exceed the catalytic activity of 4-DMAP (**27**) (in agreement with the MCA values of these systems) has been shown for intramolecular Baylis-Hillman reactions.<sup>84</sup> DBU (**36**) as the nitrogen base with the highest MCA value in Table 2.5 has also been tested in these reactions but appears to be basic enough to deprotonate the protic solvent (ethanol) to such a degree as to favor addition of alkoxide anions instead. This phenomenon has been observed in related reactions before, but it is very difficult indeed to find one mechanistic scheme fitting all published cases.<sup>80,82,85,86</sup> The high basicity of DBU may also be at the heart of its low activity as a catalyst in the acylation of alcohols with anhydrides.<sup>75</sup> The acidic side products generated in these reactions will, even when neutralized with a large excess of an auxiliary amine base, protonate (and thus deactivate) DBU in the course of the reaction. This together with the steric effects hindering the formation of a planar, resonance-stabilized acyliminium cation will limit the use of DBU as an organocatalyst to some selected cases. No such problems can be expected from catalysts combining high MCA with comparatively low PA values, and we may use the ratio MCA/PA as a quantitative guideline in this respect. A survey of these ratios in Table 2.5 immediately shows that tertiary phosphanes fare much better in this respect than all nitrogen-based compounds, underlining the promising prospects of this class of compounds in organocatalysis. Reaction rates for the acylation of tertiary alcohols with anhydrides in apolar solution catalyzed by pyridines **25**, **27**, **29**, and **32** are in full agreement with the relative MCA values of these compounds.<sup>7,11,83</sup> Most interestingly,  $\text{PBU}_3$  has been shown to be slightly more effective than 4-DMAP (**27**) in acylation reactions of secondary alcohols.<sup>87</sup> This observation is at variance with the proton affinities of 4-DMAP and, for example,  $\text{PEt}_3$  (**40**) but readily accommodated with respect to the MCA values of these two systems. A wide range of results exist for the base-catalyzed hydrolysis of carboxylic acid derivatives in water.<sup>88</sup> For some catalysts the mechanism has been clearly established to proceed through initial formation of acylammonium intermediates.<sup>89</sup> The reaction rates determined for the quinuclidine derivatives **7**, **17**, **26**, and DABCO (**19**) in their reaction with organic carbonates, for example, are in full agreement with their MCA values. We should, however, not forget that aqueous solvation leads to a dramatic reduction of nucleophilic reactivity in general and also, in part, a reordering of relative reactivities as

compared to less polar organic solvents.<sup>72</sup> Aside from correlating catalytic efficiencies with the MCA values of the corresponding catalysts and thus establishing a Brønsted-type correlation between reaction rates and groundstate affinity data, the MCA values in Table 2.5 can also be used in a more qualitative way to understand the basis of organocatalytic processes. This can be exemplified using the proline-catalyzed aldol reaction between acetone and aromatic aldehydes.<sup>90</sup> The uncatalyzed background reaction corresponds in this case to the nucleophilic addition of acetone (or, more likely, its enol) to the aromatic aldehyde. The hope for a catalytic process rests on the assumption that the enamine **31** formed by reaction of acetone and proline is more reactive toward the electrophilic aldehyde than the enol of acetone. The MCA value for enamine **31** (599.2 kJ/mol) is much higher than that of acetone enol (459.0 kJ/mol) or that of proline (**5**) itself (532.4 kJ/mol). Even when present in equal amounts in the reaction mixture **31** will react much faster with electrophiles than acetone enol or proline and thus enable a catalytic cycle. Under most experimental conditions, however, the true side reaction to proline catalysis will most likely be that of unspecific base catalysis.<sup>91</sup> The acetone enolate involved in this process will be a much better nucleophile than either acetone enol or enamine **31**. A direct comparison of these ionic and neutral nucleophiles through their MCA values will not be meaningful due to the large role played by environmental factors (solvent, counterion) in the reaction of anionic nucleophiles.

### 2.3.4 Conclusions

The MCA values presented here can be used as a guideline for the optimization of organocatalytic transformations. The mechanistic complexity of many such reactions, the presence of numerous side reactions, and the broad variety of solvents used under experimental conditions make it unlikely that quantitative predictions can be made for structurally different organocatalysts with only one single parameter. However, if the general limitation of a single parameter approach has been accepted, it is clear that the currently known catalytic activities of nitrogen and phosphorous bases are much more readily correlated with MCA than with PA or  $pK_a$  data.

### 3. Estimating the Stereoinductive Potential of Cinchona Alkaloids with a Prochiral Probe Approach

#### 3.1 Introduction

Cinchona alkaloids and their derivatives play an important role in stereoselective catalysis, both as actual catalysts as well as building blocks for ligands in transition metal complexes.<sup>34,92</sup> The frequent use of these compounds in a variety of chemically distinct transformations suggests that the intrinsic structural and electronic properties of these alkaloids make them suitable for stereoselective processes.<sup>93</sup> The most frequently used compounds of this class include cinchonidine (**12**), cinchonine (**13**), quinine (**22**), and quinidine (**18**). One of the inherently useful properties of these compounds is their commercial availability. We are testing what properties make these compounds superior to the known, but much less frequently used C9-epimers **42**, **43**, **44** and **45** by using two different cationic probes. For the sake of comparison, the chiral tertiary amines such as (*S*)-proline-derived<sup>15,94</sup> diamine **23** and sparteine **46** (Figure 3.1) will also be included.

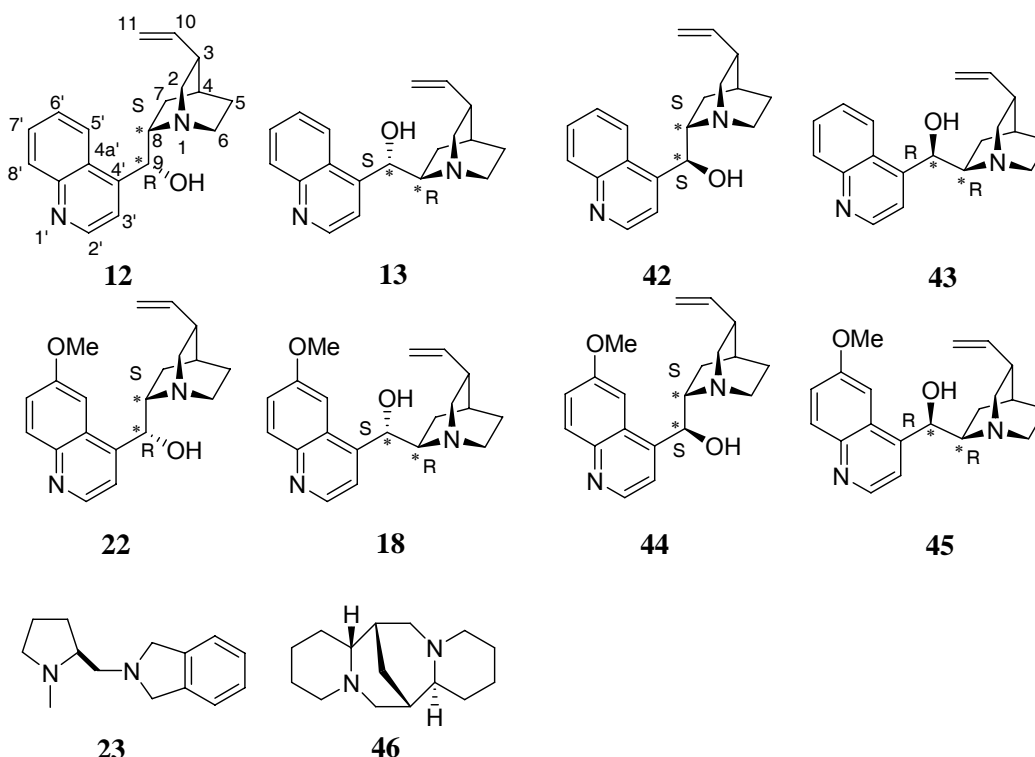
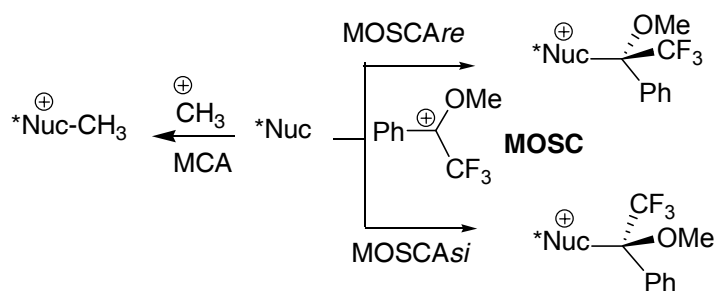


**Figure 3.1.** Cinchona Alkaloids and Selected Chiral Tertiary Amines.

In Chapter 2, a variety of N- and P- centered bases is ranked according to their affinity towards the achiral cation ( $\text{CH}_3^+$ ), and this MCA is shown to be correlated better with the experimentally observed catalytic efficiencies than PA. These studies here are extended to

include affinity values towards a prochiral cation, formally derived from  $\alpha$ -methoxy- $\alpha$ -trifluoromethyl- $\alpha$ -phenylacetic acid (MTPA, Mosher's acid,  $\text{Ph}(\text{OCH}_3)(\text{CF}_3)\text{C}-\text{CO}_2\text{H}$ ) through decarboxylation. The success of this latter acid as a derivatizing reagent for a multitude of chiral alcohols suggests that the three substituents connected to C2 (Ph,  $\text{CF}_3$ ,  $\text{OCH}_3$ ) provide a strongly differentiated environment in steric and electronic terms.<sup>95,96</sup> In order to emphasize the resemblance to Mosher's acid we will refer to this cation as "Mosher's cation" (or **MOSC**) and to the corresponding reaction enthalpies at 298 K then as "MOSCA" values. As described in Scheme 3.1, reaction of **MOSC** with chiral nucleophiles can occur from the *re* or *si* face of the cation, leading to two diastereomeric adducts with two different affinity values  $\text{MOSCA}_{re}$  and  $\text{MOSCA}_{si}$ .



**Scheme 3.1.**

The development of new chiral descriptors for stereoselective organocatalytic transformations is interesting in its own right, and the prochiral MOSCA probe proposed here is a practical approach in this direction.

### 3.2 Mosher's Cation Affinity (MOSCA) values and MCA values

The MOSCA values of compounds shown in Figure 3.1 are listed in Table 3.1, and their corresponding MCA, PA values are also included for comparison and analysis. Figure 3.2 compiles the data in Table 3.1 in a graphical manner.

**Table 3.1.** MCA, PA, MOSCA Values (in kJ/mol) of the N(sp<sup>3</sup>) Centers in Compounds Shown in Figure 3.1.

	MCA <sup>a</sup>	PA <sup>a</sup>	MOSCA <sup>a</sup>		$\Delta$ MOSCA <i>re-si</i> <sup>a</sup>	$\Delta$ MOSCA <i>re-si</i> <sup>b</sup>
			<i>re</i>	<i>si</i>		
Cinchonidine (12)	584.8	993.0	215.2	220.7	-5.5	-5.7
Cinchonine (13)	580.8	995.0	220.7	212.3	8.5	8.9
Epi-Cinchonidine (42)	562.4	990.1	197.6	188.4	9.2	9.2
Epi-Cinchonine (43)	564.4	991.1	183.7	180.0	3.7	4.0
Quinine (22)	594.7	1001.8	227.3	233.7	-6.4	-6.0
Quinidine (18)	588.6	1002.3	231.2	223.3	7.9	8.2
Epi-Quinine (44)	571.7	999.6	205.6	196.9	8.7	10.2
Epi-Quinidine (45)	572.3	998.9	193.1	189.3	3.8	3.1
<b>23</b>	574.8	1009.7	224.9	217.6	7.3	7.8
<b>46</b>	554.9	1044.4	156.3	158.6	-2.3	-1.4

<sup>a</sup> Calculated at MP2(FC)/6-31+G(2d,p)//B98/6-31G(d) level; <sup>b</sup> Calculated at MP2(FC)/6-31+G(2d,p)//MP2(FC)/6-31G(d) level.

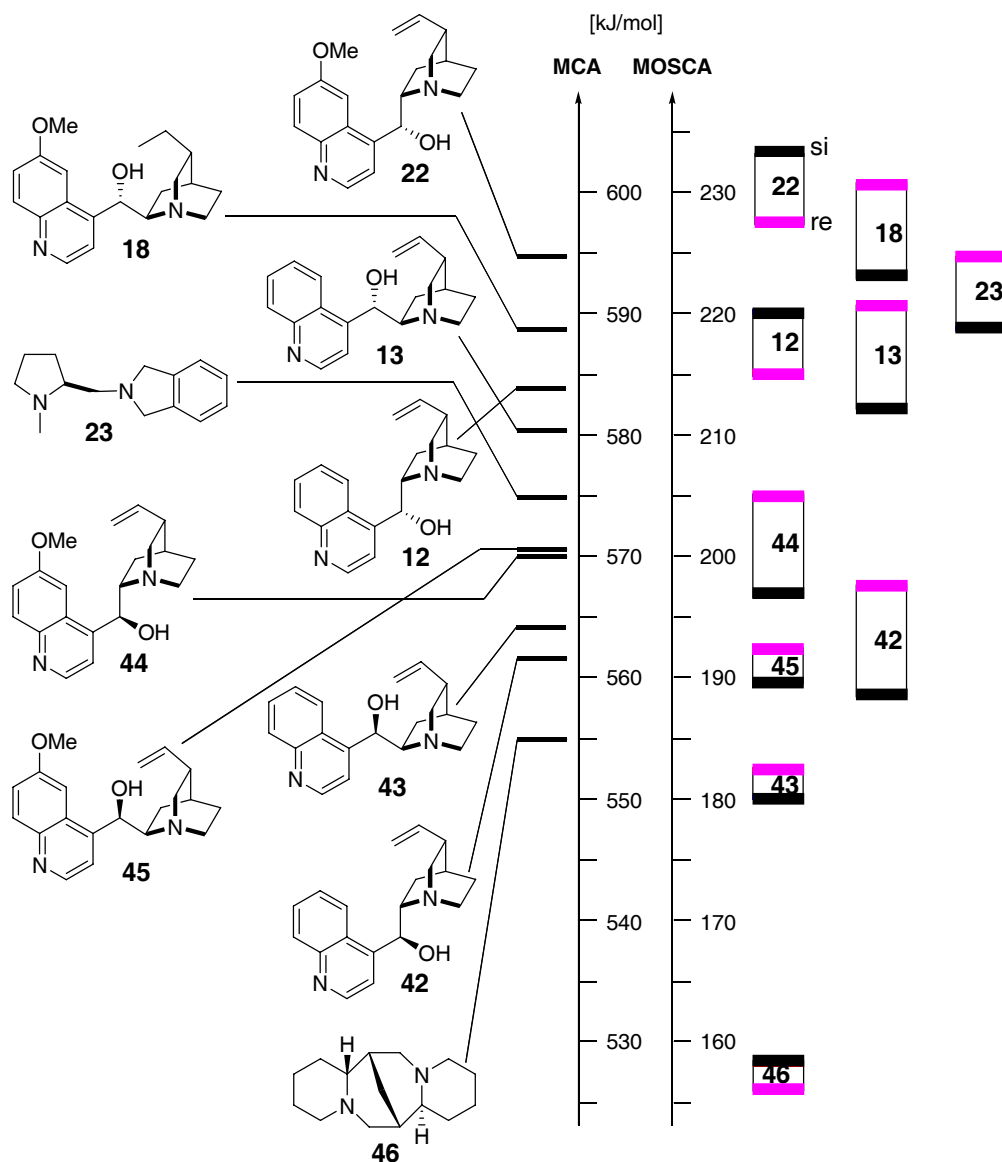


**Figure 3.2.** MCA and MOSCA Values of Compounds Shown in Figure 3.1.

The analysis concentrates here on the properties of the quinuclidine substructure in alkaloids as it has been shown earlier that the MCA values of the respective  $N(sp^3)$  center is significantly higher than that of the  $N(sp^2)$  center in the quinoline ring. The MCA values of natural cinchona alkaloids **12**, **13**, **18**, **22** are in the range of 580 - 595 kJ/mol, which are similar to those of some commonly used organocatalysts such as DMAP, 4-pyrrolidinopyridine (PPY), and quinuclidines as shown in Chapter 2. The MCA values differ by only 4 kJ/mol in the cinchona alkaloids **12** and **13**, and by about 6 kJ/mol in alkaloids **18** and **22**. However, the MCA value of epi-cinchonidine **42** is lower than that of **12** by more than 20 kJ/mol, and similarly the MCA value of epi-quinine **44** is also lower than that of **22** by

more than 20 kJ/mol. The MCA values of epi-cinchonine **43** and epi-quinidine **45** are lower than the MCA values of **13** and **18** by more than 16 kJ/mol, respectively. Comparing the relative energies for neutral molecules and adducts, respectively, the neutral epimers **42** and **44** are more stable by more than 10 kJ/mol than **12** and **22**, and the cations are less stable by 8 kJ/mol. Addition of a methoxy substituent to the quinoline ring has a surprisingly large influence on enhancing the MCA values of the quinuclidine nitrogen atom in cinchona alkaloids. This enhancement amounts to 10 kJ/mol in **12/22**, 8 kJ/mol in **13/18**, 9.3 kJ/mol in **42/44**, and 8 kJ/mol in **43/45**. The MCA value of tertiary amine **23**, frequently used in organocatalytic processes, is 574.8 kJ/mol. The MCA value of **46** is 554.9 kJ/mol, somewhat lower than the MCA values of commonly used organocatalysts. The proton affinities of all cinchona alkaloids are much less affected by changes in the stereochemistry than the MCA values, resulting in rather similar values for all cinchona alkaloids in Table 3.1.

The MOSCA<sub>re</sub> and MOSCA<sub>si</sub> values of compounds shown in Figure 3.1 (Table 3.1) are substantially smaller in absolute terms than the respective MCA values. The difference appears to be close to 370 kJ/mol for the nucleophiles selected here, but the steric bulk and internal structure of the **MOSC** leads to a significantly larger spread of MOSCA than of MCA values. The highest MOSCA values are calculated here for quinine (**22**) and quinidine (**18**), which are also the compounds with highest MCA values. Also in line with the MCA results is the finding that all natural alkaloids **12**, **13**, **18**, and **22** have higher MOSCA values than their C9 epimers. However, the MOSCA values for the non-natural alkaloids **42/43** and **44/45** are farther apart than expected based on their respective MCA data. If the qualitative correlation of carbocation affinity values with catalytic activity in Lewis base-catalyzed reactions observed earlier holds, one would conclude that **18** and **22** are the most reactive compounds and that the respective C9 epimers are significantly less reactive.

This has indeed been observed experimentally by Oda *et al.* in the alkaloid-catalyzed alcoholysis of cyclic anhydrides.<sup>97</sup> These studies, together with subsequent work by Aitken *et al.*<sup>98</sup> and by Bolm *et al.*,<sup>99</sup> also illustrate that numerous other factors contribute to the experimentally observed selectivity, one of the critical parameters being the catalyst concentration. The generally higher selectivity observed in the presence of higher catalyst concentrations indicates the presence of an unselective background process, a general phenomenon of base-catalyzed reactions of alcohols with anhydrides.<sup>9,10</sup> In addition, a catalytic effect of the protonated cinchona alkaloids cannot also be excluded. The intrinsic stereoinductive potential of the bases considered here is quantified through the difference between *re* and *si* face **MOSC** affinity values as listed in Table 3.1, a negative value

indicating preference for *si* face attack. Negative values are found here for the natural alkaloids **12** and **22**, while positive values of similar size are found for the alkaloids **13** and **18**. The opposite preferences for quinine (**22**) and quinidine (**18**) parallel numerous experimental observations in the alcoholysis of anhydrides, in which catalysis by **22** and **18** yield opposite product enantiomers.<sup>97,98,99</sup> Experimental studies involving the C9 epimeric cinchona alkaloids are much less frequent and appear to indicate the same absolute stereochemical preferences for stereochemical pairs **13/43** and **18/45**, but with lower absolute ee% values for **43** and **45**. The stereofacial preference as well as the lower absolute selectivity are closely matched by the MOSCA values computed here, predicting the same *re* facial addition preference for all four of these compounds, with MOSCA values being much smaller for **43/45** than for **13/18** (Table 3.1). It is only for compounds **42** and **44** that the experimental results observed by Oda (near-racemic product) are in clear contrast to the large positive MOSCA values calculated here. In the light of these results reexamination of the catalytic performance of these compounds under the conditions developed by Bolm *et al.* appears highly desirable.

### 3.3 Conformational Properties of Cinchona Alkaloids, Their Methyl Cation Adducts and MOSC Adducts

The conformational analysis of cinchona alkaloids, their methyl cation adducts and MOSC adducts will be helpful for understanding their affinity data discussed above. Even though the conformation of cinchona alkaloids and their desirable properties have been previously studied by force field,<sup>100,101</sup> semiempirical,<sup>102</sup> and DFT calculations or low level *ab initio* methods,<sup>103,104</sup> their cationic adducts' conformations are rarely studied. Thus, a detailed conformational analysis is discussed here.

Figure 3.3 shows a pictorial representation of the relative energies of conformers and conformer numbers in the range of 0 - 16 kJ/mol for neutral cinchona alkaloids **12**, **13**, **42**, **43** and their methyl cation adducts at MP2/6-31+G(2d,p)//B98/6-31G(d) level. Similarly, the Figure 3.4 shows the same pictorial representation for cinchona alkaloids **22**, **18**, **44**, **45** and their methyl cation adducts. The conformers with higher relative energy (>16 kJ/mol) are excluded here because their populations are less than 1%.

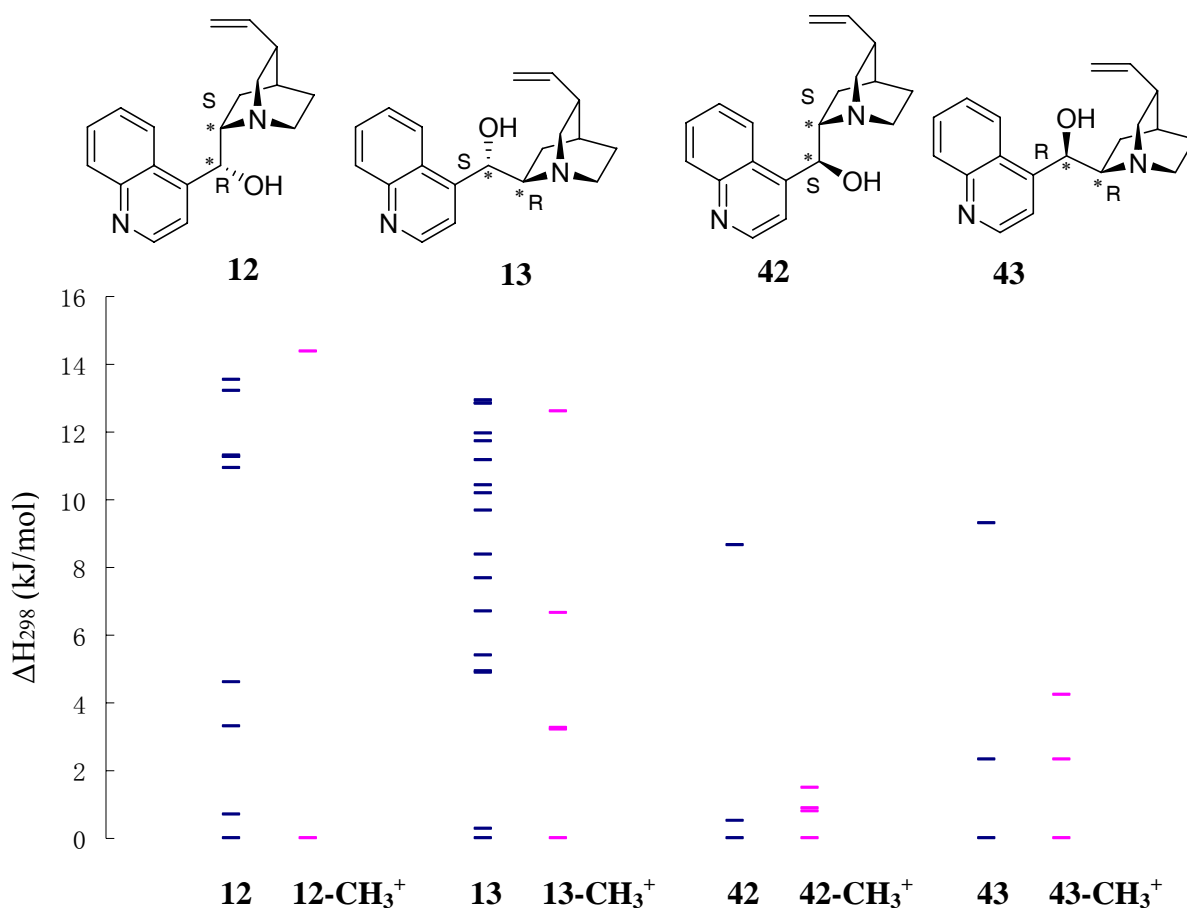


**Figure 3.3.** Relative Enthalpies of Conformers of Compounds **12**, **13**, **42**, **43** and Their Methyl Cation Adducts at MP2/6-31+G(2d,p)//B98/6-31G(d) Level within an Energy Window of 16 kJ/mol.

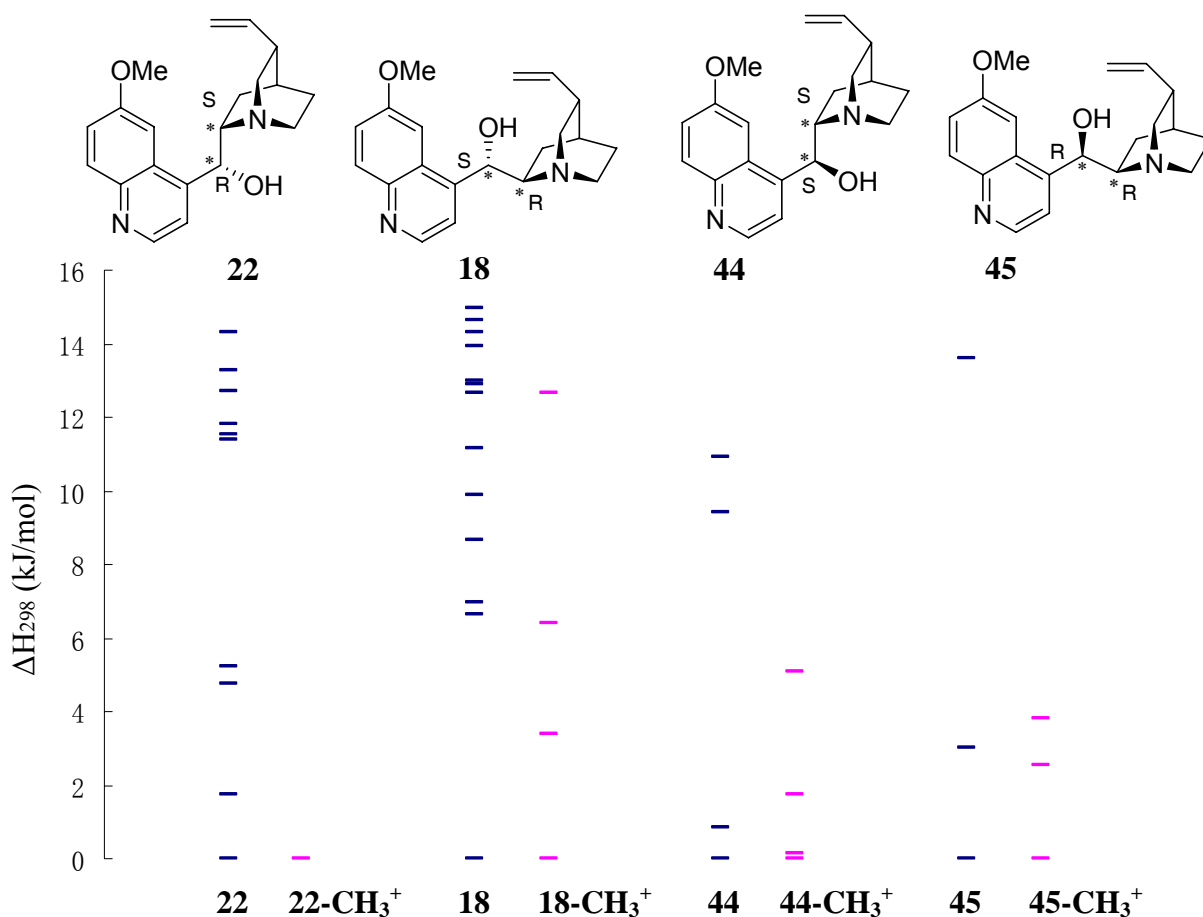
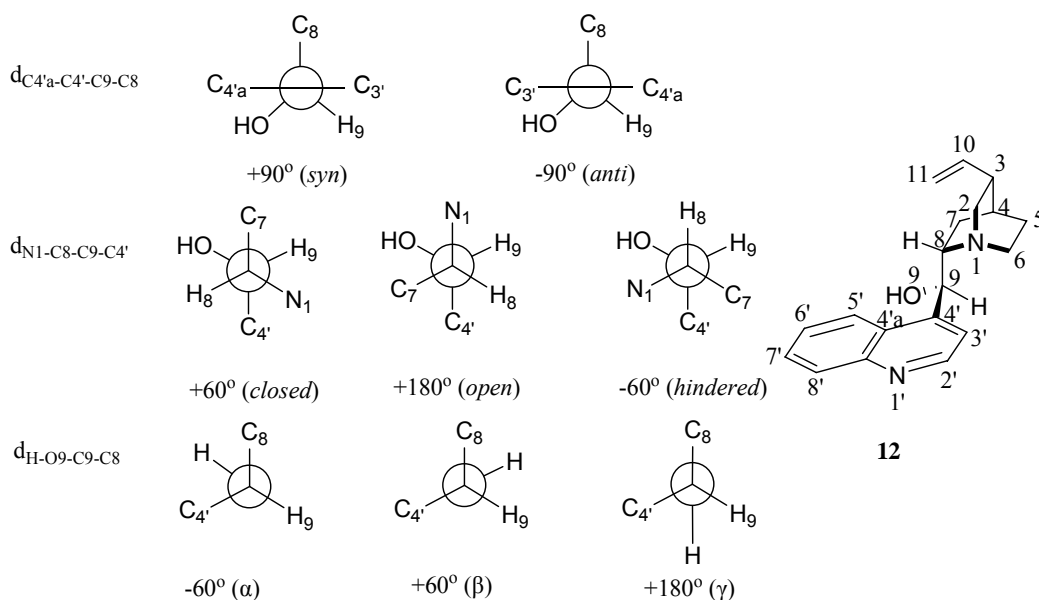


**Figure 3.4.** Relative Enthalpies of Conformers of Compounds **22**, **18**, **44**, **45** and Their Methyl Cation Adducts at MP2/6-31+G(2d,p)//B98/6-31G(d) Level within an Energy Window of 16 kJ/mol.

The conformational spaces of the neutral bases **12**, **13**, **18** and **22** are quite large; in contrast, the conformational spaces of **42** - **45** are rather narrow. Within the chosen energy window (16 kJ/mol), the conformer numbers of **12** and **13** decrease from more than 10 conformers to 2 and 5 conformers, respectively, for their methyl cation adducts. The same observation is also found for **18** and **22**, and the energy gaps among the cationic conformers increase, compared to the neutral forms. However, the conformational space change is not so obvious for **42** - **45**. These results imply that the methylation of natural cinchona alkaloids **12**, **13**, **18** and **22** leads to a reduction of the conformational space of these molecules. This finding agrees with Mueller and Zaera's finding about the protonation of cinchonidine.<sup>103</sup>

Furthermore, the structures of the lowest conformer for cinchona alkaloids shown in Figure 3.1 and their methyl cation adducts are analyzed by selected critical geometrical parameters summarized in Table 3.2. The structures of the most stable conformers for **12** and **12-CH<sub>3</sub><sup>+</sup>** at the MP2(FC)/6-31G(d)//B98/6-31G(d) level of theory are shown in Figure 3.5. The optimized geometries for **12** and **12-CH<sub>3</sub><sup>+</sup>** at MP2/6-31G(d) level have no significant difference from

B98/6-31G(d) optimized geometries. The conformations of cinchona alkaloids studied here are classified based on Agranat's definition.<sup>102</sup> Agranat classified the conformers into 18 classes by *syn/anti*, *open/closed/hindered* and  $\alpha/\beta/\gamma$ . The dihedral angle  $d_{C4'a-C4'-C9-C8}$  is expected to be ca.  $+90^\circ$  or  $-90^\circ$ , which corresponds to *syn* or *anti* conformations. *Syn/anti* refer to the conformations in which the methoxy group (or  $C_{5'}$ ) and the hydroxy group at  $C_9$  are on the same side or on the opposite side (see Scheme 3.2). The values of dihedral angle  $d_{N1-C8-C9-C4'}$  refer to the *open*, *closed* and *hindered* nomenclature of cinchona alkaloids conformation (see Scheme 3.2). In the *open* conformations, the quinuclidine N is oriented away from the quinoline moiety. In the *closed* conformations, the lone pair of N points over the quinoline moiety. In the *hindered* conformations, the two rings are on top of each other. The values of dihedral angle  $d_{H-O9-C9-C8}$  refer to the orientation of hydroxy group connected to  $C_9$  (see Scheme 3.2). The hydroxy hydrogen is staggered between  $C_8$  and  $C_{4'}$ , designated  $\alpha$ ; the hydroxy hydrogen is staggered between  $C_8$  and  $H_9$ , designated  $\beta$ ; the hydroxy hydrogen is staggered between  $C_{4'}$  and  $H_9$ , designated  $\gamma$ . The lowest energy conformation of **12**, **13**, **18**, **22** is classified as *anti-hindered- $\alpha$*  with intramolecular hydrogen bond ( $N\cdots H\cdots O_9$ ), which is not found in Agranat's semiempirical PM3 studies. Probably, the structures with intramolecular hydrogen bond in **12**, **13**, **18**, **22** cannot survive by PM3 calculations.



**Scheme 3.2.** Illustration of Classification of Conformers Using Compound **12**.

The lowest energy conformation of **42** - **45** is *anti-open- $\beta$*  also with intramolecular hydrogen bond ( $N\cdots H\cdots O_9$ ), which is in line with Agranat's finding. The methylation appears to hinder rotation around the  $C_{4'}-C_9$  and  $C_9-C_8$  bonds, which makes the quinuclidine moiety to orient

away from quinoline moiety and result in the lowest energy *hindered* conformation in **12**, **13**, **18**, **22** vanishing and narrow down their conformational space. However, the methylation does not narrow down the conformational space of **42** - **45** because the lowest energy conformation of **42** - **45** is *open* conformation.

**Table 3.2.** The Lowest Energy Conformation of Cinchona Alkaloids Shown in Figure 3.1 and Their Methyl Cation Adducts.<sup>a</sup>

	$r_{\text{N-C4}'}$ (Å)	$d_{\text{C4}'\text{-C4}'\text{-C9-C8}}$ (°)	$d_{\text{N1-C8-C9-C4}'}$ (°)	$d_{\text{H-O9-C9-C8}}$ (°)	Classification
<b>12</b>	3.373	-82.4	-85.4	-27.0	<i>anti-hindered-<math>\alpha</math></i>
<b>12</b> (MP2) <sup>b</sup>	3.280	-81.8	-81.9	-29.1	<i>anti-hindered-<math>\alpha</math></i>
<b>12-CH<sub>3</sub><sup>+</sup></b>	3.928	-78.5	175.7	-174.1	<i>anti-open-<math>\gamma</math></i>
<b>12-CH<sub>3</sub><sup>+</sup></b> (MP2) <sup>b</sup>	3.866	-73.9	178.8	-174.8	<i>anti-open-<math>\gamma</math></i>
<b>13</b>	3.372	82.3	85.9	27.0	<i>anti-hindered-<math>\alpha</math></i>
<b>13-CH<sub>3</sub><sup>+</sup></b>	3.930	78.9	-176.5	174.5	<i>anti-open-<math>\gamma</math></i>
<b>42</b>	3.814	98.9	165.8	-29.2	<i>anti-open-<math>\beta</math></i>
<b>42</b> (MP2) <sup>b</sup>	3.775	95.6	168.8	-34.1	<i>anti-open-<math>\beta</math></i>
<b>42-CH<sub>3</sub><sup>+</sup></b>	3.953	-68.3	-172.3	161.0	<i>syn-open-<math>\gamma</math></i>
<b>42-CH<sub>3</sub><sup>+</sup></b> (MP2) <sup>b</sup>	3.882	-63.9	-169.1	161.0	<i>syn-open-<math>\gamma</math></i>
<b>43</b>	3.817	-97.5	-166.8	31.9	<i>anti-open-<math>\beta</math></i>
<b>43-CH<sub>3</sub><sup>+</sup></b>	3.939	-104.6	169.7	-165.7	<i>anti-open-<math>\gamma</math></i>
<b>22</b>	3.382	-82.0	-85.5	-26.1	<i>anti-hindered-<math>\alpha</math></i>
<b>22-CH<sub>3</sub><sup>+</sup></b>	3.927	-77.9	176.0	-173.8	<i>anti-open-<math>\gamma</math></i>
<b>18</b>	3.349	82.6	83.7	28.9	<i>anti-hindered-<math>\alpha</math></i>
<b>18-CH<sub>3</sub><sup>+</sup></b>	3.928	78.9	-174.5	173.8	<i>anti-open-<math>\gamma</math></i>
<b>44</b>	3.816	98.0	165.7	-29.6	<i>anti-open-<math>\beta</math></i>
<b>44-CH<sub>3</sub><sup>+</sup></b>	3.951	-67.9	-171.0	158.6	<i>syn-open-<math>\gamma</math></i>
<b>45</b>	3.819	-97.6	-167.4	32.3	<i>anti-open-<math>\beta</math></i>
<b>45-CH<sub>3</sub><sup>+</sup></b>	3.939	-102.1	169.2	-166.0	<i>anti-open-<math>\gamma</math></i>

<sup>a</sup> Calculated at the MP2(FC)/6-31+G(2d,p)//B98/6-31G(d) level of theory; <sup>b</sup> Optimized at the MP2(FC)/6-31G(d) level of theory.

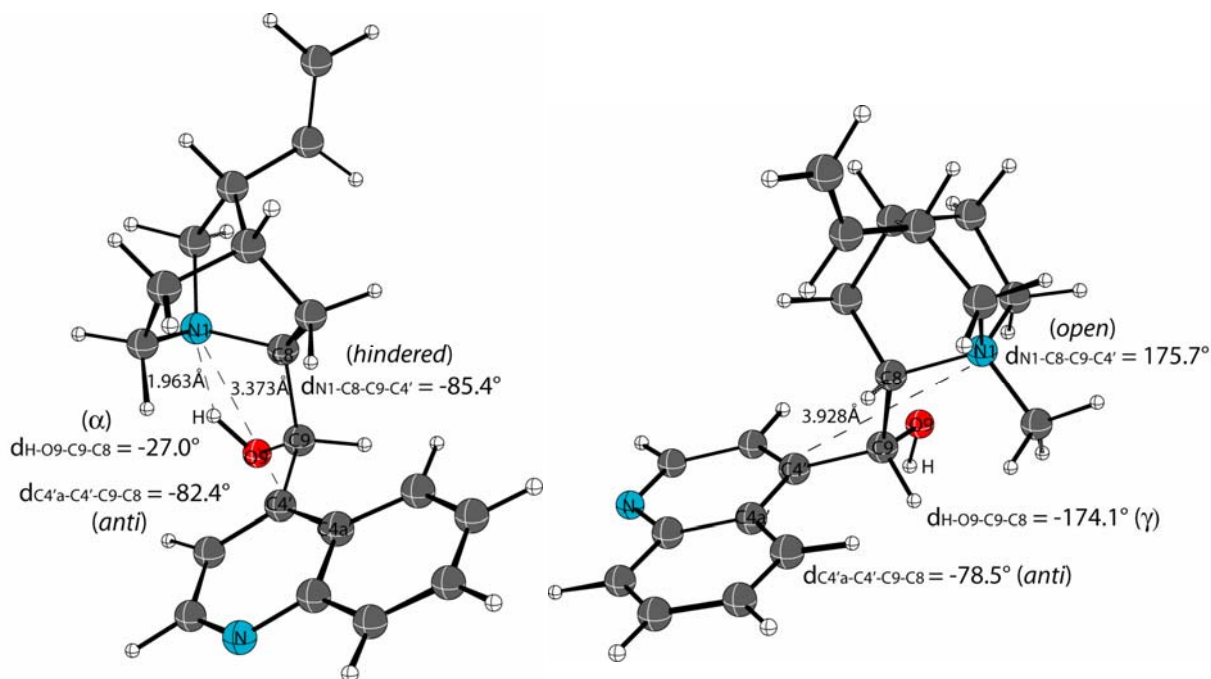
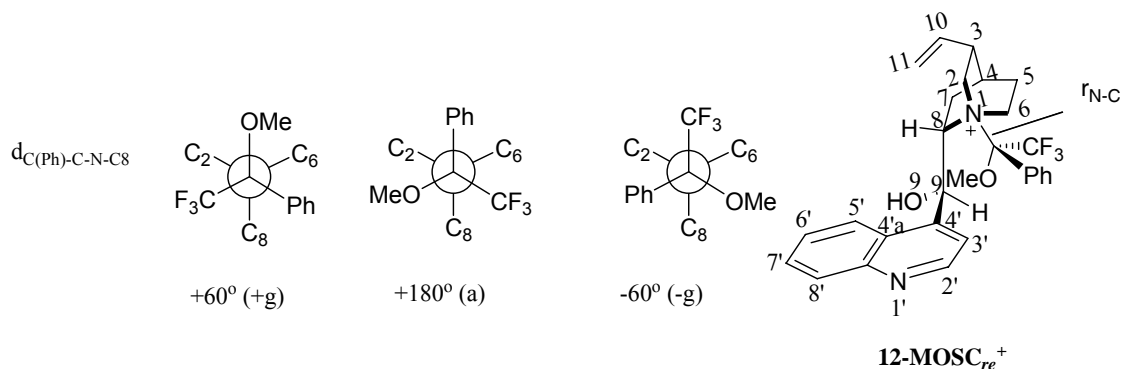


**Figure 3.5.** The Most Stable Conformer of **12** and **12-CH<sub>3</sub><sup>+</sup>** at the MP2(FC)/6-31G(d)//B98/6-31G(d) Level of Theory.

Selected geometrical parameters of the lowest conformation of their **MOSC** adducts are summarized in Table 3.3 and illustrated in Scheme 3.3. Investigating the geometrical parameters of **MOSC** adducts, we found that the dihedral angle  $d_{C8-N-C-O}$  differs only slightly between *re* face adduct and *si* face adduct for cinchona alkaloids **12**, **13**, **42**, **22**, **18**, **44** which indicates the methoxy group in **MOSC** always points to a similar position in both types of adducts. The structures of the most stable conformers for **12-MOSCre<sup>+</sup>** and **12-MOSCsi<sup>+</sup>** in Figure 3.6 show that the methoxy group in the **MOSC** prefers to approach the quinoline moiety, and the same observation is obtained for other cinchona alkaloids except for **43** and **45**. Further conformational searches involved flipping the quinoline moiety starting from the best conformer of **12-MOSCre<sup>+</sup>** and **12-MOSCsi<sup>+</sup>**, respectively. These latter modifications result in new conformers which are less stable than before by more than 10 kJ/mol. Furthermore, analysing the charge distribution in the **MOSC** adducts of **12** (see Table 3.4), we found that the methoxy group has more negative charge than the -CF<sub>3</sub> and phenyl groups, and the hydrogen atoms on the quinoline moiety have a positive charge. This may explain why the methoxy group always prefers to approach the quinoline moiety. Charge distribution also shows that the fluorine atoms in CF<sub>3</sub> have more negative charge than the carbon atom in the phenyl group. The electrostatic repulsion in **12-MOSCsi<sup>+</sup>** is probably less than that in **12-MOSCre<sup>+</sup>** because the not so negative carbon in the phenyl group is close to electronegative

hydroxy group ( $r_{\text{C(Ph)-O(H)}} = 3.17 \text{ \AA}$ ). In contrast, the more negative fluorine atoms in the  $\text{CF}_3$  group are close to the electronegative hydroxy group in **12-MOSCre**<sup>+</sup>. The same observation is obtained for **22**. The configuration of C9 in compound **13**, **42**, **18** and **44**, is changed, which results in that the less negative carbon in the phenyl group is close to the electronegative hydroxy group in their **MOSCre**<sup>+</sup> adducts, thus, their **MOSCre**<sup>+</sup> adducts are more stable.



**Scheme 3.3.** Illustration of Notation of Geometry Parameters Using Adduct **12-MOSCre**<sup>+</sup>.

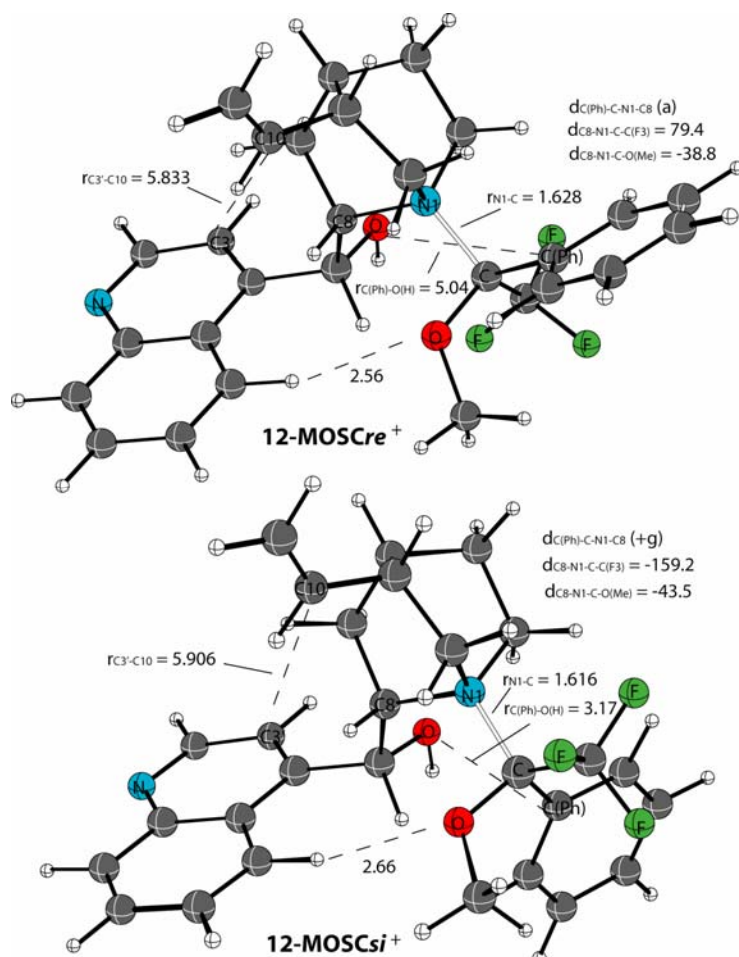


**Figure 3.6.** The Most Stable Conformer of **12-MOSCre**<sup>+</sup> and **12-MOSCSI**<sup>+</sup> at the MP2(FC)/6-31G(d)//B98/6-31G(d) Level of Theory (Bond Length in Ångstroms and Dihedral Angle in Degree (°)).

**Table 3.3.** The Lowest Energy Conformation and Selected Conformation of Cinchona Alkaloids' MOSC Adducts.

	r <sub>N-C</sub> (Å)	r <sub>C(Ph)-O(H)</sub> (Å)	r <sub>C3'-C10</sub> (Å)	d <sub>C(Ph)-C-N-C8</sub> (°)	d <sub>C8-N-C-C(F3)</sub> (°)	d <sub>C8-N-C-O(Me)</sub> (°)
<b>12-MOSCre<sup>+</sup></b>	1.628	5.04	5.833	a	79.4	-38.8
<b>12-MOSCsi<sup>+</sup></b>	1.616	3.17	5.906	+g	-159.2	-43.5
<b>13-MOSCre<sup>+</sup></b>	1.613	3.16	5.654	-g	159.6	43.9
<b>13-MOSCsi<sup>+</sup></b>	1.624	5.02	5.688	a	-78.8	39.6
<b>42-MOSCre<sup>+</sup></b>	1.607	3.83	6.821	-g	167.3	53.9
<b>42-MOSCsi<sup>+</sup></b>	1.617	4.88	6.777	a	78.9	61.3
<b>43-MOSCre<sup>+</sup></b>	1.615	3.62	6.609	-g	157.9	43.3
<b>43-MOSCre<sup>+</sup>-2<sup>a</sup></b>	1.631	4.832	3.858	a	59.8	-58.8
<b>43-MOSCsi<sup>+</sup></b>	1.648	3.298	6.082	-g	68.6	-178.3
<b>43-MOSCsi<sup>+</sup>-2<sup>b</sup></b>	1.623	3.736	3.735	+g	-165.2	-52.1
<b>22-MOSCre<sup>+</sup></b>	1.631	5.08	5.826	a	80.9	-37.5
<b>22-MOSCsi<sup>+</sup></b>	1.619	3.25	5.889	+g	-159.3	-43.5
<b>18-MOSCre<sup>+</sup></b>	1.615	3.25	5.662	-g	159.7	43.8
<b>18-MOSCsi<sup>+</sup></b>	1.627	5.08	5.752	a	-80.4	38.1
<b>44-MOSCre<sup>+</sup></b>	1.606	3.83	6.830	-g	167.5	54.2
<b>44-MOSCsi<sup>+</sup></b>	1.616	4.87	6.773	a	-57.1	61.0
<b>45-MOSCre<sup>+</sup></b>	1.614	3.607	6.134	-g	158.3	43.8
<b>45-MOSCre<sup>+</sup>-2<sup>c</sup></b>	1.628	4.798	3.888	a	58.7	-60.0
<b>45-MOSCsi<sup>+</sup></b>	1.646	3.281	6.127	-g	68.7	-178.3
<b>45-MOSCsi<sup>+</sup>-2<sup>d</sup></b>	1.620	3.729	3.747	+g	-165.5	-52.5

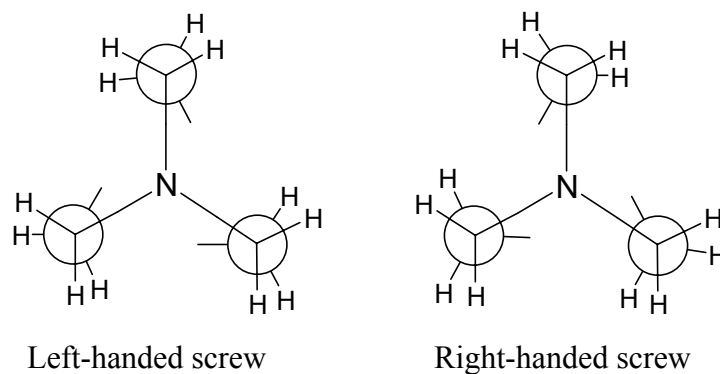
<sup>a</sup> pseudo-enantiomer of the best conformer of **42-MOSCsi<sup>+</sup>**; <sup>b</sup> pseudo-enantiomer of the best conformer of **42-MOSCre<sup>+</sup>**; <sup>c</sup> pseudo-enantiomer of the best conformer of **44-MOSCsi<sup>+</sup>**; <sup>d</sup> pseudo-enantiomer of the best conformer of **44-MOSCre<sup>+</sup>**.

**Table 3.4.** Charge Distribution in **MOSC** Adducts of **12**.

<b>12-MOSCre<sup>+</sup></b>						<b>12-MOSCst<sup>+</sup></b>					
OCH <sub>3</sub>		Ph		CF <sub>3</sub>		OCH <sub>3</sub>		Ph		CF <sub>3</sub>	
O	-0.596	C	-0.122	C	+1.117	O	-0.594	C	-0.141	C	+1.122
C	-0.321	C	-0.223	F	-0.346	C	-0.321	C	-0.233	F	-0.345
H	+0.231	C	-0.244	F	-0.337	H	+0.228	C	-0.237	F	-0.347
H	+0.240	C	-0.204	F	-0.352	H	+0.241	C	-0.208	F	-0.345
H	+0.226	C	-0.221			H	+0.227	C	-0.205		
		C	-0.208					C	-0.204		
		H	+0.249					H	+0.252		
		H	+0.249					H	+0.254		
		H	+0.259					H	+0.258		
		H	+0.259					H	+0.259		
		H	+0.259					H	+0.258		
sum	-0.221		+0.053		+0.081		-0.220		+0.052		+0.085

<sup>a</sup> NPA/MP2(FC)/6-31G(d)//MP2(FC)/6-31G(d) charges.

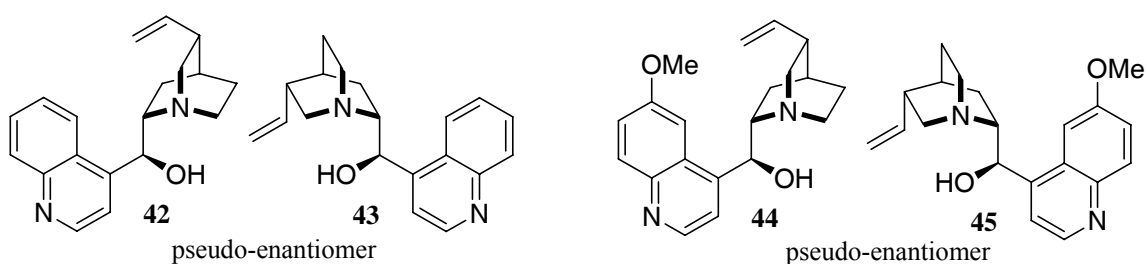
There is another conformational feature of these alkaloids, which has rarely been discussed, the conformation of the quinuclidine ring. The quinuclidine ring can twist in two different directions, either forming a right-handed screw or left-handed screw (viewed from the quinuclidine nitrogen atom along the pseudo C<sub>3</sub> symmetry axis, see the Scheme 3.4). Analysing of the lowest energy conformation of cinchona alkaloids shown in Figure 3.1, we found that the quinuclidine ring in **12**, **42**, **22** and **44** with S configuration at C8 is twisted as a left-handed screw, and that in **13**, **43**, **18** and **45** with R configuration at C8 is twisted as a right-handed screw. These results show that the configuration of C8 influences the direction of twist in the quinuclidine ring. The magnitude of the twist dihedral angle is in the range of 10 – 20°. Dijkstra *et al.* reported similar results when they investigate the conformation of the quinuclidine ring of dihydroquinine and dihydroquinidine through <sup>1</sup>H NMR spectra.<sup>101</sup> The twist direction of the quinuclidine ring is not changed in the corresponding methyl cation adducts.



**Scheme 3.4.** Schematic Drawing of the Quinuclidine Ring in Cinchona Alkaloids.

**Table 3.5.** Quinuclidine Ring Rotation Direction in Cinchona Alkaloids, Their Methyl Cation Adducts and **MOSCA** Adducts.

	Neutral molecule	Methyl cation adducts	<b>MOSCA</b> adducts	<b>MOSCA<sub>si</sub></b> adducts
<b>12</b>	left	left	left	left
<b>13</b>	right	right	right	right
<b>42</b>	left	left	right	right
<b>43</b>	right	right	right	right
<b>22</b>	left	left	left	left
<b>18</b>	right	right	right	right
<b>44</b>	left	left	right	right
<b>45</b>	right	right	right	right



**Scheme 3.5.**

Alkaloids **43** and **45** are pseudo-enantiomers with respect to compounds **42** and **44** (see Scheme 3.5), thus the **43-MOSCA<sub>si</sub><sup>+</sup>** and **45-MOSCA<sub>si</sub><sup>+</sup>** adducts are the pseudo-enantiomers of **42-MOSCA<sup>+</sup>** and **44-MOSCA<sup>+</sup>** adducts. The MOSCA values in Table 3.1 show that the **42-MOSCA<sup>+</sup>** and **44-MOSCA<sup>+</sup>** adducts are more stable than their *si* face adducts, suggesting

that the **43-MOSC***si*<sup>+</sup> and **45-MOSC***si*<sup>+</sup> adducts should be more stable than their *re* face adducts. However, the *si* face adducts are found to be slightly less stable than *re* facial adducts. In order to verify that this is not due to any missing conformers, we choose the best conformers of the **42-MOSC***re*<sup>+</sup> and **44-MOSC***re*<sup>+</sup> adducts and manually built their pseudo-enantiomers that are **43-MOSC***si*<sup>+</sup> and **45-MOSC***si*<sup>+</sup> adducts as the initial structures, and then reoptimized them at B98/6-31G(d) level. The final conformers obtained in this way are less stable than the best conformers we found before for **43-MOSC***si*<sup>+</sup> and **45-MOSC***si*<sup>+</sup>. Analysis of the internal quinuclidine ring distortion in the best conformer of each compound's **MOSC** adducts (see Table 3.5) reveals that the direction of distortion in the **MOSC** adducts of **12**, **13**, **43**, **22**, **18**, **45** remains the same as in the respective neutral compounds and methyl adducts, but is changed in the **MOSC** adducts of **42** and **44**. This raises the question why the rotation direction of the quinuclidine ring changes in **MOSC** adducts of epimers **42** and **44** and makes the **MOSC** adducts of these compounds more stable, while this is not so in the **MOSC** adducts of **43** and **45**. The rotation direction of the quinuclidine ring in epimers **42** and **44** changes probably because the repulsion between the incoming **MOSC** and the OH group on C9 is larger than in the adducts of natural cinchona alkaloids. Through the analysis of conformation (see Table 3.3), we found that the distance between C10 and C3' in the best conformers of **MOSC** adducts of **42** and **44** is large, which indicates the vinyl group is far away from the quinoline moiety and will not induce any repulsion between the vinyl group and the quinoline moiety. However, the distance between C10 and C3' in the conformations generated for **43-MOSC** and **45-MOSC** from mirror images of **42-MOSC** and **44-MOSC** is much shorter than in other cinchona alkaloids' **MOSC** adducts, leading to an increase in repulsive forces. Thus, the supposedly good conformers are not the best ones and other conformers without change of rotation direction of the quinuclidine ring stand for the best ones. This may be the reason why **43/45** have the least **MOSCA** values compared to other cinchona alkaloids, and also have small  $\Delta$ **MOSCA***re-si* values.

### 3.4 Correlation of MOSCA Values with Other Properties

One further finding concerns the overall dipole moment of **MOSC** adducts for the cinchona alkaloids (Table 3.6), which shows a moderate correlation with the MOSCA values (see Figure 3.7). This correlation implies that the energetically most favourable **MOSC** adducts are those with overall lower dipole moments. However, as exemplified by the results for **23**, such a correlation appears not to be of general validity.

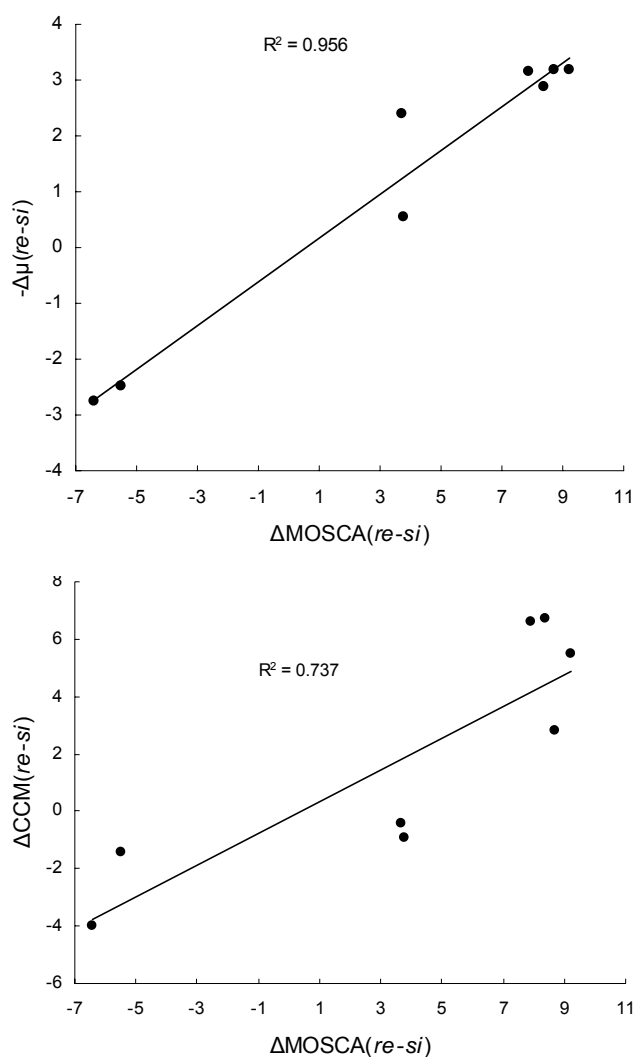


**Figure 3.7.** Correlation of  $\Delta\text{MOSCA}$  with Other Properties for Cinchona Alkaloids.

**Table 3.6.** MOSCA values (kJ/mol), CCM and Dipole Moments (D) for Compounds Shown in Figure 3.1.

	MOSCA		$\Delta$ MOSCA	CCM		$\Delta$ CCM	$\mu$		$\Delta\mu$
	<i>re</i>	<i>si</i>	<i>re-si</i>	<i>re</i>	<i>si</i>	<i>re-si</i>	<i>re</i>	<i>si</i>	<i>re-si</i>
Cinchonidine ( <b>12</b> )	215.2	220.7	-5.5	13.8	15.2	-1.4	6.98	4.51	2.47
Cinchonine ( <b>13</b> )	220.7	212.3	8.5	16.8	10.1	6.7	4.16	7.04	-2.88
Epi- Cinchonidine ( <b>42</b> )	197.6	188.4	9.2	16.1	10.6	5.5	3.51	6.68	-3.17
Epi- Cinchonine ( <b>43</b> )	183.7	180.0	3.7	16.8	17.2	-0.4	2.99	5.37	-2.38
Quinine ( <b>22</b> )	227.3	233.7	-6.4	16.2	20.2	-4.0	6.49	3.72	2.77
Quinidine ( <b>18</b> )	231.2	223.3	7.9	16.2	9.6	6.6	3.42	6.57	-3.15
Epi-Quinine ( <b>44</b> )	205.6	196.9	8.7	15.9	13.1	2.8	3.14	6.31	-3.17
Epi- Quinidine ( <b>45</b> )	193.1	189.3	3.8	18.8	19.7	-0.9	6.05	6.6	-0.55
<b>23</b>	224.9	217.6	7.3	9.1	4.3	4.8	4.53	8.34	-3.81
<b>46</b>	156.3	158.6	-2.3	12.4	8.8	3.6	1.61	2.86	-1.25

The continuous chirality measure (CCM) developed by Avnir<sup>105</sup> is a general approach to measure the deviation of the structure of a chiral molecule from having an achiral point group. The CCM can be used as a quantitative measurement of the intrinsic chirality of molecular systems. CCM values have been calculated for the lowest energy conformations of compounds shown in Figure 3.1. There is no quantitative correlation between MOSCA values and CCM for the set of compounds studied here. However, there is a moderate correlation between  $\Delta$ MOSCA<sub>*re-si*</sub> of cinchona alkaloids **12**, **13**, **18**, **22**, **43** - **45** and their respective  $\Delta$ CCM<sub>*re-si*</sub> values (see Figure 3.7).

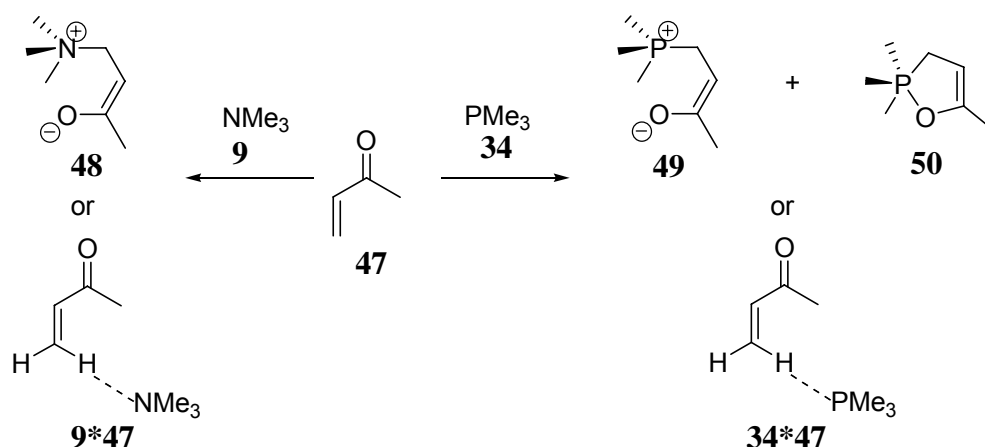
### 3.5 Conclusions

Taken together the MOSCA values determined here for a series of tertiary amines represent a quantitative and easily computable measure of the stereoinductive potential of these nucleophiles. These data, together with the methyl cation affinity (MCA) values, are expected to facilitate the development of new, more effective and more selective catalysts, in particular in an area where initial experiments have already been performed. The stereoinductive potential is one of the key factors determining the stereoselectivity in catalytic processes. Whether or not such a process is successful depends on a host of additional factors, the absolute catalytic efficiency being one of the most relevant. The MOSCA probe studied here appears to capture both the catalytic efficiency as well as the stereoselectivity. For the systems studied here the most reactive and selective compounds appear to be quinine (**22**) and quinidine (**18**), while sparteine (**46**) appears to be neither particularly selective nor reactive. The conformational space of natural cinchona alkaloids **12**, **13**, **18**, **22** are narrowed down and much more defined after they are combined with electrophiles. This could be a scientific reason why they are used frequently in asymmetric organocatalysis.

## 4. The Performance of Computational Methods in Locating the Charge-Separated Intermediates in Organocatalytic Transformations

### 4.1 Introduction

In Chapter 2 and Chapter 3 we have benchmarked and discussed the formation of cationic adducts in catalytic transformations using the selected cations as probes. However, in many of these reactions neutral electrophiles react with neutral nucleophiles to give zwitterionic adducts at some stage of the catalytic cycle. Recent theoretical studies of these types of processes have indicated that some of the most frequently used theoretical methods in computational chemistry such as the hybrid functional B3LYP do not describe these zwitterionic adducts as minima on the potential energy surface in the gas phase.<sup>31,32,33</sup> This precludes the use of compound energy methods such as the G3B3 or G3MP2B3<sup>40,41</sup> schemes for the determination of accurate reaction energies. The use of continuum solvation methods may, in part, alleviate the problem due to selective stabilization of structures with large dipole moment, but the overall results then rest on a quantum mechanical foundation of unknown (and possibly also uncertain) quality. In order to identify theoretical methods suitable for the reliable description of these types of processes we have selected here the gas phase reaction of methylvinylketone (MVK, **47**) with trimethylamine (**9**) and with trimethylphosphine (**34**) as model systems (Scheme 4.1). These addition reactions correspond to the first step in the amine- or phosphine-catalyzed Baylis-Hillman and Rauhut-Currier reactions, but may also be relevant for many other reactions involving Lewis base catalysis.



Scheme 4.1.

The stationary points expected in the reaction of **9** and **47** include the reactant complex **9\*47** between these two components and the zwitterionic adduct **48**. Similarly, the reaction of

phosphane **34** with **47** may yield the reactant complex **34\*47**, the zwitterionic adduct **49**, and also the neutral adduct **50** with pentacoordinated phosphorous.

The performance of a range of computational methods is evaluated based on the model systems. A rigorous comparison leads us to propose a new and effective computational scheme which is applicable to the larger systems that include more ubiquitously used electrophile-nucleophile combination in organocatalysis.

#### 4.2 Geometries and Energies of Zwitterionic Adducts

Geometry optimizations were initially performed using those electronic structure methods typically used in the G2,<sup>39</sup> G3,<sup>40,41</sup> G4<sup>106</sup> and W1<sup>42,43</sup> compound energy schemes. This includes optimizations at HF, MP2 and B3LYP levels. The hybrid density functional method mPW1K developed by Truhlar *et al.* has also been included here since promising results have recently been obtained with this method (Table 4.1).<sup>107</sup>

The results compiled in Table 4.1 show that reactant complex **9\*47** and zwitterionic adduct **48** can be located as stationary points at RHF level with a variety of basis sets, while **48** is not a stationary point at B3LYP level, irrespective of the basis set choice. Somewhat surprisingly **48** does not exist as a local minimum at MP2(FC)/6-31G(d) level, but it does exist when MP2(FC) calculations are performed with larger basis sets including diffuse basis functions. Whether or not the frozen core (FC) approximation is used in these calculations is of little consequences for the final results. This is an important result as this precludes use of the standard G2, G3 or G4 schemes for this type of stationary point, with the exception of the G2+ and G2(+) schemes developed by Gronert<sup>108</sup> and by Radom *et al.*<sup>109</sup> for calculations of charged systems. These latter two compound schemes involve geometry optimizations at MP2(FULL)/6-31+G(d,p) and MP2(FC)/6-31+G(d) level. The inability to locate zwitterionic adduct **48** at B3LYP level also precludes the use of the highly accurate W1 scheme recently proposed by Martin *et al.*<sup>42,43</sup> Similar to the results obtained at RHF level, all combinations of the mPW1K functional with Pople style basis sets predict zwitterionic adduct **48** and reactant complex **9\*47** as local minima. The reaction energies are, however, significantly closer to those obtained at MP2 than at RHF level. Table 4.1 lists reaction energies obtained from total electronic energies together with those obtained using enthalpies at 298.15 K. The latter are systematically less stabilizing as can be expected due to the loss of translational and rotational degrees of freedom. The magnitude of this effect is rather similar for all methods listed in Table 4.1, irrespective of whether or not zwitterionic adduct **48** exists as a stationary point on

the potential energy surface. The following discussion will therefore be based on reaction energies obtained from enthalpies at 298.15 K exclusively.

**Table 4.1.** Energies and Structural Data for Stationary Points in the Reaction of MVK (**47**) with NMe<sub>3</sub> (**9**).<sup>a</sup>

level of theory	reactant complex <b>9*47</b>			zwitterionic adduct <b>48</b>		
	E <sub>tot</sub> (kJ/mol)	H <sub>298</sub> (kJ/mol)	r(C-N) (pm)	E <sub>tot</sub> (kJ/mol)	H <sub>298</sub> (kJ/mol)	r(C-N) (pm)
HF/6-31G(d)	-10.94	-5.05	372.4	113.19	125.31	163.8
HF/6-31+G(d)	-7.42	-1.84	380.3	106.43	119.37	160.9
HF/6-31+G(2d)	-5.26	-0.22	387.7	114.19	127.02	160.4
HF/6-31+G(2d,p)	-5.25	-0.21	385.1	113.34	126.04	160.1
HF/6-311+G(2d,p)	-5.14	-0.09	386.0	113.59	126.43	159.8
B3LYP/6-31G(d) <sup>a</sup>	-16.19	-9.89	353.8	-	-	-
B3LYP/6-31G(2df,p) <sup>b</sup>	-17.47	-11.09	352.0	-	-	-
B3LYP/cc-pVTZ+d <sup>c</sup>	-10.41	-4.84	362.3	-	-	-
B3LYP /6-31+G(d)	-8.40	-2.58	360.8	-	-	-
B3LYP /6-31+G(2d)	-6.77	-1.38	364.2	-	-	-
B3LYP /6-31+G(2d,p)	-6.90	-1.51	363.3	-	-	-
B3LYP /6-311+G(2d,p)	-6.31	-0.92	363.1	-	-	-
mPW1K/6-31G(d)	-15.56	-9.44	345.9	44.60	55.56	165.2
mPW1K /6-31+G(d)	-9.46	-4.09	351.2	40.15	51.55	161.3
mPW1K/6-31+G(2d)	-7.63	-2.34	357.9	46.80	58.36	160.5
mPW1K/6-31+G(2d,p)	-8.00	-2.69	355.2	45.45	56.92	160.0
mPW1K/6-311+G(2d,p)	-8.12	-2.73	354.9	45.52	57.02	160.0
MP2(FC)/6-31G(d)	-24.64	-18.45	345.0	-	-	-
MP2(FULL)/6-31G(d) <sup>d</sup>	-25.21	-18.97	343.9	-	-	-
MP2(FC)/6-31+G(d)	-21.53	-16.38	347.0	22.39	33.77	163.4
MP2(FULL)/6-31+G(d)	-21.80	-16.91	346.8	20.44	31.54	162.8
MP2(FC)/6-31+G(2d)	-19.63	-14.57	349.0	22.50	32.98	163.4
MP2(FC)/6-31+G(2d,p)	-18.55	-13.62	348.9	23.01	33.32	163.3
MP2(FC)/6-311+G(2d,p)	-18.46	-13.34	348.0	20.49	31.45	162.8
QCISD/6-31+G(d) <sup>e</sup>	-18.93	-14.06	353.9	49.27	60.37	162.2
QCISD/6-31+G(2d) <sup>f</sup>	-17.45	-12.39	355.4	51.54	62.02	162.1

<sup>a</sup> All attempts to locate a cyclic minimum similar to structure **50** also for the nitrogen-based system failed, giving the acyclic structure **48** instead; <sup>b</sup> level of theory used for geometry optimizations in the G3B3 and G3(MP2)B3 schemes; <sup>c</sup> level of theory used for geometry optimization in the G4 scheme; <sup>d</sup> level of theory used for geometry optimization in W1 theory; <sup>e</sup> level of theory used for geometry optimizations in the G2 and G3 schemes; <sup>f</sup> thermal corrections taken from the MP2/6-31+G(d) level of theory; <sup>g</sup> thermal corrections taken from the MP2/6-31+G(2d) level of theory.

**Table 4.2.** Energies and Structural Data for Stationary Points in the Reaction of MVK (**47**) with PMe<sub>3</sub> (**34**).

level of theory	reactant complex <b>34*47</b>		zwitterionic adduct <b>49</b>		cyclic adduct <b>50</b>	
	$\Delta H_{298}$ (kJ/mol)	r(C-P) (pm)	$\Delta H_{298}$ (kJ/mol)	r(C-P) (pm)	$\Delta H_{298}$ (kJ/mol)	r(C-P) (pm)
HF/6-31G(d)	-3.57	439.5	101.92	182.3	60.87	185.3
HF/6-31+G(d)	-1.75	442.8	87.15	182.4	61.95	185.0
HF/6-31+G(2d)	-0.46	446.2	81.63	181.5	55.51	184.3
HF/6-31+G(2d,p)	-0.43	445.0	80.85	181.5	56.62	184.3
HF/6-311+G(2d,p)	-0.60	446.3	78.43	181.1	55.33	184.1
B3LYP/6-31G(d) <sup>a</sup>	-6.66	414.7	65.22	186.4	15.46	187.5
B3LYP/6-31G(2df,p) <sup>b</sup>	-7.03	413.7	55.77	184.0	2.80	186.6
B3LYP/cc-pVTZ+d <sup>c</sup>	-2.79	418.6	47.21	182.7	3.01	185.9
B3LYP /6-31+G(d)	-1.98	420.2	55.48	185.7	20.23	187.1
B3LYP /6-31+G(2d)	-1.05	419.3	49.94	184.0	13.57	186.0
B3LYP /6-31+G(2d,p)	-1.06	417.9	48.44	184.0	13.25	186.0
B3LYP /6-311+G(2d,p)	-0.41	420.6	48.56	183.5	13.15	185.9
mPW1K/6-31G(d)	-6.42	408.7	29.97	180.9	-30.92	184.8
mPW1K /6-31+G(d)	-3.20	412.4	19.79	181.3	-28.49	183.7
mPW1K/6-31+G(2d)	-2.00	413.1	13.41	180.2	-36.06	183.7
mPW1K/6-31+G(2d,p)	-2.20	409.7	11.69	180.1	-35.86	183.7
mPW1K/6-311+G(2d,p)	-2.39	408.5	9.53	179.7	-37.89	183.5
MP2(FC)/6-31G(d)	-13.77	405.3	-	-	-25.35	185.8
MP2(FULL)/6-31G(d) <sup>d</sup>	-14.78	402.9	-	-	-30.81	185.5
MP2(FC)/6-31+G(d)	-14.93	406.4	14.90	181.4	-34.53	185.5
MP2(FULL)/6-31+G(d)	-16.07	403.5	10.88	181.0	-40.57	185.2
MP2(FC)/6-31+G(2d)	-12.53	406.0	5.99	180.8	-47.09	185.1
MP2(FC)/6-31+G(2d,p)	-11.83	405.7	7.20	180.9	-48.01	185.2
MP2(FC)/6-311+G(2d,p)	-11.13	406.2	4.32	180.3	-49.96	184.8
QCISD/6-31+G(d) <sup>e</sup>	-12.35	412.5	46.11	182.0	-1.47	185.7
QCISD/6-31+G(2d) <sup>f</sup>	-10.12	414.0	39.93	181.5	-10.94	185.4

<sup>a</sup> level of theory used for geometry optimizations in the G3B3 and G3(MP2)B3 schemes; <sup>b</sup> level of theory used for geometry optimization in the G4 scheme; <sup>c</sup> level of theory used for geometry optimization in W1 theory; <sup>d</sup> level of theory used for geometry optimizations in the G2 and G3 schemes; <sup>e</sup> thermal corrections taken from the MP2/6-31+G(d) level of theory; <sup>f</sup> thermal corrections taken from the MP2/6-31+G(2d) level of theory.

The results obtained for PMe<sub>3</sub> (**34**) as the nucleophile differ from those obtained for NMe<sub>3</sub> (**9**) in that the zwitterionic adduct (**49**) corresponds to a local minimum with all methods considered here - with the exception of the MP2/6-31G(d) level. Whether or not the frozen core (FC) approximation is used in MP2 calculations is again of little consequence for the final results. Essentially the same results are obtained using different exponents for the d-type polarization functions, indicating that the choices made in the standard 6-31G(d) basis sets for N and P are not responsible for the failure to locate zwitterionic adducts **48** and **49** at MP2

level. The energetics of adduct formation as well as the length of the newly formed C-P bond are, however, distinctly different at B3LYP level as compared to MP2 and mPW1K levels.

The optimized geometries of adducts **48**, **49**, **50** at the mPW1K/6-31+G(d) and QCISD/6-31+G(2d) level of theories are shown in Figure 4.1. The structures as computed at these two levels are very similar in practically all details. The zwitterionic character of adducts **48** and **49** has been assessed by calculating the overall charge of the NMe<sub>3</sub> and PMe<sub>3</sub> moieties in these adducts at the NPA/mPW1K/6-31+G(d) level. The overall charge of the nucleophile NMe<sub>3</sub> in **48** is quite moderate and amounts to +0.50 e, while the charge of PMe<sub>3</sub> in **49** and **50** amounts to +1.02 e and +0.92 e, respectively. This illustrates that a significantly larger charge-transfer occurs from PMe<sub>3</sub> to the MVK (**47**) reactant than is the case for NMe<sub>3</sub>. This also illustrates that the Lewis structure shown in Scheme 4.1 for adduct **50** may not be fully appropriate.

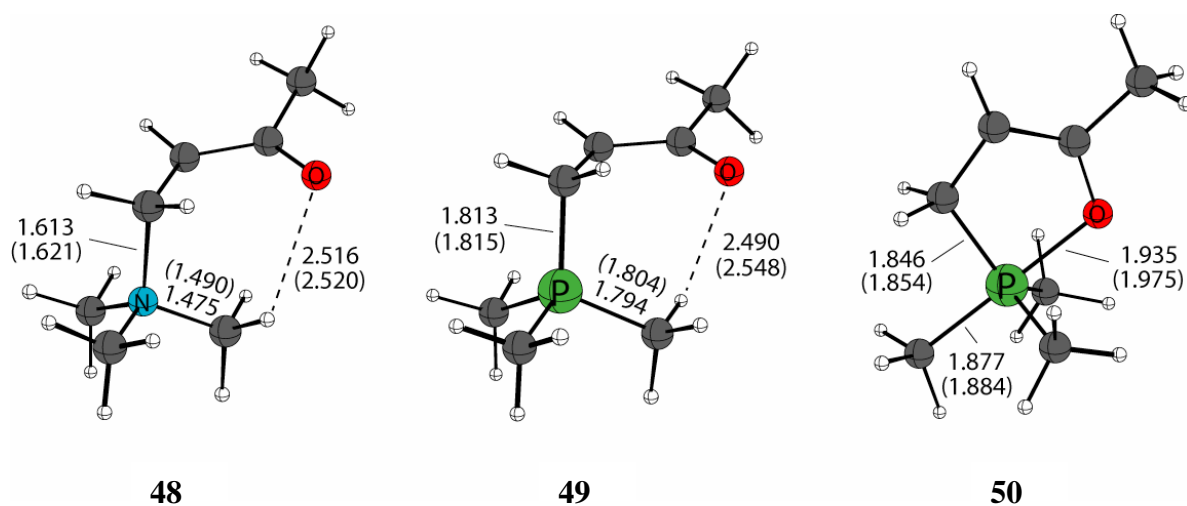


**Figure 4.1.** The Structures of Adducts **48** – **50** Optimized at mPW1K/6-31+G(d) Level. Geometric Parameters Obtained at the QCISD/6-31+G(2d) Level are Shown in Brackets. All Distances are in Ångstroms.

### 4.3 Theoretical Benchmarking of Reaction Energies

Relative energies have been calculated for all stationary points located before for the two model systems (Table 4.3) using G3-type compound energy schemes. In the first set of calculations termed "G3(+)" we retain all single point energy calculations of the original G3 scheme,<sup>41</sup> but vary the nature of thermal corrections and geometry optimizations. The most accurate results of these variants use geometries optimized at QCISD/6-31+G(2d) level and thermal corrections obtained from (unscaled) harmonic MP2(FC)/6-31+G(2d) frequencies. The reaction energies for formation of zwitterionic adducts **48** and **49** of +44.4 and +11.6 kJ/mol, respectively, are closely matched by all other variants considered here. This includes the most economical approach using geometries and thermal corrections obtained at mPW1K/6-31+G(d) level. Given the large influence of diffuse basis functions on the stabilities of zwitterionic adducts **48** and **49**, we have additionally calculated reaction energies using a modified G3 scheme termed here "G3+". In this modification the combination of QCISD(T)/6-31G(d) single point energies and correction for diffuse functions at MP4 level of the G3-scheme are replaced by one single point calculation at QCISD(T)/6-31+G(d) level. The reaction energies obtained with this scheme vary by no more than 0.6 kJ/mol from those using the G3(+) scheme on the same geometries. Whether these reaction energies can also be reproduced using a variant of the much more economical G3(MP2) scheme has been tested using geometries obtained at mPW1K/6-31+G(d) level (Table 4.3). This "G3(MP2)(+)" approach yields reaction energies deviating by up to 4.1 kJ/mol from the best (G3+) values, making it less appropriate for the calculation of benchmark quality data. We can thus conclude that combination of the original G3 single point energy scheme with mPW1K/6-31+G(d) geometries and thermal corrections provides the most economical way for the determination of reliable stabilities of zwitterionic structures. This level will in the following be referred to as "G3mPW1K(+)", and includes the following series of calculations:

- Optimization and frequency calculation at the mPW1K/6-31+G(d) level of theory
- QCISD(T,FC)/6-31G(d)//mPW1K/6-31+G(d) single point
- MP4(FC)/6-31+G(d)//mPW1K/6-31+G(d) single point
- MP4(FC)/6-31G(2df,p)//mPW1K/6-31+G(d) single point
- MP2(Full)/G3large//mPW1K/6-31+G(d) single point

The G3mPW1K(+) enthalpy at 298 K is defined as eq. 4.1.

$$\Delta H_{298} = E[\text{MP4(FC)/6-31G(d)//mPW1K/6-31+G(d)}] + \Delta E(+)$$

$$+ \Delta E(2\text{df,p}) + \Delta E(\text{QCI}) + \Delta E(\text{G3Large}) + H_{\text{corr}} \quad (4.1)$$

$$\Delta E(+)= E[\text{MP4(FC)/6-31+G(d)//mPW1K/6-31+G(d)}]-$$

$$E[\text{MP4(FC)/6-31G(d)//mPW1K/6-31+G(d)}]$$

$$\Delta E(2\text{df,p})= E[\text{MP4(FC)/6-31G(2df,p)//mPW1K/6-31+G(d)}]-$$

$$E[\text{MP4(FC)/6-31G(d)//mPW1K/6-31+G(d)}]$$

$$\Delta E(\text{QCI})= E[\text{QCISD(T,FC)/6-31+G(d)//mPW1K/6-31+G(d)}]-$$

$$E[\text{MP4(FC)/6-31G(d)//mPW1K/6-31+G(d)}]$$

$$\Delta E(\text{G3Large})= E[\text{MP2(Full)/G3Large//mPW1K/6-31+G(d)}]- E[\text{MP2(FC)/6-}$$

$$31\text{G(2df,p)//mPW1K/6-31+G(d)}]-E[\text{MP2(FC)/6-31+G(d)//mPW1K/6-31+G(d)}]+$$

$$E[\text{MP2(FC)/6-31G(d)//mPW1K/6-31+G(d)}]$$

$H_{\text{corr}}$ : ZPE + thermal correction to enthalpy (298 K) at mPW1K/6-31+G(d) level

**Table 4.3.** G3 Reaction Enthalpies at 298.15 K ( $\Delta H_{298}$ ) for Reaction of MVK (**47**) with NMe<sub>3</sub> (**9**) and PMe<sub>3</sub> (**34**) (kJ/mol).

geometries	thermal corrections <sup>a</sup>	MVK ( <b>47</b> ) + NMe <sub>3</sub> ( <b>9</b> )		MVK ( <b>47</b> ) + PMe <sub>3</sub> ( <b>34</b> )		
		<b>9*47</b>	<b>48</b>	<b>34*47</b>	<b>49</b>	<b>50</b>
<b>G3(+)</b>						
MP2/6-31+G(d)	HF/6-31+G(d) <sup>b</sup>	-12.77	+44.34	-11.59	+11.34	-48.54
MP2/6-31+G(d)	MP2/6-31+G(d)	-12.93	+44.57	-11.26	+13.11	-47.68
QCISD/6-31+G(d)	MP2/6-31+G(d)	-12.80	+45.08	-11.05	+14.16	-47.45
mPW1K/6-31+G(d)	mPW1K/6-31+G(d)	-12.29	+44.56	-10.66	+12.25	-47.90
MP2/6-31+G(2d)	HF/6-31+G(2d) <sup>b</sup>	-12.85	+44.99	-11.74	+10.92	-48.35
MP2/6-31+G(2d)	MP2/6-31+G(2d)	-12.68	+44.36	-11.51	+11.26	-48.61
QCISD/6-31+G(2d)	MP2/6-31+G(2d)	-12.60	+44.38	-11.28	+11.62	-48.71
mPW1K/6-31+G(2d)	mPW1K/6-31+G(2d)	-12.01	+43.09	-10.63	+10.51	-48.24
<b>G3+</b>						
QCISD/6-31+G(d)	MP2/6-31+G(d)	-13.16	+45.31	-11.41	+14.57	-46.92
QCISD/6-31+G(2d)	MP2/6-31+G(2d)	-12.94	+44.63	-11.62	+12.14	-48.19
<b>G3(MP2)(+)</b>						
mPW1K/6-31+G(d)	mPW1K/6-31+G(d)	-11.57	+46.26	-9.59	+16.06	-44.04

<sup>a</sup> based on unscaled harmonic frequencies except for HF level; <sup>b</sup> scale factor for harmonic frequency is 0.8929.

Formation of zwitterionic adduct **48** from NMe<sub>3</sub> (**9**) and MVK (**47**) is endothermic by 44.6 kJ/mol for the best G3+ method considered here. How does this value compare to the energies

obtained directly from geometry optimization as compiled in Table 4.1? Choosing the results obtained with the largest basis sets in Table 4.1 (6-311+G(2d,p)) we can see that RHF reaction energies are much less favourable (+126 kJ/mol), while reaction energies obtained from MP2(FC) or mPW1K calculations are much closer to the G3+ value at +31 and +57 kJ/mol, respectively. Similar observations can also be made for zwitterionic adduct **49**, whose formation is endothermic by 12.1 kJ/mol at G3+ level. Reaction energies are least favorable at RHF level (+78 kJ/mol), also unfavourable at B3LYP level (+48 kJ/mol), and close to thermoneutral at MP2(FC) and mPW1K level with values of +4 and +9 kJ/mol, respectively.

**Table 4.4.** Reaction Enthalpies at 298.15 K ( $\Delta H_{298}$ ) for Reaction of MVK (**47**) with NMe<sub>3</sub> (**9**) and PMe<sub>3</sub> (**34**) (kJ/mol).

Level of theory	MVK( <b>47</b> ) + NMe <sub>3</sub> ( <b>9</b> )		MVK ( <b>47</b> ) + PMe <sub>3</sub> ( <b>34</b> )			MAD <sup>a</sup>
	<b>9*47</b>	<b>48</b>	<b>34*47</b>	<b>49</b>	<b>50</b>	
mPW1K/G3large//	-2.25	+57.10	-2.29	+3.96	-49.51	8.40
mPW1K/6-31+G(d)						
mPW1K/6-311+G(3df,2pd)//	-1.90	+56.48	-1.91	+4.81	-48.13	8.00
mPW1K/6-31+G(d)						
MP2(FC)/G3MP2large//	-12.38	+27.66	-10.62	-9.65	-68.70	12.17
mPW1K/6-31+G(d)						
MP2(Full)/G3large//	-12.63	+26.78	-11.13	-12.70	-71.72	13.40
mPW1K/6-31+G(d)						
B2-PLYP/6-31+G(2d)//	-8.60	+60.42	-7.02	+30.23	-13.64	15.47
mPW1K/6-31+G(d) <sup>b</sup>						
B2-PLYP/G3large//	-5.70	+64.78	-4.84	+23.58	-23.75	14.01
mPW1K/6-31+G(d)						
B2-PLYP-M1/6-31+G(2d)//	-12.52	+42.14	-10.04	+15.87	-32.22	4.51
mPW1K/6-31+G(d) <sup>c</sup>						
B2-PLYP-M2/6-31+G(2d)//	-13.42	+37.92	-10.74	+12.55	-36.51	3.91
mPW1K/6-31+G(d) <sup>d</sup>						
B2-PLYP-M2/G3large//	-8.96	+44.73	-7.31	+7.20	-44.91	3.32
mPW1K/6-31+G(d) <sup>d</sup>						
B2-PLYP-M3/6-31+G(2d)//	-11.34	+49.00	-9.17	+24.11	-20.99	9.52
mPW1K/6-31+G(d) <sup>e</sup>						
B2K-PLYP/6-31+G(2d)//	-12.38	+46.98	-10.19	+16.41	-32.67	4.83
mPW1K/6-31+G(d)						
G3+//QCISD/6-31+G(2d)	-12.94	+44.63	-11.62	+12.14	-48.19	

<sup>a</sup>Mean Absolute Deviation from G3+//QCISD/6-31+G(2d) results; <sup>b</sup>using original B2-PLYP parameters b=0.73 and c=0.27 as recommended by *Grimme et al.*,<sup>110,111</sup> <sup>c</sup>using parameters b=0.73 and c=0.40; <sup>d</sup>using parameters b=0.73 and c=0.43; <sup>e</sup>using parameters b = 0.57 and c = 0.43.

Whether an approach solely based on energy calculations at either density functional or MP2 level can be identified that more closely approximates the G3mPW1K(+) results has been further explored in Table 4.4. The MAD values reported here refer to the results obtained at

the G3+//QCISD/6-31+G(2d) level described in Table 4.3, and other single point calculations are based on structures obtained at mPW1K/6-31+G(d) level. A first attempt involves mPW1K calculations using significantly larger basis sets than those used in Table 4.1 for geometry optimizations. The final MAD values obtained are quite good, but not small enough for high-precision predictions. This is also true for MP2 calculations using larger basis sets. The double-hybrid B2-PLYP scheme has recently been proposed by Grimme as a systematic improvement over both hybrid DFT and MP2 theories.<sup>110,111</sup> The exchange-correlation energies are calculated in this scheme according to eq. (4.2):

$$E_{xc} = (1-a_x) E_x^{GGA} + a_x E_x^{HF} + b E_c^{GGA} + c E_c^{PT2} \quad (4.2)$$

The mixing parameter  $a_x$  is used here to weigh the relative contributions of exact exchange  $E_x^{HF}$  and GGA exchange  $E_x^{GGA}$ . The correlation energies are equally calculated as a mix of GGA-derived correlation energy (using the LYP functional) and correlation energy calculated using second-order perturbation energy (PT2). This latter calculation is based on KS orbitals (and thus differs from MP2 energies based on HF orbitals). The mixing parameters  $a_x = 0.53$ ,  $b = 0.73$  and  $c = 0.27$  have been optimized by Grimme using the G2/97 thermochemical data set.<sup>111</sup> For the systems studied here we find that the overall MAD values are slightly higher for B2-PLYP than those obtained for MP2 calculations. The results obtained for the small 6-31+G(2d) basis set are very similar to those obtained for the larger G3large basis set, indicating little dependence of the results on the particular choice of the basis set. In a more recent study Martin *et al.* showed that the mixing parameters for exchange and correlation energies used in the B2-PLYP scheme take on quite different values when optimized for different sets of reference data.<sup>112</sup> As a result a new mixing scheme termed "B2K-PLYP" with broader applicability has been proposed using  $a_x = 0.72$ ,  $b = 0.58$  and  $c = 0.42$ . The MAD value for B2K-PLYP is significantly smaller at 4.8 kJ/mol than for B2-PLYP when using the 6-31+G(2d) basis set. Using  $c = 0.40$  (B2-PLYP-M1 in Table 4.4) gives MAD = 4.5 kJ/mol for the data set chosen here, indicating a large dependence of the stability of zwitterionic intermediates on the particular choice of this parameter. Using  $c = 0.43$  (B2-PLYP-M2 in Table 4.4) gives MAD = 3.9 kJ/mol, a value surprisingly similar to that used in the B2K-PLYP scheme. That this is mainly due to the treatment of correlation energies has been shown here by keeping the mixing parameters for exchange energies  $a_x$  and for GGA-derived correlation  $b$  at the original B2-PLYP values (using  $a_x = 0.53$ ,  $b = 0.73$ ), while searching for the optimal choice of parameter  $c$  describing the admixture of PT2 correlation energies. The

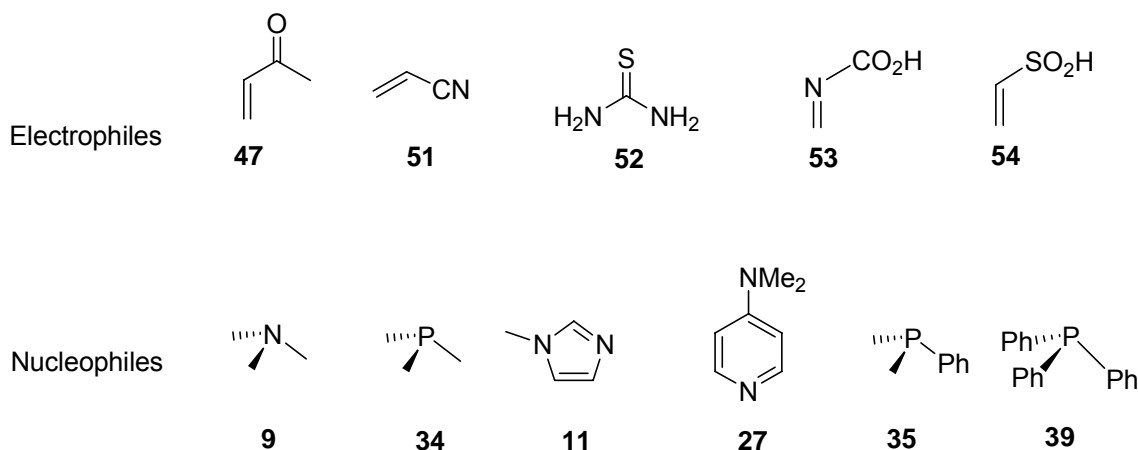
MAD value can be lowered further when using the larger G3large basis set (instead of 6-31+G(2d)), giving MAD = 3.3 kJ/mol at the B2-PLYP-M2/G3large//mPW1K/6-31+G(d) level. Rescaling of the PT2 correlation energies is, in principle, rather similar to the strategy pursued in "scaling all correlation" (SAC) methods such as SAC/3 or PCI-X, in which it is assumed that correlation energy calculations such as MP2 recover only a limited amount of the overall correlation energy.<sup>113,114</sup> Best results are indeed obtained here for combinations with  $b + c > 1$ , which effectively corresponds to scaling up correlation energies in absolute terms. This can also be verified by combining the optimized  $c = 0.43$  parameter with  $b = 0.57$ . This B2-PLYP-M3 variant gives significantly inferior results as compared to B2-PLYP-M2. The similarity of the results obtained with B2-PLYP-M2 and B2K-PLYP and the inferior results obtained with B2-PLYP-M3 also illustrates that rescaling the correlation energies (as in B2-PLYP-M2) and rebalancing the mixture of exchange energies (as in B2K-PLYP) have rather similar consequences for the dataset chosen here. Considering the limited size of this data set this conclusion cannot be made in general terms at the moment, but certainly suggests that departure from the  $b + c = 1$  recipe pursued in developing the B2-PLYP and B2K-PLYP models offers one more opportunity of optimizing the performance of double-hybrid functionals.

Beyond resolving methodological issues, the results compiled in Tables 4.3 and 4.4 also illustrate quite clearly how much stronger  $\text{PMe}_3$  binds to a neutral electrophile such as MVK ( $H_{298} = +12.1$  kJ/mol) as compared to  $\text{NMe}_3$  ( $H_{298} = +44.6$  kJ/mol). The binding energy difference at the reference G3+//QCISD/6-31+G(2d) level amounts to 32.5 kJ/mol in favor of  $\text{PMe}_3$ , which parallels the higher binding affinity of  $\text{PMe}_3$  to methyl cations ( $H_{298} = -604.7$  kJ/mol) as compared to that of  $\text{NMe}_3$  ( $H_{298} = -540.7$  kJ/mol). As a second point we note that the cyclic adduct **50** is energetically much more favourable than zwitterionic adduct **49** at all levels of theory considered here. The relative stability of these two structures will, of course, depend on the polarity of the reaction medium to some extent. The high stability of **50** is nevertheless noteworthy as this type of intermediate is typically excluded from considerations in phosphine-mediate Baylis-Hillman reactions.

#### 4.4 Extension to Larger Systems

In order to verify that the observations made for the small nucleophiles  $\text{NMe}_3$  (**9**) and  $\text{PMe}_3$  (**34**) are also valid for larger electrophile/nucleophile combinations, we have calculated the stability of zwitterionic adducts between the electrophiles and nucleophiles shown in Scheme 4.2. The list of nucleophiles includes commonly used catalytic N-centered bases such as N-

methylimidazole (NMI, **11**) and N,N-dimethylaminopyridine (DMAP, **27**) as well as phenyl-substituted phosphines **35** and **39**. On the side of the electrophiles we include additional alkenes bearing electron-withdrawing substituents such as **51** and **54**, as well as the weakly electrophilic thiourea **52** and the strongly electrophilic imine **53**.



**Scheme 4.2.**

**Table 4.5.** Reaction Enthalpies at 298.15 K ( $\Delta H_{298}$ ) for Reaction of Selected Nucleophiles and Electrophiles (kJ/mol).<sup>a</sup>

	<b>9</b>	<b>34</b>	<b>11</b>	<b>27</b>	<b>35</b>	<b>39</b>
B2PLYP-M2/6-31+G(2d)//mPW1K/6-31+G(d)						
<b>47</b>	+37.92	+12.55	+40.40	+35.42	+13.39	+22.79
<b>51</b>	-	+59.49	-	-	+53.51	+61.69
<b>52</b>	-	+50.33	+99.79	+79.02	+48.62	+60.68
<b>53</b>	-16.53	-32.73	+13.60	-20.54	-33.93	-24.05
<b>54</b>	-	+16.48	+43.64	+31.52	+15.06	+30.90
G3(MP2)mPW1K(+)						
<b>47</b>	+46.26	+16.06	+53.56	+41.61	+12.66	/
<b>51</b>	-	+64.87	-	-	+57.05	/
<b>52</b>	-	+34.31	+92.85	+68.52	+33.28	/
<b>53</b>	-15.38	-32.10	+22.25	-10.17	-31.33	/
<b>54</b>	-	+8.31	+46.93	+38.98	+8.57	/
G3mPW1K(+)						
<b>47</b>	+44.56	+12.25	+49.70	/	/	/
<b>51</b>	-	+62.74	-	-	/	/
<b>52</b>	-	+32.31	+90.70	/	/	/
<b>53</b>	-17.71	-36.59	+18.75	/	/	/
<b>54</b>	-	+4.26	+43.51	/	/	/

<sup>a</sup> only acyclic zwitterionic adduct considered here;  
 - no stable zwitterionic adduct at mPW1K/6-31+G(d) level.

The results obtained for these systems are collected in Table 4.5. For reaction of acrylonitrile (**51**) with N-centered nucleophiles **9**, **11**, and **27**, and also for the reaction of electrophiles **52**

and **54** with NMe<sub>3</sub> (**9**) no stable zwitterionic adducts could be found at the mPW1K/6-31+G(d) level. For all other combinations reaction energies have been calculated at B2-PLYP-M2/6-31+G(2d) level, and for selected systems also at G3(MP2)mPW1K(+) and G3mPW1K(+) level. The results obtained at this latter level for reactions of PMe<sub>3</sub> (**34**) show that reaction energies with the electrophiles selected here cover a range of almost 100 kJ/mol with **51** being the least effective and **53** being the most effective electrophile. The results obtained at G3(MP2)mPW1K(+) differ from the G3mPW1K(+) values by no more than 4.4 kJ/mol, while deviations of up to 18 kJ/mol occur at B2-PLYP-M2/6-31+G(2d) level. A similar comparison involving all nucleophiles could not be led to completion due to size limitations, but the B2-PLYP-M2/6-31+G(2d) level results indicate that PMe<sub>3</sub> (**34**) is the most and NMI (**11**) is the least effective nucleophile with reaction energy differences of 27.9 kJ/mol. The phosphines **34** and **35** give reaction energies of comparable size, while reaction of PPh<sub>3</sub> (**39**) is slightly less favorable. This finding is different from the one obtained in Chapter 2, in which the MCA value of PPh<sub>3</sub> (**39**) is larger than those of **34** and **35**. Analysis of the mPW1K/6-31+G(d) optimized structures reveals that the newly formed C-P bond in the zwitterionic adduct between PPh<sub>3</sub> (**39**) and MVK (**47**) is 184.2 pm, which is longer than the newly formed C-P bond (181.3 pm) in adduct **49** by 3 pm or so. The difference of the newly formed C-P bond in their corresponding methyl cation adducts is only 1.5 pm or so. It may indicate that the steric repulsion between the MVK (**47**) and phenyl substituents in PPh<sub>3</sub> (**39**) probably leads to the zwitterionic adduct less stable than the adduct between the MVK (**47**) and PMe<sub>3</sub> (**34**), which is not an issue for methyl cation adducts because the methyl cation is such a small electrophile.

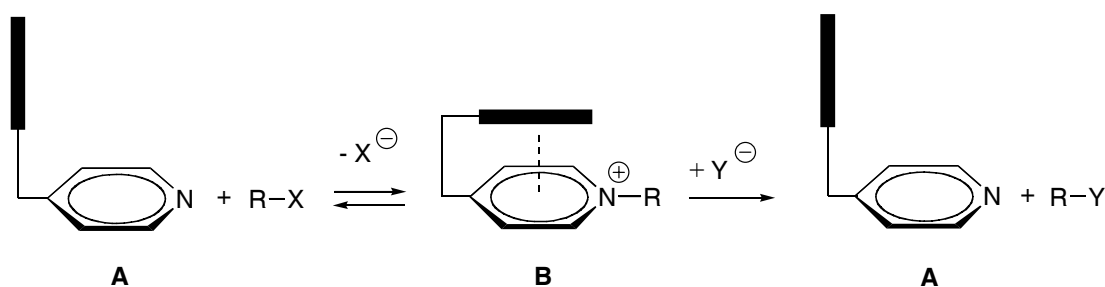
#### 4.5 Conclusions

The commonly used hybrid density functional B3LYP fails to give correct adduct geometries for nitrogen-containing nucleophiles, whether combined with Pople type basis sets or correlation consistent basis sets. The MP2/6-31G(d) level of theory does not give correct adduct geometries either. Geometry optimizations at the mPW1K/6-31+G(d) level provide a reliable basis for the development of compound energy schemes for the accurate description of zwitterionic adducts between neutral nucleophiles and electrophiles. Accurate energetics can be obtained using modified G3 schemes as well as double-hybrid DFT methods such as B2K-PLYP or B2-PLYP-M2. This latter class of methods also allows for the systematic investigation of large systems typically formed as intermediates in organocatalytic reactions.

## 5. Critical Design Elements for Acyl-Transfer Catalysts

### 5.1 Introduction

Using chiral pyridine derivatives based on DMAP (4-(dimethylamino)pyridine, **27**) or PPY (4-(N-pyrrolidino)pyridine, **29**) major advances have recently been made in kinetic resolution experiments, in particular in those involving secondary alcohols as substrates.<sup>8,90,115,116</sup> The design of these catalysts requires a delicate balance between two partially opposing effects: (a) the use of steric effects for the shielding of parts of the reaction center and thus the control over the conformational space of the selectivity-determining transition states; and (b) the rate enhancement of substrate turnover as compared to the uncatalyzed background reaction. In order to avoid an overly large reduction of the rate of the catalyzed process through steric effects, some of the catalyst designs involve the use of stacking interactions between the core pyridine ring and some side chain functional groups. How these interactions can lead to enhanced rates and to enhanced control of the conformational space at the same time can be illustrated with the minimal two-step sequence for the catalyzed group-transfer process in Scheme 5.1.

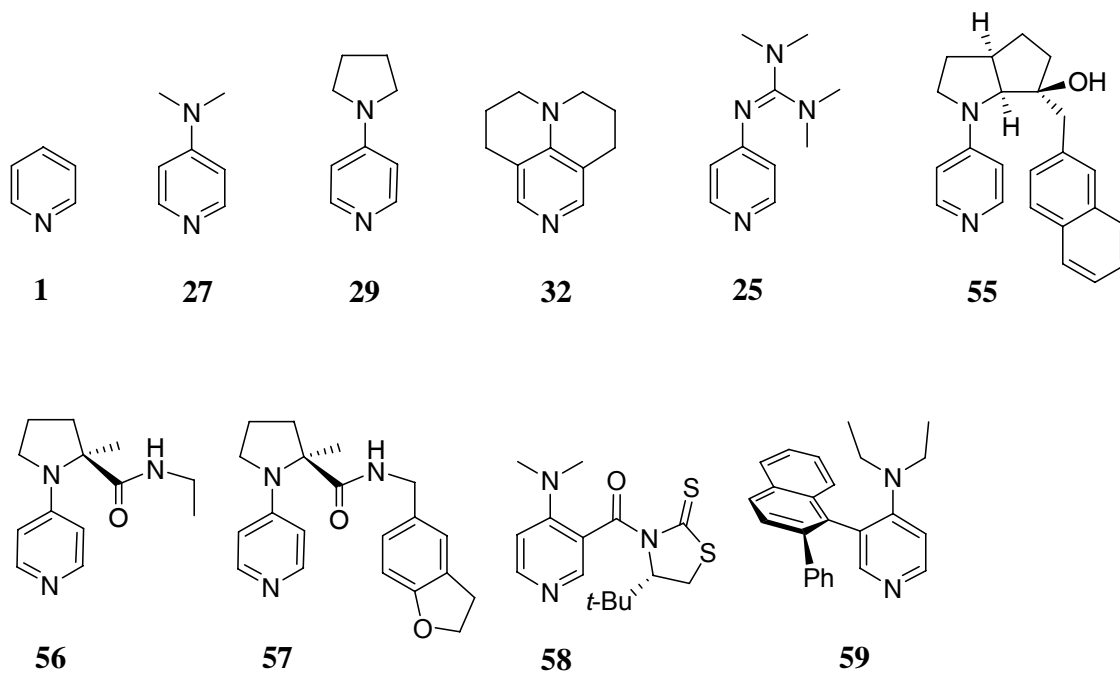


**Scheme 5.1.**

Initial reaction of the catalyst **A** with the electrophilic reagent  $RX$  (with  $R$  often being an acyl group) generates the cationic intermediate **B**. Subsequent reaction of **B** with the nucleophilic reagent  $Y^-$  regenerates the catalyst **A** and produces the product  $RY$ . Intermediate **B** is usually not detected directly under experimental conditions, but most indirect evidence points to the fact that the first of these steps is fast and reversible as compared to the second, product-forming step. Stabilization of intermediate **B** through stacking interactions will under these conditions translate into an overall enhanced rate of reaction. That the stacking interactions are more favorable at the pyridinium cation stage **B** than in the neutral catalyst is plausible in

systems containing electron-rich  $\pi$ -systems connected to the pyridine ring through a flexible linker unit.

In order to probe the involvement of stacking interactions in catalysts based on the pyridine nucleus in a systematic manner, a series of selected catalysts (see Scheme 5.2) are studied using several different theoretical methods. For the sake of computational accuracy, a rigorous and fast conformational search is required for the flexible catalysts **55** – **59**. Thus, the OPLS-AA force field, which lacks appropriate parameters for the systems studied here, is first developed and then implemented for conformational search. The performance of various theoretical methods for describing stacking interactions is compared and discussed. The conformational properties of acylpyridinium-cations predicted theoretically are discussed and also compared to experimental results. Their catalytic potential is explored and compared to several achiral pyridine derivatives, whose catalytic potential has been tested in the past.<sup>10,71,83</sup>



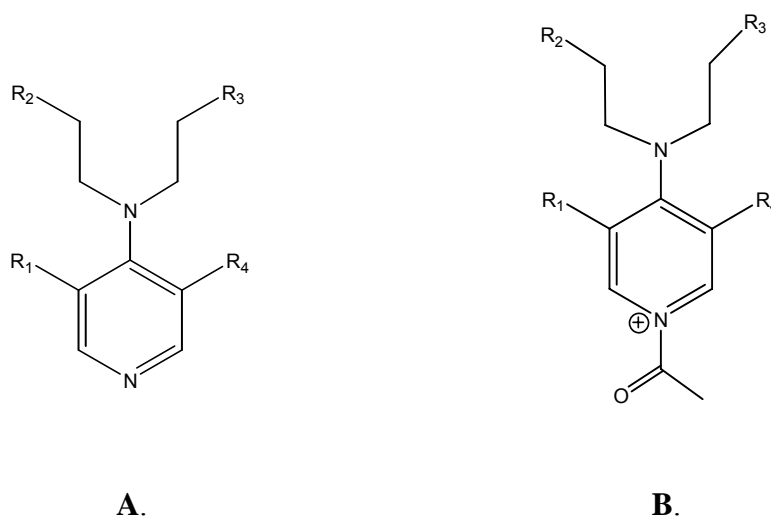
**Scheme 5.2.**

## 5.2 Force Field Development and Selection of Methods

### 5.2.1 Development of OPLS All-Atom Force Field and Conformational Search

The conformational space of all systems presented in this chapter has initially been studied with the OPLS-AA force field as implemented in BOSS 4.6.<sup>117</sup> Potential parameters for the description of 4-aminopyridines and their acetylpyridinium cations are currently not part of the default OPLS-AA force field.<sup>118</sup>

Two sets of OPLS-AA force field parameters for calculation on 4-aminopyridines (**A**) and 4-aminopyridinium cations (**B**) have been developed.



Most atom types are taken from AMBER atom type defined in Ref. 119. A new atom type is defined for the nitrogen atom connected to C4 position of pyridine ring and is termed as “NN” in both cases.

In both cases, Coulomb parameters have been derived using the CM1 procedure with the AM1 wavefunction. Lennard-Jones parameters are taken from similar compounds, such as pyridines, and tertiary amines in OPLS-AA force field. Bond and angle parameters are also chosen from OPLS-AA force field. For missing bond stretching and angle bending parameters, the equilibrium bond length  $r_{eq}$  and bond angle  $\theta_{eq}$  are taken from MP2(FC)/6-31G(d) optimized geometry, and force constants  $K_r$  and  $K_\theta$  are also taken from similar compounds in the OPLS-AA force field. Most dihedral parameters are chosen from similar compounds again, special dihedral parameters are selected to reproduce the potential energy profile at the B3LYP/6-31G(d) level of theory (see Figure 5.1) for conformational isomers of **A** with R<sub>1</sub>=R<sub>4</sub>=H, R<sub>2</sub>=R<sub>3</sub>=Me.

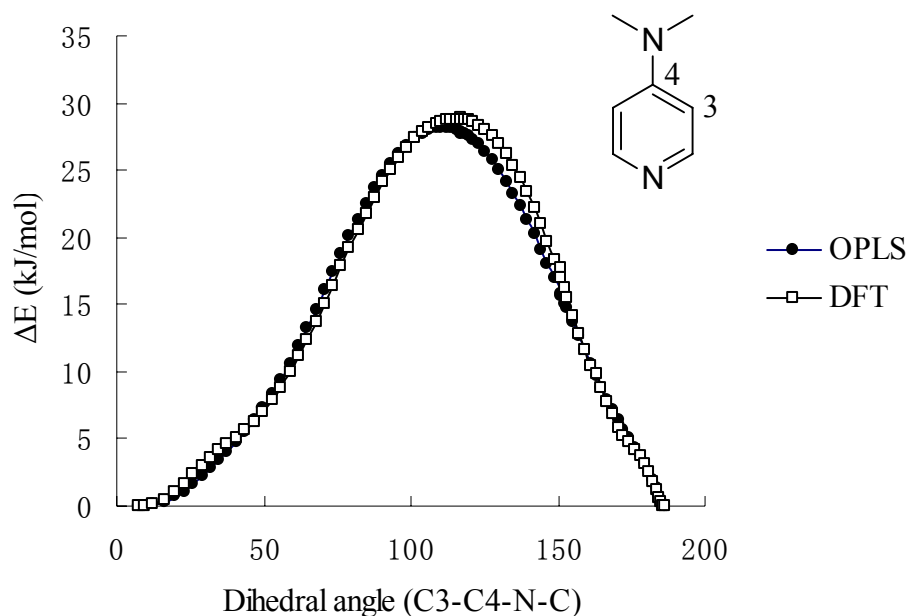


**Figure 5.1.** Potential Energy Profiles at the B3LYP/6-31G(d) and OPLS-AA Levels of Theory.

All of force field parameters are summarized in Appendix 9.5.2. The conformational space of both types of species has then been searched by systematic conformational search using the Monte Carlo search facility implemented in BOSS 4.6. The procedure of conformational search by BOSS 4.6 is also described in detail in Appendix 9.5.2. The structures of identified conformers by OPLS-AA were used for the subsequent quantum chemistry calculations.

### 5.2.2 Selection of Methods

It is known from theoretical studies of supramolecular complexes of a variety of  $\pi$ -systems such as benzene, naphthalene and the DNA bases that a correct description of dispersion interactions is required already at the stage of geometry optimization.<sup>63,120-122</sup> It is widely recognized that Hartree–Fock calculations describe dispersion interactions rather poorly due to their neglect of correlation effects. Good results are often obtained already at the MP2 level. An overestimation of dispersion forces observed in some cases at this latter level can be remedied either through more highly correlated single reference approaches such as CCSD(T)<sup>123</sup> or through rescaling the MP2 correlation energies according to the SCS-MP2 procedure.<sup>63,121,122</sup> Unfortunately, gradient-corrected density functional methods such as BLYP and hybrid functionals such as Becke3LYP are not able to describe dispersion interactions correctly in a systematic fashion due the essentially local design of these functionals.<sup>63,121,122</sup> How far a correlated treatment is also required for the correct description of conformational properties of the catalysts under study here is investigated using catalyst **55** as a test case. A rigorous conformational search has first been performed for **55** and its acetyl intermediate by modified OPLS-AA force field, then the identified conformers were reoptimized at the B3LYP/6-31G(d) level of theory, identifying 24 conformers for neutral **55** and 54 conformers for the corresponding acetyl intermediate **55Ac**. The potential of this level of theory was tested in earlier studies of the catalytic potential of pyridine bases.<sup>10,71,83</sup> Based on the Boltzmann-averaged enthalpies calculated at the B3LYP/6-311+G(d,p)//B3LYP/6-31G(d) level approximately 30 conformations make a significant contribution (>1%) to the conformational ensemble at 298 K, the energetically most favorable conformer of **55Ac** contributing 9.5%. The existence of stacked conformations in pyridinium cations can be determined in structural terms using the distance between the center of the pyridine ring and the center of the closest lying six membered aromatic ring (as indicated in Figure 5.2). This distance amounts to 5.20 Å in the most favorable conformer optimized at the B3LYP/6-31G(d) level, which is not a  $\pi$ – $\pi$  stacking structure and does not agree with the spectroscopic studies performed by Kawabata and coworkers.<sup>17</sup> Kawabata and coworkers have studied catalyst **55** and its acyl intermediate using <sup>1</sup>H NMR in CDCl<sub>3</sub> at 20 °C. Based on an analysis of the chemical shift and NOE data, an “open” conformation with little interaction between the pyridine nucleus and the naphthalene  $\pi$ -system was predicted for **55** in its neutral form and a “closed” conformation for the acylpyridinium cation formed from **55** and isobutyryl chloride (see Figure 5.2). The chemical shift data also indicates that the pyridine ring is conformationally flexible in neutral **55** (leading to identical resonances for the C2/C6 and

C3/C5 protons), but conformationally restricted in the corresponding acyl intermediate (giving four different signals for the four pyridine protons). However, more problematic is the fact that none of the other 52 conformational isomers found at the B3LYP level shows any type of stacking interactions. Repeating the conformational search at the RHF/3-21G level<sup>124</sup> again yields a large number of conformational isomers for **55Ac** (52 structures), this time including stacked conformations. Additional consideration of MP2(FC)/6-31G(d) single point energies makes one of the stacked conformations the energetically most favorable one. In order to verify that this single point approach does not lead to artefactual results, the six best conformations obtained at the MP2(FC)/6-31G(d)//RHF/3-21G level have been reoptimized at the MP2(FC)/6-31G(d) level. The results collected for these conformers in Table 5.1 indicate that the relative ordering is identical at both levels.

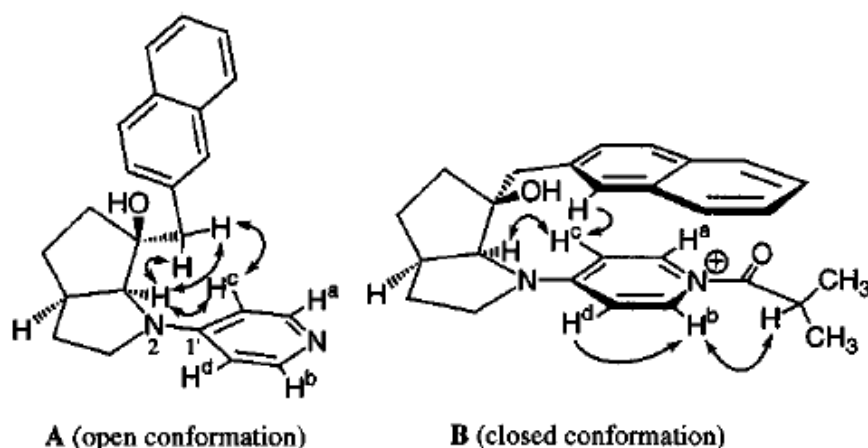


**Figure 5.2.** <sup>1</sup>H NMR Study of **55** (**A**) and Its Acyliminium Ion (**B**) in CDCl<sub>3</sub> at 20 °C. Arrows Denote the Observed NOEs. In **A**, Protons H<sup>a</sup>, H<sup>b</sup> and H<sup>c</sup>, H<sup>d</sup> Appear at δ 8.01 and 6.37 ppm, Respectively. In **B**, Protons H<sup>a</sup>, H<sup>b</sup>, H<sup>c</sup>, and H<sup>d</sup> Appear Independently at δ 7.45, 8.73, 5.69, and 6.87 ppm, Respectively.<sup>17</sup>

The stacked conformation **55Ac-1** is even more stabilized when relative energies are calculated at the MP2(FC)/6-311+G(d,p)//MP2(FC)/6-31G(d) level, predicting an energy gap in excess of 10 kJ/mol between stacked and non-stacked conformations. Application of the SCS-MP2 scaling protocol<sup>63</sup> to the MP2(FC)/6-311+G(d,p)//MP2(FC)/6-31G(d) energies for **55Ac** does indeed reduce the energy difference between stacked and other conformations to 4.9 kJ/mol, while the relative conformational ordering remains approximately the same as before (Table 5.1).

**Table 5.1.** Relative Enthalpies (in kJ/mol) for Selected Conformers of **55Ac** at Different Levels of Theory.

	<b>55Ac-1</b>	<b>55Ac-2</b>	<b>55Ac-3</b>	<b>55Ac-4</b>	<b>55Ac-5</b>	<b>55Ac-6</b>
$\Delta H_{298}$ HF/3-21G	18.30	0	8.95	2.81	10.18	14.27
$\Delta H_{298}$ HF/MIDI!	12.33	0	4.39	2.79	5.88	13.67
$\Delta H_{298}$ MP2/6-31G(d)//HF/3-21G	0	1.24	3.09	3.66	6.05	6.07
$\Delta H_{298}$ MP2/6-31G(d)//HF/MIDI!	0	2.30	6.24	5.39	8.11	8.33
$\Delta H_{298}$ MP2/6-31G(d)	0	0.63	2.05	5.79	12.76	13.25
$\Delta H_{298}$ MP2/6-311+G(d,p)// MP2/6-31G(d)	0	11.53	14.46	14.61	27.63	24.56
$\Delta H_{298}$ SCS-MP2/6-311+G(d,p)// MP2/6-31G(d)	0	4.90	8.25	9.00	17.75	17.94

Finally, we have also tested geometry optimizations at the RHF/MIDI! level in combination with MP2/6-31G(d) single point calculations as the basis of conformational searches. Despite the fact that the MIDI! basis set<sup>125</sup> yields better structural data as compared to the smaller 3-21G basis set, there is no significant improvement here as compared to MP2(FC)/6-31G(d)//RHF/3-21G. We may thus conclude that the sequence of full conformational screening at the MP2(FC)/6-31G(d)//RHF/3-21G level, reoptimization of the best conformers at MP2(FC)/6-31G(d) level, and calculation of SCS-MP2(FC)/6-311+G(d,p)//MP2(FC)/6-31G(d) single point energies for the best conformers appears to represent the best protocol for the determination of high level results. The following discussion of structural properties of catalysts **55** – **59** and their acetyl intermediates is therefore based on the results obtained in this fashion.

### 5.3 Conformational Properties of Acylpyridinium-Cations

The energetically most favorable conformer of catalyst **55** is shown in Figure 5.3 together with the two best conformers of the acetyl intermediate **55Ac**.

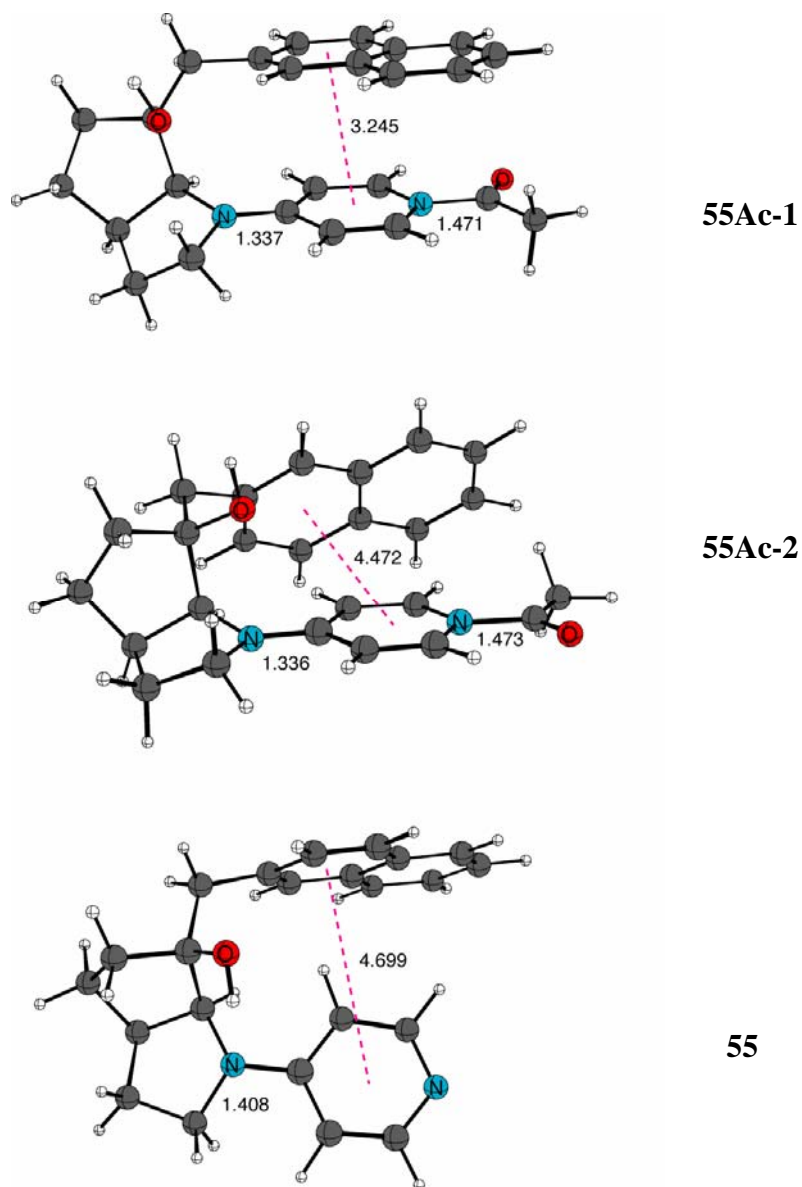


**Figure 5.3.** Structures of the Energetically Most Favorable Conformers of Catalyst **55** and Its Acetylated Form **55-Ac** as Optimized at the MP2(FC)/6-31G(d) Level of Theory. Distances Are Given in Ångstroms.

In the more favorable of these latter structures **55Ac-1** the naphthalene ring is positioned quite ideally on top of the pyridinium ring, while the second best conformer **55Ac-2** may best be described as “side-on” in the sense that the C–H bonds of the pyridinium ring point towards the naphthalene  $\pi$ -system. The different relative orientation of the two  $\pi$ -systems is clearly reflected in the different values of the stacking parameter (3.25 vs. 4.47 Å, Table 5.2), but has little effect on other key structural variables such as the C–N bond distance between acetyl group and pyridine ring (1.471 vs. 1.473 Å). This latter bond distance has earlier been found to be a sensitive structural probe for the stability of the acetyl intermediates of differently substituted pyridines as exemplified in Table 5.2 with the values for catalysts **1**, **25**, **27**, **29**, **32**.<sup>71</sup> For these latter systems a good correlation is also found between the overall charge of the acetyl group and the C–N bond distance, with shorter bonds correlating with lower overall (positive) charges. However, the charge of the acetyl group is largely constant for the six best conformers of **55Ac** as are the respective C–N bond distances (Table 5.2). This implies that the energy differences between these conformers (up to 18 kJ/mol) do not result from differences in the stabilization of the overall positive charge of the system. One further difference between **55Ac-1** and **55Ac-2** concerns the orientation of the acetyl group oxygen atom, which points in the direction of the naphthalene side chain in **55Ac-1** and in the opposite direction in **55Ac-2**. The former orientation had been predicted by Kawabata *et al.* based on NOE measurements between the acetyl group hydrogen atoms and the pyridine ring protons.<sup>17</sup> Aside from the stacked and side-on conformers described in Table 5.2 and Figure 5.3 additional structures of **55Ac** exist in which the naphthalene ring is rotated away from the pyridine ring with stacking parameters beyond 6 Å. These structures contribute very little to the conformational ensemble at 298 K (<1%) and are therefore not explicitly discussed here. In conclusion it is only conformer **55Ac-1** which is in line with all direct and indirect conclusions derived from the NMR data for this system. The most favorable conformer found for the neutral catalyst **55** can best be described as “T-shaped”. This structure alone is insufficient to explain the rapid interconversion of the C2–C6 protons of the pyridine ring in **55**, but not in **55Ac**. However, one major difference between these two systems is the much shorter (1.337 vs. 1.408 Å) and thus stronger C–N bond connecting the pyridine ring to the amino-substituent at C4. Rotation around this bond (which has partial double bond character in **55Ac**, but not in **55**) is required for rapid equilibration of the hydrogen atoms on the two sides of the pyridine ring and the barrier for rotation around this bond is certainly higher in **55Ac** than in **55**.

The conformational properties of the acetyl intermediates of catalysts **56** – **59** can easily be classified based on the structures shown in Figure 5.4 and the structural and charge data in Table 5.2.

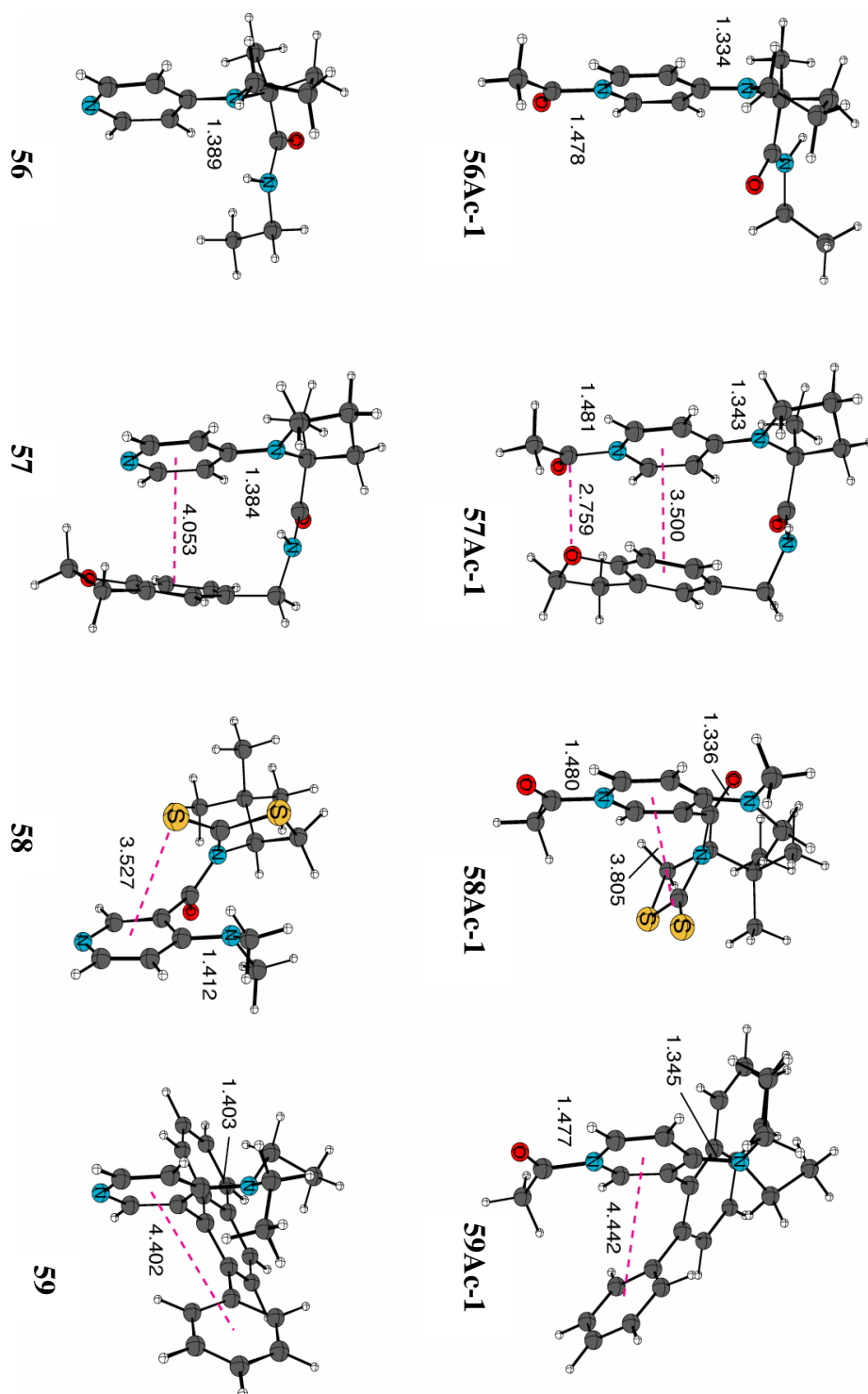


**Figure 5.4.** Structures of the Energetically Most Favorable Conformers of Catalysts **56** – **59** and Their Respective Acetylated Forms as Optimized at the MP2(FC)/6-31G(d) Level of Theory. Distances are given in Ångstroms.

**Table 5.2** Structural and Electronic Characteristics of Acetyl Intermediates of Catalysts Shown in Scheme 5.2.

system	R(C-N) <sup>a</sup> (Å) RHF/3-21G	R(C-N) <sup>a</sup> (Å) MP2/6-31G(d)	q(Ac) <sup>b</sup> NPA	q(Ac) <sup>c</sup> NPA	Stacking parameters <sup>d</sup> (Å) HF/3-21G	Stacking parameters <sup>d</sup> (Å) MP2/6-31G(d)	ΔE <sup>e</sup> (kJ/mol)	ΔE <sup>f</sup> (kJ/mol)
<b>1Ac</b>	1.500	1.540	+0.368	+0.380	-	-	-	-
<b>27Ac</b>	1.459	1.486	+0.303	+0.314	-	-	-	-
<b>29Ac</b>	1.456	1.482	+0.296	+0.307	-	-	-	-
<b>32Ac</b>	1.451	1.478	+0.287	+0.298	-	-	-	-
<b>25Ac</b>	1.445	1.472	+0.273	+0.287	-	-	-	-
<b>55Ac-1</b>	1.448	1.471	+0.281	+0.285	3.57	3.25	0.0	0.0
<b>55Ac-2</b>	1.447	1.473	+0.279	+0.287	5.23	4.47	11.53	4.90
<b>55Ac-3</b>	1.448	1.474	+0.280	+0.289	5.18	4.60	14.46	8.25
<b>55Ac-4</b>	1.447	1.471	+0.279	+0.287	5.32	4.29	14.61	9.00
<b>55Ac-5</b>	1.448	1.472	+0.279	+0.288	5.20	4.65	27.63	17.75
<b>55Ac-6</b>	1.451	1.478	+0.285	+0.296	4.70	4.57	24.56	17.94
<b>56Ac</b>	1.453	1.478	+0.291	+0.301	-	-	-	-
<b>57Ac-1</b>	1.458	1.481	+0.290	+0.293	3.68	3.50	0.0	0.0
<b>57Ac-2</b>	1.458	1.482	+0.284	+0.292	4.51	4.41	12.69	7.59
<b>58Ac-1</b>	1.457 <sup>g</sup>	1.480	+0.299	+0.307	3.83	3.81	0.0	0.0
<b>58Ac-2</b>	1.458 <sup>g</sup>	1.481	+0.301	+0.309	3.83	3.70	0.48	0.78
<b>59Ac-1</b>	1.450	1.477	+0.294	+0.299	4.41	4.44	0.0	0.00
<b>59Ac-2</b>	1.450	1.476	+0.295	+0.298	4.32	4.39	1.86	1.74

<sup>a</sup> Bond distance between pyridine nitrogen and acetyl carbon atoms; <sup>b</sup> NPA/MP2/6-31G(d)//HF/3-21G charges; <sup>c</sup> NPA/MP2/6-31G(d)//MP2/6-31G(d) charges; <sup>d</sup> Distance between the center of pyridine ring and the center of the closest aromatic ring (or C=S group); <sup>e</sup> Energy differences (in kJ/mol) between conformers calculated from H<sub>298</sub>(MP2(FC)/6-311+G(d,p)//MP2(FC)/6-31G(d)) data; <sup>f</sup> Energy differences (in kJ/mol) between conformers calculated from H<sub>298</sub>(SCS-MP2(FC)/6-311+G(d,p)//MP2(FC)/6-31G(d)) data; <sup>g</sup> Geometries of systems **58Ac** and **58** optimized at HF/3-21G\* level.

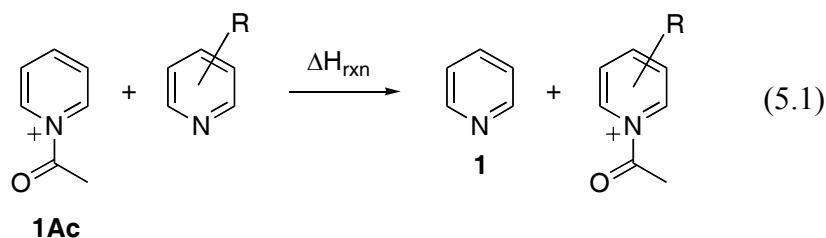
A comparison of the related systems **56** and **57** shows that catalyst **57** contains a  $\pi$ -system capable of stacking interactions, while **56** does not. A close contact between the pyridinium  $\pi$ -system and the benzene ring contained in the amide side chain of **57Ac** is indeed visible in the energetically most favorable conformer of this system displayed in Figure 5.4. However, the distance between the ring midpoints of 3.50 Å is significantly longer than the distance between the acetyl group and the oxygen atom of the dihydrobenzofuran side chain of 2.76 Å. This latter contact appears to originate from electrostatic complementarity of the most electronegative center of the side chain and the partially positively charged acetyl group in **57Ac**. It is clear from this description that further variation of the side chain heteroatoms may result in even stronger electrostatic interactions, implying more stable acetyl intermediates and better conformational control. The second best conformer of **57Ac-2** orients the side chain in a side-on fashion to the pyridinium ring and is less stable than **57Ac-1** by 7.6 kJ/mol. No spectroscopic data appear to exist for the acyl intermediates of **56** and **57**. However, **57** has been found to give slightly better selectivities than **56** in kinetic resolution experiments of alcohols.<sup>18</sup>

Catalyst **58** differs from the previous systems in that close contacts between the pyridine ring and parts of the side chain (here: the thiocarbonyl group) exist at both the neutral and the cationic stage. The stacking distance is even smaller for neutral **58** than for **58Ac**. One major difference between the neutral and cationic forms of **58** concerns the orientation of the *tert*-butyl group, which points towards the dimethylamino group in acetyl-intermediate **58Ac**, and in the opposite direction in neutral catalyst **58**. Non-stacking conformations are energetically very unfavorable for both species. Yamada and coworkers have studied catalyst **58** and its alkyl- and acyl-pyridinium derivatives by <sup>1</sup>H NMR measurements.<sup>20</sup> Through comparison to model compounds lacking the thiocarbonyl moiety it was concluded that acylation of **58** leads to a “conformationally locked” pyridinium cation involving stacking interactions between the pyridinium nucleus and the thiocarbonyl bond. Calculations performed on the isobutyrylpyridinium-cation of **58** at the B3LYP/6-31G(d) level of theory also show that these intermediates have clear conformational preferences with respect to the orientation of the *tert*-butyl side chain.<sup>20</sup> The orientation of the *tert*-butyl side chain is directly comparable to what is found here for the acetyl intermediate. However, while no significant conformational preference exists for the acetyl group in **58Ac** (*syn* and *anti* conformer differ by less than 1 kJ/mol at all levels studied here), a clear preference for an *anti* conformation (pointing the carbonyl oxygen atom away from the substituent at C3) has been found experimentally for the isobutyryl group.

No stacking interactions between the pyridine ring and the phenyl side chain exist in the neutral or cationic forms of catalyst **59**. Still the rigid phenylnaphthyl side chain has clear conformational preferences at both stages, orienting the phenyl substituent towards the acetyl group in cation **59Ac** and towards the diethylamino group in neutral **59**. Previous theoretical studies of the conformational space of catalyst **59** at the PM3 level as well as the X-ray crystal structure of protonated **59** shows that the  $\pi$ -systems contained in **59** are connected in a rather rigid manner. This excludes the conformational rearrangement described in Scheme 5.1. The most favorable orientation of the acetyl group in **59Ac-1** is in line with the assignment made for the situation in solution based on  $^1\text{H}$  NMR spectroscopic results.<sup>126</sup>

#### 5.4 Reaction Enthalpies for Acetyl Group Transfer

The stability of acetyl intermediates of catalysts shown in Scheme 5.2 has been assessed using the reaction enthalpy at 298.15 K for the isodesmic reaction (5.1) shown in Scheme 5.3.



Scheme 5.3

Previous results for catalysts **1**, **25**, **27**, **29**, **32** have been obtained at the B3LYP/6-311+G(d,p)//B3LYP/6-31G(d) level of theory.<sup>71</sup> Given the problematic performance of this level in describing the conformational properties of the larger catalysts **55** – **59** we concentrate here on the results obtained from calculations at Hartree–Fock and MP2 levels of theory (Table 5.3).

Perusal of the results for the non-stacking catalysts **1**, **25**, **27**, **29**, **32** shows a clear trend to smaller reaction enthalpies on going from the B3LYP/6-311+G(d,p)//B3LYP/6-31G(d) to the MP2(FC)/6-31G(d)//RHF/3-21G level. This reduction is still visible when MP2(FC)/6-31G(d) optimized geometries are used and thus reflects the intrinsic properties of the MP2 method. Additional consideration of SCS-MP2 single point energies calculated with the large 6-311+G(d,p) basis set predicts practically the same values. Comparison of the results obtained from the most economical and the most expensive MP2 versions considered here (MP2(FC)/6-31G(d)//RHF/3-21G vs. SCS-MP2(FC)/6-311+G(d,p)//MP2(FC)/6-31G(d)) shows these to be strikingly similar for most systems. The relative ordering of the stabilities of catalysts **1**, **25**, **27**, **29**, **32** is practically identical at all levels selected here with one exception: while catalyst **25** is predicted to give more stable intermediates than catalyst **32** at the Hartree–Fock and B3LYP levels, largely similar values are obtained at the MP2 levels for both systems.

**Table 5.3.** Stabilities of Acetyl Intermediates of Catalysts Shown in Scheme 5.2 as Expressed through the Heat of Reaction  $\Delta H_{\text{rxn}}$  of Isodesmic Reaction (5.1) at 298.15 K (in kJ/mol).

system	$\Delta H_{\text{rxn}}$ RHF-1 <sup>a</sup>	$\Delta H_{\text{rxn}}$ RHF-2 <sup>a</sup>	$\Delta H_{\text{rxn}}$ B3LYP-1 <sup>a</sup>	$\Delta H_{\text{rxn}}$ B3LYP-2 <sup>a</sup>	$\Delta H_{\text{rxn}}$ MP2-1 <sup>a</sup>	$\Delta H_{\text{rxn}}$ MP2-2 <sup>a</sup>	$\Delta H_{\text{rxn}}$ MP2-3 <sup>a</sup>	$\Delta H_{\text{rxn}}$ MP2-4 <sup>a</sup>	$\Delta H_{\text{rxn}}$ MP2-5 <sup>a</sup>	$\Delta H_{\text{rxn}}$ RHF-4
<b>1</b>	0.0	0.0	0.0	0.0	0.0	0.0	0.0	0.0	0.0	0.0
<b>27</b>	-89.24	-85.47	-82.54	-82.08	-78.97	-77.19	-77.67	-76.16	-78.77	-82.79
<b>29</b>	-99.67	-95.15	-93.42	-93.1	-88.49	-89.21	-89.84	-86.20	-89.11	-94.39
<b>32</b>	-110.58	-102.07	-107.06	-108.9	-101.75	-100.60	-101.51	-99.48	-101.41	-107.27
<b>25</b>	-117.76	-106.46	-114.27	-113.1	-99.98	-102.17	-99.22	-94.74	-98.50	-115.73
<b>55</b>	-116.22	-104.36	-110.84	-110.19	-109.77	-109.91	-119.16	-130.32	-120.93	-90.96
<b>56</b>	-87.56	-	-	-	-81.95	-	-84.60	-82.36	-85.37	-90.00
<b>57</b>	-113.30	-	-	-	-114.44	-	-106.08	-110.43	-105.78	-110.01
<b>58</b>	-80.27	-	-	-	-69.48	-	-69.76	-70.28	-74.03	-76.27
<b>59</b>	-109.18	-	-102.89	-105.25	-92.31	-	-92.93	-91.03	-93.09	-96.34

<sup>a</sup> The following abbreviations have been used: "RHF-1" = RHF/3-21G//RHF/3-21G; "RHF-2" = RHF/MIDI//RHF/MIDI; "B3LYP-1" = B3LYP/6-31G(d)//B3LYP/6-31G(d); "B3LYP-2" = B3LYP/6-311+G(d,p)//B3LYP/6-31G(d); "MP2-1" = MP2(FC)/6-31G(d)//RHF/3-21G; "MP2-2" = MP2(FC)/6-31G(d)//RHF/MIDI; "MP2-3" = MP2(FC)/6-31G(d)//MP2(FC)/6-31G(d); "MP2-4" = MP2(FC)/6-311+G(d,p)//MP2(FC)/6-31G(d); "MP2-5" = SCS-MP2(FC)/6-311+G(d,p)//MP2(FC)/6-31G(d); "RHF-4" = RHF/6-311+G(d,p)//MP2/6-31G(d).

Turning to the results obtained for catalysts **55** – **59** we note that the two “ $\pi$ -stacking” catalysts **55** and **57** give particularly stable acetyl intermediates. The actual stability values for these two systems depend much more on the computational level than those for all other systems. Concentrating on the results obtained at the SCS-MP2(FC)/6-311+G(d,p)//MP2(FC)/6-31G(d) level (“MP2-5”), the most stable acetyl intermediate is formed by catalyst **55** (–120.9 kJ/mol). The magnitude of the correlation contribution to this reaction energy of 30.0 kJ/mol (obtained as the difference between SCS-MP2(FC)/6-311+G(d,p)//MP2(FC)/6-31G(d) and RHF/6-311+G(d,p)//MP2(FC)/6-31G(d) energies) is in clear support of strong dispersion interactions<sup>121</sup> between the naphthalene side chain and the pyridinium ring system in **55Ac**.

The involvement of  $\pi$ -stacking interactions in acyl intermediates of catalyst **57** can be assessed through comparison to catalyst **56**, whose acetyl intermediates differ in stability by 20.4 kJ/mol. To equate this difference to the magnitude of dispersion interactions is, however, not correct considering the stability difference between **56** and **57** of 20.0 kJ/mol predicted at RHF/6-311+G(d,p)//MP2(FC)/6-31G(d) level. The absence of a notable correlation effect on the stabilization energies together with the structural characteristics for the acetyl intermediate **57Ac-1** noted above suggests that the higher stabilization energy of **57Ac** as compared to **56Ac** is mainly due to electrostatic effects between the acetyl group and the side chain. Stacking interactions appear not to play a prominent role in catalysts **58** and **59**. In catalyst **58** the balance between the inductive electron-withdrawing power of the acyl substituent at C3 of the pyridine ring and the stacking interactions between the thiocarbonyl group and the pyridine ring in its cationic form appear to result in net destabilization compared to DMAP **27**. That dispersion interactions are indeed not decisive for the stabilization of **58Ac** relative to **58** is also reflected in a negative correlation contribution of –2.2 kJ/mol for this system. In catalyst **59** this is certainly due to the rigid  $\sigma$ -bond framework preventing the large-scale conformational rearrangement described in Scheme 5.1, but inductive substituent effects appear to be sufficiently large to make the acetyl intermediate **59Ac** quite stable even in the absence of stacking interactions. With respect to the general reaction scheme described in Scheme 5.1 we may expect catalysts **55**, **56**, **57**, and **59** to be more reactive than DMAP (**27**) at ambient temperature or above since their acetyl intermediates are more stable than that of DMAP.

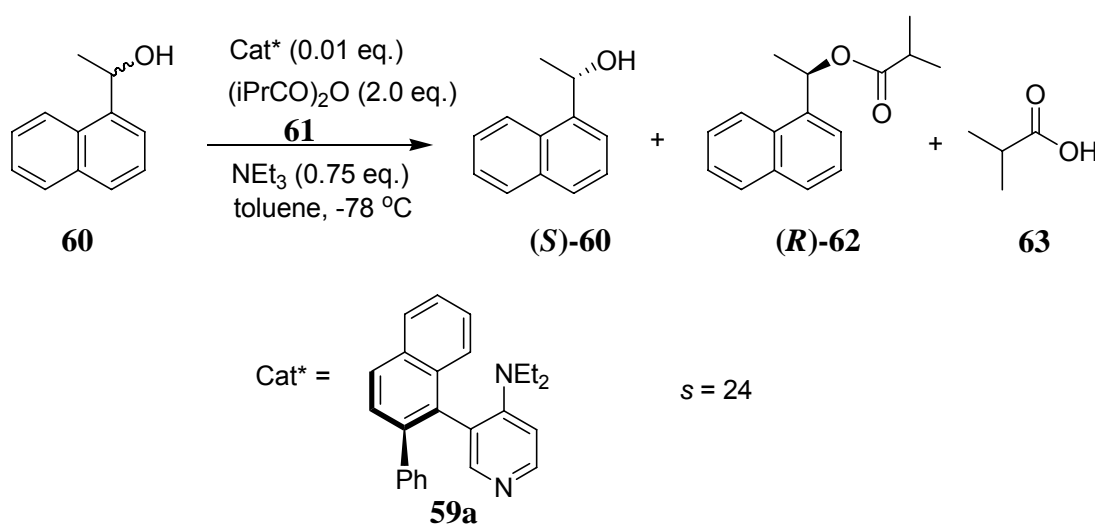
## 5.5 Conclusions

The conformational preferences of catalysts **55** – **59** studied at the SCS-MP2(FC)/6-311+G(d,p)//MP2(FC)/6-31G(d) level are in line with the limited existing experimental data available for these systems. Stacking conformations dominate the appearance of the acetylpyridinium intermediates of catalysts **55**, **57**, and **58**. Dispersion interactions are mainly responsible for this situation in **55Ac**, while electrostatic effects dominate in **57Ac**. The conformational preferences of the acetyl intermediates of **58** and **59** are mainly enforced by the rigidity of the  $\sigma$ -framework, leading to a stacking conformation in **58Ac** and a non-stacking conformation in **59Ac**. Large conformational changes still occur in both of these latter systems on formation of the acetyl intermediate, supporting the “conformational switch” picture derived from experimental  $^1\text{H}$  NMR studies. In methodological terms we have shown that studies of the acetyl intermediates of catalysts **55** – **59** require correlated levels, the MP2(FC)/6-31G(d)//RHF/3-21G level providing a reasonable lower limit of effort. DFT methods such as the popular B3LYP hybrid functional are not able to describe stacking interactions induced through dispersion interactions properly.

## 6. Optimal Selectivity of Chiral Analogues of 4-(Dimethylamino)Pyridine for Nonenzymatic Enantioselective Acylations: a Theoretical Investigation

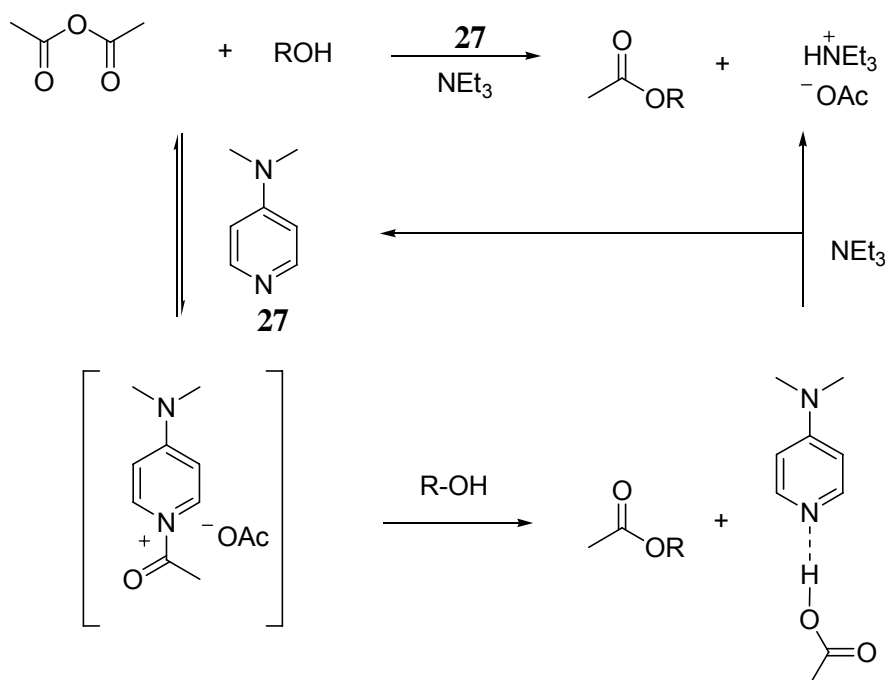
### 6.1 Introduction

Organocatalysis has been at the forefront of research in organic chemistry in recent years, and one of the most studied fields concerns acyl group transfer reactions mediated by chiral catalysts. Chiral catalysts based on amine and phosphine structural motifs have been designed and synthesized for kinetic resolution (KR) of alcohols and related stereoselective transformations.<sup>7,127</sup> Chiral dimethylamino-pyridine (DMAP) catalysts have been demonstrated to be good catalysts for enantioselective acyl-transfer reactions by Vedejs,<sup>115,128</sup> Fuji,<sup>16,17</sup> Fu,<sup>8,129</sup> and Spivey.<sup>23,130</sup> Spivey's group<sup>130</sup> has developed a series of axially chiral, atropisomeric derivatives of 4-dialkylaminopyridines as catalysts for the KR of racemic *sec*-alcohols. KR experiments proceeded using racemic 1-(1-naphthyl)-ethanol **60** as the substrate and isobutyric anhydride **61** as acyl donor (see Scheme 6.1) in the presence of the enantiomerically pure biaryl catalyst **59a**. The alcohol (*R*)-**60** reacts faster than the alcohol (*S*)-**60** with **61** to produce ester (*R*)-**62** and carboxylic acid **63** using the catalyst **59a**, and the selectivity factor (*s*) of 24 was obtained at -78 °C. In the similar manner, KR experiments were performed using a series of atropisomeric derivatives with various 4-dialkylamino groups. They found that the selectivities of these catalysts are dependent on the nature of the 4-dialkylamino group, but have not offered an explanation on why this is so. Spivey's findings have motivated us to perform theoretical investigations for better understanding the acylation reaction of racemic alcohols and the factors influencing the selectivities of these catalysts.



Scheme 6.1.

The mechanisms of DMAP-catalyzed acetylation of alcohols have been investigated theoretically in detail by Zipse's group.<sup>10</sup> The currently accepted consensus mechanism for acylation reactions of alcohols is described in Scheme 6.2, which involves the preequilibrium formation of an acylpyridinium cation, and then its reaction with the alcohol in the rate-determining second step to form the ester product with the protonated catalyst, and finally regeneration of the activated catalyst with an auxiliary base. An alternative mechanism is the deprotonation of the alcohol by catalyst and subsequent attack of the alkoxide at the acyl donor; however, previous DFT calculations show that it is much less favorable.<sup>10</sup> Whether this finding persists for the acylation of racemic secondary alcohols is still a question, therefore, we investigate the mechanism carefully again using Spivey's catalyst **59a** and *sec*-alcohol **60**.



**Scheme 6.2.**

In order to shed light on the enantioselectivities of chiral DMAP-catalysts for acyl-transfer reactions, we have investigated theoretically the acylation of racemic secondary alcohols by a series of Spivey's catalysts and substrates in detail. The most important question we concern is whether the enantioselectivities of chiral DMAP-catalyzed acyl-transfer reactions can be rationalized with the transition state in the rate-determining step that is also considered as the selectivity-determining step. The possible role of 4-dialkylamino substituents on the chiral transformation is discussed and a catalyst modification to improve the enantioselectivity is suggested.

## 6.2 Nucleophilic Catalysis vs. Base Catalysis

In order to check whether the commonly accepted mechanism persists, we have first investigated the nucleophilic and general base catalysis pathways for the reaction of racemic 1-(1-naphthyl)ethanol (**60**) with isobutyric anhydride (**61**) catalyzed by **59a** at the B3LYP/6-311+G(d,p)//B3LYP/6-31G(d) level of theory used in the previous theoretical studies of DMAP-catalyzed acetylation of alcohols.<sup>10</sup> All conformers of reactants **60** and **61**, and products **62** and **63** have been searched carefully and optimized at B3LYP/6-31G(d) level and obtained the relative enthalpies at the B3LYP/6-311+G(d,p)//B3LYP/6-31G(d) level of theory. The conformational spaces of the transition states (TSs) along the nucleophilic catalysis pathway were searched by modified OPLS-AA force field and then the identified conformers were reoptimized at B3LYP/6-31G(d) level in order to obtain the relative enthalpies at the B3LYP/6-311+G(d,p)//B3LYP/6-31G(d) level of theory. The IRC calculations have been run using the best conformer of TS to obtain the reactant complex, intermediate, and product complex. The TSs along the base-catalyzed pathway were located based on the previously suggested “four-membered” and “six-membered” structures<sup>10</sup> and optimized at B3LYP/6-31G(d) level. Using these structures the relative enthalpies at the B3LYP/6-311+G(d,p)//B3LYP/6-31G(d) level of theory have been calculated. The nucleophilic and general base catalysis pathways are plotted in Figure 6.1 by using the lowest-energy conformer and the relative enthalpies for stationary points located on the potential energy surface are shown in Table 6.1. The diastereomeric transition states and intermediates are denoted as (*R*)-\* and (*S*)-\*, which represent the corresponding configuration of the involved alcohol.

The reaction is initiated through formation of a ternary complex **64** of reactants **60**, **61** and catalyst **59a** for both the nucleophilic and general base catalysis pathway. Along the nucleophilic catalysis pathway, the reactant complex **64** passes through the first TS **65** to yield intermediates **66**, which then pass through the second TS **67** with concomitant proton transfer to product complex **68**. The alternative base-catalyzed reaction pathway proceeds through concerted TSs **69** to product complex **68** in one single step. The diastereomers including R-configuration alcohol are always a few kJ/mol lower than those including S-configuration alcohol. The most energetically favorable transition state (*R*)-**69** along the base catalysis pathway is located 40 kJ/mol or so above the transition state (*R*)-**65** and 53 kJ/mol or so above the transition state (*R*)-**67**. Single point calculations have also been done at the MP2/6-31G(d)//B3LYP/6-31G(d) level of theory for the best conformers of (*R*)-**65**, (*R*)-**67**, (*R*)-**69**. The energy of (*R*)-**69** is also higher than that of (*R*)-**65** and (*R*)-**67** by more than 30

kJ/mol at MP2/6-31G(d)//B3LYP/6-31G(d) level. This indicates that the nucleophilic catalysis pathway is more favorable than the general base catalysis pathway, which is in line with Zipse group's previous finding on DMAP-catalyzed reaction of acetic anhydride and *tert*-butanol.

**Table 6.1.** Relative Enthalpies (in kJ/mol) for Stationary Points Located on the Potential Energy Surface at B3LYP/6-311+G(d, p)//B3LYP/6-31G(d) Level.

$\Delta H_{298}$ (gas phase)	
Nucleophilic catalysis	
<b>59a+60+61</b>	0.00
<b>(R)-64</b> (reactant complex)	-22.98
<b>(S)-64</b> (reactant complex)	-22.54
<b>(R)-65</b> (first TS)	26.80
<b>(S)-65</b> (first TS)	34.29
<b>(R)-66</b> (intermediate)	7.56
<b>(S)-66</b> (intermediate)	11.72
<b>(R)-67</b> (second TS)	14.06
<b>(S)-67</b> (second TS)	20.10
<b>(R)-68</b> (product complex)	-87.35
<b>(S)-68</b> (product complex)	-86.87
<b>59a+(R)-62 +63</b>	-21.61
Base catalysis (concerted)	
<b>59a+60+61</b>	0.00
<b>(R)-64</b> (reactant complex)	-22.98
<b>(S)-64</b> (reactant complex)	-22.54
<b>(R)-69</b> (TS)	67.23
<b>(S)-69</b> (TS)	77.49
<b>(R)-68</b> (product complex)	-87.35
<b>(S)-68</b> (product complex)	-86.87
<b>59a+(R)-62+63</b>	-21.61

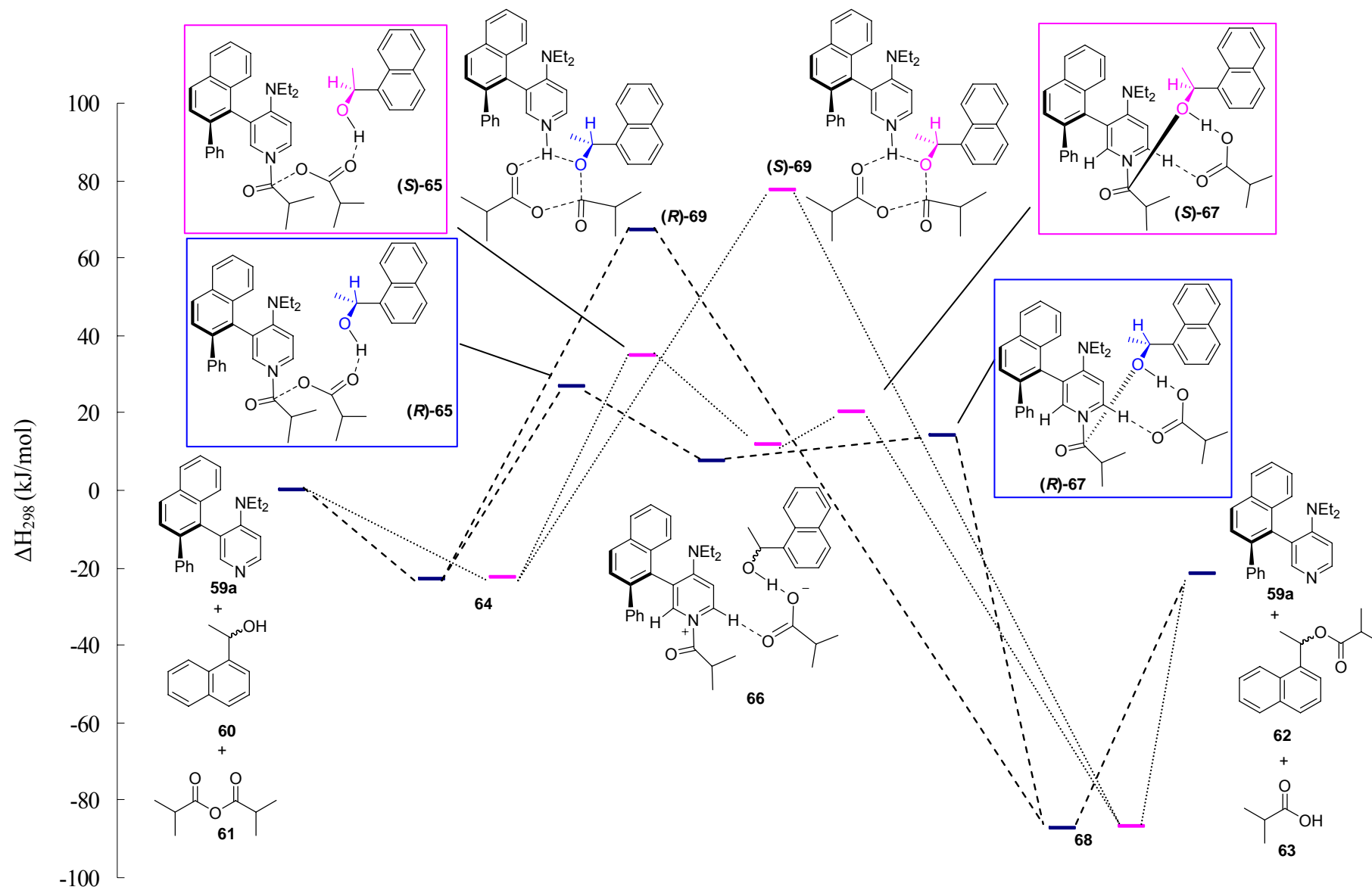


**Figure 6.1.** Gas Phase Enthalpy Profile ( $\Delta H_{298}$ ) Calculated at the B3LYP/6-311+G(d,p)//B3LYP/6-31G(d) Level of Theory.

### 6.3 Reaction Barriers and Conformational Space of TSs

The energy difference between the diastereomeric TSs of the rate-determining step is the key point to predict the enantioselectivity. Thus, the enthalpy profile including TSs and intermediates along the nucleophilic catalysis pathway shown in Figure 6.1 is chosen particularly to put in Figure 6.2 in order to discuss the reaction barriers and the conformational space of TSs in detail.

The systems investigated here are very flexible and have a large conformational space. A systematic conformational search of TSs **65** and **67** was first done using a modified OPLS-AA force field, and then the conformers identified by force field within the energy window of 40 kJ/mol were reoptimized at the B3LYP/6-31G(d) level of theory, and single point calculations were done at the B3LYP/6-311+G(d, p) level of theory. Figure 6.2 shows a pictorial representation of the relative energies of all conformers of transition states **65** and **67**.

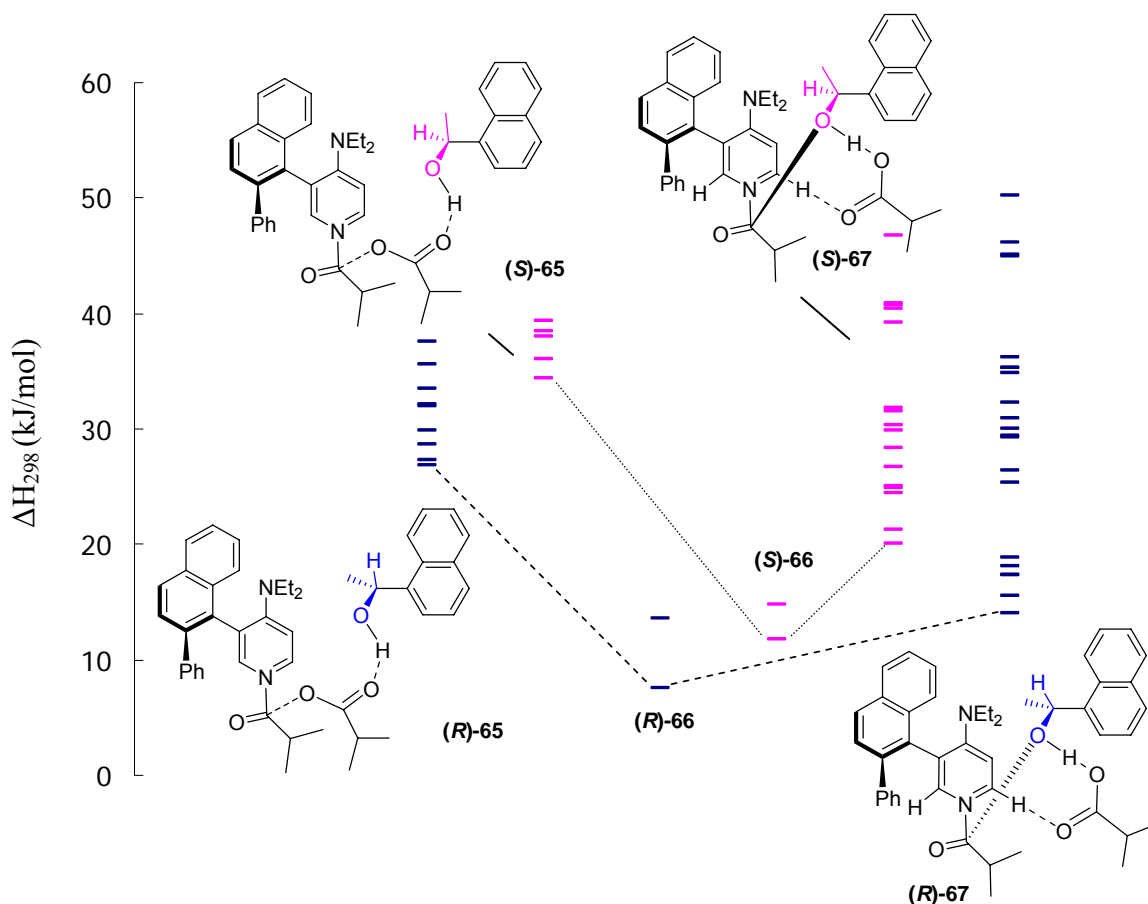


**Figure 6.2.** Relative Energies (Relative to the Best Conformers of **59a+60+61**) of All Conformers of Transition States **65** and **67** and the Intermediate **66** at B3LYP/6-311+G(d, p)//B3LYP/6-31G(d) Level.

Surprisingly, the energy of first TS **65** in the formation of an acylpyridinium cation is higher than that of the second step commonly considered as the rate-determining step by 13 kJ/mol or so at B3LYP/6-311+G(d,p)//B3LYP/6-31G(d) level. In order to see whether this observation also persists by other theoretical methods, we chose several other theoretical methods to do single point calculations again based on the optimized B3LYP/6-31G(d) structures. The DFT methods with dispersion corrections (DFT-D) and MP2 methods are chosen because we assume that the dispersion interactions may exist and play some roles due to the system studied here including several aromatic rings, however, the popular B3LYP functional cannot predict this type of interaction accurately. The single point calculations were done at different theoretical levels of theories for conformers whose populations are more than 1% at B3LYP/6-311+G(d,p)//B3LYP/6-31G(d) level. The relative Boltzman-averaged enthalpies between (**R**)-**65** and (**R**)-**67** at different levels of theories are investigated carefully and compared (see Figure 6.3). In order to avoid the basis set superposition error (BSSE), the relative enthalpies are calculated with respect to the reactant complex instead of the separated reactants.

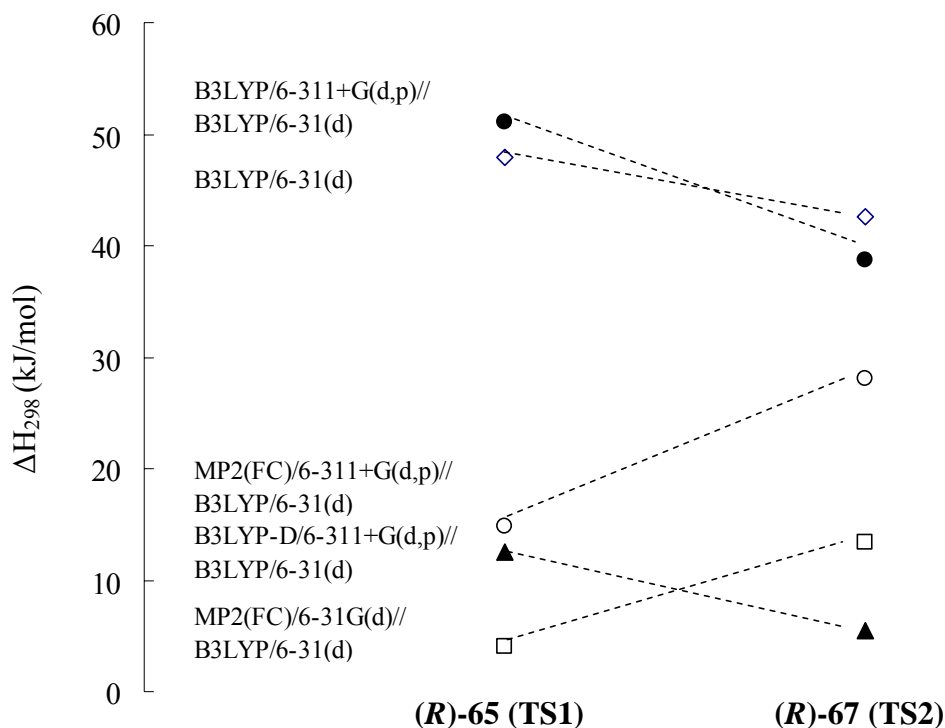


**Figure 6.3.** Relative Energies of (**R**)-**65** and (**R**)-**67** with Respect to the Reactant Complex at Different Levels of Theories.

The energy difference between (*R*)-**65** and (*R*)-**67** varies with theoretical methods, the variation is in the range of -14 kJ/mol and +14 kJ/mol. Thus, different theoretical methods predict different rate-determining steps using the same model system. At this point, it is hard to pin down which method is more reliable without higher level theoretical benchmark data that are too difficult to get for such a big system. MP2 results seem more basis sets dependent and they are much more computationally costly than DFT methods for the system studied here. We will use the economic DFT methods B3LYP/6-311+G(d,p)//B3LYP/6-31G(d) and B3LYP-D/6-311+G(d,p)//B3LYP/6-31G(d) to calculate the catalytic selectivity in section 6.4 and to see which calculated results are in line with Spivey's experimental results.

In principle, the rate-determining step is also considered to be the selectivity-determining step. Thus, it is difficult to predict which step is the selectivity-determining step due to the uncertainty of rate-determining step described above. We have tried to calculate the free energy difference of diastereomers in these two steps to match the experimental value (see Table A9.6.1 in Appendix). It turns out that the free energy difference of the diastereomers of TS **67** is closer to experimental values. The detailed theoretical prediction of catalytic selectivity is discussed in the section 6.4. We focus our attention here on the structures and the energy difference of the diastereomers of TS **67** to investigate the possible factors influencing the stereoselectivity of catalyst **59a**.

Through analysis of the optimized geometries of transition state **67**, we found that all conformers can be classified into the four types shown in Scheme 6.3. Figure 6.4 shows a pictorial representation of the relative energies of the conformers of (*R*)-**67** and (*S*)-**67**, respectively. Generally speaking, the carboxylate group is bonded to the left or right side of the pyridine ring by weak hydrogen bonding and the alcohol approaches the reaction center either from the front face or the back face of the pyridine ring. Type **67-I** shows that the carboxylate group is bonded to the right side of the pyridine ring and the alcohol approaches the reaction center from the back side. For this type the conformers with R-configuration alcohol are more stable than the conformer with S-configuration alcohols by more than 20 kJ/mol. In type **67-II** and **67-III**, the conformers with S-configuration alcohol are more stable than the conformers with R-configuration alcohol. Conformers in type **67-IV** have poor stabilities, no matter including either R-configuration or S-configuration alcohol. The most stable conformer with R-configuration alcohol belongs to the type **67-I**, which is more stable than the most stable conformer with S-configuration alcohol classified into the type **67-III** by 6.1 kJ/mol.

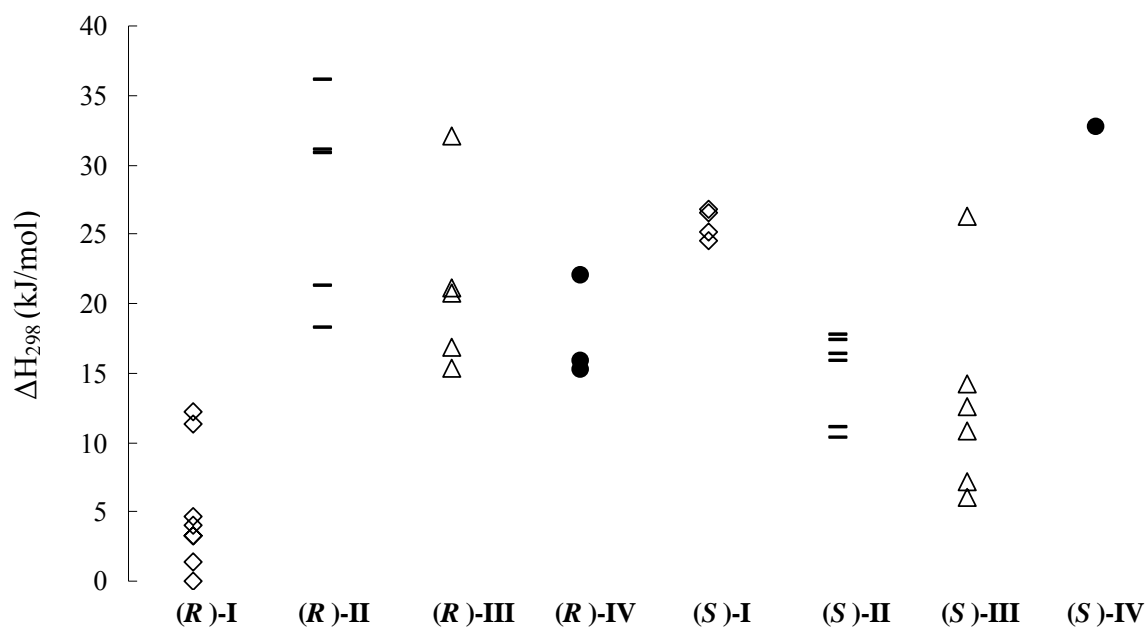
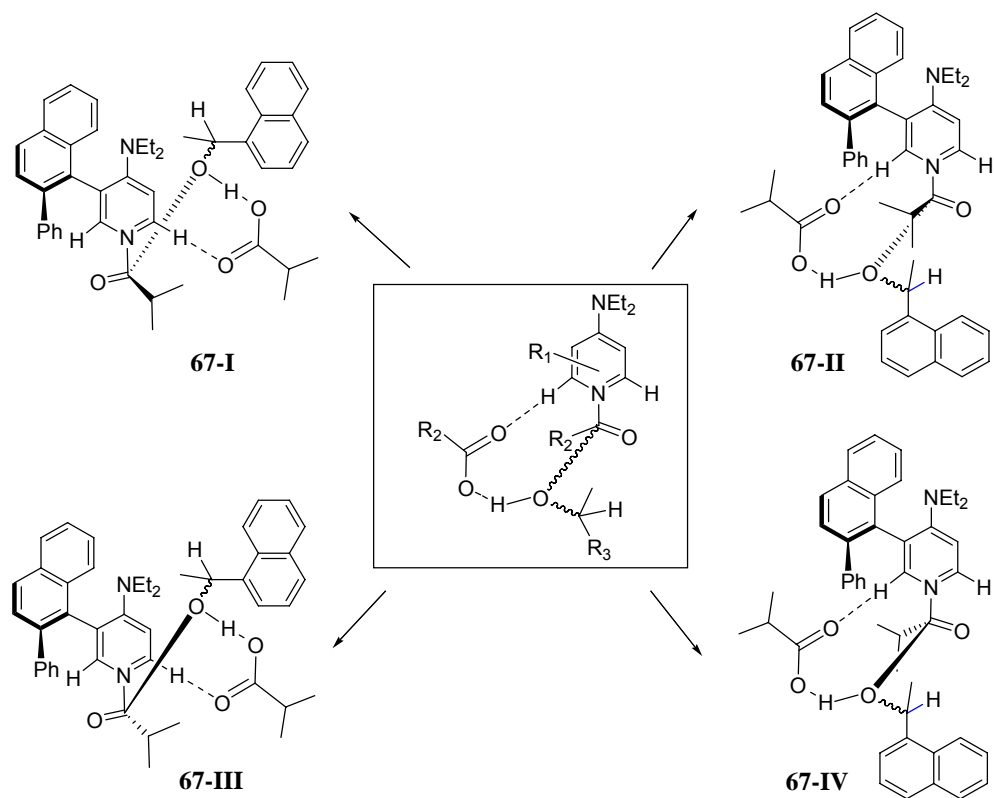
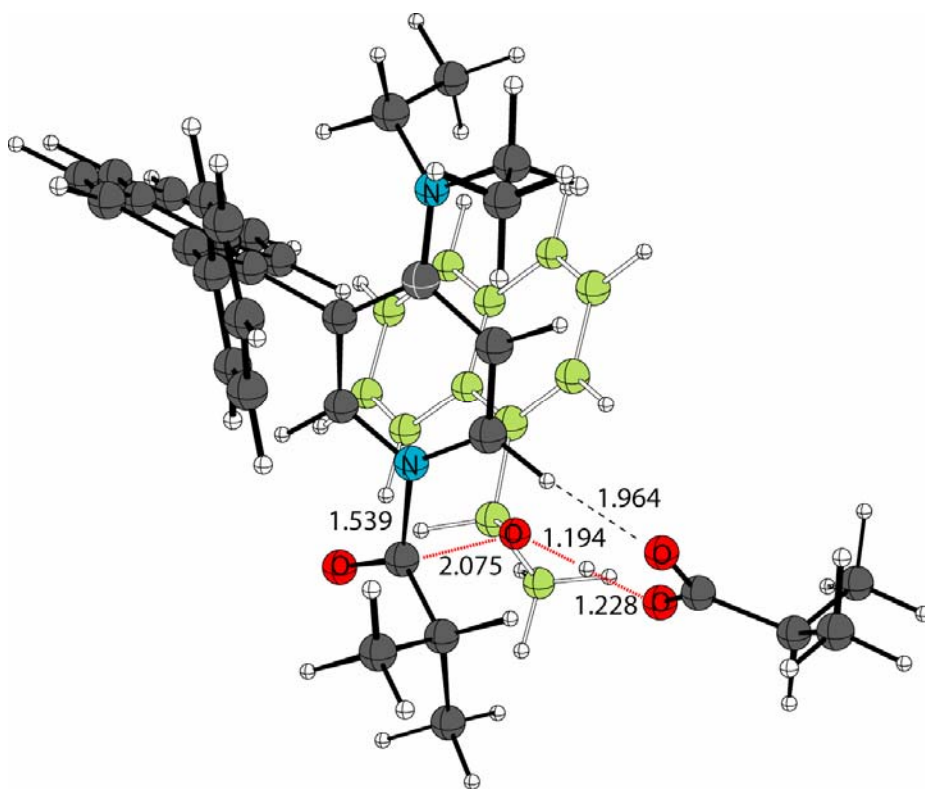
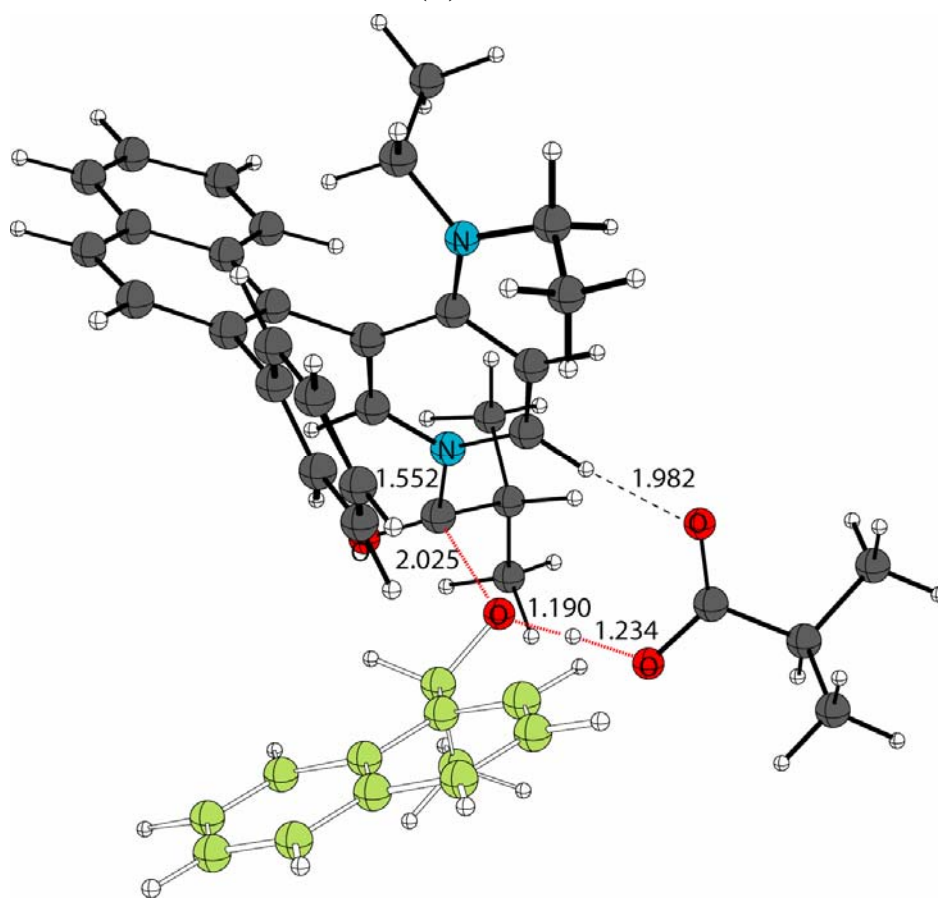


**Figure 6.4.** Relative Energies (kJ/mol) of Conformers of TS **67**.

The B3LYP/6-31G(d) optimized structures of the most stable conformers of (*R*)-**67** and (*S*)-**67** are shown in Figure 6.5. Analysis of the structures reveals that the alcohol **60** (shown by light green color in Figure 6.5) approaches the reaction center from the back face of the pyridine ring in (*R*)-**67** and the front face of the pyridine ring in (*S*)-**67**. There is no significant steric hindrance when alcohol approaches the reaction center from the back face of the pyridine in (*R*)-**67**. In contrast, alcohol approaching the reaction center from the front face of the pyridine in (*S*)-**67**, the steric repulsion between the tilted phenyl ring of the catalyst **59a** and the naphthyl ring of alcohol **60** may lead to the energy of (*S*)-**67** higher than that of (*R*)-**67** by 6 kJ/mol or so.



**(R)-67**



**(S)-67**

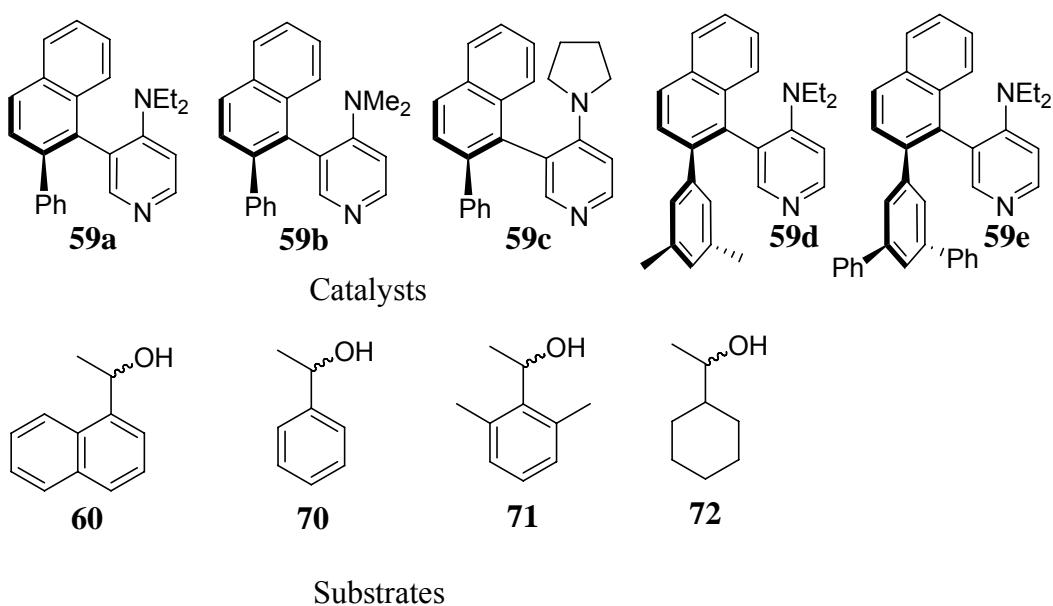
**Figure 6.5.** The Most Stable Conformer of **(R)-67** and **(S)-67** at the B3LYP/6-311+G(d,p)//B3LYP/6-31G(d) Level of Theory.

#### 6.4 Theoretical Prediction of Selectivity and a Modification of Catalyst

Spivey *et al.* have reported that varying the 4-dialkylamino substituents influence the selectivities of catalysts, however, there is no clear correlation between the selectivity of catalyst and the steric bulk or chain length of alkyl groups. We choose a series of catalysts **59a** - **59c** (shown in Scheme 6.4) and use the same substrate **60** to investigate their selectivity theoretically and compare them with experimental results. The experimental selectivity factors (*s*) of catalysts **59a** - **59c** and transformed free energy difference ( $\Delta G_{195,\text{exp}}$ ) are collected in the first column of Table 6.2. The relation formula between selectivity factors (*s*) and transformed free energy difference is shown as follows.

$$\text{Selectivity factor } s = \frac{k_r}{k_s} \quad (6.1)$$

$$\ln s = \ln \left( \frac{k_r}{k_s} \right) = -\frac{\Delta\Delta G^\ddagger}{RT} = -\frac{\Delta G_r^\ddagger - \Delta G_s^\ddagger}{RT} = \frac{G_s^{\text{TS}} - G_r^{\text{TS}}}{RT} = \frac{\Delta G^{\text{TS}}}{RT} \quad (6.2)$$



**Scheme 6.4.** Catalysts and Substrates Used to Model Kinetic Resolution of *sec*-Alcohols.

The enthalpy and free energy difference between the diastereomers of the TS **67** considered as the selectivity-determining TS for **59a**, **59b**, **59c** were calculated by DFT methods and also listed in Table 6.2. The conformational space of TS **67** for **59b** and **59c** were also searched in the similar way as for catalyst **59a** by modified OPLS-AA force field and then the identified conformers were reoptimized at B3LYP/6-31G(d) level. Experimental results show that the pyrrolidino-substituted catalyst **59c** is the least selective catalyst and the 4-dimethylaminopyridine based catalyst **59b** and 4-diethylaminopyridine based catalyst **59a**

have better selectivity. The enthalpy differences  $\Delta H_{298}$  for the TS **67** of catalysts **59a** - **59c** calculated at B3LYP/6-311+G(d,p)//B3LYP/6-31G(d) level have no significant difference, and cannot reflect the experimental trends of  $\Delta G_{195,\text{exp}}$ . The calculated free energy differences  $\Delta G_{298}$  for the TS of catalysts **59a** - **59c** calculated at the same level theory cannot reproduce experimental results either and even predict the opposite result that the pyrrolidino-substituted catalyst **59c** should have higher selectivity than **59a** and **59b**. If we obtain  $\Delta S_{298}$  by formula 6.3 and we assume that the  $\Delta H_{298}$  and  $\Delta S_{298}$  approximately have the same value as  $\Delta H_{195}$  and  $\Delta S_{195}$ , respectively, we get  $\Delta G_{195}$  by formula 6.4. The free energy difference  $\Delta G_{195}$  estimated at experimental temperature (195 K) does not improve theoretical results either.

$$\Delta S_{298} = \frac{\Delta H_{298} - \Delta G_{298}}{298} \quad (6.3)$$

$$\Delta G_{195} = \Delta H_{195} - 195 * \Delta S_{195} \quad (6.4)$$

**Table 6.2.** Comparison of Experimental and Calculated Energy Difference (in kJ/mol) for the Diastereomers of TS **67** for Catalysts **59a** - **59c**.

Cat.	Experimental (195 K) <sup>a</sup>		Theoretical <sup>b</sup>				Theoretical <sup>c</sup>			
	<i>s</i>	$\Delta G_{195,\text{exp}}$	<i>s</i>	$\Delta G_{195}$	$\Delta G_{298}$	$\Delta H_{298}$	<i>s</i>	$\Delta G_{195}$	$\Delta G_{298}$	$\Delta H_{298}$
<b>59a</b>	24	5.16	36	5.82	5.65	6.13	15.9	4.48	6.09	1.42
<b>59b</b>	10	3.74	35	5.78	5.60	6.12	2.5	1.51	1.60	1.34
<b>59c</b>	3.5	2.03	150	8.12	9.38	5.73	4.8	2.55	4.03	-0.26

<sup>a</sup> *s* values are taken from experimental results and temperature is 195 K, and  $\Delta G_{195,\text{exp}}$  is obtained based on equation (6.2); <sup>b</sup> B3LYP/6-311+G(d,p)//B3LYP/6-31G(d), Boltzmann-weighted average; <sup>c</sup> B3LYP-D/6-311+G(d,p)//B3LYP/6-31G(d), Boltzmann-weighted average.

The thermal corrections recalculated at 195 K do not improve the results (see Table A9.6.2 in Appendix). After addition of dispersion corrections, the enthalpy differences  $\Delta H_{298}$  for the TS of catalysts **59a** - **59c** are significantly smaller, but both free energy difference  $\Delta G_{298}$  and  $\Delta G_{195}$  cannot reproduce the experimental results. Failure to reproduce experimental results leads us to doubt whether we find the right TS models or we cannot calculate free energy accurately although the TS models are chosen correctly. If the free energy differences of TS **67** used above cannot be correlated to experimental results correctly, the free energy differences of TS **65** or intermediate **66** might be correlated to experimental results correctly. Thus, we chose catalyst **59a** and substrate **60** to investigate their free energy differences of TS **65** or intermediate **66**. Disappointingly, they are not able to be correlated with

experimental results correctly either (see Table 9.6.1 in Appendix). The experimental results show that the free energy differences  $\Delta G_{195,\text{exp}}$  for different catalysts are less than 4 kJ/mol, which indicates the influence of 4-dialkylamino substituents to the selectivity is not so dramatic and makes the theoretical predictions very difficult. The possible reason for deviation of theoretical results from experimental results could be that the 4-dialkylamino substituents are far away from the reaction center and variation of 4-dialkylamino substituents mainly induces entropy variations, which are small values; because the structural changes of catalysts are just variations of 4-dialkylamino groups from restricted pyrrolidino ring to more flexible alkyl chains. Unfortunately, it is a challenge to evaluate the entropy change accurately by commonly used theoretical methods.

Further we did theoretical selectivity predictions for one catalyst **59a** with various substrates **60**, **70-72** shown in Scheme 6.4, which leads to the changes near the reaction center. In order to save computational costs, we just use the best conformers obtained at the B3LYP/6-311+G(d,p)//B3LYP/6-31G(d) level of theory to predict the free energy difference of TS (**R**)-**67** and (**S**)-**67** for the catalyst **59a** instead of using Boltzman-averaged values of all conformers. The enthalpy difference  $\Delta H_{298}$  only varies by 0.2 kJ/mol from using the enthalpy of one best conformer to using the average enthalpies of all of conformers (see Figure 6.6). Thus, using one best conformer's enthalpy will not lose the calculation accuracy significantly. The variation of substrates is assumed not to change the conformational space of TS **67** dramatically shown in Figure 6.4. We use the best conformers of TS type (**R**)-**67-I** and (**S**)-**67-III** with substrate **60** as our TS template to get the new TS with other substrates. We keep the main part of (**R**)-**67-I** and (**S**)-**67-III** and just vary the substrate part to build the initial input structure, and then reoptimize the structure to obtain the TSs (**R**)-**67** and (**S**)-**67** with a series of substrates. The free energy and enthalpy difference of TS (**R**)-**67** and (**S**)-**67** for the catalyst **59a** with a series of substrates are calculated at B3LYP/6-311+G(d,p)//B3LYP/6-31G(d) level and compiled in Table 6.3. Inspection of Table 6.3 reveals that the calculated enthalpy differences  $\Delta H_{298}$  have the same trend as the experimental results; however, the calculated free energy differences are not fully in line with the experimental results. Figure 6.7 shows clearly that the  $\Delta H_{298}$  is moderately correlated to  $\Delta G_{195,\text{exp}}$ , which supports our suggested TS models are appropriate for modelling the changes near the reaction center. The TS models we found may be used as templates to predict the potential selectivity of new catalysts if we modify some part of catalyst near the reaction center.

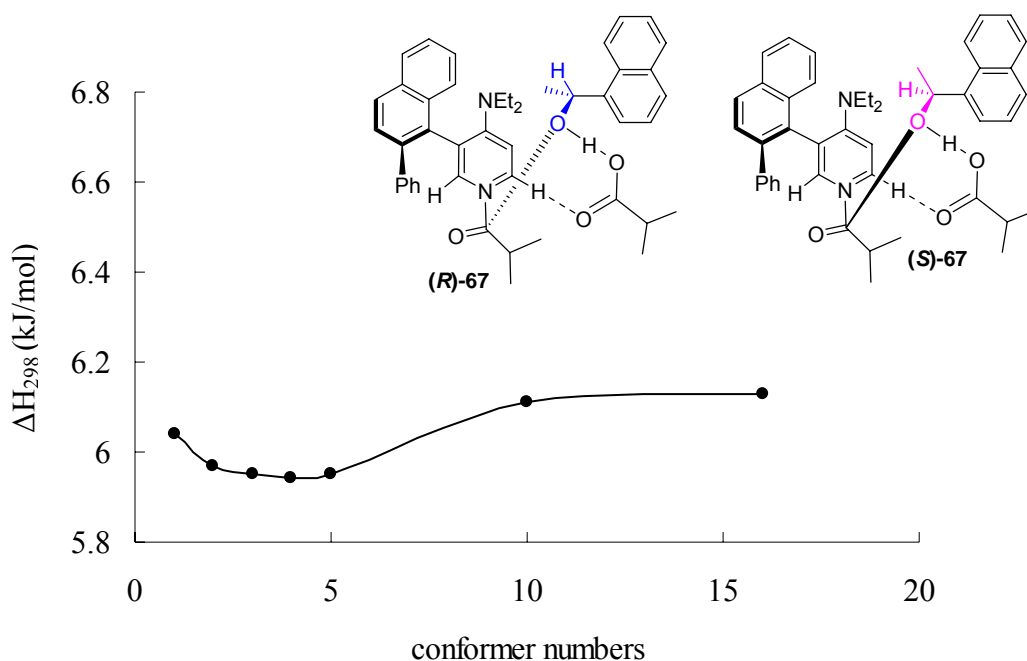


**Figure 6.6.** The Number of Conformers Required to Calculate Accurate Energy Difference.

**Table 6.3.** Comparison of Experimental and Calculated Energy Difference (in kJ/mol) for the Diastereomers of TS **67** for Catalysts **59a – 59d** and Substrates **60, 70 – 72**.<sup>a</sup>

Cat.	Sub.	Experimental (195 K)		TS ( <b>67</b> )			
		<i>s</i>	$\Delta G_{195,exp}$	<i>s</i>	$\Delta G_{195}$	$\Delta G_{298}$	$\Delta H_{298}$
<b>59a</b>	<b>60</b>	24	5.16	23.5	5.12	4.63	6.04
<b>59b</b>	<b>60</b>	10	3.74	35.3	5.78	5.60	6.12
<b>59c</b>	<b>60</b>	3.5	2.03	149.7	8.12	9.38	5.73
<b>59d</b>	<b>60</b>	-	-	1808.9 (118 <sup>b</sup> )	12.16 (7.74 <sup>b</sup> )	13.23	10.13
<b>59a</b>	<b>60</b>	24	5.16	23.5	5.12	4.63	6.04
<b>59a</b>	<b>70</b>	13	4.16	248.2	8.94	11.88	3.38
<b>59a</b>	<b>71</b>	25	5.22	27.1	5.35	5.26	5.51
<b>59a</b>	<b>72</b>	8.4	3.45	4.42	2.41	2.15	2.91

<sup>a</sup> Using the best conformers of (**R**)-**67-I** and (**S**)-**67-III**; <sup>b</sup>  $\Delta G_{195,exp}$  obtained through the equation  $\Delta H_{298} = 1.7465 * \Delta G_{195,exp} - 3.3948$ , and then transformed to selectivity factor.

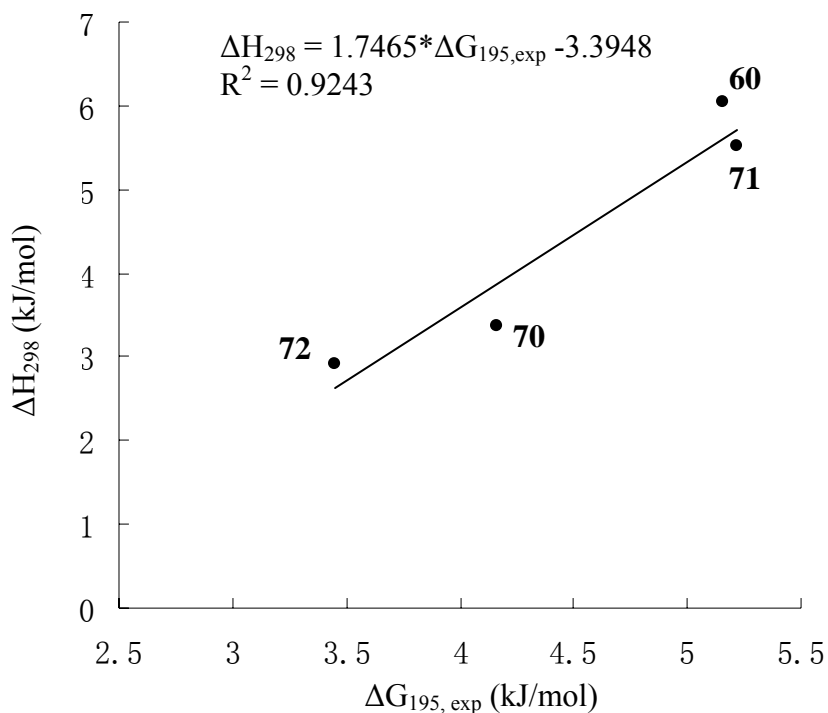


**Figure 6.7.** Correlation between Experimental and Calculated Energies for the Enantioselectivity.

Based on our TS models, the attached blocking groups on the phenyl ring of catalysts can block the alcohols to approach the reaction center from the front face of pyridine ring, which is the favorite position for S-configuration alcohol to approach the reaction center, thus the reaction rate of S-configuration alcohol is much slower, and results in higher enantioselectivity. Thus, we suggest adding groups such as methyl groups on the tilted phenyl group as “blocking groups” to make new catalyst **59d** shown in Scheme 6.4, and it may improve catalytic selectivity. Inspection of our TS conformational space shown in Figure 6.4 reveals that the (*R*)-**67-I** type TS wins a lot by energy than other types of TS, therefore we just investigated the best conformer of this type of TS for TSs involving R-configuration alcohols. We reoptimized the new TS by using the conformer identified previously and replaced the catalyst part by new catalyst **59d**. However, for TSs involving S-configuration alcohols the most stable TS type (*S*)-**67-III** with catalyst **59a** may not be the most stable one with catalyst **59d** due to the steric hindrance, and the (*S*)-**II** type of TS may become the most stable type because this type of TS is only 5 kJ/mol or so above (*S*)-**67-III**. Thus the best conformers of both (*S*)-**67-III** and (*S*)-**67-II** types were investigated with catalyst **59d** to avoid overlooking an important conformer. In this case, the (*S*)-**67-II** type TS

is more stable than **(S)-67-III** type TS. Then, we calculated the total energy difference  $\Delta E_{\text{tot}}$ , enthalpy difference  $\Delta H_{298}$ , free energy difference  $\Delta G_{298}$  between **(R)-67-I** and **(S)-67-II** with new catalyst **59d**, and obtained the extrapolated  $\Delta G_{195,\text{exp}}$  based on their correlation equation obtained above, and the selectivity factor is  $s = 118$  (see Table 6.3), which indicates the catalyst **59d** with potential high selectivity. Recently, experimental results of Spivey's group gave some evidences for this. They synthesized a new catalyst in which phenyl groups were added on the tilted phenyl group as "blocking groups" to get catalyst **59e** (shown in Scheme 6.4). Their results have shown the catalytic selectivity factor of the new catalyst can be improved to  $s = 39$ , however, the reaction rate is lower by a factor of 2 as compared to the catalyst **59a**. The phenyl "blocking" groups in catalyst **59e** maybe too big and hinder the alcohol to approach the reaction center, which leads to its low reactivity. In our suggested catalyst **59d**, the methyl "blocking" groups are rather small. Thus, it may improve the catalytic selectivity and keep high catalytic activity simultaneously.

## 6.5 Conclusions

Similar to the acylation reactions with achiral catalysts, the commonly accepted nucleophilic mechanism is more favorable than the general base mechanism for the reaction of racemic 1-(1-naphthyl)ethanol (**60**) with isobutyric anhydride (**61**). The identified TS models in the selectivity-determining step reveal that alcohols with different configuration prefer different directions to approach the reaction center. The key TS model is helpful for catalyst design, thus a new catalyst with potential high selectivity is suggested and its selectivity is predicted theoretically. Whether this theoretical prediction is true still requires experimental evidence.

## 7. Tautomeric Equilibria in 3-Amino-1-(2-aminoimidazol-4-yl)-prop-1-ene, a Central Building Block of Marine Alkaloids

### 7.1 Introduction

3-Amino-1-(2-aminoimidazol-4-yl)-prop-1-ene (**73**) is a metabolite of the 2-aminoimidazole class of natural products holding a central position in the modular synthesis of a large variety of marine alkaloids.<sup>131-135</sup> The flexible use of this building block in the biosynthesis of pyrrol-imidazole alkaloids has recently been suggested to be due to the variable reactivity of **73**, acting as a nucleophile in one tautomeric form and as an electrophile in another. Equilibration between the respective tautomeric forms thus stands at the center of a comprehensive biosynthetic scheme proposed by Al-Mourabit *et al.*<sup>131</sup> In order to support the participation of different tautomeric forms of **73** along various biosynthetic pathways, Al-Mourabit *et al.* have recently described the results of theoretical studies suggesting the comparable stability of the four tautomeric forms I - IV of **73** shown in Figure 7.1. Based on the assumption of the comparable stability of its various tautomeric forms, **73** may be an ideal starting point for the development of new organocatalysts due to the existence of its potentially four different active sites. However, we found that the theoretical evidences provided by Al-Mourabit *et al.* were not rigorous and convincing. We have therefore revisited the question of thermodynamic stability of tautomeric forms of **73**, using selected theoretical methods known for their performance in the prediction of thermodynamic stabilities.<sup>70,136,137</sup>

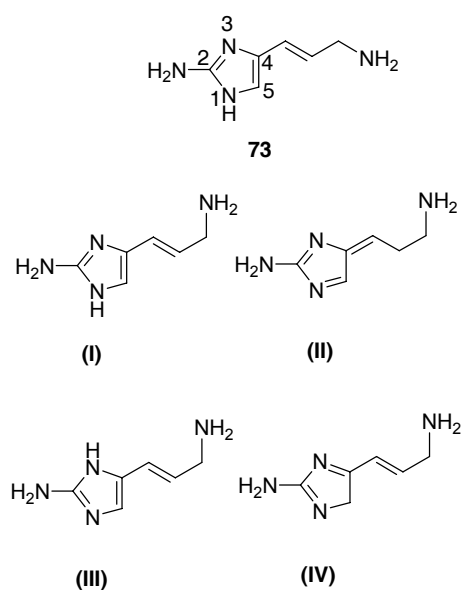


**Figure 7.1.** 2-Aminoimidazole Metabolite **73** and its Tautomers I - IV.

## 7.2 Stabilities of Neutral Tautomers

### 7.2.1 Tautomeric Equilibria in Gas Phase

Initial studies were performed at the RHF/6-31G(d) level of theory, the same level used by Al-Mourabit *et al.* (Table 7.1).<sup>132</sup> The first entry of Table 7.1 is taken from Ref. <sup>132</sup> and shows tautomer IV to be more stable than the other tautomers by around 5 kJ/mol. Carefully searching the conformational space of all four systems by rotation around all rotatable bonds, we identified 18 conformers for tautomers I, III, and IV, and 9 conformers for II, respectively (see Table A33 in Appendix 9.8). According to this conformational analysis, the results reported in Ref. <sup>132</sup> are based on the best conformer for IV, but higher energy conformers of tautomers I - III. Using the best conformers for all four tautomers, the relative energies reported in the second row of Table 7.1 are obtained. Accordingly, tautomer III is the most stable one at the RHF/6-31G(d) level, the other forms being less stable by, at most, 6 kJ/mol. Including thermal corrections to enthalpies at 298.15 K ( $\Delta H_{298}$  in Table 7.1) does not lead to any significant changes in relative energies. The relative enthalpies have subsequently been recalculated with three other theoretical methods known for their performance in predicting accurate thermochemical data. This includes calculations for all conformers with Becke's B98 hybrid functional<sup>50</sup> in combination with the 6-31G(d) basis set, the MP2(FC)/6-31+G(2d,p)//B98/6-31G(d) level recently identified as a reliable method for the calculation of proton and methyl cation affinities of N- and P-bases,<sup>137</sup> and the G3MP2B3 compound method developed by Curtiss *et al.*<sup>40,68</sup> The G3MP2B3 level is considered to be the most accurate in this series of methods.<sup>40,138</sup>

All methods agree in that tautomers I and III, which include the aromatic imidazole ring system in its standard tautomeric form, are of almost identical stability, while tautomers II and IV are much less stable. At G3MP2B3 level tautomers II and IV are predicted to be less favorable than III by 21.8 kJ/mol and 22.9 kJ/mol, respectively. Thus, tautomers II and IV are unlikely to coexist with the other tautomers in the gas phase. The non-aromatic C2-H tautomer of **73** is ruled out here because it is much less stable than all other tautomers. The calculation at B98/6-31G(d) level indicate relative energies between III and the C2-H tautomer in excess of 90 kJ/mol.

**Table 7.1.** Relative Energies (kJ/mol) of the Best Conformer of Tautomers I – IV of Compound **73** Shown in Figure 7.1.

	Level of theory	I	II	III	IV
$\Delta E_{\text{tot}}^{\text{a}}$	RHF/6- 31G(d)	4.9	5.0	5.9	0.0
$\Delta E_{\text{tot}}^{\text{b}}$	RHF/6- 31G(d)	0.5	6.0	0.0	1.7
$\Delta H_{298}$	RHF/6- 31G(d)	0.1	4.9	0.0	0.2
$\Delta H_{298}$	B98/6-31G(d)	1.2	12.0	0.0	15.3
$\Delta H_{298}^{\text{c}}$	MP2/6-31+G(2d,p)//B98/6-31G(d)	1.4	27.5	0.0	32.9
$\Delta H_{298}$	G3MP2B3	0.1	21.8	0.0	22.9

<sup>a</sup> Ref. 132; <sup>b</sup> This work; <sup>c</sup> Thermochemical corrections calculated at B98/6-31G(d) level.

The structures of the energetically most favorable conformers at the MP2(FC)/6-31+G(2d,p)//B98/6-31G(d) level of theory for I - IV are shown in Figure 7.2. All structures have in common that both amino groups are non-planar in all four tautomers, and that the side chain attached to the C4 position assumes an extended conformation.

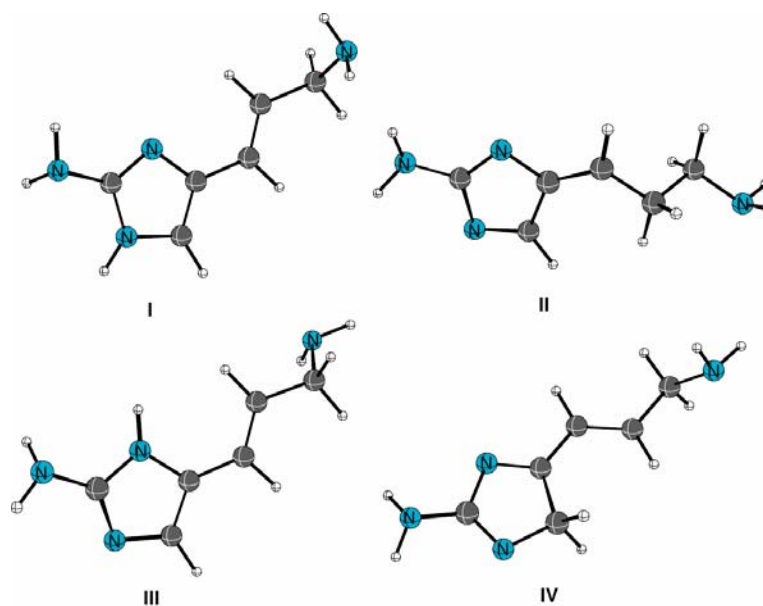


**Figure 7.2.** Structures of the Best Conformer of Tautomers I - IV of Compound **73** at the MP2(FC)/6-31+G(2d,p)//B98/6-31G(d) Level of Theory.

Conditions favoring tautomeric equilibration between isomers I - IV will also allow for the E/Z-isomerization of the C=C double bond in **73**. While Z-configured alkenes are usually considered to be less stable than the corresponding E-isomers, other effects may compensate these differences in polyfunctional systems such as **73**. We have therefore also studied tautomers V – VIII (Figure 7.3) derived from I - IV through E/Z isomerization.

Conformational searches performed at RHF/6-31G(d) and B98/6-31G(d) level again identified a large number of different conformers. The energetically most favorable conformer was subsequently used for comparison to isomer III (Table 7.2).

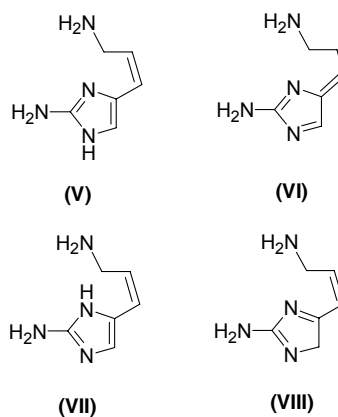


**Figure 7.3.** E/Z-Isomers of Tautomers I – IV of Compound **73**.

**Table 7.2.** Stabilities (kJ/mol) of the Best Conformer of Tautomers V-VIII (Figure 7.3) Relative to Tautomer III.<sup>a</sup>

	Level of theory	V	VI	VII	VIII
$\Delta H_{298}$	RHF/6-31G(d)	10.2	-3.0	-3.8	11.5
$\Delta H_{298}$	B98/6-31G(d)	13.7	4.0	-17.7	22.5
$\Delta H_{298}$	MP2/6-31+G(2d,p)//B98/6-31G(d)	3.7	19.6	-15.4	39.5
$\Delta H_{298}$	G3MP2B3	2.5	14.6	-12.3	29.7

<sup>a</sup>Using the best conformer of III as the reference.

All methods agree that tautomer VII is more stable than III. Concentrating on the best (G3MP2B3) results, this stability difference amounts to -12.3 kJ/mol. Inspection of the structure of VII (Figure 7.4) identifies the formation of an intramolecular hydrogen bond between the terminal NH<sub>2</sub> group and the imidazole ring system as the cause for this enhanced stability. E/Z-isomerization of the other three tautomers I, II, and IV also leads to some changes in their relative stability, but the effects are smaller than observed for III. In conclusion we can thus state that gas phase enthalpies predict isomer VII as the only significantly populated tautomeric/isomeric form of **73** under equilibrating conditions.

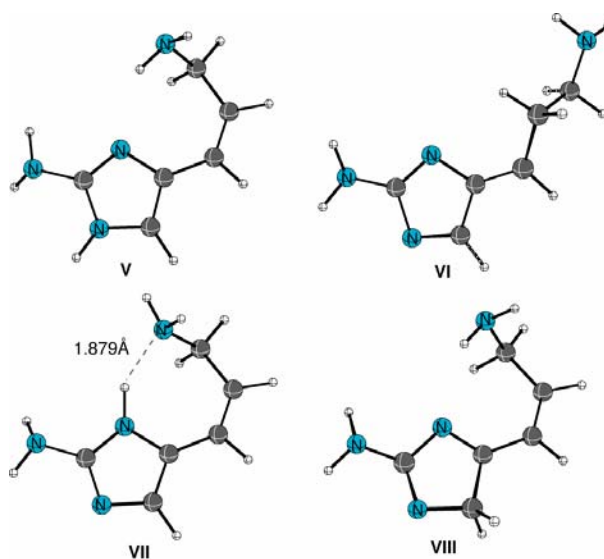


**Figure 7.4.** Structures of the Best Conformer of Tautomers V -VIII of Compound **73** at the MP2(FC)/6-31+G(2d,p)//B98/6-31G(d) Level of Theory.

### 7.2.2 Tautomeric Equilibria in Water

In order to test the influence of aqueous solvation effects on this conclusion, we have calculated solvation free energies in water  $\Delta G_{\text{solv}}$  for all conformers of tautomers I - VIII at the PCM/UAHF/RHF/6-31G(d) level<sup>139-141</sup> using the previously optimized gas phase structures. Combination of these solvation free energies with gas phase enthalpies obtained at either MP2(FC)/6-31+G(2d,p)//B98/6-31G(d) or G3MP2B3 level yields the relative enthalpies in water  $\Delta H_{298}$  (water) compiled in Table 7.3 in columns 3 and 4. Structural relaxation in aqueous solution can, of course, lead to significant changes in relative stabilities. The solvation free energies  $\Delta G_{\text{solv}}$  for all conformers of tautomers I - VIII were therefore calculated again at the PCM/UAHF/RHF/6-31G(d) level using the optimized structures in aqueous solution at PCM/UAHF/B98/6-31G(d) level. The solvation free energies  $\Delta G_{\text{solv}}$  are calculated at PCM/UAHF/RHF/6-31G(d) level because the PCM/UAHF model has been parameterized at Hartree-Fock level. The solvation free energies  $\Delta G_{\text{solv}}$  are also calculated at PCM/UAHF/B98/6-31G(d) level with optimized B98/6-31G(d) gas phase geometries and solution phase geometries, respectively, and combined with either MP2(FC)/6-31+G(2d,p)//B98/6-31G(d) or G3MP2B3 level to yield the relative enthalpies in water  $\Delta H_{298}$  (water) (compiled in Table A9.7.1, see Appendix 9.7). The resulting relative stabilities of tautomers I - VIII are essentially identical to those reported in Table 7.3. In the same manner, combination of these solvation free energies with gas phase enthalpies obtained at either

MP2(FC)/6-31+G(2d,p)//B98/6-31G(d) or G3MP2B3 level yields the relative enthalpies in water  $\Delta H_{298}$  (water) compiled in Table 7.3 in columns 5 and 6. The numbers shown for isomers I - VIII are those for the most stable conformers in water.

Comparison of relative enthalpies in the gas phase  $\Delta H_{298}$  (gas, G3MP2B3) and in aqueous solution  $\Delta H_{298}$  (water, G3MP2B3) shows the most significant changes for the stability of isomer VII. From the results obtained at G3MP2B3 level with relaxed geometries in aqueous solution (column 6 in Table 7.3) it is evident that conformer VII is much less well solvated than all other tautomers, which, in essence, means that the benefit of the intramolecular hydrogen bond is lost in a strongly polar medium such as water. Z-isomer VII therefore ends up being less stable by 4.5 kJ/mol than E-isomer III under aqueous conditions. Surveying the results for all other systems in Table 7.3 we note that isomer I is predicted to be equally stable as III. Most importantly we also note that isomers void of the aromatic imidazole ring system (II, IV, VI, and VIII) are rather unstable also under aqueous conditions. Comparison of the results obtained at MP2 and G3MP2B3 level indicates that none of these conclusions depends on the particular choice of gas phase energies. Also, the influence of solution phase relaxation on the relative stability of tautomers I - VIII is rather minor.

**Table 7.3.** Relative Energies (kJ/mol) of Isomers of I -VIII in the Gas Phase and in Water.<sup>a</sup>

Isomer	G3MP2B3	MP2	G3MP2B3	MP2	G3MP2B3
	$\Delta H_{298}^b$ (gas)	$\Delta H_{298}^c$ (water)	$\Delta H_{298}^d$ (water)	$\Delta H_{298}^e$ (water)	$\Delta H_{298}^f$ (water)
	gas phase geometries			solution phase geometries	
I	0.1	0.5	-0.1	0.4	-0.2
II	21.8	34.5	29.7	36.7	31.8
III	0.0	0.0	0.0	0.0	0.0
IV	22.9	25.4	15.2	28.3	19.9
V	2.5	10.8	10.2	10.0	9.5
VI	14.6	29.9	25.7	31.6	27.4
VII	-12.3	-1.7	2.8	0.7	4.5
VIII	29.7	40.0	29.9	42.1	32.1

<sup>a</sup> Using the best conformer of III as the reference; <sup>b</sup> The best conformer G3MP2B3 gas phase data; <sup>c</sup> Sum of  $H_{298}$ (gas phase, MP2/6-31G+(2d,p)//B98/6-31G(d)) and  $\Delta G_{solv}$  calculated at PCM/UAHF/RHF/6-31G(d)//B98/6-31G(d) level; <sup>d</sup> Sum of  $H_{298}$ (gas phase, G3MP2B3) and  $\Delta G_{solv}$  calculated at PCM/UAHF/HF/6-31G(d)//B98/6-31G(d) level; <sup>e</sup> Sum of  $H_{298}$ (gas phase, MP2/6-31G+(2d,p)//B98/6-31G(d)) and  $\Delta G_{solv}$  calculated at PCM/UAHF/RHF/6-31G(d)//PCM/UAHF/B98/6-31G(d) level; <sup>f</sup> Sum of  $H_{298}$ (gas phase, G3MP2B3) and  $\Delta G_{solv}$  calculated at PCM/UAHF/HF/6-31G(d)//PCM/UAHF/B98/6-31G(d) level.

### 7.3 Stabilities of Protonated Forms

The low thermodynamic stability of tautomeric forms II and IV casts some doubt on their proposed involvement as electrophiles in synthetic and biosynthetic reactions.<sup>131,132</sup> Especially under acidic conditions it would seem conceivable that the protonated forms of **73** are much more likely to act as electrophiles. The actual availability of the cationic forms depend, of course, on the basicity of **73** in aqueous solution and we use the thermodynamic cycle shown in Figure 7.5 to derive a quantitative estimate for the  $pK_a$  of the protonated form of **73** in aqueous solution under standard conditions. The basicity of **73** is compared here to that of 2-aminoimidazole **74**, whose protonated form is known to have  $pK_a = +8.5$ .<sup>142</sup> The reaction free energy in the gas phase  $\Delta G_{rxn,gas}$  can accurately be calculated using the same methods as before and a value of -16.4 kJ/mol is obtained at G3MP2B3 level. Additional consideration of solvation effects at the PCM/UAHF/RHF/6-31G(d)//PCM/UAHF/B98/6-31G(d) level leads to a reaction free energy in solution  $\Delta G_{rxn,sol}$  of -13.8 kJ/mol based on the equation 7.1.

$$\Delta G_{\text{rxn,sol}} = -\Delta G_{\text{solv}}(\mathbf{74}\text{-H}^+) - \Delta G_{\text{solv}}(\mathbf{73}) + \Delta G_{\text{rxn,gas}} + \Delta G_{\text{solv}}(\mathbf{74}) + \Delta G_{\text{solv}}(\mathbf{73}\text{-3H}^+) \quad (7.1)$$

This implies that metabolite **73** is more basic than 2-aminoimidazole **74** by 2.4  $pK_a$  units with  $pK_a(\mathbf{73}\text{-H}^+) = +10.9$ . Under the, in part, strongly acidic reaction conditions employed in transformations of **73** and its derivatives involving either mineral acids or  $\text{CH}_3\text{SO}_3\text{H}$  ( $pK_a = -0.6$  in aqueous solution)<sup>132,143</sup> we can thus assume that **73** is present quantitatively in its protonated form. The reactivity of **73** under these conditions will thus be that of  $\text{I-3H}^+$  or one of its tautomeric forms. In order to explore the possibility that the energetically unfavorable neutral tautomers II and IV are stabilized at the protonated stage we have used the same theoretical methods as before to compare the relative stabilities of the three tautomers shown in Figure 7.6. The relative energies of these systems are compiled in Table 7.4. As expected the tautomer  $\text{I-3H}^+$  is the most stable one. The tautomer  $\text{IV-1H}^+$  is less stable than  $\text{I-3H}^+$  by 7.6 kJ/mol in aqueous solution, which represents a much smaller energy difference of these tautomers as compared to the neutral stage (19.9 kJ/mol). A second tautomer  $\text{IV-3H}^+$  is much less stable than  $\text{IV-1H}^+$  and therefore most likely not involved in reactions under acidic conditions.

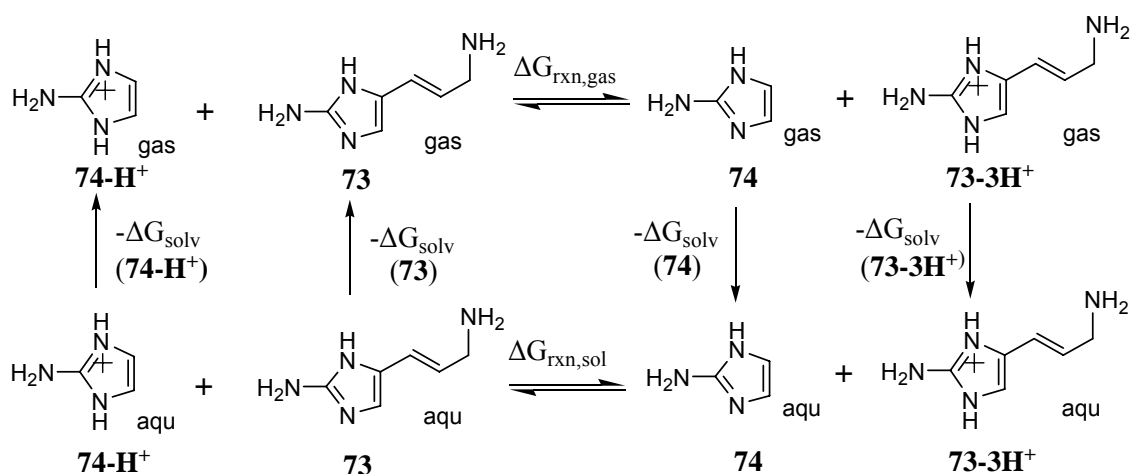


**Figure 7.5.** The Thermodynamic Cycle Used to Calculate Relative  $pK_a$  in Aqueous Solution.

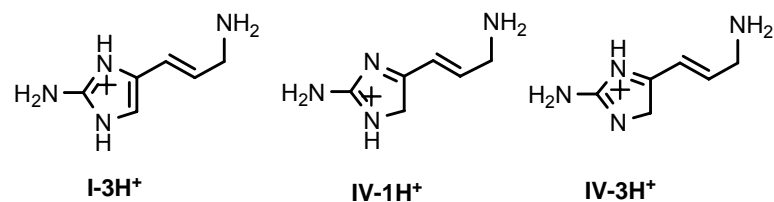


**Figure 7.6.** Tautomeric Forms of Protonated Metabolite **73**.

**Table 7.4.** Relative Energies (kJ/mol) of Cationic Tautomers in the Gas Phase and in Water.<sup>a</sup>

Isomer	G3MP2B3	MP2	G3MP2B3	MP2	G3MP2B3
	$\Delta H_{298}^b$ (gas)	$\Delta H_{298}^c$ (water)	$\Delta H_{298}^d$ (water)	$\Delta H_{298}^e$ (water)	$\Delta H_{298}^f$ (water)
	gas phase geometries			solution phase geometries	
I-3H <sup>+</sup>	0.0	0.0	0.0	0.0	0.0
IV-1H <sup>+</sup>	13.4	12.8	8.7	12.4	7.6
IV-3H <sup>+</sup>	68.2	63.5	57.4	61.4	55.4

<sup>a</sup> Using the best conformer of I-3H<sup>+</sup> as the reference; <sup>b</sup> The best conformer G3MP2B3 gas phase data; <sup>c</sup> Sum of  $H_{298}$ (gas phase, MP2/6-31G+(2d,p)//B98/6-31G(d)) and  $\Delta G_{solv}$  calculated at PCM/UAHF/RHF/6-31G(d)//B98/6-31G(d) level; <sup>d</sup> Sum of  $H_{298}$ (gas phase, G3MP2B3) and  $\Delta G_{solv}$  calculated at PCM/UAHF/HF/6-31G(d)//B98/6-31G(d) level; <sup>e</sup> Sum of  $H_{298}$ (gas phase, MP2/6-31G+(2d,p)//B98/6-31G(d)) and  $\Delta G_{solv}$  calculated at PCM/UAHF/RHF/6-31G(d)//PCM/UAHF/B98/6-31G(d) level; <sup>f</sup> Sum of  $H_{298}$ (gas phase, G3MP2B3) and  $\Delta G_{solv}$  calculated at PCM/UAHF/HF/6-31G(d)//PCM/UAHF/B98/6-31G(d) level.

One example where occurrence of the unstable neutral tautomer IV has been suggested concerns the H/D exchange reactions in compound **75** in refluxing deuterated trifluoroacetic acid (Figure 7.7).<sup>132</sup> If we assume the basicity of **75** to parallel that of **73** then **75** will be fully protonated under these conditions. Selective H/D exchange at position C5 as well as *cis/trans* isomerization to yield product **76** without H/D exchange at C7 can be rationalized with the three protonated forms **77**, **78** and **79**. As already implied by Al-Mourabit *et al.* H/D exchange at all heteroatoms can be expected to be fast under these conditions as compared to *cis/trans* isomerization. This latter process can be initiated through formation of C5-protonated tautomer **77** and subsequent cyclization to intermediate **78**. Ring-opening to intermediate **79** and isomerization between the C5- and N1-protonated forms complete the reaction sequence. Other processes, in which neutral **73** has been suggested to act as electrophile,<sup>131</sup> may similarly involve the protonated form of **73** instead.

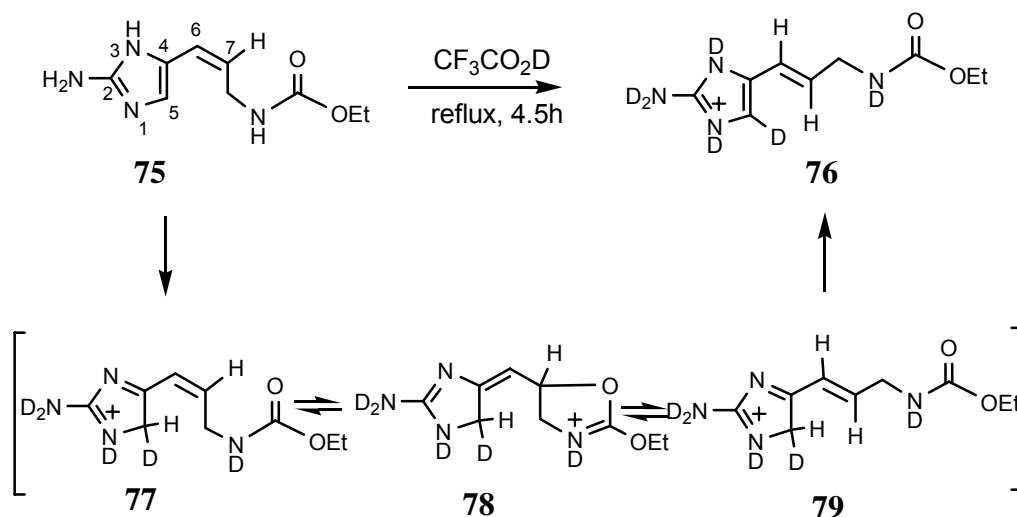


**Figure 7.7.** H/D-Exchange and *cis/trans* Isomerization of **75** under Acidic Conditions as Reported in Ref. 132.

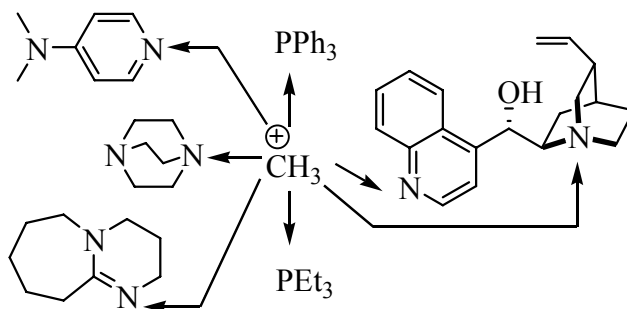
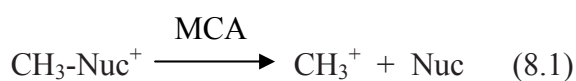
#### 7.4 Conclusions

In conclusion, the tautomers II and IV of 2-aminoimidazole metabolite **73** reported as energetically favorable before<sup>132</sup> are unlikely to coexist with tautomers I and III, in the gas phase as well as in water. The tautomers I and III have almost identical stability in the gas phase and in water, and thus will both be accessible in solution. The *Z*-isomer of III, tautomer VII, should not be ignored because it is more stable than any other tautomer in the gas phase and competitive with I and III in water. These conclusions are independent of the particular theoretical methods chosen for solution phase calculations. The low thermodynamic stability of tautomers II and IV casts some doubt on the role of these isomers as electrophiles in synthetic and biosynthetic reactions.<sup>131</sup> The protonated form of the 2-aminoimidazole moiety, which is present in many synthetically used derivatives of **73**, may fill this role much more comfortably and with much less thermodynamic effort.<sup>133,134,135</sup> The calculated  $pK_a$  of **73-H<sup>+</sup>** of +10.9 in aqueous solution indeed suggests that **73** is present quantitatively in its protonated form even under mildly acidic reaction conditions. Protonation also decreases the stability difference between the most stable tautomer III and the less stable tautomer IV, offering an explanation for the apparent involvement of this latter tautomer in H/D exchange experiments.

## 8. Summary and General Conclusions

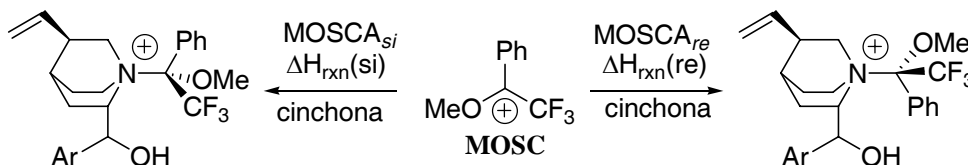
In the present work, the theoretical benchmarking has been done for studying the issues in organocatalytic processes and other chemical process such as tautomeric equilibrium, and the descriptors for organocatalytic activities and selectivities are developed, meanwhile the activities and selectivities of organocatalysts for acyl transfer reactions are studied theoretically. The key results of the thesis are summarized as follows.

(1) Methyl Cation Affinities (MCAs) are defined in this context as the reaction enthalpies at 298 K for the transformations shown in equation 8.1. MCA for a large variety of neutral and anionic bases can be predicted accurately with compound methods such as G2, G3 or W1. The predictive ability of MP2 calculations is slightly lower, but still practically useful. The performance of the B98 hybrid functional depends strongly on the size of the systems at hand. The calculated MCAs depend little on the methods used for structure optimization and the MP2(FC)/6-31+G(2d,p)//B98/6-31G(d) method is identified to offer an affordable option for the characterization of even the largest currently used organocatalysts. The identified method is used to calculate the MCA values of a set of commonly used N- and P-based organocatalysts (see Scheme 8.1). The MCA values presented here can be used as a guideline for the optimization of organocatalytic transformations. The mechanistic complexity of many such reactions, the presence of numerous side reactions, and the broad variety of solvents used under experimental conditions make it unlikely that quantitative predictions can be made for structurally different organocatalysts with only one single parameter. However, if the general limitation of a single parameter approach has been accepted, it is clear that the currently known catalytic activities of nitrogen and phosphorus bases are much more readily correlated with MCA than with PA or  $pK_a$  data.



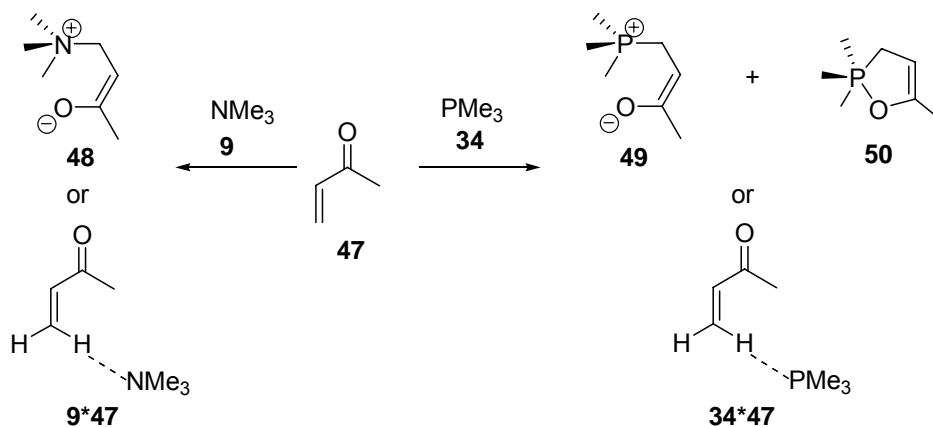
**Scheme 8.1.**

(2) The new concept of Mosher's cation affinities (MOSCA) is defined (see Scheme 8.2) and developed. Taken together the MOSCA values determined for a series of tertiary amines represent a quantitative and easily computable measure of the stereoinductive potential of these nucleophiles. These data, together with the MCA values, are expected to facilitate the development of new, more effective and more selective catalysts, in particular in an area where initial experiments have already been performed. The stereoinductive potential is one of the key factors determining the stereoselectivity in catalytic processes. Whether or not such a process is successful depends on a host of additional factors, the absolute catalytic efficiency being one of the most relevant. The MOSCA probe studied here appears to capture both the catalytic efficiency as well as the stereoselectivity. For the cinchona alkaloids and selected tertiary amines studied the most reactive and selective compounds appear to be quinine (**22**) and quinidine (**18**), while sparteine (**46**) appears to be neither particularly selective nor reactive.



**Scheme 8.2.**

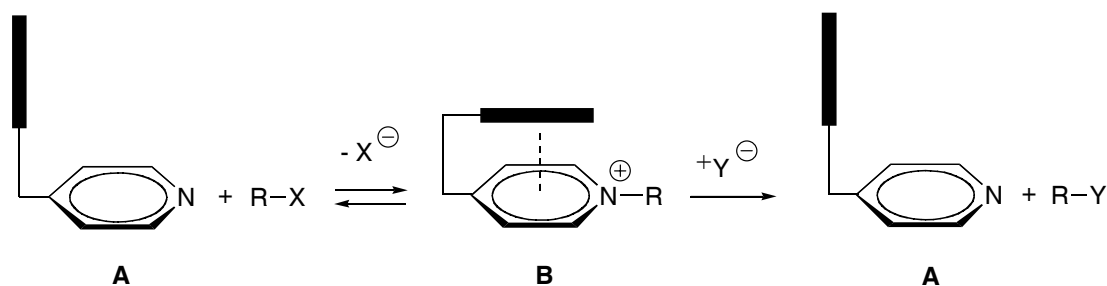
(3) In many organocatalytic transformations neutral electrophiles react with neutral nucleophiles to give zwitterionic adducts at some stage of the catalytic cycle such as in the Morita-Baylis-Hillman (MBH) reaction. A series of theoretical methods have been studied systematically in order to identify theoretical methods appropriate for the reliable description of the formation of zwitterionic adducts using the model systems shown in Scheme 8.3.



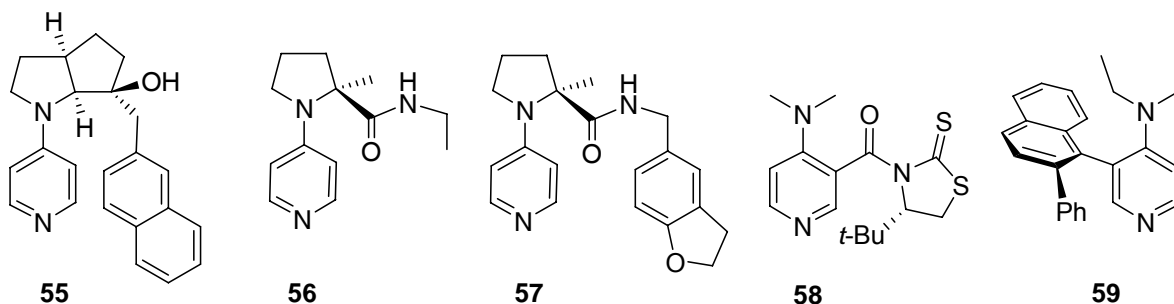
**Scheme 8.3.**

The commonly used hybrid density functional B3LYP in computational studies of organic reactions fails to give correct adduct geometry for nitrogen-containing nucleophile, whether combined with Pople type basis sets or with correlation consistent basis sets. Geometry optimizations at the mPW1K/6-31+G(d) level provide a reliable basis for the development of compound energy schemes for the accurate description of zwitterionic adducts between neutral nucleophiles and electrophiles. Accurate energetics can be obtained using modified G3 schemes as well as double-hybrid DFT methods such as B2K-PLYP or B2-PLYP-M2. This latter class of methods also allows for the systematic investigation of large systems typically formed as intermediates in organocatalytic reactions.

(4) The conformational preferences of 4-DMAP derivatived catalysts studied at the SCS-MP2(FC)/6-311+G(d,p)//MP2(FC)/6-31G(d) level are in line with the limited existing experimental data available for these systems. It has been shown that stacking interactions can play a decisive role in the stability as well as the conformational preferences of these transient intermediates (see Scheme 8.4). Stacking conformations dominate the appearance of the acetylpyridinium intermediates of catalysts **55**, **57**, and **58**.



Scheme 8.4.

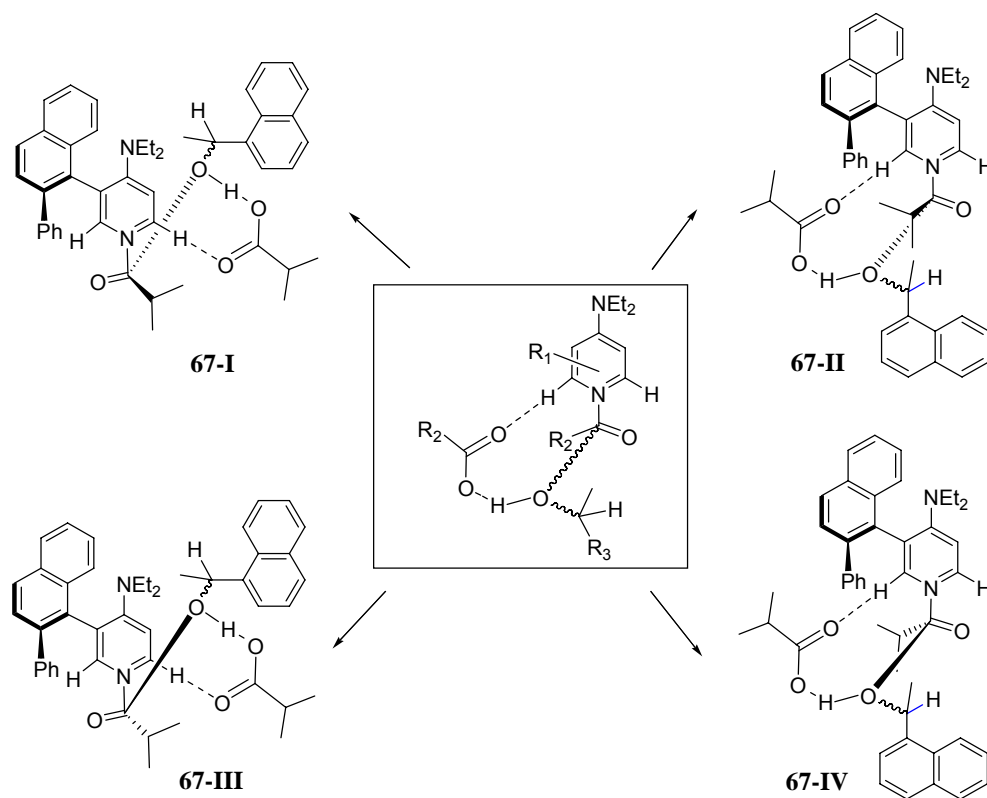


Scheme 8.5.

Dispersion interactions are mainly responsible for this situation in **55Ac**, while electrostatic effects dominate in **57Ac**. The conformational preferences of the acetyl intermediates of **58** and **59** are mainly enforced by the rigidity of the  $\sigma$ -framework, leading to a stacking

conformation in **58Ac** and a non-stacking conformation in **59Ac**. Still, large conformational changes occur in both of these latter systems on formation of the acetyl intermediate, supporting the “conformational switch” picture derived from experimental  $^1\text{H}$  NMR studies. In methodological terms we have shown that studies of the acetyl intermediates of catalysts **55** – **59** require correlated levels, the MP2(FC)/6-31G(d)//RHF/3-21G level providing a reasonable lower limit of effort. DFT methods such as the popular B3LYP hybrid functional are not able to describe stacking interactions induced through dispersion interactions properly.

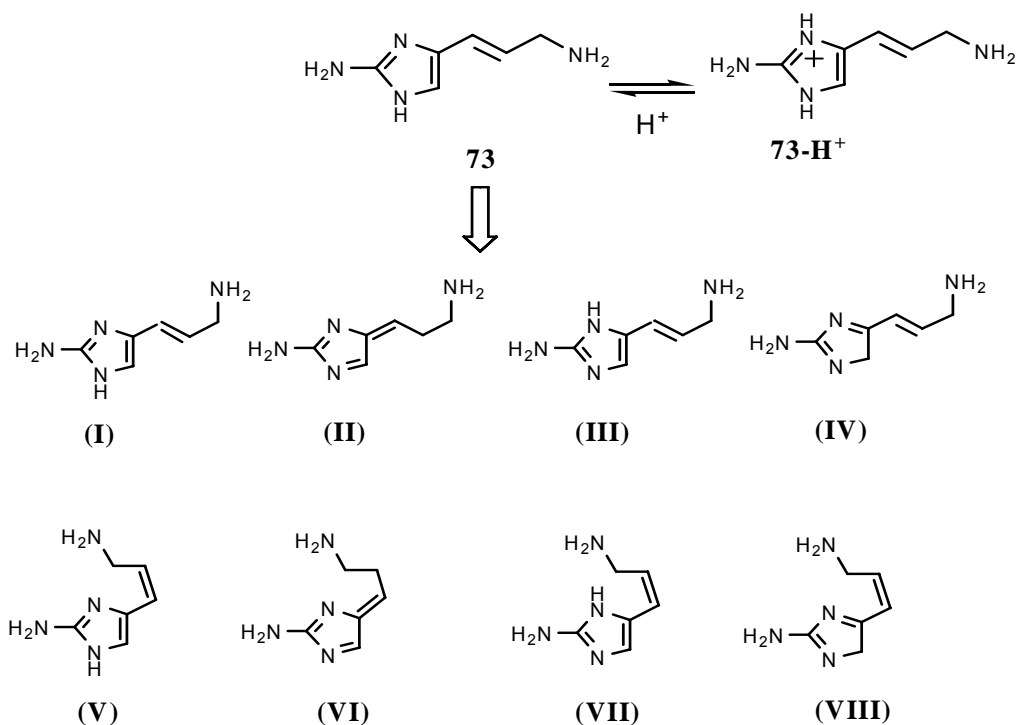
(5) Similar to acylation reactions with achiral catalysts, the commonly accepted nucleophilic mechanism is more favorable than the general base mechanism for the reaction of racemic 1-(1-naphthyl)ethanol (**60**) with isobutyric anhydride (**61**). The identified TS models in the selectivity-determining step can be classified into four types (see Scheme 8.6) and reveal that alcohols with different configuration prefer different directions to approach the reaction center. The key TS model is helpful for catalyst design, thus a new catalyst with potential high selectivity is suggested and its selectivity is predicted theoretically.



**Scheme 8.6.**

(6) The tautomers II and IV of 2-aminoimidazole metabolite **73** reported as energetically favorable before<sup>132</sup> are unlikely to coexist with tautomers I and III, in the gas phase as well as

in water. The tautomers I and III have almost identical stability in the gas phase and in water, and thus will both be accessible in solution. The Z-isomer of III, tautomer VII, should not be ignored because it is more stable than any other tautomer in the gas phase and competitive with I and III in water. These conclusions are independent of the particular theoretical methods chosen for solution phase calculations. The low thermodynamic stability of tautomers II and IV casts some doubt on the role of these isomers as electrophiles in synthetic and biosynthetic reactions.<sup>131</sup> The protonated form of the 2-aminoimidazole moiety, which is present in many synthetically used derivatives of **73**, may fill this role much more comfortably and with much less thermodynamic effort.<sup>133,134,135</sup> The calculated  $pK_a$  of **73-H<sup>+</sup>** of +10.9 in aqueous solution indeed suggests that **73** is present quantitatively in its protonated form even under mildly acidic reaction conditions. Protonation also decreases the stability difference between the most stable tautomer III and the less stable tautomer IV, offering an explanation for the apparent involvement of this latter tautomer in H/D exchange experiments.



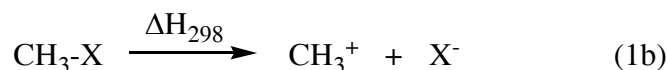
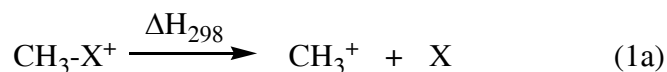
**Scheme 8.7.**

Our findings are helpful for better understanding the properties of organocatalysts and the mechanism of organocatalytic processes and help organocatalyst design. We hope that we can improve the models for helping the organocatalyst design more quickly and efficiently in the future.

## 9. Appendix

### 9.1 Computational Details for MCA

The MCA values computed in assessment of theoretical methods for calculation of MCA have been determined as the heat of reaction  $\Delta H_{\text{rxn}}$  at 298.15 K for reaction (1a) for neutral nucleophiles (X) and for reaction (1b) for anionic nucleophiles (X<sup>-</sup>).



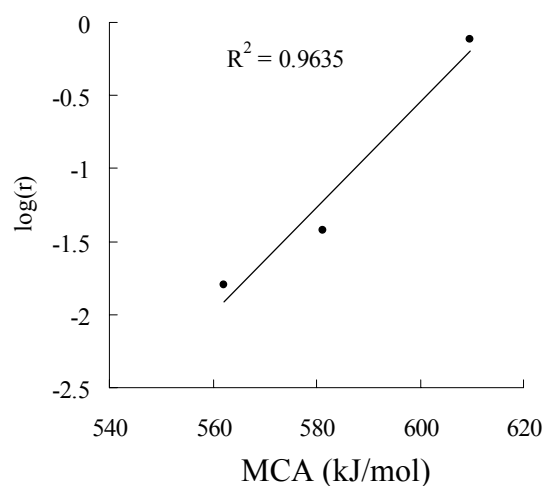
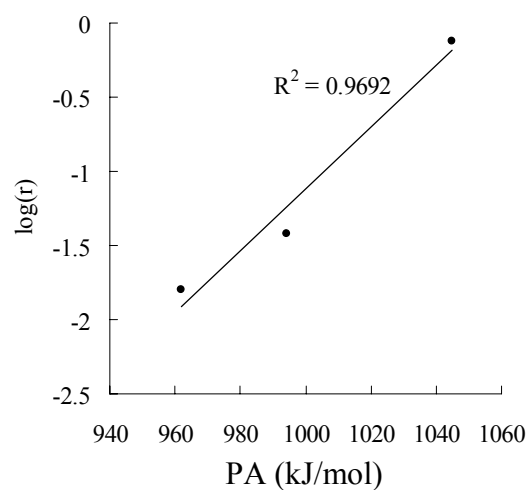
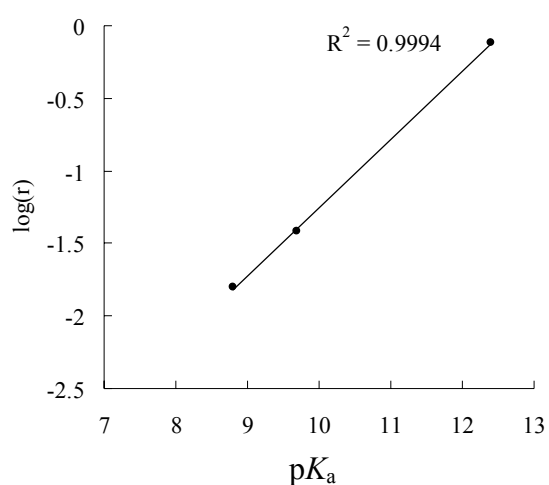
If not mentioned otherwise, thermal corrections to enthalpies at 298.15 K have been calculated at the same level as geometry optimizations using the rigid rotor/harmonic oscillator approximation. All data refer to true minima on the potential energy surface with all-positive vibrational frequencies. All calculations were carried out with Gaussian 03 suite of programs.<sup>144</sup> Geometry optimizations at CCSD(T) level have been performed with MOLPRO 2002.6.<sup>145</sup>

For all N- and P-centered organocatalysts presented in Chapter 2, the geometries have been optimized at the B98/6-31G(d) level of theory. The conformational space of flexible organocatalysts has first been searched using the MM3 force field and the systematic search routine in the TINKER program.<sup>146</sup> All stationary points located at force field level have then been reoptimized at B98/6-31G(d) level as described before. Starting geometries for the cationic adducts have been generated from the neutral structures through addition of a proton or methyl cation, followed by subsequent reoptimization at B98/6-31G(d) level. Thermochemical corrections to 298.15 K have been calculated for all minima from unscaled vibrational frequencies obtained at this same level. The thermochemical corrections have been combined with single-point energies calculated at the MP2(FC)/6-31+G(2d,p)//B98/6-31G(d) level to yield enthalpies  $H_{298}$  at 298.15 K. In conformationally flexible systems enthalpies have been calculated as Boltzmann-averaged values over all available conformers. This procedure has recently been found to reproduce G3 methyl cation affinity values of selected small- and medium-sized organocatalysts within 4.0 kJ/mol. All quantum mechanical calculations have been performed with Gaussian 03.<sup>144</sup>

## 9.2 Correlation of $pK_a$ , PA, and MCA Values with Available Experimental Rate Data of Organocatalytic Processes.

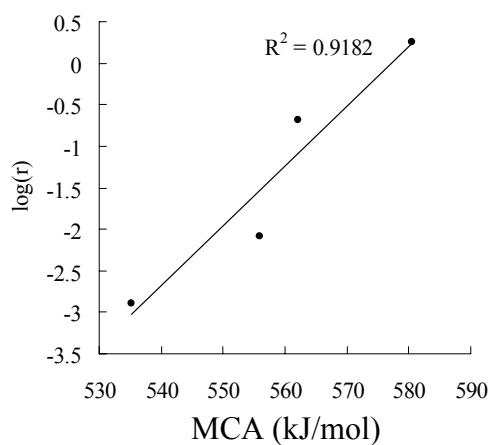
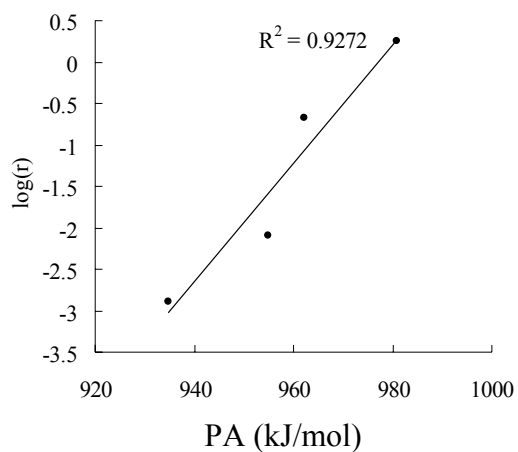
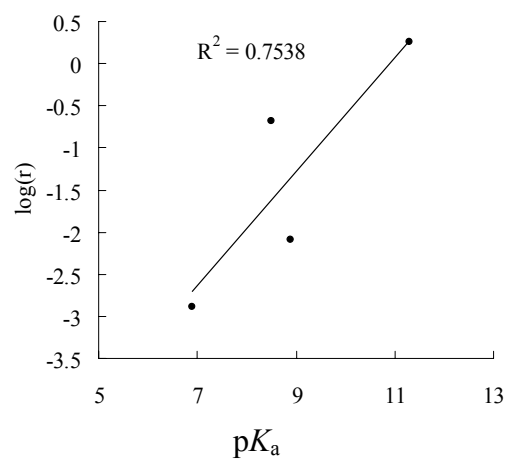
	Reaction rate <sup>a</sup>	log (rate)	$pK_a$ <sup>b</sup>	PA <sup>c</sup> (kJ/mol)	MCA <sup>c</sup> (kJ/mol)
DABCO ( <b>19</b> )	0.016	-1.8	8.8	962.1	562.2
4-DMAP ( <b>27</b> )	0.038	-1.42	9.7	994.1	581.2
DBU ( <b>36</b> )	0.762	-0.12	12.4	1044.8	609.6

<sup>a</sup> Reaction rate data from Ref. 82; <sup>b</sup>  $pK_a$  values from Ref. 7; <sup>c</sup> Calculated at MP2/6-31+G(2d,p)//B98/6-31G(d) level.



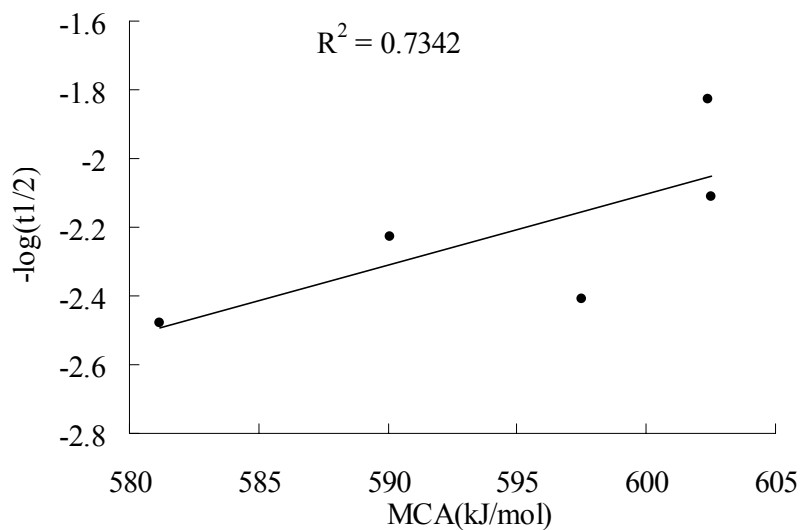
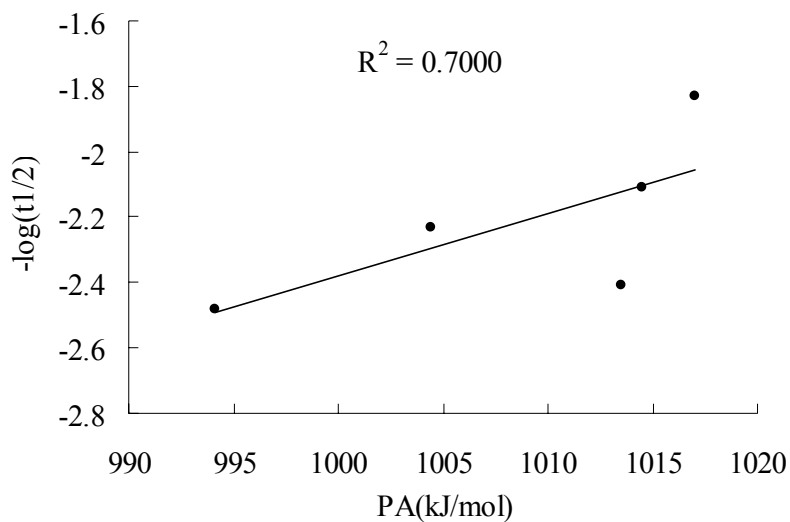
	Reaction rate <sup>a</sup>	log (rate)	pK <sub>a</sub> <sup>a</sup>	PA <sup>b</sup> (kJ/mol)	MCA <sup>b</sup> (kJ/mol)
3-quinuclidinone ( <b>7</b> )	0.0013	-2.89	6.9	934.7	535.2
3-chloroquinuclidine ( <b>17</b> )	0.0082	-2.09	8.9	955.0	555.9
DABCO ( <b>18</b> )	0.21	-0.68	8.5	962.1	562.2
quinuclidine ( <b>26</b> )	1.8	0.26	11.3	980.8	580.6

<sup>a</sup> Reaction rate data and pK<sub>a</sub> values from Ref. 81 ; <sup>b</sup> Calculated at MP2/6-31+G(2d,p)//B98/6-31G(d) level.



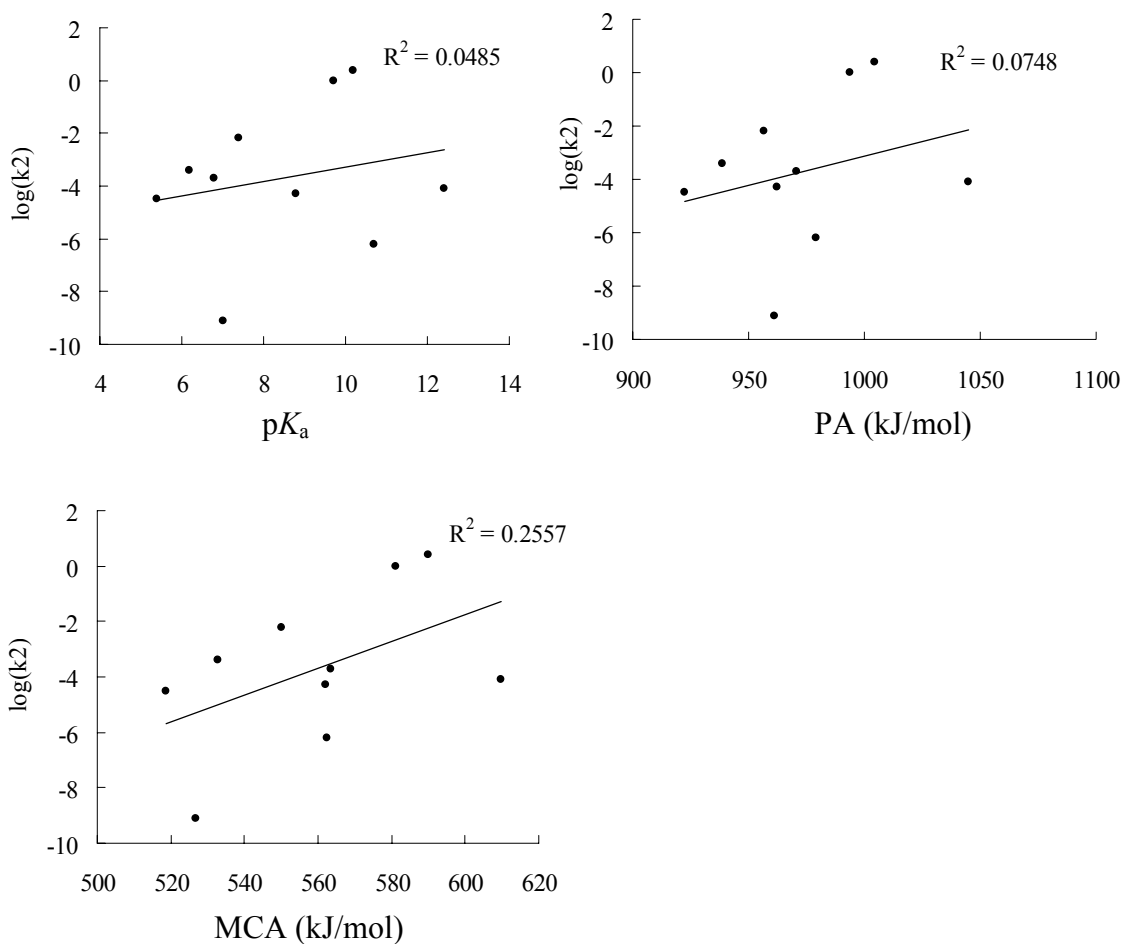
	Reaction half-lives <sup>a</sup> ( $\tau_{1/2}$ , min)	$-\log(\tau_{1/2})$	PA <sup>b</sup> (kJ/mol)	MCA <sup>b</sup> (kJ/mol)
<b>32</b>	67	-1.83	1017.0	602.4
<b>33</b>	129	-2.11	1014.5	602.5
PPY ( <b>29</b> )	171	-2.23	1004.4	590.1
4-DMAP ( <b>27</b> )	304	-2.48	994.1	581.2
<b>25</b>	260	-2.41	1013.5	597.5

<sup>a</sup> Reaction rate data from Ref.11 ; <sup>b</sup> Calculated at MP2/6-31+G(2d,p)//B98/6-31G(d) level.

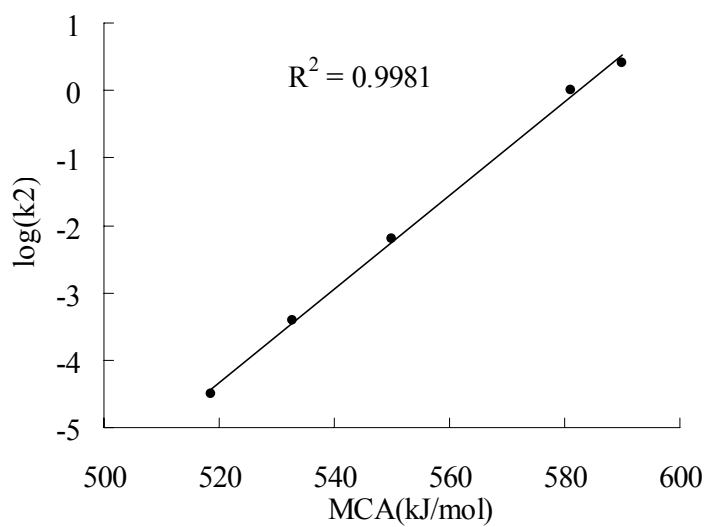
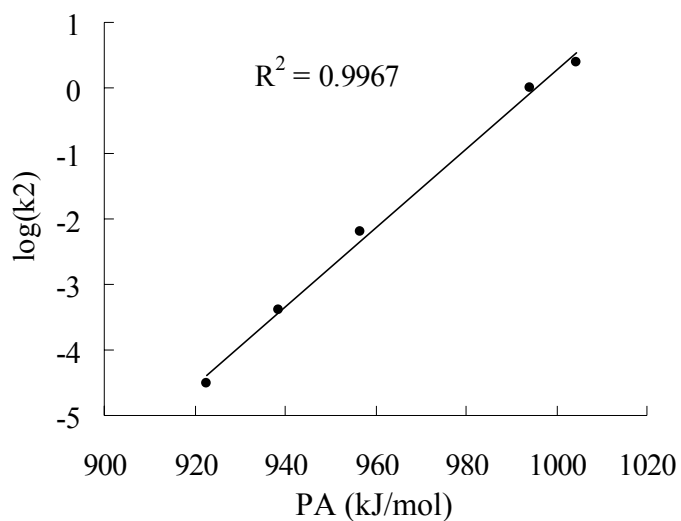
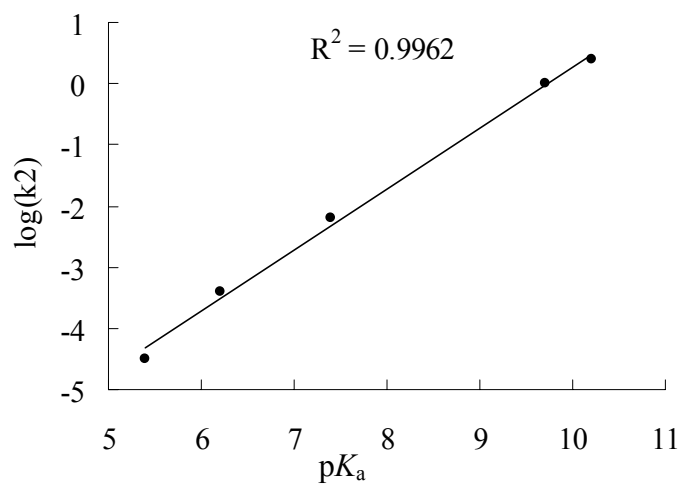


	$\log(k_2)^a$	$pK_a^a$	PA <sup>b</sup> (kJ/mol)	MCA <sup>b</sup> (kJ/mol)
PPY ( <b>29</b> )	0.4	10.2	1004.4	590.1
4-DMAP ( <b>27</b> )	0.0	9.7	994.1	581.2
N-methylimidazole ( <b>11</b> )	-2.2	7.4	956.5	550.0
4-methylpyridine ( <b>6</b> )	-3.4	6.2	938.7	532.8
3-DMAP ( <b>21</b> )	-3.7	6.8	970.8	563.4
DBU ( <b>36</b> )	-4.1	12.4	1044.8	609.6
DABCO ( <b>19</b> )	-4.3	8.8	962.1	562.2
Pyridine ( <b>1</b> )	-4.5	5.4	922.6	518.7
NEt <sub>3</sub> ( <b>20</b> )	-6.2	10.7	979.2	562.3
2-DMAP ( <b>2</b> )	-9.1	7	961.3	526.7

<sup>a</sup> Reaction rate data and  $pK_a$  values from Ref. 7; <sup>b</sup> Calculated at MP2/6-31+G(2d,p)/B98/6-31G(d) level.



Correlation of  $pK_a$ , PA and MCA with the rate data for the acylation reaction described in Ref. 7, including 4-substituted pyridines **1**, **6**, **27**, and **29**, and N-methylimidazole (**11**).



### 9.3 Computational Details for MOSCA

The geometries of all systems have been optimized at the B98/6-31G(d) level of theory. The conformational space of cinchona alkaloids has first been searched using the MM3 force field and the systematic search routine in the TINKER program.<sup>146</sup> The conformers of **46** were taken from Wiberg's previous studies.<sup>147</sup> All stationary points located at force field level have then been reoptimized at B98/6-31G(d) level as described before. Starting geometries for the cationic adducts have been generated from the neutral structures through addition of a methyl cation, followed by subsequent reoptimization at B98/6-31G(d) level. For conformational search of **MOSC** adducts, the best conformer of the methyl cation adducts was chosen as the central structure. The methyl cation was replaced by **MOSC**, and then the new C-N bond was rotated to search possible conformers, and for cinchona alkaloids the rotation of hydroxy group was also considered. In order to avoid missing important conformers, we also checked the conformers by flipping the quinoline moiety and twisting the quinuclidine ring of the best conformer of **12-MOSCre<sup>+</sup>** and **12-MOSCsi<sup>+</sup>**, respectively. It turns out that these conformers are less stable than before by more than 10 kJ/mol. Thermochemical corrections to 298.15 K have been calculated for all minima from unscaled vibrational frequencies obtained at this same level. The thermochemical corrections have been combined with single-point energies calculated at the MP2(FC)/6-31+G(2d,p)//B98/6-31G(d) level to yield enthalpies  $H_{298}$  at 298.15 K. In conformationally flexible systems enthalpies have been calculated as Boltzmann-averaged values over all available conformers. All quantum mechanical calculations have been performed by Gaussian 03.<sup>148</sup>

#### 9.4 Computational Details for the Stability of Zwitterionic Adducts

All data refer to true minima on the potential energy surface with all-positive vibrational frequencies. All calculations were carried out with Gaussian 03 suite of programs.<sup>144</sup> Thermochemical corrections to 298.15 K have been calculated for all minima from unscaled vibrational frequencies. B2-PLYP and related calculations can be performed in Gaussian03 using the generalized input format for DFT methods in combination with extra overlays for the PT2 calculation. One sample input file is shown as follows.

```
%chk=/home/yin/bhr/nme3_mpw1k_6-31+gd.chk
%mem=2000mb
%nproc=2
#P BLYP/6-31+G(2d) scf=tight geom=check guess=read iop(3/76=0470005300,3/78=0730007300)
extraoverlay

8/10=90/1; 9/16=-3/6;

nme3_mpw1k_6-31+g2d-spb2

0 1
```

In the output file:

```
SCF Done: E(RB+HF-LYP) = -174.064195599 A.U. after 10 cycles
```

```
.....
```

```
E2 = -0.7746642262D+00 EUMP2 = -0.17483885982487D+03
```

Then,  $E_{\text{tot}}(\text{B2-PLYP})$  can be calculated as follows.

```
 $E_{\text{tot}}(\text{B2-PLYP}) = E(\text{RB+HF-LYP}) + 0.27 * E2 = -174.2733549$ 
```

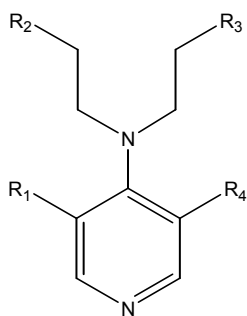
## 9.5 Computational Details for Chapter 5

### 9.5.1 Theoretical Methods

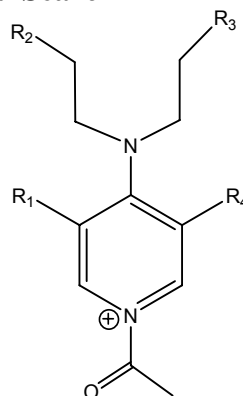
The conformational space of all systems studied here has initially been studied with the OPLS-AA force field as implemented in BOSS 4.6.<sup>117</sup> Potential parameters for the description of 4-aminopyridines and their acetylpyridinium cations are currently not part of the default OPLS-AA force field.<sup>118</sup> The nitrogen atom attached to C4 of the pyridine ring has therefore been defined as a new nitrogen atom type. Appropriate force field parameters for the neutral catalysts and the acetylpyridinium cations have then been developed from a series of *ab initio* calculations at the B3LYP/6-31G(d) and MP2/6-31G(d) level of theory. Coulomb parameters have been derived using the CM1 procedure with the AM1 wavefunction. The conformational space of both types of species has then been searched using the Monte Carlo conformational search facility implemented in BOSS 4.6.

All conformers identified in this way have subsequently been reoptimized at the RHF/3-21G level of theory. For some of the systems optimizations at the RHF/MIDI! and B3LYP/6-31G(d) levels of theory have also been performed. Finally, geometry optimizations have also been performed at the MP2(FC)/6-31G(d) level for the best conformers identified at the MP2(FC)/6-31G(d)//RHF/3-21G level. For the best conformers identified at fully optimized MP2(FC)/6-31G(d) level additional single point calculations have been performed at the MP2(FC)/6-311+G(d,p) level of theory. In all cases default convergence criteria have been used. Thermochemical corrections to enthalpies at 298.15 K ( $H_{298}$ ) have been calculated at the same level as that used for geometry optimization. The only exception concerns geometries optimized at MP2(FC)/6-31G(d) level. In this latter case thermochemical corrections have been taken from the HF/3-21G level. All calculations have been performed with Gaussian 03.<sup>144</sup>

## 9.5.2 Force Field Parameters and Conformational Search



**A**



**B**

### List of atom types for **A** and **B**

Atom type	Description	$\sigma$ , Å	$\epsilon$ , kcal/mol
CT	Any $sp^3$ carbon	3.500	0.066
CA	Any aromatic $sp^2$ carbon	3.550	0.070
C	Any carbonyl $sp^2$ carbon	3.750	0.105
NC	Nitrogen in pyridine ring	3.250	0.170
NN	Nitrogen in amino group connected to pyridine ring	3.250	0.170
N	Nitrogen in amide group	3.250	0.170
O	Carbonyl oxygen or in amides	2.960	0.210
OH	Oxygen in hydroxyl group	3.120	0.170
OS	$sp^3$ oxygen in five- membered ring	2.900	0.140
S	S in five-membered ring	3.550	0.250
S=	In C=S group	3.550	0.250
HC	hydrogen attached to aliphatic carbon	2.420	0.030
HA	Hydrogen attached to aromatic carbon	2.420	0.030
HO	Alcohol hydrogen	0.000	0.000
H	Amide hydrogen	0.000	0.000

Bond and Angle Parameters for A

Type	$r_{eq}$ or $\theta_{eq}$	$K_r$	Source <sup>a</sup>
CA-CA	1.400	469.0	old
CA-NC	1.339	483.0	old
CA-HA	1.080	367.0	old
CA-NN	1.360	529.0	new
CT-NN	1.456	337.0	new
CT-HC	1.090	340.0	old
CT-CT	1.529	268.0	old
CA-CT	1.510	317.0	old
CT-OH	1.410	320.0	old
OH-HO	0.945	553.0	old
C –O	1.212	570.0	old
C -CT	1.500	317.0	new
CT-N	1.335	490.0	old
C -N	1.449	337.0	old
N –H	1.010	434.0	old
CT-OS	1.410	320.0	old
CA-OS	1.364	450.0	new
C –S=	1.640	400.0	old
C –S	1.760	250.0	old
CT-S	1.810	220.0	new
CA-CA-CA	120.0	63.0	old
CA-CA-NC	124.0	70.0	old
CA-NC-CA	117.0	70.0	old
HA-CA-CA	120.0	35.0	old
HA-CA-NC	116.0	35.0	old
NN-CA-CA	121.4	70.0	new
NN-CT-CT	102.0	65.0	new
CT-NN-CA	117.6	150.0	new
CT-NN-CT	116.0	30.0	new
CT-NN-CT in five- membered ring	110.0	60.0	new
NN-CT-HC	109.5	35.0	new
HC-CT-HC	107.8	33.0	old
HC-CT-CT	110.7	37.5	old
CT-CT-CT	112.7	58.35	old
CT-OH-HO	108.5	55.0	old
OH-CT-CT	109.5	50.0	old
CA-CT-CT	114.0	63.0	old
CT-CA-CA	120.0	63.0	old
C -CT-CT	111.1	63.0	old
CT-C –N	116.6	70.0	old
C –N –H	119.8	35.0	old
N –C –O	122.9	80.0	old
H –N –CT	118.4	38.0	old
CT-CT-N	109.7	80.0	old
HC-CT-N	109.5	35.0	old
CA-C –O	120.4	80.0	new
CA-OS-CT	111.8	100.0	new

Type	$r_{eq}$ or $\theta_{eq}$	$K_r$	Source <sup>a</sup>
N-CT-CA	111.2	80.0	new
CA-CA-OS	109.5	50.0	old
CT-CT-OS	120.0	70.0	new
HC-CT-OS	109.5	35.0	old
N-C-S=	125.0	70.0	new
S-C-S=	125.0	70.0	new
C-S-CT	98.9	62.0	new
S-CT-CT	114.7	50.0	old

a. old parameters published in literatures<sup>117,118,149</sup>

## Dihedral angle parameters for A

Dihedral angle	V1	V2	V3	V4	Source <sup>a</sup>
HC-CT-CT-HC	0.0	0.0	0.30	0.0	old
HC-CT-CT-CT	0.0	0.0	0.30	0.0	old
CT-CT-CT-CT	6.622	-2.6	-0.4	1.3	new
CA-CA-CA-CA	0.0	7.250	0.0	0.0	old
CA-CA-CA-NC	0.0	7.250	0.0	0.0	old
CA-CA-NC-CA	0.0	7.250	0.0	0.0	old
HA-CA-CA-CA	0.0	7.250	0.0	0.0	old
HA-CA-CA-HA	0.0	7.250	0.0	0.0	old
HA-CA-CA-NC	0.0	7.250	0.0	0.0	old
CT-CA-CA-CA	0.0	7.250	0.0	0.0	old
CT-NN-CT-CT	0	1.2	0	0.7	new
CA-CA-NN-CT	0	3.75	1.0	0	new
CA-NN-CT-HC	0	0	0.35	0	new
CT-NN-CT-HC	0	0	0.435	0	new
CA-NN-CT-CT	0	1.2	0	0.7	new
CA-N-CT-CT	0	1.2	0	0.7	new
NN-CT-CT-CT	2.392	-0.674	-0.6	0	new
NN-CT-CT-OH	6.28	-5.1	2.03	0	new
CT-C-N-H	0.0	4.9	0.0	0.0	old
CT-C-N-CT	2.3	6.089	0.0	0.0	old
NN-CT-C-O	0.0	0.0	0.0	0.0	new
H-N-CT-CT	0.0	0.0	0.0	0.0	old
H-N-CT-CA	0.0	0.0	0.0	0.0	old
CT-CT-C-O	0.0	1.166	0.0	0.0	old
O-C-N-H	0.0	4.90	0.0	0.0	old
H-N-CT-HC	0.0	0.0	0.0	0.0	old
N-CT-CT-HC	0.0	0.0	0.464	0.0	old
HC-CT-CA-CA	0.0	0.0	0.0	0.0	old
CT-CA-CA-HA	0.0	7.25	0.0	0.0	old
CA-CA-CA-OS	0.0	7.25	0.0	0.0	new
CT-CA-CA-OS	0.0	7.25	0.0	0.0	new
CA-CT-CT-OS	-1.336	0.00	0.00	0.00	new
CA-OS-CT-CT	0.650	-0.250	0.670	0.0	new
CT-OS-CA-CA	0.0	3.0	0.0	0.0	new
CA-CA-C-O	0.0	0.0	0.0	0.0	new
CA-CA-C-N	0.0	1.1	0.0	0.0	new
CA-C-N-C	2.30	6.089	0.0	0.0	new
CA-CA-CA-C	0.0	7.250	0.0	0.0	new
S=C-N-C	0.0	6.50	0.0	0.0	new
C-N-CT-CT	-1.396	-0.427	0.0	0.0	new
CT-CT-S-C	0.925	-0.576	0.677	0.0	new
HC-CT-S-C	0.0	0.0	0.647	0.0	new
S=C-S-CT	0.0	6.5	0.0	0.0	new

<sup>a</sup> old parameters published in literatures.<sup>117,118,149</sup>

### Bond and Angle parameters for **B**<sup>a</sup>

Type	$r_{eq}$ or $\theta_{eq}$	$K_r$	Source <sup>b</sup>
CA-CA	1.412	469.0	new
CA-NC	1.369	483.0	new
CA-NN	1.320	483.0	new
CT-NN	1.448	483.0	new
CT-C	1.500	317.0	new
NC-C -CT	116.6	700.0	new
NC-C -O	122.5	80.0	new
O -C -CT	120.4	80.0	old
CT-NN-CT	119.0	60.0	new
CT-NN-CT	108.0	60.0	new
in five-membered ring			
CA-NN-CA	117.6	150.0	new

<sup>a</sup> only listing parameters different from **A**; <sup>b</sup> old parameters published in literatures.<sup>117,118,149</sup>

### Dihedral angle parameters for **B**<sup>a</sup>

Dihedral angle	V1	V2	V3	V4	Source <sup>b</sup>
CA-CA-NN-CT	0.0	4.50	1.0	0.0	new
CA-NC-C -O	0.0	7.5	0.0	0.0	new
CA-NC-C -CT	0.0	14.0	0.0	0.0	new
O -C -CT-HC	0.0	0.0	0.0	0.0	new
NN-CT-CT-OH	7.5	0.0	3.0	0.0	new
NC-C -CT-HC	0.0	0.0	0.0	0.0	new

<sup>a</sup> only listing parameters different from **A**; <sup>b</sup> old parameters published in literatures.<sup>117,118,149</sup>

### How to run conformational search by BOSS4.6?

The Z-matrix for the BOSS input file can be converted from **PDB** or **mol** file by **xPDBZ** or **xMOLZ** scripts included in the BOSS4.6 program suit. The atom type and parameters should be described in the parameter files. The correct atom type No. for each atom is required to be specified manually in BOSS input file, which should correspond to the atom type No. in the parameter file. First of all, all charges are set to zero in the parameter file, CM1 charges can be calculated by script **xAM1CM1**, and then the obtained CM1A charges are inserted in the parameter file. Then a Monte Carlo conformational search can be run by script **xCS** included in the BOSS4.6 program suit, and the number of trial structures can be varied by changing variable “configurations” in script **xCS**. Monte Carlo conformational searching results are written to the **\*.out** file and the Cartesian coordinates of all optimized conformers are summarized in the **\*.plt** file in **mol** format. The utility program **csmol** in the BOSS4.6 program suit is used to separate the concatenated **\*.plt.mol** file.

## 9.6 Computational Details for Chapter 6

Stationary points (reactant, product and transition state geometries) were optimized and characterized by frequency analysis at the B3LYP/6-31G(d) level of theory. The conformational space of transition states TS **65** and TS **67** for catalyst **59a** with substrate **60** has initially been studied with the OPLS-AA force field as implemented in BOSS 4.6.<sup>117</sup> The conformational space of transition state TS **67** for catalyst **59b** and **59c** with substrate **60** has also initially been studied with the OPLS-AA force field. In order to save computational cost, the structures of transition state TS **67** for catalyst **59a** with substrates **70** – **72** were initially built based on the best conformers of TS **67** for catalyst **59a** with substrate **60** and then reoptimized at the B3LYP/6-31G(d) level of theory. A similar technique was used to obtain TS **67** for the new suggested catalyst **59d**. Potential parameters for the description of 4-aminopyridines and their acetylpyridinium cations are currently not part of the default OPLS-AA force field.<sup>118</sup> The nitrogen atom attached to C4 of the pyridine ring has therefore been defined in the section 9.5. Appropriate force field parameters for the transition states have then been developed from a series of *ab initio* calculations at the B3LYP/6-31G(d) level of theory. Coulomb parameters have been derived using the CM1 procedure with the AM1 wavefunction. The conformational space of both types of species has then been searched using the Monte Carlo conformational search facility implemented in BOSS 4.6. The energetically most favorable conformers identified in this way have subsequently been reoptimized at the B3LYP/6-31G(d) level of theory, and single point calculations have been performed at the B3LYP/6-311+G(d, p) level of theory with Gaussian 03 D.01.<sup>148</sup> Dispersion corrections to DFT (termed DFT-D) proposed by S. Grimme<sup>150</sup> were used to calculate the accurate dispersion interaction by the ORCA 2.6.4 program package.<sup>151</sup> Thermochemical corrections to free energies ( $G_{298}$ ) and enthalpies at 298.15 K ( $H_{298}$ ) have been calculated at the same level as that used for geometry optimization.

**Table A9.6.1.** Comparison of Experimental Values with Calculated Energy Difference (in kJ/mol) for the Diastereomers of TS **67**, TS **65** and Intermediate **66** of Catalyst **59a**, Respectively.<sup>a</sup>

Cat.	Sub.	Experimental (195 K)			TS ( <b>67</b> )	
		<i>s</i>	$\Delta G_{\text{exp}}$	$\Delta G_{195}$	$\Delta G_{298}$	$\Delta H_{298}$
<b>59a</b>	<b>60</b>	24	5.16	5.82	5.65	6.13
					TS ( <b>65</b> )	
				3.2	0.92	7.57
				Intermediate ( <b>66</b> )		
				2.3	1.35	4.15

<sup>a</sup> Using the best conformers identified at the B3LYP/6-311+G(d,p)/B3LYP/6-31G(d) level of theory.

**Table A9.6.2.** Comparison of Experimental and Calculated Energy Difference (in kJ/mol) for the Diastereomers of TS **67** for Catalysts **59a** -**59c**.

Cat.	Experimental (195 K)		Theoretical <sup>a</sup>		
	<i>s</i>	$\Delta G_{\text{exp}}$	<i>s</i>	$\Delta G_{195}$	$\Delta H_{195}$
<b>59a</b>	24	5.16	110.6	7.63	5.99
<b>59b</b>	10	3.74	74.1	6.98	6.26
<b>59c</b>	3.5	2.03	457.1	9.93	5.43

<sup>a</sup> Frequency calculations recalculated at 195 K and obtained thermal corrections at 195 K at the B3LYP/6-31G(d) level of theory, where the  $\Delta G_{195}$  and  $\Delta H_{195}$  are different from those estimated  $\Delta G_{195}$  and  $\Delta H_{195}$  shown in Table 6.2.

## 9.7 Computational Details for Chapter 7

Geometry optimizations of all systems have been performed at the RHF/6-31G(d) and the B98/6-31G(d) level of theory. Thermochemical corrections to enthalpies at 298.15 K have been calculated at the same level of theory using the rigid rotor/harmonic oscillator model. Single point calculations at MP2(FC)/6-31+G(2d,p) level have been calculated based on the B98/6-31G(d) geometries. Combination of these energies with thermochemical corrections obtained at B98/6-31G(d) level yield enthalpies described as " $H_{298}(\text{MP2(FC)/6-31+G(2d,p)/B98/6-31G(d)})$ " in the text. For the four best conformers obtained at MP2(FC)/6-31+G(2d,p)/B98/6-31G(d) level refined relative enthalpies have been calculated using the G3(MP2)B3 compound method developed by Curtiss *et al.*<sup>40,68</sup> For the sake of consistency identical B98/6-31G(d) geometries were used in the MP2(FC)/6-31+G(2d,p) and G3(MP2)B3 calculations. Solvent effects have been calculated using the PCM continuum solvation model in its IEF-PCM incarnation<sup>139,141,152</sup> in combination with UAHF radii.<sup>139,140</sup> All calculations have been performed with Gaussian 03, Revision D.01.<sup>148</sup>

**Table 9.7.1.** Relative energies (kJ/mol) of isomers of I -VIII of compound **73** in the gas phase and in water.<sup>a</sup>

Isomer	G3MP2B3	MP2	G3MP2B3	PCM												
	$\Delta H_{298}^b$ (gas)	$\Delta H_{298}^c$ (water)	$\Delta H_{298}^d$ (water)	$\Delta G_{\text{solv}}$	$\Delta H_{298}^e$ (water)	$\Delta H_{298}^f$ (water)	$\Delta G_{\text{solv}}$	$\Delta H_{298}^g$ (water)	$\Delta H_{298}^h$ (water)	$\Delta G_{\text{solv}}$	$\Delta H_{298}^i$ (water)	$\Delta H_{298}^j$ (water)	$\Delta G_{\text{solv}}$			
	gas phase geometries				solution phase geometries				gas phase geometries				solution phase geometries			
I	0.1	0.5	-0.1	-78.2	0.4	-0.2	-77.2	-0.6	-1.6	-72.9	-1.2	-2.1	-76.6			
II	21.8	34.5	29.7	-71.0	36.7	31.8	-67.8	35.1	29.6	-63.2	37.0	31.6	-64.4			
III	0.0	0.0	0.0	-79.8	0.0	0.0	-78.7	0.0	0.0	-70.1	0.0	0.0	-73.3			
IV	22.9	25.4	15.2	-86.2	28.3	19.9	-81.6	27.5	17.5	-77.2	29.1	19.3	-78.6			
V	2.5	10.8	10.2	-77.2	10.0	9.5	-76.8	9.3	8.1	-71.4	8.3	7.1	-75.6			
VI	14.6	29.9	25.7	-67.1	31.6	27.4	-64.2	29.6	24.7	-60.1	31.6	26.7	-61.3			
VII	-12.3	-1.7	2.8	-63.7	0.7	4.5	-60.9	-4.1	-0.9	-59.5	-3.5	-0.3	-62.1			
VIII	29.7	40.0	29.9	-82.6	42.1	32.1	-80.5	41.3	30.6	-74.0	42.0	30.6	-77.2			

<sup>a</sup> Using the best conformer of III as the reference; <sup>b</sup> The best conformer G3MP2B3 gas phase data; <sup>c</sup> Sum of  $H_{298}$ (gas phase, MP2/6-31G+(2d,p)//B98/6-31G(d)) and  $\Delta G_{\text{solv}}$  calculated at PCM/UAHF/RHF/6-31G(d)//B98/6-31G(d) level; <sup>d</sup> Sum of  $H_{298}$ (gas phase, G3MP2B3) and  $\Delta G_{\text{solv}}$  calculated at PCM/UAHF/HF/6-31G(d)//B98/6-31G(d) level; <sup>e</sup> Sum of  $H_{298}$ (gas phase, MP2/6-31G+(2d,p)//B98/6-31G(d)) and  $\Delta G_{\text{solv}}$  calculated at PCM/UAHF/RHF/6-31G(d)//PCM/UAHF/B98/6-31G(d) level; <sup>f</sup> Sum of  $H_{298}$ (gas phase, G3MP2B3) and  $\Delta G_{\text{solv}}$  calculated at PCM/UAHF/HF/6-31G(d)//PCM/UAHF/B98/6-31G(d) level; <sup>g</sup> Sum of  $H_{298}$ (gas phase, MP2/6-31G+(2d,p)//B98/6-31G(d)) and  $\Delta G_{\text{solv}}$  calculated at PCM/UAHF/B98/6-31G(d)//B98/6-31G(d) level; <sup>h</sup> Sum of  $H_{298}$ (gas phase, G3MP2B3) and  $\Delta G_{\text{solv}}$  calculated at PCM/UAHF/B98/6-31G(d)//B98/6-31G(d) level; <sup>i</sup> Sum of  $H_{298}$ (gas phase, MP2/6-31G+(2d,p)//B98/6-31G(d)) and  $\Delta G_{\text{solv}}$  calculated at PCM/UAHF/B98/6-31G(d)//PCM/UAHF/B98/6-31G(d) level; <sup>j</sup> Sum of  $H_{298}$ (gas phase, G3MP2B3) and  $\Delta G_{\text{solv}}$  calculated at PCM/UAHF/B98/6-31G(d)//PCM/UAHF/B98/6-31G(d) level.

## 9.8 Energies of All Compounds

**Table A1.** Energy Components (in Hartree) Used in Compound Methods.

	$E_{\text{MP2/6-311G(d,p)}}$	$E_{\text{MP4/6-311G(d,p)}}$	$E_{\text{QCISD(T)}}$	$E_{\text{MP2/6-311+G(d,p)}}$	$E_{\text{MP4/6-311+G(d,p)}}$	$E_{\text{MP2/6-311G(2df,p)}}$	$E_{\text{MP4/6-311G(2df,p)}}$	$E$ (G2)			
<b>CH<sub>3</sub><sup>+</sup></b>	-39.356173	-39.3796871	-39.3810565	-39.3563022	-39.379823	-39.3693997	-39.3935637	-39.375147	-39.385587		
<b>NH<sub>3</sub></b>	-56.408752	-56.4280383	-56.4284262	-56.4152414	-56.4343359	-56.4356164	-56.456560	-56.450543	-56.458644		
<b>NH<sub>3</sub>-CH<sub>3</sub><sup>+</sup></b>	-95.949810	-95.9895208	-95.9907232	-95.9506444	-95.9904424	-95.9910081	-96.0329236	-96.005603	-96.007798		
<b>PH<sub>3</sub></b>	-342.612249	-342.641293	-342.643089	-342.612962	-342.642092	-342.638995	-342.672753	-342.646761	-342.679022		
<b>PH<sub>3</sub>-CH<sub>3</sub><sup>+</sup></b>	-382.148413	-382.195036	-382.197122	-382.149572	-382.196325	-382.191011	-382.196325	-382.204451	-382.229601		
	$E_{\text{MP2/6-31G(d)}}$	$E_{\text{MP4/6-31G(d)}}$	$E_{\text{QCISD(T)}}$	$E_{\text{MP2/6-31+G(d)}}$	$E_{\text{MP4/6-31+G(d)}}$	$E_{\text{MP2/6-31G(2df,p)}}$	$E_{\text{MP4/6-31G(2df,p)}}$	$E_{\text{MP2/GTLarge}}$	$E$ (G3)		
<b>CH<sub>3</sub><sup>+</sup></b>	-39.325375	-39.3461692	-39.3474594	-39.3257779	-39.3466708	-39.3602393	-39.3842278	-39.4161441	-39.4305791		
<b>NH<sub>3</sub></b>	-56.354212	-56.3712589	-56.3720978	-56.3630364	-56.3800587	-56.4148069	-56.4354807	-56.4930272	-56.5070204		
<b>NH<sub>3</sub>-CH<sub>3</sub><sup>+</sup></b>	-95.868201	-95.903027	-95.9048088	-95.8700788	-95.9052871	-95.9632777	-96.0043073	-96.0896105	-96.1014963		
<b>PH<sub>3</sub></b>	-342.551705	-342.578315	-342.580626	-342.553371	-342.580063	-342.612923	-342.646168	-342.940711	-342.978514		
<b>PH<sub>3</sub>-CH<sub>3</sub><sup>+</sup></b>	-382.054772	-382.096063	-382.098770	-382.056589	-382.098133	-382.155787	-382.205766	-382.539553	-382.574097		
	$E_{\text{MP2/6-31G(d)}}$	$E_{\text{MP4/6-31G(d)}}$	$E_{\text{QCISD(T)}}$	$E_{\text{MP2/6-31+G(d)}}$	$E_{\text{MP4/6-31+G(d)}}$	$E_{\text{MP2/6-31G(2df,p)}}$	$E_{\text{MP4/6-31G(2df,p)}}$	$E_{\text{MP2/GTLarge}}$	$E$ (G3B3)		
<b>CH<sub>3</sub><sup>+</sup></b>	-39.325307	-39.3462055	-39.3475151	-39.3257113	-39.3467107	-39.3601836	-39.3842477	-39.4159518	-39.4313689		
<b>NH<sub>3</sub></b>	-56.3541849	-56.3713001	-56.3721478	-56.3629145	-56.380006	-56.4147932	-56.4355054	-56.492865	-56.508301		
<b>NH<sub>3</sub>-CH<sub>3</sub><sup>+</sup></b>	-95.868174	-95.903068	-95.9048591	-95.8700568	-95.9053365	-95.9631954	-96.0042907	-96.0894534	-96.103415		
<b>PH<sub>3</sub></b>	-342.551493	-342.578347	-342.580723	-342.553127	-342.580064	-342.612745	-342.646094	-342.940462	-342.980048		
<b>PH<sub>3</sub>-CH<sub>3</sub><sup>+</sup></b>	-382.054650	-382.096185	-382.098925	-382.056463	-382.098254	-382.155524	-382.205676	-382.538965	-382.576073		
	$E_{\text{SCF(D)}}$	$E_{\text{SCF(T)}}$	$E_{\text{SCF(Q)}}$	$E_{\text{CCSD(D)}}$	$E_{\text{CCSD(T)}}$	$E_{\text{CCSD(Q)}}$	$E_{\text{CCSD(T)(D)}}$	$E_{\text{CCSD(T)(T)}}$	$E_{\text{nocore}}$	$E_{\text{core+relativistic}}$	$E(\text{W1})$
<b>CH<sub>3</sub><sup>+</sup></b>	-39.235814	-39.247671	-39.249979	-39.367153	-39.402063	-39.410925	-39.369119	-39.405138	-39.408494	-39.472562	-39.483495
<b>NH<sub>3</sub></b>	-56.204899	-56.220044	-56.223777	-56.417907	-56.471167	-56.486415	-56.423109	-56.479421	-56.479725	-56.561568	-56.586358
<b>NH<sub>3</sub>-CH<sub>3</sub><sup>+</sup></b>	-95.591187	-95.618280	-95.624515	-95.955712	-96.046293	-96.071399	-95.964859	-96.060175	-96.067344	-96.214075	-96.248084
<b>PH<sub>3</sub></b>	-342.480525	-342.490809	-342.493955	-342.652845	-342.692440	-342.702993	-342.657635	-342.699626	-342.698609	-343.815853	-343.834150
<b>PH<sub>3</sub>-CH<sub>3</sub><sup>+</sup></b>	-381.866048	-381.890040	-381.895946	-382.187554	-382.266499	-382.287628	-382.196452	-382.279392	-382.281795	-383.463072	-383.495102

**Table A2.** Total Energies, Enthalpies, Free energies (in Hartree).

system	PBEPBE/6-31++G(d, p)			MPWB95/6-31++G(d, p)			B3LYP/6-31++G(d, p)		
	$E_{\text{tot}}$	$H_{298}$	$G_{298}$	$E_{\text{tot}}$	$H_{298}$	$G_{298}$	$E_{\text{tot}}$	$H_{298}$	$G_{298}$
$\text{CH}_3^+$	-39.4114936	-39.377083	-39.400000	-39.4455635	-39.411277	-39.434192	-39.484827	-39.449647	-39.472537
$\text{NH}_3$	-56.4901538	-56.452683	-56.474560	-56.5362699	-56.498932	-56.520808	-56.5671081	-56.528897	-56.550750
$\text{NH}_3\text{-CH}_3^+$	-96.0913366	-96.009312	-96.036936	-96.1681475	-96.086417	-96.114045	-96.2282966	-96.144459	-96.172058
$\text{PH}_3$	-342.9536698	-342.926500	-342.950396	-343.1524863	-343.125449	-343.149341	-343.146994	-343.119135	-343.142992
$\text{PH}_3\text{-CH}_3^+$	-382.5479531	-382.479220	-382.508961	-382.7771739	-382.708621	-382.738363	-382.8017229	-382.731269	-382.760923
	B98/6-31G(d)			B98/6-31++G(d, p)			B98/6-31++G(2df, p)		
	$E_{\text{tot}}$	$H_{298}$	$G_{298}$	$E_{\text{tot}}$	$H_{298}$	$G_{298}$	$E_{\text{tot}}$	$H_{298}$	$G_{298}$
$\text{CH}_3^+$	-39.4629215	-39.427481	-39.450370	-39.4672005	-39.432002	-39.454894	-39.4678459	-39.432812	-39.455706
$\text{NH}_3$	-56.5246395	-56.486143	-56.507987	-56.5425519	-56.504184	-56.526035	-56.5450007	-56.506780	-56.528629
$\text{NH}_3\text{-CH}_3^+$	-96.1766453	-96.092221	-96.119817	-96.1895229	-96.105488	-96.133076	-96.1916132	-96.107929	-96.135526
$\text{PH}_3$	-343.0846545	-343.056498	-343.080340	-343.0910288	-343.063053	-343.086902	-343.0956863	-343.067855	-343.091706
$\text{PH}_3\text{-CH}_3^+$	-382.7205109	-382.649500	-382.679119	-382.7304879	-382.659938	-382.689591	-382.7380616	-382.667973	-382.697595
	B98/6-311+G(2df, p)			B98/cc-pVTZ+d					
	$E_{\text{tot}}$	$H_{298}$	$G_{298}$	$E_{\text{tot}}$	$H_{298}$	$G_{298}$			
$\text{CH}_3^+$	-39.474864	-39.439894	-39.462781	-39.4771006	-39.442169	-39.465054			
$\text{NH}_3$	-56.5596843	-56.521532	-56.543379	-56.5599807	-56.521833	-56.543673			
$\text{NH}_3\text{-CH}_3^+$	-96.2125935	-96.128946	-96.156545	-96.2179613	-96.134335	-96.161955			
$\text{PH}_3$	-343.1198154	-343.092077	-343.115928	-343.1261069	-343.098235	-343.122080			
$\text{PH}_3\text{-CH}_3^+$	-382.7703092	-382.700328	-382.729936	-382.7789325	-382.708894	-382.738494			

Table A2. Continued

	B3LYP/6-31G(d)			B3LYP/6-311++G(d, p)			B3LYP/cc-pVTZ+d		
	E <sub>tot</sub>	H <sub>298</sub>	G <sub>298</sub>	E <sub>tot</sub>	H <sub>298</sub>	G <sub>298</sub>	E <sub>tot</sub>	H <sub>298</sub>	G <sub>298</sub>
CH <sub>3</sub> <sup>+</sup>	-39.4803875	-39.44499	-39.466187	-39.4914712	-39.456518	-39.479406	-39.4951851	-39.460203	-39.483083
NH <sub>3</sub>	-56.5479476	-56.509624	-56.531469	-56.582722	-56.544638	-56.566488	-56.5847251	-56.546681	-56.568520
NH <sub>3</sub> <sup>-</sup> CH <sub>3</sub> <sup>+</sup>	-96.2148647	-96.130638	-96.158242	-96.2490586	-96.165513	-96.193107	-96.2576794	-96.174162	-96.201779
PH <sub>3</sub>	-343.1402806	-343.112204	-343.136055	-343.173329	-343.145604	-343.169464	-343.1824695	-343.154737	-343.178586
PH <sub>3</sub> -CH <sub>3</sub> <sup>+</sup>	-382.791348	-382.72045	-382.750089	-382.8349804	-382.764904	-382.794557	-382.8510126	-382.780989	-382.810592
	B3LYP/aug-cc-pVDZ+2df// B3LYP/6-31G(d)		B3LYP/6-31++G(2df,p)// B3LYP/6-31G(d)		B98/6-31++G(2df, p)// B98/6-31G(d)				
	E <sub>tot</sub>	H <sub>298</sub>	E <sub>tot</sub>	H <sub>298</sub>	E <sub>tot</sub>	H <sub>298</sub>			
CH <sub>3</sub> <sup>+</sup>	-39.4808922	-39.4454947	-39.4849782	-39.4495807	-39.467844	-39.432403			
NH <sub>3</sub>	-56.57075	-56.5324264	-56.56903	-56.5307064	-56.544909	-56.506412			
NH <sub>3</sub> <sup>-</sup> CH <sub>3</sub> <sup>+</sup>	-96.2271944	-96.1429677	-96.2295844	-96.1453577	-96.191588	-96.107164			
PH <sub>3</sub>	-343.1697534	-343.1416768	-343.1511162	-343.1230396	-343.095684	-343.067527			
PH <sub>3</sub> -CH <sub>3</sub> <sup>+</sup>	-382.8226991	-382.7518011	-382.8081611	-382.7372631	-382.737986	-382.666975			
	MP2(FC)/6-31G(d, p)			MP2(FC)/6-31++G(d, p)			MP2(FULL)/6-31++G(d, p)		
	E <sub>tot</sub>	H <sub>298</sub>	G <sub>298</sub>	E <sub>tot</sub>	H <sub>298</sub>	G <sub>298</sub>	E <sub>tot</sub>	H <sub>298</sub>	G <sub>298</sub>
CH <sub>3</sub> <sup>+</sup>	-39.3466256	-39.310184	-39.333043	-39.3474824	-39.311036	-39.333896	-39.3521523	-39.315671	-39.338528
NH <sub>3</sub>	-56.3832165	-56.343945	-56.365771	-56.3925249	-56.353408	-56.375240	-56.3963329	-56.357181	-56.379011
NH <sub>3</sub> <sup>-</sup> CH <sub>3</sub> <sup>+</sup>	-95.9164643	-95.830482	-95.858001	-95.9183628	-95.832597	-95.860124	-95.9276312	-95.841765	-95.869288
PH <sub>3</sub>	-342.5785766	-342.549520	-342.573329	-342.5805271	-342.551515	-342.575324	-342.5928861	-342.563802	-342.587610
PH <sub>3</sub> -CH <sub>3</sub> <sup>+</sup>	-382.1030677	-382.030199	-382.059682	-382.1055001	-382.032807	-382.062296	-382.1237074	-382.050872	-382.080340

Table A2. Continued

	MP2(FC)/aug-cc-pVDZ			MP2(FC)/aug-cc-pVTZ				
	E <sub>tot</sub>	H <sub>298</sub>	G <sub>298</sub>	E <sub>tot</sub>	H <sub>298</sub>	G <sub>298</sub>		
CH <sub>3</sub> <sup>+</sup>	-39.3451925	-39.309465	-39.332363	-39.380956	-39.345242	-39.368108		
NH <sub>3</sub>	-56.4048893	-56.366718	-56.388579	-56.4605409	-56.422151	-56.443989		
NH <sub>3</sub> <sup>-</sup> CH <sub>3</sub> <sup>+</sup>	-95.9266144	-95.842460	-95.870034	-96.0208043	-95.936293	-95.963871		
PH <sub>3</sub>	-342.6140542	-342.585821	-342.609687	-342.6612883	-342.632914	-342.656750		
PH <sub>3</sub> -CH <sub>3</sub> <sup>+</sup>	-382.1327532	-382.062067	-382.091692	-382.2235166	-382.152281	-382.181818		
	MP2(FC)/6-311G(d, p)// MP2(FULL)/6-31G(d)		MP2(FC)/6-311+G(d, p)// MP2(FULL)/6-31G(d)		MP2(FC)/6-311G(2df, p)// MP2(FULL)/6-31G(d)		MP2(FC)/6-311+G(3df, 2p)// MP2(FULL)/6-31G(d)	
	E <sub>tot</sub>	H <sub>298</sub>	E <sub>tot</sub>	H <sub>298</sub>	E <sub>tot</sub>	H <sub>298</sub>	E <sub>tot</sub>	H <sub>298</sub>
CH <sub>3</sub> <sup>+</sup>	-39.3561733	-39.32227117	-39.3563022	-39.32240007	-39.3693997	-39.33549757	-39.3751466	-39.34124447
NH <sub>3</sub>	-56.4087524	-56.37190527	-56.4152414	-56.37839427	-56.4356164	-56.39876927	-56.4505427	-56.41369557
NH <sub>3</sub> <sup>-</sup> CH <sub>3</sub> <sup>+</sup>	-95.9498098	-95.86932567	-95.9506444	-95.87016027	-95.9910081	-95.91052397	-96.0056033	-95.92511917
PH <sub>3</sub>	-342.6122485	-342.5850134	-342.6129617	-342.5857266	-342.6389946	-342.6117595	-342.6467605	-342.6195254
PH <sub>3</sub> -CH <sub>3</sub> <sup>+</sup>	-382.1484134	-382.0803303	-382.149572	-382.0814889	-382.1910109	-382.1229278	-382.2044508	-382.1363677
	MP2(FC)/AVDZ+2df// B3LYP/cc-pVTZ+d		MP2(FC)/AVTZ+2df// B3LYP/cc-pVTZ+d		MP2(FC)/AVQZ+2df// B3LYP/cc-pVTZ+d		MP2(FULL)/6-31G(d) <sup>a</sup>	
	E <sub>tot</sub>	H <sub>298</sub>	E <sub>tot</sub>	H <sub>298</sub>	E <sub>tot</sub>	H <sub>298</sub>	E <sub>tot</sub>	H <sub>298</sub>
CH <sub>3</sub> <sup>+</sup>	-39.3450761	-39.310094	-39.3809167	-39.3459346	-39.3913418	-39.3563597	-39.3294346	-39.29553247
NH <sub>3</sub>	-56.4048022	-56.3667581	-56.4605317	-56.4224876	-56.47774	-56.4396959	-56.3573778	-56.32053067
NH <sub>3</sub> <sup>-</sup> CH <sub>3</sub> <sup>+</sup>	-95.9263483	-95.8428309	-96.020752	-95.9372346	-96.049291	-95.9657736	-95.876174	-95.79568987
PH <sub>3</sub>	-342.6255651	-342.5978326	-342.6660404	-342.6383079	-342.6780135	-342.650281	-342.5622591	-342.535024

Table A2. Continued

$\text{PH}_3\text{-CH}_3^+$	-382.1480408	-382.0780172	-382.2299733	-382.1599497	-382.253881	-382.1838574	-382.0703814	-382.0022983
	SCS-MP2(FC)/AVDZ+2df// B3LYP/cc-pVTZ+d		SCS-MP2(FC)/AVTZ+2df// B3LYP/cc-pVTZ+d		SCS-MP2(FC)/AVQZ+2df// B3LYP/cc-pVTZ+d			
	$E_{\text{tot}}$	$H_{298}$	$E_{\text{tot}}$	$H_{298}$	$E_{\text{tot}}$	$H_{298}$		
$\text{CH}_3^+$	-39.35431818	-39.31933608	-39.39270271	-39.35772061	-39.40424974	-39.36926764		
$\text{NH}_3$	-56.40471108	-56.36666698	-56.46254896	-56.42450486	-56.48120973	-56.44316563		
$\text{NH}_3\text{-CH}_3^+$	-95.92998284	-95.84646544	-96.02823253	-95.94471513	-96.05922366	-95.97570626		
$\text{PH}_3$	-342.6333656	-342.6056331	-342.6765331	-342.6488006	-342.689805	-342.6620725		
$\text{PH}_3\text{-CH}_3^+$	-382.1579499	-382.0879263	-382.2445422	-382.1745186	-382.2708392	-382.2008156		
	MP2(FC)/6-31++G(d,p)// B98/6-31G(d)		MP2(FC)/6-31++G(2d,p)// B98/6-31G(d)		MP2(FC)/6-31+G(2d,p)// B98/6-31G(d)		CCSD(T)/aug-cc-pVQZ	
	$E_{\text{tot}}$	$H_{298}$	$E_{\text{tot}}$	$H_{298}$	$E_{\text{tot}}$	$H_{298}$	$E_{\text{tot}}$	$H_{298}$
$\text{CH}_3^+$	-39.3472954	-39.3118544	-39.35271	-39.317269	-39.3523703	-39.3169293	-39.41446811	-39.38056598
$\text{NH}_3$	-56.3922142	-56.3537172	-56.4084832	-56.3699862	-56.4081946	-56.3696976	-56.49520549	-56.45835836
$\text{NH}_3\text{-CH}_3^+$	-95.9181921	-95.8337681	-95.9378347	-95.8534107	-95.9373165	-95.8528925	-96.08694074	-96.00645661
$\text{PH}_3$	-342.58018	-342.552023	-342.5944711	-342.566314	-342.5942623	-342.5661053	-342.7093457	-342.6821105
$\text{PH}_3\text{-CH}_3^+$	-382.105133	-382.0341218	-382.1253799	-382.054369	-382.1248738	-382.0538628	-382.299433	-382.2313498

**Table A3.** Energy Components (in Hartree) Used in Compound Methods.

	$E_{\text{MP2/6-311G(d,p)}}$	$E_{\text{MP4/6-311G(d,p)}}$	$E_{\text{QCISD(T)}}$	$E_{\text{MP2/6-311+G(d,p)}}$	$E_{\text{MP4/6-311+G(d,p)}}$	$E_{\text{MP2/6-311G(2df,p)}}$	$E_{\text{MP4/6-311G(2df,p)}}$	$E_{\text{MP2/6-311+G(3df,2p)}}$	$E$ (G2)
<b>H<sub>2</sub>O</b>	-76.2636539	-76.2760675	-76.2760682	-76.2745467	-76.2869005	-76.2989426	-76.3134592	-76.3181084	-76.3320551
<b>H<sub>2</sub>O – CH<sub>3</sub><sup>+</sup></b>	-115.7418351	-115.7758378	-115.7765544	-115.7443563	-115.778578	-115.7930759	-115.8297244	-115.8088658	-115.8202133
<b>HF</b>	-100.2667223	-100.2737373	-100.2734582	-100.2784688	-100.3196208	-100.3099778	-100.3196208	-100.3291624	-100.3500024
<b>HF – CH<sub>3</sub><sup>+</sup></b>	-139.6794291	-139.7097307	-139.7099896	-139.6826326	-139.7134397	-139.7406416	-139.7741023	-139.7569892	-139.7804386
<b>H<sub>2</sub>S</b>	-398.8464033	-398.8708497	-398.871991	-398.8474222	-398.8720092	-398.8846984	-398.915636	-398.8931709	-398.9307055
<b>H<sub>2</sub>S – CH<sub>3</sub><sup>+</sup></b>	-438.3414728	-438.3869299	-438.3889048	-438.3428497	-438.3883975	-438.3949372	-438.4463998	-438.4082902	-438.4420025
<b>HCl</b>	-460.2439949	-460.2627779	-460.2633628	-460.2446732	-460.2636034	-460.2913067	-460.3184956	-460.2987361	-460.3401763
<b>HCl – CH<sub>3</sub><sup>+</sup></b>	-499.6800815	-499.7212771	-499.7229007	-499.6825626	-499.7239069	-499.7430762	-499.792483	-499.7574104	-499.7993944
<b>NH<sub>2</sub><sup>-</sup></b>	-55.7033584	-55.7206462	-55.7206628	-55.7550372	-55.7713574	-55.7358816	-55.7551733	-55.796123	-55.8174306
<b>NH<sub>2</sub><sup>-</sup> – CH<sub>3</sub><sup>+</sup></b>	-95.587429	-95.625426	-95.6262548	-95.5936211	-95.6316241	-95.6332419	-95.6736198	-95.6522254	-95.6669114
<b>OH<sup>-</sup></b>	-75.5734647	-75.5831861	-75.5829333	-75.6397948	-75.6497547	-75.6144489	-75.6267351	-75.688111	-75.7127714
<b>OH<sup>-</sup> – CH<sub>3</sub><sup>+</sup></b>	-115.4362047	-115.4684746	-115.4687664	-115.4448553	-115.4773327	-115.492731	-115.5278737	-115.5136598	-115.5349074
<b>F<sup>-</sup></b>	-99.6132607	-99.6170987	-99.6168155	-99.6786867	-99.6844252	-99.661476	-99.6683231	-99.7321343	-99.7605987
<b>F<sup>-</sup> – CH<sub>3</sub><sup>+</sup></b>	-139.4379569	-139.4662011	-139.4660127	-139.4471949	-139.4759304	-139.5049317	-139.5366384	-139.5250964	-139.5542149
<b>PH<sub>2</sub><sup>-</sup></b>	-342.007302	-342.0325443	-342.0338521	-342.0110183	-342.0366089	-342.0427836	-342.0735216	-342.054701	-342.0949421
<b>PH<sub>2</sub><sup>-</sup> – CH<sub>3</sub><sup>+</sup></b>	-381.8099322	-381.8560422	-381.8580367	-381.8111779	-381.8574545	-381.8569491	-381.9082766	-381.8699132	-381.9060371
<b>SH<sup>-</sup></b>	-398.270903	-398.2908558	-398.2916407	-398.2732325	-398.2935269	-398.318382	-398.3452208	-398.3292224	-398.3715768
<b>SH<sup>-</sup> – CH<sub>3</sub><sup>+</sup></b>	-438.0349851	-438.0367079	-438.0784717	-438.0367079	-438.078974	-438.0941867	-438.1432716	-438.1070487	-438.1484647
<b>Cl<sup>-</sup></b>	-459.7002638	-459.7142799	-459.7145205	-459.7035702	-459.7181627	-459.7565305	-459.7792463	-459.7654629	-459.8089958
<b>Cl<sup>-</sup> – CH<sub>3</sub><sup>+</sup></b>	-499.4262789	-499.4632312	-499.4642332	-499.4284828	-499.46574	-499.4958597	-499.5418767	-499.5078424	-499.5538301

Table A3. Continued

	$E_{\text{MP2/6-31G(d)}}$	$E_{\text{MP4/6-31G(d)}}$	$E_{\text{QCISD(T)}}$	$E_{\text{MP2/6-31+G(d)}}$	$E_{\text{MP4/6-31+G(d)}}$	$E_{\text{MP2/6-31G(2df,p)}}$	$E_{\text{MP4/6-31G(2df,p)}}$	$E_{\text{MP2/GTLarge}}$	$E(\text{G3})$
<b>H<sub>2</sub>O</b>	-76.1968478	-76.2073266	-76.2078917	-76.209702	-76.2203046	-76.2670957	-76.281815	-76.3616032	-76.3820445
<b>H<sub>2</sub>O – CH<sub>3</sub><sup>+</sup></b>	-115.6458511	-115.6752243	-115.6765192	-115.6501491	-115.6800422	-115.7531739	-115.7895456	-115.8932148	-115.9148666
<b>HF</b>	-100.1821715	-100.1884344	-100.1884269	-100.2028717	-100.2095363	-100.2532943	-100.2639553	-100.3733753	-100.4011055
<b>HF – CH<sub>3</sub><sup>+</sup></b>	-139.5717365	-139.5984594	-139.5987566	-139.5787823	-139.6063009	-139.6803946	-139.7145114	-139.8421534	-139.8762893
<b>H<sub>2</sub>S</b>	-398.7884133	-398.8119981	-398.8133937	-398.7901901	-398.8138912	-398.8541231	-398.8850194	-399.1951051	-399.2383723
<b>H<sub>2</sub>S – CH<sub>3</sub><sup>+</sup></b>	-438.2506351	-438.2922796	-438.2946316	-438.2526567	-438.2945658	-438.3550781	-438.4057343	-438.7513225	-438.7944814
<b>HCl</b>	-460.1923572	-460.210878	-460.2115698	-460.194414	-460.2130797	-460.2555299	-460.2828801	-460.6074144	-460.6546645
<b>HCl – CH<sub>3</sub><sup>+</sup></b>	-499.5951716	-499.6332052	-499.6349421	-499.5975385	-499.6358842	-499.6992388	-499.7481471	-500.1067473	-500.1582113
<b>NH<sub>2</sub><sup>-</sup></b>	-55.6469426	-55.6625353	-55.6630989	-55.7076649	-55.7225299	-55.7058268	-55.7250843	-55.8362354	-55.8638397
<b>NH<sub>2</sub><sup>-</sup> – CH<sub>3</sub><sup>+</sup></b>	-95.5065291	-95.5398446	-95.5413523	-95.5155673	-95.5492274	-95.6017196	-95.6411677	-95.7356467	-95.7601223
<b>OH<sup>-</sup></b>	-75.5131415	-75.5213761	-75.521828	-75.5883569	-75.5966723	-75.5744104	-75.5873945	-75.7287895	-75.7602389
<b>OH<sup>-</sup> – CH<sub>3</sub><sup>+</sup></b>	-115.3461339	-115.3738528	-115.3748548	-115.357706	-115.3859979	-115.4490143	-115.4837442	-115.5976121	-115.6292246
<b>F<sup>-</sup></b>	-99.5266066	-99.5307477	-99.530704	-99.6238467	-99.62975	-99.5837754	-99.5927206	-99.7736485	-99.8091883
<b>F<sup>-</sup> – CH<sub>3</sub><sup>+</sup></b>	-139.3358539	-139.3606801	-139.3605832	-139.3532406	-139.3788664	-139.4385448	-139.4708204	-139.6098531	-139.6496423
<b>PH<sub>2</sub><sup>-</sup></b>	-341.9406873	-341.9646155	-341.966272	-341.9612127	-341.9855402	-342.0023881	-342.0333789	-342.3499756	-342.3964133
<b>PH<sub>2</sub><sup>-</sup> – CH<sub>3</sub><sup>+</sup></b>	-381.7211928	-381.7628851	-381.7654993	-381.7245506	-381.7665403	-381.8197833	-381.8702134	-382.2055908	-382.2512697
<b>SH<sup>-</sup></b>	-398.2104514	-398.2299729	-398.2308468	-398.2296044	-398.2495555	-398.2739882	-398.3013357	-398.6320254	-398.6806093
<b>SH<sup>-</sup> – CH<sub>3</sub><sup>+</sup></b>	-437.9526647	-437.9914968	-437.9932967	-437.955745	-437.9949283	-438.053285	-438.1017907	-438.4505858	-438.501628
<b>Cl<sup>-</sup></b>	-459.6521044	-459.6662592	-459.6665483	-459.6711454	-459.6858399	-459.7082425	-459.7314657	-460.0746719	-460.1235999
<b>Cl<sup>-</sup> – CH<sub>3</sub><sup>+</sup></b>	-499.3545576	-499.388677	-499.3898387	-499.3574609	-499.3919573	-499.4506048	-499.4962323	-499.8574906	-499.9130225

Table A3. Continued

	E <sub>MP2/6-31G(d)</sub>	E <sub>MP4/6-31G(d)</sub>	E <sub>QCISD(T)</sub>	E <sub>MP2/6-31+G(d)</sub>	E <sub>MP4/6-31+G(d)</sub>	E <sub>MP2/6-31G(2df,p)</sub>	E <sub>MP4/6-31G(2df,p)</sub>	E <sub>MP2/GTLarge</sub>	E (G3B3)
<b>H<sub>2</sub>O</b>	-76.1968451	-76.2073245	-76.2078898	-76.2096739	-76.220278	-76.2671089	-76.2818268	-76.3615987	-76.3837249
<b>H<sub>2</sub>O – CH<sub>3</sub><sup>+</sup></b>	-115.645785	-115.6752171	-115.6765104	-115.6500936	-115.680049	-115.7531439	-115.7895811	-115.8931989	-115.9169751
<b>HF</b>	-100.1821715	-100.1884343	-100.1884268	-100.2028711	-100.2095356	-100.2532962	-100.2639572	-100.3733769	-100.4027805
<b>HF – CH<sub>3</sub><sup>+</sup></b>	-139.5716854	-139.598521	-139.5988308	-139.5788377	-139.6064741	-139.6803758	-139.714602	-139.842112	-139.8778114
<b>H<sub>2</sub>S</b>	-398.7883098	-398.812039	-398.8134686	-398.7900884	-398.8139354	-398.8539529	-398.8849269	-399.1948494	-399.2398373
<b>H<sub>2</sub>S – CH<sub>3</sub><sup>+</sup></b>	-438.2502873	-438.292295	-438.2947189	-438.2523044	-438.2945826	-438.3547596	-438.4057129	-438.7506468	-438.796703
<b>HCl</b>	-460.1923035	-460.2108867	-460.2115945	-460.1943718	-460.2131004	-460.2554106	-460.2827982	-460.6072522	-460.6561245
<b>HCl – CH<sub>3</sub><sup>+</sup></b>	-499.5945306	-499.6329972	-499.634839	-499.5969146	-499.6357028	-499.6985248	-499.7478978	-500.1057431	-500.1600253
<b>NH<sub>2</sub><sup>-</sup></b>	-55.6468384	-55.6626363	-55.6632096	-55.7070814	-55.7221122	-55.7055258	-55.7249224	-55.835573	-55.8648525
<b>NH<sub>2</sub><sup>-</sup> – CH<sub>3</sub><sup>+</sup></b>	-95.5064917	-95.5398909	-95.5414081	-95.5155238	-95.5492689	-95.6016371	-95.6411381	-95.7354694	-95.7623002
<b>OH<sup>-</sup></b>	-75.5131039	-75.5214157	-75.5218792	-75.5882803	-75.5966461	-75.5741983	-75.5872386	-75.7285308	-75.7616558
<b>OH<sup>-</sup> – CH<sub>3</sub><sup>+</sup></b>	-115.3460757	-115.3738476	-115.374855	-115.3575822	-115.3859276	-115.4490037	-115.4837592	-115.5974953	-115.6317384
<b>F<sup>-</sup></b>	-99.5266066	-99.5307477	-99.530704	-99.6238467	-99.62975	-99.5837754	-99.5927206	-99.7736485	-99.8114563
<b>F<sup>-</sup> – CH<sub>3</sub><sup>+</sup></b>	-139.3357595	-139.3606356	-139.3605501	-139.3529295	-139.3785973	-139.438607	-139.4708966	-139.6096806	-139.6520607
<b>PH<sub>2</sub><sup>-</sup></b>	-341.9405805	-341.9646649	-341.9663609	-341.9610292	-341.98551	-342.0020599	-342.0331555	-342.3495878	-342.3976641
<b>PH<sub>2</sub><sup>-</sup> – CH<sub>3</sub><sup>+</sup></b>	-381.720988	-381.7629753	-381.7656533	-381.7243382	-381.7666251	-381.8195179	-381.8701407	-382.2050579	-382.2532821
<b>SH<sup>-</sup></b>	-398.210406	-398.2300052	-398.2308956	-398.2295509	-398.2495753	-398.2738123	-398.3012183	-398.6318269	-398.6819578
<b>SH<sup>-</sup> – CH<sub>3</sub><sup>+</sup></b>	-437.9524538	-437.9915533	-437.993397	-437.9555565	-437.9950132	-438.0529778	-438.1017083	-438.4499936	-438.5036817
<b>Cl<sup>-</sup></b>	-459.6521044	-459.6662592	-459.6665483	-459.6711454	-459.6858399	-459.7082425	-459.7314657	-460.0746719	-460.1258679
<b>Cl<sup>-</sup> – CH<sub>3</sub><sup>+</sup></b>	-499.3543147	-499.3886843	-499.3898784	-499.357256	-499.392009	-499.4503507	-499.4962149	-499.8570295	-499.9151909

Table A3. Continued

	$E_{\text{SCF(D)}}$	$E_{\text{SCF(T)}}$	$E_{\text{SCF(Q)}}$	$E_{\text{CCSD(D)}}$	$E_{\text{CCSD(T)}}$	$E_{\text{CCSD(Q)}}$	$E_{\text{CCSD(T)(D)}}$	$E_{\text{CCSD(T)(T)}}$	$E_{\text{nocore}}$	$E_{\text{core+relativistic}}$	$E(\text{W1})$
<b>H<sub>2</sub>O</b>	-76.040697	-76.060203	-76.065649	-76.266789	-76.332818	-76.353858	-76.271707	-76.341387	-76.341421	-76.448751	-76.483034
<b>H<sub>2</sub>O – CH<sub>3</sub><sup>+</sup></b>	-115.365029	-115.398190	-115.406120	-115.740332	-115.844906	-115.875457	-115.749391	-115.859109	-115.867059	-116.039026	-116.080838
<b>HF</b>	-100.032733	-100.060691	-100.068237	-100.258414	-100.341565	-100.368821	-100.262400	-100.349072	-100.350619	-100.495430	-100.537719
<b>HF – CH<sub>3</sub><sup>+</sup></b>	-139.299620	-139.341267	-139.351342	-139.672125	-139.793305	-139.829715	-139.680493	-139.806656	-139.815071	-140.024194	-140.074443
<b>H<sub>2</sub>S</b>	-398.704016	-398.716159	-398.719392	-398.886787	-398.936111	-398.949439	-398.892156	-398.944944	-398.942619	-400.333038	-400.357604
<b>H<sub>2</sub>S – CH<sub>3</sub><sup>+</sup></b>	-438.043618	-438.069457	-438.075400	-438.382585	-438.470275	-438.493355	-438.392939	-438.485753	-438.487339	-439.942523	-439.979007
<b>HCl</b>	-460.095437	-460.108675	-460.112004	-460.280759	-460.338894	-460.356192	-460.285595	-460.347923	-460.345067	-462.072931	-462.104837
<b>HCl – CH<sub>3</sub><sup>+</sup></b>	-499.377995	-499.406305	-499.412324	-499.719313	-499.817764	-499.844172	-499.729504	-499.833883	-499.834825	-501.627345	-501.670256
<b>NH<sub>2</sub><sup>-</sup></b>	-55.534309	-55.547278	-55.550794	-55.760252	-55.810546	-55.825360	-55.768400	-55.822614	-55.787342	-55.868857	-55.928901
<b>NH<sub>2</sub><sup>-</sup> – CH<sub>3</sub><sup>+</sup></b>	-95.229871	-95.255240	-95.261360	-95.599455	-95.688874	-95.713927	-95.609755	-95.704399	-95.707773	-95.854415	-95.892353
<b>OH<sup>-</sup></b>	-75.394777	-75.411576	-75.416505	-75.633758	-75.696056	-75.716510	-75.641400	-75.708284	-75.667528	-75.774694	-75.849322
<b>OH<sup>-</sup> – CH<sub>3</sub><sup>+</sup></b>	-115.060812	-115.091825	-115.099473	-115.442193	-115.545136	-115.575604	-115.452303	-115.560902	-115.564710	-115.736727	-115.782829
<b>F<sup>-</sup></b>	-99.428282	-99.450807	-99.457462	-99.662690	-99.739301	-99.765819	-99.668634	-99.749538	-99.711293	-99.855988	-99.937440
<b>F<sup>-</sup> – CH<sub>3</sub><sup>+</sup></b>	-139.056857	-139.096979	-139.106622	-139.435299	-139.555703	-139.592303	-139.444340	-139.570138	-139.575091	-139.784514	-139.838841
<b>PH<sub>2</sub><sup>-</sup></b>	-341.881510	-341.891098	-341.893965	-342.055547	-342.095726	-342.106478	-342.061786	-342.105192	-342.088544	-343.205552	-343.240213
<b>PH<sub>2</sub><sup>-</sup> – CH<sub>3</sub><sup>+</sup></b>	-381.520332	-381.542835	-381.548334	-381.851595	-381.929603	-381.950116	-381.861900	-381.944655	-381.945548	-383.127691	-383.160630
<b>SH<sup>-</sup></b>	-398.136023	-398.146284	-398.149182	-398.317865	-398.365941	-398.380008	-398.324283	-398.376612	-398.359177	-399.749318	-399.790626
<b>SH<sup>-</sup> – CH<sub>3</sub><sup>+</sup></b>	-437.735380	-437.759833	-437.765485	-438.076350	-438.164364	-438.187566	-438.087340	-438.181157	-438.180572	-439.635835	-439.675045
<b>Cl<sup>-</sup></b>	-459.563645	-459.573481	-459.576353	-459.744538	-459.799177	-459.817752	-459.749772	-459.809281	-459.791917	-461.519446	-461.568383
<b>Cl<sup>-</sup> – CH<sub>3</sub><sup>+</sup></b>	-499.123966	-499.149673	-499.155427	-499.465324	-499.562460	-499.589815	-499.475656	-499.579330	-499.578076	-501.370720	-501.417712

**Table A4.** Total Energies, Enthalpies, Free energies (in Hartree).

	B3LYP/cc-pVTZ+d			B3LYP/6-311++G(d, p)			B98/6-31++G(2df, p)// B98/6-31G(d)		MP2/6-31G(d, p)		
	$E_{\text{tot}}$	$H_{298}$	$G_{298}$	$E_{\text{tot}}$	$H_{298}$	$G_{298}$	$E_{\text{tot}}$	$H_{298}$	$E_{\text{tot}}$	$H_{298}$	$G_{298}$
<b>H<sub>2</sub>O</b>	-76.4598397	-76.434769	-76.456191	-76.45853077	-76.433462	-76.454884	-76.411043	-76.385873	-76.2197857	-76.194121	-76.215545
<b>H<sub>2</sub>O</b> –	-116.073157	-116.004624	-116.032472	-116.0628916	-115.994362	-116.022202	-115.995104	-115.925902	-115.68943352	-115.618830	-115.646496
<b>CH<sub>3</sub><sup>+</sup></b>											
<b>HF</b>	-100.483571	-100.47095	-100.490665	-100.48238309	-100.469748	-100.489459	-100.422392	-100.409896	-100.19463907	-100.181786	-100.201496
<b>HF</b> –	-140.038457	-139.98520	-140.013508	-140.02566045	-139.972686	-140.000999	-139.945354	-139.891631	-139.6051299	-139.550033	-139.578026
<b>CH<sub>3</sub><sup>+</sup></b>											
<b>H<sub>2</sub>S</b>	-399.432964	-399.414116	-399.437460	-399.42264789	-399.403852	-399.427210	-55.883197	-55.861653	-398.81009809	-398.790430	-398.813747
<b>H<sub>2</sub>S</b> –	-439.064109	-439.003078	-439.032277	-439.04603648	-438.985011	-439.014243	-95.833629	-95.764776	-438.2930985	-438.229485	-438.258513
<b>CH<sub>3</sub><sup>+</sup></b>											
<b>HCl</b>	-460.844003	-460.833990	-460.855174	-460.83401919	-460.824045	-460.845238	-75.773857	-75.76263	-460.2054468	-460.195037	-460.216204
<b>HCl</b> –	-500.420954	-500.370323	-500.399546	-500.40255045	-500.351928	-500.381162	-115.695345	-115.639499	-499.629579	-499.576760	-499.605718
<b>CH<sub>3</sub><sup>+</sup></b>											
<b>NH<sub>2</sub><sup>-</sup></b>	-55.895647	-55.873944	-55.895426	-55.925398289	-55.903188	-55.924644	-99.821956	-99.819596	-55.6694656	-55.646985	-55.668469
<b>NH<sub>2</sub><sup>-</sup></b>	-95.899974	-95.831825	-95.859140	-95.893888543	-95.825708	-95.853036	-139.708936	-139.665524	-95.5939205	-95.524456	-95.551700
<b>-CH<sub>3</sub><sup>+</sup></b>											
<b>OH<sup>-</sup></b>	-75.7904039	-75.778927	-75.798497	-75.827448163	-75.815608	-75.835169	-399.340712	-399.321748	-75.52606950	-75.514348	-75.533923
<b>OH<sup>-</sup></b> –	-115.772250	-115.716896	-115.743947	-115.76499937	-115.709662	-115.736733	-438.946315	-438.884494	-115.3820093	-115.324822	-115.351762
<b>CH<sub>3</sub><sup>+</sup></b>											
<b>F<sup>-</sup></b>	-99.850177	-99.847817	-99.864336	-99.88869321	-99.886333	-99.902852	-460.746741	-460.736712	-99.52660657	-99.524246	-99.540765
<b>F<sup>-</sup></b> –	-139.799833	-139.756876	-139.783190	-139.7913724	-139.748492	-139.774824	-500.298386	-500.247171	-139.360097	-139.315580	-139.341879
<b>CH<sub>3</sub><sup>+</sup></b>											
<b>PH<sub>2</sub><sup>-</sup></b>	-342.574482	-342.558030	-342.581538	-342.58035608	-342.563820	-342.587334	-342.500314	-342.483873	-341.9600264	-341.942721	-341.966199
<b>PH<sub>2</sub><sup>-</sup></b> –	-382.515042	-382.456087	-382.485384	-382.50182309	-382.442836	-382.472134	-382.402093	-382.342318	-381.7637955	-381.702408	-381.731556
<b>CH<sub>3</sub><sup>+</sup></b>											
<b>SH<sup>-</sup></b>	-398.853665	-398.844427	-398.865583	-398.85895804	-398.849717	-398.870882	-398.773701	-398.764543	-398.2221489	-398.212590	-398.233734
<b>SH<sup>-</sup></b> –	-438.757730	-438.707316	-438.736114	-438.74349752	-438.693058	-438.721844	-438.639967	-438.589038	-437.9877848	-437.935304	-437.963943
<b>CH<sub>3</sub><sup>+</sup></b>											
<b>Cl<sup>-</sup></b>	-460.297536	-460.295175	-460.312558	-460.30372718	-460.301367	-460.318750	-460.212111	-460.209751	-459.65210438	-459.649744	-459.667127
<b>Cl<sup>-</sup></b> –	-500.165390	-500.123809	-500.151444	-500.15187767	-500.110248	-500.137894	-500.043397	-500.001311	-499.3782038	-499.335002	-499.362557
<b>CH<sub>3</sub><sup>+</sup></b>											

Table A4. Continued

	MP2/6-31++G(d, p)			MP2/6-31++G(d,p)// B98/6-31G(d)		MP2/6-31++G(2d,p)// B98/6-31G(d)		MP2/6-31+G(2d,p)// B98/6-31G(d)	
	E <sub>tot</sub>	H <sub>298</sub>	G <sub>298</sub>	E <sub>tot</sub>	H <sub>298</sub>	E <sub>tot</sub>	H <sub>298</sub>	E <sub>tot</sub>	H <sub>298</sub>
<b>H<sub>2</sub>O</b>	-76.2333759	-76.207969	-76.229394	-76.2333078	-76.2081378	-76.2617508	-76.2365808	-76.2616118	-76.2364418
<b>H<sub>2</sub>O – CH<sub>3</sub><sup>+</sup></b>	-115.6936152	-115.623237	-115.650930	-115.693484	-115.6242819	-115.7248867	-115.655685	-115.7245305	-115.6553285
<b>HF</b>	-100.2159192	-100.203232	-100.222952	-100.215904	-100.2034077	-100.2527867	-100.240291	-100.2527867	-100.2402907
<b>HF – CH<sub>3</sub><sup>+</sup></b>	-139.61246657	-139.557818	-139.585981	-139.612142	-139.5584189	-139.6546912	-139.600968	-139.6544008	-139.6006778
<b>H<sub>2</sub>S</b>	-398.8122181	-398.792577	-398.815894	-55.7309528	-55.7094088	-55.7506778	-55.7291338	-55.749791	-55.728247
<b>H<sub>2</sub>S – CH<sub>3</sub><sup>+</sup></b>	-438.2957965	-438.232373	-438.261402	-95.5592078	-95.4903548	-95.5818373	-95.5129843	-95.5813702	-95.5125172
<b>HCl</b>	-460.2077632	-460.197369	-460.218538	-75.6025028	-75.5912758	-75.6322485	-75.6210215	-75.631849	-75.620622
<b>HCl – CH<sub>3</sub><sup>+</sup></b>	-499.6324664	-499.579784	-499.608749	-115.39355	-115.3377035	-115.4277147	-115.371869	-115.4273908	-115.3715448
<b>NH<sub>2</sub><sup>-</sup></b>	-55.7320642	-55.709317	-55.730768	-99.6238467	-99.6214867	-99.6594279	-99.6570679	-99.6594279	-99.6570679
<b>NH<sub>2</sub><sup>-</sup> –CH<sub>3</sub><sup>+</sup></b>	-95.5595242	-95.489262	-95.516494	-139.376662	-139.3332495	-139.4182667	-139.374855	-139.418347	-139.374935
<b>OH<sup>-</sup></b>	-75.6026568	-75.590674	-75.610242	-398.811848	-398.7928836	-398.8305352	-398.811571	-398.8303632	-398.8113992
<b>OH<sup>-</sup> – CH<sub>3</sub><sup>+</sup></b>	-115.3938995	-115.337025	-115.364041	-438.295108	-438.2332872	-438.3203389	-438.258518	-438.3197511	-438.2579301
<b>F<sup>-</sup></b>	-99.6238467	-99.621486	-99.638005	-460.207517	-460.1974884	-460.2285295	-460.218501	-460.2284004	-460.2183714
<b>F<sup>-</sup> – CH<sub>3</sub><sup>+</sup></b>	-139.3773615	-139.333034	-139.359361	-499.631664	-499.5804487	-499.6596658	-499.608451	-499.6591775	-499.6079625
<b>PH<sub>2</sub><sup>-</sup></b>	-341.9810056	-341.963683	-341.987158	-341.980639	-341.9641983	-341.9990677	-341.982627	-341.9984752	-341.9820342
<b>PH<sub>2</sub><sup>-</sup> – CH<sub>3</sub><sup>+</sup></b>	-381.7675862	-381.706508	-381.735664	-381.767197	-381.7074224	-381.7900043	-381.730229	-381.7894744	-381.7296994
<b>SH<sup>-</sup></b>	-398.2415756	-398.232018	-398.253162	-398.24133	-398.2321719	-398.2655131	-398.256355	-398.2653748	-398.2562168
<b>SH<sup>-</sup> – CH<sub>3</sub><sup>+</sup></b>	-437.991256	-437.939071	-437.967733	-437.990722	-437.9397925	-438.0174778	-437.966549	-438.0170264	-437.9660974
<b>Cl<sup>-</sup></b>	-459.671145	-459.668785	-459.686168	-459.671145	-459.6687854	-459.6979091	-459.695549	-459.6979091	-459.6955491
<b>Cl<sup>-</sup> – CH<sub>3</sub><sup>+</sup></b>	-499.3813075	-499.338325	-499.365887	-499.380914	-499.3388281	-499.4109623	-499.368876	-499.4106808	-499.3685948

**Table A5.** Energy Components (in Hartree) Used in G3.

	$E_{\text{MP2/6-31G(d)}}$	$E_{\text{MP4/6-31G(d)}}$	$E_{\text{QCISD(T)}}$	$E_{\text{MP2/6-31+G(d)}}$	$E_{\text{MP4/6-31+G(d)}}$	$E_{\text{MP2/6-31G(2df,p)}}$	$E_{\text{MP4/6-31G(2df,p)}}$	$E_{\text{MP2/GTLarge}}$	E (G3)
<b>pyrrole</b>	-209.480830	-209.5392877	-209.5382593	-209.4964473	-209.5549701	-209.6393209	-209.7053776	-209.9361593	-210.005008
<b>pyrrole-CH<sub>3</sub><sup>+</sup></b>	-248.999848	-249.0811821	-249.0828866	-249.0080542	-249.0899276	-249.1942066	-249.2861353	-249.5373548	-249.615147
<b>pyrazole</b>	-225.503526	-225.5577504	-225.5549956	-225.5196429	-225.5741285	-225.6613392	-225.7237234	-225.9660856	-226.040138
<b>pyrazole-CH<sub>3</sub><sup>+</sup></b>	-265.027154	-265.1002785	-265.0989861	-265.0362896	-265.1100706	-265.2257905	-265.309399	-265.5790957	-265.656309
<b>N-methyl-pyrrole</b>	-248.644006	-248.7180912	-248.7169399	-248.6605179	-248.7349603	-248.838428	-248.9224572	-249.1913352	-249.270822
<b>N-methyl-pyrrole-CH<sub>3</sub><sup>+</sup></b>	-288.172259	-288.2693895	-288.2710348	-288.181812	-288.2797348	-288.4028811	-288.5128668	-288.8025172	-288.890959
<b>pyridine</b>	-247.482518	-247.5529096	-247.5512206	-247.498312	-247.5688412	-247.656671	-247.7356984	-248.0048474	-248.092899
<b>pyridine-CH<sub>3</sub><sup>+</sup></b>	-287.019171	-287.1071207	-287.1061879	-287.0285649	-287.1169809	-287.2336694	-287.332638	-287.6307554	-287.719344
<b>imidazole</b>	-225.519198	-225.573979	-225.5717214	-225.5356519	-225.5907735	-225.6772422	-225.7402134	-225.9825993	-226.057889
<b>imidazole-CH<sub>3</sub><sup>+</sup></b>	-265.063019	-265.1356042	-265.1344617	-265.0718603	-265.1451546	-265.2606753	-265.3437562	-265.6138166	-265.690020
<b>quinoline</b>	-400.640977	-400.7524494	-400.7476536	-400.664985	-400.7766027	-400.9180001	-401.0419096	-401.486926	-401.629249
<b>quinoline-CH<sub>3</sub><sup>+</sup></b>	-440.182783	-440.312324	-440.308330	-440.199561	-440.3296156	-440.5011429	-440.6455051	-441.118608	-441.261624
<b>pyrrolidine</b>	-211.827206	-211.900702	-211.902816	-211.840003	-211.914494	-212.0174003	-212.1023486	-212.3167399	-212.376014
<b>Pyrrolidine-CH<sub>3</sub><sup>+</sup></b>	-251.374954	-251.4665189	-251.4693917	-251.3824189	-251.4750799	-251.6027771	-251.708221	-251.9507785	-252.009361
<b>NMe<sub>3</sub></b>	-173.828591	-173.893607	-173.8958721	-173.8394348	-173.9053762	-173.9950051	-174.0708542	-174.2411839	-174.287611
<b>NMe<sub>3</sub>-CH<sub>3</sub><sup>+</sup></b>	-213.374536	-213.4571903	-213.4600224	-213.3810555	-213.4648003	-213.5805824	-213.6765099	-213.8766135	-213.921541
<b>N-methyl-imidazole</b>	-264.683017	-264.7535311	-264.751103	-264.7002739	-264.771430	-264.877052	-264.9581217	-265.238341	-265.324326
<b>N-methyl-imidazole-CH<sub>3</sub><sup>+</sup></b>	-304.233176	-304.3215089	-304.320233	-304.243005	-304.332287	-304.466789	-304.567972	-304.8763183	-304.963387

**Table A5. Continued**

	$E_{\text{MP2/6-31G(d)}}$	$E_{\text{MP4/6-31G(d)}}$	$E_{\text{QCISD(T)}}$	$E_{\text{MP2/6-31+G(d)}}$	$E_{\text{MP4/6-31+G(d)}}$	$E_{\text{MP2/6-31G(2df,p)}}$	$E_{\text{MP4/6-31G(2df,p)}}$	$E_{\text{MP2/GTLarge}}$	$E(\text{G3})$
<b>DABCO</b>	-344.158803	-344.2691002	-344.2705728	-344.1767329	-344.2888792	-344.4477919	-344.575089	-344.9220447	-345.022541
<b>DABCO- CH<sub>3</sub><sup>+</sup></b>	-383.711830	-383.8398802	-383.8419238	-383.7261682	-383.8562133	-384.0404943	-384.1878485	-384.5646917	-384.664242
<b>quinuclidine</b>	-328.155211	-328.2687536	-328.270712	-328.1700263	-328.2851647	-328.4417032	-328.571922	-328.9059934	-328.999220
<b>Quinuclidine -CH<sub>3</sub><sup>+</sup></b>	-367.714997	-367.8459942	-367.8484667	-367.7266416	-367.8592964	-368.0411988	-368.1911446	-368.5561793	-368.647631
<b>PMe<sub>3</sub></b>	-460.068688	-460.1405533	-460.1436557	-460.0767557	-460.1492122	-460.243071	-460.3275004	-460.7465137	-460.809805
<b>PMe<sub>3</sub>-CH<sub>3</sub><sup>+</sup></b>	-499.630406	-499.7170346	-499.7204397	-499.6361986	-499.7236427	-499.8468508	-499.9482905	-500.4064054	-500.468867
<b>PMe<sub>2</sub>Ph</b>	-651.203074	-651.3255148	-651.3256122	-651.2247381	-651.3477819	-651.4997256	-651.6388061	-652.2796972	-652.413246
<b>PMe<sub>2</sub>Ph-CH<sub>3</sub><sup>+</sup></b>	-690.767703	-690.9049877	-690.9054216	-690.7847800	-690.9228728	-691.1074045	-691.2636195	-691.9420731	-692.074754

**Table A6.** Total Energies, Enthalpies (in Hartree).

	B98/6-31G(d)		B98/6-31++G(2df,p) //B98/6-31G(d)		MP2/6-31++G(d,p)//B98/6-31G(d)		MP2/6-31++G(2d,p)//B98/6-31G(d)	
	E <sub>tot</sub>	H <sub>298</sub>	E <sub>tot</sub>	H <sub>298</sub>	E <sub>tot</sub>	H <sub>298</sub>	E <sub>tot</sub>	H <sub>298</sub>
<b>pyrrole</b>	-210.0799588	-209.992376	-210.110411	-210.0228282	-209.537954	-209.450372	-209.5824402	-209.4948582
<b>pyrrole-CH<sub>3</sub><sup>+</sup></b>	-249.740246	-249.609948	-249.767197	-249.636899	-249.0705122	-248.9402142	-249.1202098	-248.9899118
<b>pyrazole</b>	-226.1084608	-226.032319	-226.137783	-226.0616412	-225.5523962	-225.4762542	-225.599795	-225.523653
<b>pyrazole-CH<sub>3</sub><sup>+</sup></b>	-265.7731898	-265.653899	-265.8022003	-265.6829095	-265.0908652	-264.9715742	-265.1447094	-265.0254184
<b>N-methyl-pyrrole</b>	-249.3749806	-249.257842	-249.4066678	-249.2895292	-248.7164907	-248.5993517	-248.7691369	-248.6519979
<b>N-methyl-pyrrole-CH<sub>3</sub><sup>+</sup></b>	-289.04323	-288.883358	-289.0718547	-288.9119827	-288.2589878	-288.0991158	-288.3167589	-288.1568869
<b>pyridine</b>	-248.181760	-248.087612	-248.209349	-248.115201	-247.5372975	-247.4431495	-247.5897175	-247.4955695
<b>pyridine-CH<sub>3</sub><sup>+</sup></b>	-287.8560148	-287.71821	-287.88373	-287.7459252	-287.0898118	-286.9520068	-287.1480953	-287.0102903
<b>imidazole</b>	-226.124982	-226.048948	-226.1551651	-226.0791311	-225.5686262	-225.4925912	-225.616203	-225.540168
<b>imidazole-CH<sub>3</sub><sup>+</sup></b>	-265.8066334	-265.686827	-265.8354572	-265.7156508	-265.1266437	-265.0068367	-265.1796182	-265.0598112
<b>quinoline</b>	-401.7646227	-401.621226	-401.806169	-401.6627723	-400.7198073	-400.5764103	-400.8059884	-400.6625914
<b>quinoline-CH<sub>3</sub><sup>+</sup></b>	-441.4454425	-441.258155	-441.486672	-441.299384	-440.2767169	-440.0894289	-440.3696719	-440.1823839
<b>pyrrolidine</b>	-212.4964237	-212.360236	-212.524057	-212.3878693	-211.9131765	-211.7769885	-211.9585779	-211.8223899
<b>pyrrolidine-CH<sub>3</sub><sup>+</sup></b>	-252.1783399	-251.99731	-252.204353	-252.0233231	-251.4764613	-251.2954313	-251.5267993	-251.3457693
<b>NMe<sub>3</sub></b>	-174.4007171	-174.273292	-174.4233976	-174.2959725	-173.9118556	-173.7844306	-173.9494999	-173.8220749
<b>NMe<sub>3</sub>-CH<sub>3</sub><sup>+</sup></b>	-214.0771833	-213.904726	-214.0994996	-213.9270423	-213.4745742	-213.3021172	-213.5182938	-213.3458368
<b>N-methyl-imidazole</b>	-265.4208789	-265.315183	-265.452295	-265.346599	-264.7477155	-264.6420195	-264.803554	-264.697858
<b>N-methyl-imidazole-CH<sub>3</sub><sup>+</sup></b>	-305.1086479	-304.959284	-305.139144	-304.9897797	-304.3123599	-304.1629969	-304.373845	-304.224482

**Table A6.** Continued

	B98/6-31G(d)		B98/6-31++G(2df,p) //B98/6-31G(d)		MP2/6-31++G(d,p)//B98/6-31G(d)		MP2/6-31++G(2d,p)//B98/6-31G(d)	
	E <sub>tot</sub>	H <sub>298</sub>	E <sub>tot</sub>	H <sub>298</sub>	E <sub>tot</sub>	H <sub>298</sub>	E <sub>tot</sub>	H <sub>298</sub>
<b>pyrrole</b>	-345.1949681	-345.003513	-345.2303471	-345.038892	-344.2721013	-344.0806453	-344.3471564	-344.1557004
<b>pyrrole-CH<sub>3</sub><sup>+</sup></b>	-384.8798256	-384.643824	-384.9152469	-384.6792453	-383.84272	-383.606718	-383.923029	-383.687027
<b>pyrazole</b>	-329.1799428	-328.976697	-329.2137268	-329.010481	-328.274072	-328.070826	-328.3444978	-328.1412518
<b>pyrazole-CH<sub>3</sub><sup>+</sup></b>	-368.8701586	-368.622359	-368.904329	-368.6565294	-367.8513201	-367.6035201	-367.9273934	-367.6795934
<b>N-methyl-pyrrole</b>	-460.9963707	-460.875351	-461.0211789	-460.9001592	-460.1498089	-460.0287889	-460.1918918	-460.0708718
<b>N-methyl-pyrrole-CH<sub>3</sub><sup>+</sup></b>	-500.6907246	-500.527994	-500.721378	-500.5586474	-499.7298604	-499.5671294	-499.7806752	-499.6179442
<b>pyridine</b>	-652.6503727	-652.472848	-652.694197	-652.5166727	-651.3134565	-651.1359325	-651.394642	-651.217118
<b>pyridine-CH<sub>3</sub><sup>+</sup></b>	-692.3483077	-692.129002	-692.396961	-692.1776556	-690.8945806	-690.6752756	-690.985272	-690.765967
	MP2/6-31+G(2d,p)// B98/6-31G(d)		MP2/6-311+G(2d,p)// B98/6-31G(d)					
	E <sub>tot</sub>	H <sub>298</sub>	E <sub>tot</sub>	H <sub>298</sub>				
<b>pyrrole</b>	-209.5821559	-209.4945731	-209.640727	-209.5531442				
<b>pyrrole-CH<sub>3</sub><sup>+</sup></b>	-249.1195815	-248.9892835	-249.1868016	-249.0565036				
<b>pyrazole</b>	-225.5995288	-225.523387	-225.6658105	-225.5896687				
<b>pyrazole-CH<sub>3</sub><sup>+</sup></b>	-265.144227	-265.0249362	-265.2203643	-265.1010735				
<b>N-methyl-pyrrole</b>	-248.7686435	-248.6515049	-248.8388805	-248.7217419				
<b>N-methyl-pyrrole-CH<sub>3</sub><sup>+</sup></b>	-288.3159368	-288.1560648	-288.3947599	-288.2348879				
<b>pyridine</b>	-247.5894387	-247.4952907	-247.6567807	-247.5626327				
<b>pyridine-CH<sub>3</sub><sup>+</sup></b>	-287.1475701	-287.0097653	-287.2243864	-287.0865816				

Table A6. Continued

	MP2/6-31+G(2d,p)// B98/6-31G(d)		MP2/6-311+G(2d,p)// B98/6-31G(d)	
	E <sub>tot</sub>	H <sub>298</sub>	E <sub>tot</sub>	H <sub>298</sub>
<b>imidazole</b>	-225.6159541	-225.5399201	-225.682212	-225.606178
<b>imidazole- CH<sub>3</sub><sup>+</sup></b>	-265.1791648	-265.0593584	-265.2552292	-265.1354228
<b>quinoline</b>	-400.8056985	-400.6623018	-400.9122748	-400.7688781
<b>quinoline- CH<sub>3</sub><sup>+</sup></b>	-440.3690547	-440.1817672	-440.4853338	-440.2980463
<b>pyrrolidine</b>	-211.9577559	-211.8215682	-212.0199662	-211.8837785
<b>pyrrolidine -CH<sub>3</sub><sup>+</sup></b>	-251.5257262	-251.3446963	-251.5964754	-251.4154455
<b>NMe<sub>3</sub></b>	-173.9486359	-173.8212108	-174.0014971	-173.874072
<b>NMe<sub>3</sub>-CH<sub>3</sub><sup>+</sup></b>	-213.5172576	-213.3448003	-213.5786899	-213.4062326
<b>N-methyl- imidazole</b>	-264.8031187	-264.6974228	-264.8809526	-264.7752567
<b>N-methyl- imidazole- CH<sub>3</sub><sup>+</sup></b>	-304.3732	-304.2238361	-304.4607248	-304.3113609
<b>pyrrole</b>	-344.3461625	-344.1547074	-344.4469658	-344.2555107
<b>pyrrole- CH<sub>3</sub><sup>+</sup></b>	-383.9217601	-383.6857585	-384.031602	-383.7956004
<b>pyrazole</b>	-328.3433046	-328.1400588	-328.4368633	-328.2336175
<b>pyrazole- CH<sub>3</sub><sup>+</sup></b>	-367.9259362	-367.6781366	-368.0284465	-367.7806469
<b>N-methyl- pyrrole</b>	-460.1908641	-460.0698444	-460.2520868	-460.1310671
<b>N-methyl- pyrrole- CH<sub>3</sub><sup>+</sup></b>	-499.7796327	-499.6169021	-499.8500326	-499.687302
<b>pyridine</b>	-651.3935886	-651.2160639	-651.502793	-651.3252683
<b>pyridine- CH<sub>3</sub><sup>+</sup></b>	-690.9840525	-690.7647468	-691.1026503	-690.8833446

**Table A7.** Total Energies and Enthalpies (in Hartree) as Calculated at the B98/6-31G(d) and MP2(FC)/6-31+G(2d,p)//B98/6-31G(d) Level of Theory for all Systems. If More than One Conformer Exist at 298.15 K, Total Energies Represent the Total Energy of the Best Conformer and Enthalpies Represent Boltzmann-Averaged Values over all Conformers.

	B98/6-31G(d)		MP2(FC)/6-31+G(2d,p)//B98/6-31G(d)	
	E <sub>tot</sub>	H <sub>298</sub>	E <sub>tot</sub>	H <sub>298</sub>
<b>CH<sub>3</sub><sup>+</sup></b>	-39.462922	-39.427481	-39.3523703	-39.3169293
<b>enol</b>	-193.050400	-192.959496	-192.6113911	-192.5204561
<b>enol-Me<sup>+</sup></b>	-232.706588	-232.573288	-232.1456101	-232.0121949
<b>enol-H<sup>+</sup></b>	-193.403147	-193.300102	-192.9488006	-192.8457561
<b>1</b>	-248.181760	-248.087612	-247.5894387	-247.4952907
<b>1-Me<sup>+</sup></b>	-287.856015	-287.718210	-287.1475701	-287.0097653
<b>1-H<sup>+</sup></b>	-248.555059	-248.446502	-247.9528770	-247.8443199
<b>2</b>	-382.107033	-381.935289	-381.1857028	-381.0139584
<b>2-Me<sup>+</sup></b>	-421.783395	-421.567596	-420.7472882	-420.5314891
<b>2-H<sup>+</sup></b>	-382.496991	-382.310686	-381.5640595	-381.3777545
<b>3</b>	-226.124982	-226.048948	-225.6159541	-225.5399201
<b>3-Me<sup>+</sup></b>	-265.806633	-265.686827	-265.1791648	-265.0593584
<b>3-H<sup>+</sup></b>	-226.503808	-226.413502	-225.9842830	-225.8939773
<b>4</b>	-401.764623	-401.621226	-400.8056985	-400.6623018
<b>4-Me<sup>+</sup></b>	-441.445443	-441.258155	-440.3690547	-440.1817672
<b>4-H<sup>+</sup></b>	-402.148068	-401.990339	-401.1763456	-401.0186162
<b>5</b>	-401.004097	-400.849695	-400.1314281	-399.9769728
<b>5-Me<sup>+</sup></b>	-440.682182	-440.483764	-439.6951018	-440.4837637
<b>5-H<sup>+</sup></b>	-401.382624	-401.213650	-400.5012983	-400.3323197
<b>6</b>	-287.484718	-287.361209	-286.7872853	-286.6637767
<b>6-Me<sup>+</sup></b>	-327.165207	-326.998151	-326.3506969	-326.1836411
<b>6-H<sup>+</sup></b>	-287.864936	-287.727193	-287.1566838	-287.0189408
<b>7</b>	-403.168063	-402.983620	-402.2223122	-402.0378693
<b>7-Me<sup>+</sup></b>	-442.842228	-442.613615	-441.7872526	-441.5586397
<b>7-H<sup>+</sup></b>	-403.543450	-403.343717	-402.5912529	-402.3915201
<b>8</b>	-212.496424	-212.360108	-211.9581467	-211.8219125
<b>8-Me<sup>+</sup></b>	-252.178340	-251.997101	-251.5257262	-251.3444449
<b>8-H<sup>+</sup></b>	-212.878286	-212.726750	-212.3328616	-212.1813258
<b>9</b>	-174.400717	-174.273292	-173.9486359	-173.8212108
<b>9-Me<sup>+</sup></b>	-214.077183	-213.904726	-213.5172576	-213.3448003
<b>9-H<sup>+</sup></b>	-174.779434	-174.636045	-174.3233160	-174.1799269
<b>10</b>	-441.066943	-440.893993	-440.0039989	-439.8310488
<b>10-Me<sup>+</sup></b>	-480.752394	-480.535599	-479.5714640	-479.3546690
<b>10-H<sup>+</sup></b>	-441.455576	-441.268467	-440.3792438	-440.1921351
<b>11</b>	-265.420879	-265.315183	-264.8031187	-264.6974228
<b>11-Me<sup>+</sup></b>	-305.108648	-304.959284	-304.3732000	-304.2238361
<b>11-H<sup>+</sup></b>	-265.806634	-265.686824	-265.1791652	-265.0593555
<b>12</b>	-921.587985	-921.190927	-919.4118894	-919.0138350
<b>12-1-Me<sup>+</sup></b>	-961.279105	-921.191485	-958.9951260	-958.5535059
<b>12-2-Me<sup>+</sup></b>	-961.276693	-960.836390	-958.9821855	-958.5411577
<b>12-1-H<sup>+</sup></b>	-921.986184	-921.573309	-919.8026136	-919.3896852
<b>12-2-H<sup>+</sup></b>	-921.980666	-921.569875	-919.7903104	-919.3789374
<b>13</b>	-921.588951	-921.191340	-919.4139549	-919.0157722

**Table A7. Continued**

<b>13-1-Me<sup>+</sup></b>	-961.2801043	-960.8381939	-958.9958574	-958.5539275
<b>13-2-Me<sup>+</sup></b>	-961.2787468	-960.8371362	-958.9849166	-958.5429850
<b>13-1-H<sup>+</sup></b>	-921.9867974	-921.5740867	-919.8055074	-919.3924041
<b>13-2-H<sup>+</sup></b>	-921.9827175	-921.5706552	-919.7928420	-919.3806086
<b>14</b>	-370.8853042	-370.6087365	-369.9124608	-369.6357009
<b>14-Me<sup>+</sup></b>	-410.5629096	-410.2408639	-409.4854796	-409.1635616
<b>14-H<sup>+</sup></b>	-371.2825205	-370.9903894	-370.3041895	-370.0119822
<b>15</b>	-251.7924062	-251.6273323	-251.1462691	-250.9811893
<b>15-Me<sup>+</sup></b>	-291.4740218	-291.2640310	-290.7193361	-290.5093453
<b>15-H<sup>+</sup></b>	-252.1783395	-251.9971093	-251.5257247	-251.3444513
<b>16</b>	-555.5467330	-555.3384240	-554.2472113	-554.0389023
<b>16-Me<sup>+</sup></b>	-595.2368724	-594.9846790	-593.8196714	-593.5674780
<b>16-H<sup>+</sup></b>	-555.9402491	-555.7178320	-554.6276035	-554.4051864
<b>17</b>	-788.7246836	-788.5293730	-787.3925616	-787.1972510
<b>17-Me<sup>+</sup></b>	-828.4036671	-828.1639465	-826.965584	-826.7259070
<b>17-H<sup>+</sup></b>	-789.1050837	-788.8943370	-787.769372	-787.5586253
<b>18</b>	-1036.067474	-1035.635678	-1033.657729	-1033.224549
<b>18-1-Me<sup>+</sup></b>	-1075.763966	-1075.286566	-1073.243065	-1072.765658
<b>18-2-Me<sup>+</sup></b>	-1075.762467	-1075.285896	-1073.232839	-1072.755469
<b>18-1-H<sup>+</sup></b>	-1036.470314	-1036.022111	-1034.05259	-1033.603882
<b>18-2-H<sup>+</sup></b>	-1036.466421	-1036.019537	-1034.041028	-1033.593499
<b>19</b>	-345.1949681	-345.0035130	-344.3461625	-344.1547074
<b>19-Me<sup>+</sup></b>	-384.8798256	-384.6438240	-383.9217601	-383.6857585
<b>19-H<sup>+</sup></b>	-345.5814154	-345.3741460	-344.726064	-344.5187946
<b>20</b>	-292.2934858	-292.0758704	-291.5262623	-291.3086717
<b>20-Me<sup>+</sup></b>	-331.9764071	-331.7138439	-331.1023150	-330.8397663
<b>20-H<sup>+</sup></b>	-292.6860655	-292.4528767	-291.912289	-291.6792654
<b>21</b>	-382.0956934	-381.9237610	-381.1761503	-381.0042179
<b>21-Me<sup>+</sup></b>	-421.7865302	-421.5708770	-420.7514068	-420.5357536
<b>21-H<sup>+</sup></b>	-382.4871894	-382.3008200	-381.5579681	-381.3716077
<b>22</b>	-1036.067788	-1035.635220	-1033.655591	-1033.222081
<b>22-1-Me<sup>+</sup></b>	-1075.762849	-1075.285972	-1073.242374	-1072.765521
<b>22-2-Me<sup>+</sup></b>	-1075.759675	-1075.284637	-1073.230128	-1072.753789
<b>22-1-H<sup>+</sup></b>	-1036.469727	-1036.021287	-1034.049578	-1033.601276
<b>22-2-H<sup>+</sup></b>	-1036.463726	-1036.018176	-1034.038380	-1033.591662
<b>23</b>	-654.7532243	-654.418466	-653.1369481	-652.8021802
<b>23-1-Me<sup>+</sup></b>	-694.4415762	-694.061436	-692.7181950	-692.3380578
<b>23-2-Me<sup>+</sup></b>	-694.4388145	-694.058543	-692.7149422	-692.3345524
<b>23-1-H<sup>+</sup></b>	-655.1579200	-654.807365	-653.5349398	-653.1843848
<b>23-2-H<sup>+</sup></b>	-655.1572657	-654.806566	-653.5336947	-653.1829948
<b>24</b>	-344.0216398	-343.856129	-343.0281551	-343.0281205
<b>24-Me<sup>+</sup></b>	-383.7165495	-383.507383	-382.7709504	-382.5618212
<b>24-H<sup>+</sup></b>	-344.4151170	-344.235536	-343.5772715	-343.3977086
<b>25</b>	-609.4372775	-609.163890	-607.9908239	-607.7174364
<b>25-1-Me<sup>+</sup></b>	-649.1479473	-648.830334	-647.5795424	-647.2619291
<b>25-2-Me<sup>+</sup></b>	-649.1299472	-648.812498	-647.5712874	-647.2538382
<b>25-1-H<sup>+</sup></b>	-609.8510049	-609.562806	-608.3893029	-608.101104
<b>25-2-H<sup>+</sup></b>	-609.8406764	-609.552738	-608.3842239	-608.0962855
<b>26</b>	-329.1799428	-328.976697	-328.3433046	-328.1400588

**Table A7. Continued**

<b>26-Me<sup>+</sup></b>	-368.8701586	-368.622359	-367.9259362	-367.6781366
<b>26-H<sup>+</sup></b>	-329.5722501	-329.353098	-328.7304067	-328.5112546
<b>27</b>	-382.1009636	-381.928966	-381.179961	-381.0079634
<b>27-Me<sup>+</sup></b>	-421.8014546	-421.58545	-420.7622566	-420.546252
<b>27-H<sup>+</sup></b>	-382.503394	-382.316683	-381.5709543	-381.3842433
<b>28</b>	-368.4785695	-368.245952	-367.5397612	-367.3071437
<b>28-Me<sup>+</sup></b>	-408.1695073	-407.8919619	-407.1232858	-406.8457582
<b>28-H<sup>+</sup></b>	-368.874974	-368.626692	-367.9301149	-367.6818329
<b>29</b>	-459.4989989	-459.289442	-458.3839094	-458.1743525
<b>29-Me<sup>+</sup></b>	-499.2030482	-498.949398	-497.9696878	-497.7160376
<b>29-H<sup>+</sup></b>	-459.905327	-459.68109	-458.7787879	-458.5545509
<b>30</b>	-742.1562367	-741.9858568	-740.8412091	-740.6708473
<b>30-Me<sup>+</sup></b>	-781.8594432	-781.6450973	-780.4285638	-780.2141553
<b>30-H<sup>+</sup></b>	-742.563026	-742.3781526	-741.2384344	-741.053508
<b>31</b>	-517.6681344	-517.448974	-516.4978850	-516.278861
<b>31-Me<sup>+</sup></b>	-557.3745239	-557.1119377	-556.0866146	-555.824032
<b>31-H<sup>+</sup></b>	-518.0758504	-517.8440739	-516.8925636	-516.660784
<b>32</b>	-536.9056041	-536.6584017	-535.6024802	-535.3552285
<b>32-Me<sup>+</sup></b>	-576.6143642	-576.3229749	-575.1929957	-574.9015947
<b>32-H<sup>+</sup></b>	-537.3171484	-537.0551323	-536.0022547	-535.7402266
<b>33</b>	-514.8206196	-514.593191	-513.5930440	-513.3656154
<b>33-Me<sup>+</sup></b>	-554.5300414	-554.258542	-553.1835305	-552.9120311
<b>33-H<sup>+</sup></b>	-515.2323777	-514.99011	-513.9919080	-513.7496403
<b>34</b>	-460.9963707	-460.875351	-460.1908641	-460.0698444
<b>34-Me<sup>+</sup></b>	-500.6907246	-500.527994	-499.7796327	-499.6169021
<b>34-H<sup>+</sup></b>	-461.3693484	-461.236986	-460.5620179	-460.4296555
<b>35</b>	-652.6503727	-652.472848	-651.3935886	-651.2160639
<b>35-Me<sup>+</sup></b>	-692.3483077	-692.129002	-690.9840525	-690.7647468
<b>35-H<sup>+</sup></b>	-653.0292176	-652.840324	-651.7674173	-651.5785237
<b>36</b>	-461.902429	-461.6446806	-460.7547154	-460.4970074
<b>36-Me<sup>+</sup></b>	-501.6127554	-501.3104093	-500.3484611	-500.0461154
<b>36-H<sup>+</sup></b>	-462.3236859	-462.0508904	-461.1653635	-460.8925754
<b>37</b>	-383.3193429	-383.122174	-382.3792999	-382.1821883
<b>37-Me<sup>+</sup></b>	-423.0310319	-422.7893121	-421.9737231	-421.7319592
<b>37-H<sup>+</sup></b>	-383.7355338	-383.5234792	-382.7851391	-382.5730755
<b>38</b>	-808.6312857	-808.35591	-806.9763546	-806.7009789
<b>38-Me<sup>+</sup></b>	-848.3339353	-848.016778	-846.5703723	-846.253215
<b>38-H<sup>+</sup></b>	-809.0171876	-808.730614	-807.3541824	-807.0676088
<b>39</b>	-1035.959842	-1035.669198	-1033.807456	-1033.516812
<b>39-Me<sup>+</sup></b>	-1075.664295	-1075.331649	-1073.401913	-1073.069267
<b>39-H<sup>+</sup></b>	-1036.34727	-1036.045204	-1034.184602	-1033.882536
<b>40</b>	-578.8822586	-578.670407	-577.7606731	-577.5489056
<b>40-Me<sup>+</sup></b>	-618.583634	-618.3298341	-617.3568199	-617.1029126
<b>40-H<sup>+</sup></b>	-579.2650593	-579.0417938	-578.1405306	-577.9171214
<b>41</b>	-925.3080029	-924.965507	-923.3652768	-923.0227097
<b>41-Me<sup>+</sup></b>	-965.0151849	-964.6312421	-962.9640597	-962.5798677
<b>41-H<sup>+</sup></b>	-925.6982276	-925.3449745	-923.7476453	-923.3942718

**Table A8.** Total Energies and Enthalpies of Cinchona Alkaloids and Selected Tertiary Amines and Their Methyl Cation Adducts, Protonated Adducts, MOSC Adducts (in Hartree).

	B98/6-31G(d)		MP2/6-31+G(2d,p)// B98/6-31G(d)	
	$E_{\text{tot}}$	$H_{298}$	$E_{\text{tot}}$	" $H_{298}$ "
<b>12_008</b>	-921.5879846	-921.190399	-919.4118894	-919.014304
<b>12_005</b>	-921.5887599	-921.191542	-919.4112625	-919.014045
<b>12_004</b>	-921.5861511	-921.189323	-919.4098786	-919.013050
<b>12_010</b>	-921.5850499	-921.188253	-919.4093451	-919.012548
<b>12_012</b>	-921.5847805	-921.187330	-919.4075947	-919.010144
<b>12_011</b>	-921.5853952	-921.188392	-919.4070268	-919.010024
<b>12_006</b>	-921.5836642	-921.186572	-919.4071052	-919.010013
<b>12_003</b>	-921.5814097	-921.184408	-919.4070086	-919.010007
<b>12_007</b>	-921.5803058	-921.183339	-919.4062430	-919.009276
<b>12_001</b>	-921.5844783	-921.187465	-919.4061593	-919.009146
<b>12_002</b>	-921.5831212	-921.186301	-919.4053166	-919.008496
<b>12_009</b>	-921.5788877	-921.181005	-919.4002252	-919.002343
	B98/6-31G(d)		MP2/6-31+G(2d,p)// B98/6-31G(d)	
	$E_{\text{tot}}$	$H_{298}$	$E_{\text{tot}}$	" $H_{298}$ "
<b>12-CH<sub>3</sub><sup>+</sup>_001</b>	-961.2750362	-960.833308	-958.9897808	-958.548053
<b>12-CH<sub>3</sub><sup>+</sup>_002</b>	-961.2729819	-960.831512	-958.9864824	-958.545013
<b>12-CH<sub>3</sub><sup>+</sup>_003</b>	-961.2667798	-960.824939	-958.9824507	-958.540610
<b>12-CH<sub>3</sub><sup>+</sup>_004</b>	-961.2707320	-960.829516	-958.9876091	-958.546393
<b>12-CH<sub>3</sub><sup>+</sup>_005</b>	-961.2791045	-960.837507	-958.9951260	-958.553528
<b>12-CH<sub>3</sub><sup>+</sup>_006</b>	-961.2688374	-960.827676	-958.9854097	-958.544248
<b>12-CH<sub>3</sub><sup>+</sup>_007</b>	-961.2695624	-960.828243	-958.9861051	-958.544786
<b>12-CH<sub>3</sub><sup>+</sup>_009</b>	-961.2580714	-960.816486	-958.9713196	-958.529734
	B98/6-31G(d)		MP2/6-31+G(2d,p)// B98/6-31G(d)	
	$E_{\text{tot}}$	$H_{298}$	$E_{\text{tot}}$	" $H_{298}$ "
<b>12-H<sup>+</sup>_001</b>	-921.9812139	-921.568876	-919.795519	-919.3831811
<b>12-H<sup>+</sup>_002</b>	-921.9807072	-921.568392	-919.7941734	-919.3818582
<b>12-H<sup>+</sup>_003</b>	-921.9832872	-921.570825	-919.8001008	-919.3876387
<b>12-H<sup>+</sup>_004</b>	-921.9845865	-921.572551	-919.8013306	-919.3892951
<b>12-H<sup>+</sup>_005</b>	-921.9852028	-921.573164	-919.800081	-919.3880422
<b>12-H<sup>+</sup>_007</b>	-921.9861841	-921.57385	-919.8026136	-919.3902795
<b>12-H<sup>+</sup>_009</b>	-921.9763229	-921.563592	-919.7901916	-919.3774608
<b>12-H<sup>+</sup>_010</b>	-921.9833979	-921.571368	-919.8010638	-919.3890339
	B98/6-31G(d)		MP2/6-31+G(2d,p)// B98/6-31G(d)	
	$E_{\text{tot}}$	$H_{298}$	$E_{\text{tot}}$	$H_{298}$
<b>12-MOSCre<sup>+</sup>_01</b>	-1643.602930	-1643.032404	-1639.993862	-1639.423336
<b>12-MOSCre<sup>+</sup>_02</b>	-1643.601236	-1643.030904	-1639.992030	-1639.421698
<b>12-MOSCre<sup>+</sup>_03</b>	-1643.600849	-1643.030787	-1639.991977	-1639.421915
<b>12-MOSCre<sup>+</sup>_05</b>	-1643.595435	-1643.025021	-1639.986320	-1639.415906
<b>12-MOSCre<sup>+</sup>_06</b>	-1643.599146	-1643.029188	-1639.990915	-1639.420957
<b>12-MOSCre<sup>+</sup>_07</b>	-1643.594642	-1643.024441	-1639.985503	-1639.415302
<b>12-MOSCre<sup>+</sup>_09</b>	-1643.592851	-1643.022340	-1639.983368	-1639.412857

**Table A8.** Continued

<b>12-MOSCsi<sup>+</sup>_08</b>	-1643.602689	-1643.031704	-1639.996189	-1639.425204
<b>12-MOSCsi<sup>+</sup>_01</b>	-1643.605550	-1643.035196	-1639.993215	-1639.422862
<b>12-MOSCsi<sup>+</sup>_02</b>	-1643.603083	-1643.032750	-1639.991598	-1639.421265
<b>12-MOSCsi<sup>+</sup>_04</b>	-1643.601347	-1643.030613	-1639.991998	-1639.421264
<b>12-MOSCsi<sup>+</sup>_03</b>	-1643.598675	-1643.028064	-1639.988820	-1639.418209
<b>12-MOSCsi<sup>+</sup>_09</b>	-1643.595219	-1643.024596	-1639.988626	-1639.418002
<b>12-MOSCsi<sup>+</sup>_05</b>	-1643.599268	-1643.028681	-1639.986674	-1639.416088
<b>12-MOSCsi<sup>+</sup>_07</b>	-1643.591629	-1643.021710	-1639.982643	-1639.412724
	B98/6-31G(d)		MP2/6-31+G(2d,p)// B98/6-31G(d)	
	$E_{\text{tot}}$	$H_{298}$	$E_{\text{tot}}$	" $H_{298}$ "
<b>13_001</b>	-921.5866549	-921.189726	-919.4101728	-919.013244
<b>13_003</b>	-921.5852231	-921.188083	-919.4070412	-919.009901
<b>13_004</b>	-921.5889509	-921.191435	-919.4139549	-919.016439
<b>13_005</b>	-921.5813729	-921.184376	-919.4085544	-919.011558
<b>13_009</b>	-921.5860240	-921.189099	-919.4104425	-919.013518
<b>13_010</b>	-921.5894842	-921.192199	-919.4118589	-919.014574
<b>13_014</b>	-921.5877194	-921.190186	-919.4138594	-919.016326
<b>13_017</b>	-921.5836673	-921.186535	-919.4074266	-919.0102943
<b>13_019</b>	-921.5851201	-921.188262	-919.4083658	-919.0115076
<b>13_020</b>	-921.5867529	-921.189183	-919.4119593	-919.0143894
<b>13_021</b>	-921.5844605	-921.187680	-919.4086645	-919.011884
<b>13_024</b>	-921.5870239	-921.189772	-919.4100112	-919.0127592
<b>13_027</b>	-921.5862640	-921.189359	-919.4094697	-919.0125648
<b>13_028</b>	-921.5851751	-921.188372	-919.4092765	-919.0124734
<b>13_032</b>	-921.5842770	-921.187439	-919.4088214	-919.0119835
<b>13_035</b>	-921.5881224	-921.190711	-919.4119798	-919.0145683
<b>13_036</b>	-921.5889490	-921.191737	-919.4110959	-919.0138839
<b>13_037</b>	-921.5845324	-921.187662	-919.4060303	-919.009160
<b>13_041</b>	-921.5849067	-921.187900	-919.4085541	-919.0115474
<b>13_042</b>	-921.5864488	-921.189296	-919.4093327	-919.0121799
	B98/6-31G(d)		MP2/6-31+G(2d,p)// B98/6-31G(d)	
	$E_{\text{tot}}$	$H_{298}$	$E_{\text{tot}}$	" $H_{298}$ "
<b>13-CH<sub>3</sub><sup>+</sup>_001</b>	-961.2701738	-960.82892	-958.9863796	-958.5451258
<b>13-CH<sub>3</sub><sup>+</sup>_003</b>	-961.2761329	-960.83452	-958.9912918	-958.5496789
<b>13-CH<sub>3</sub><sup>+</sup>_005</b>	-961.2708816	-960.829177	-958.9887915	-958.5470869
<b>13-CH<sub>3</sub><sup>+</sup>_009</b>	-961.2698625	-960.828676	-958.9864472	-958.5452607
<b>13-CH<sub>3</sub><sup>+</sup>_010</b>	-961.2801043	-960.838721	-958.9958574	-958.5544741
<b>13-CH<sub>3</sub><sup>+</sup>_017</b>	-961.2695043	-960.828426	-958.9869748	-958.5458964
<b>13-CH<sub>3</sub><sup>+</sup>_019</b>	-961.2688022	-960.827719	-958.9848667	-958.5437834
<b>13-CH<sub>3</sub><sup>+</sup>_020</b>	-961.2683003	-960.826648	-958.9866331	-958.5449808
<b>13-CH<sub>3</sub><sup>+</sup>_021</b>	-961.2685341	-960.827574	-958.9849461	-958.543986
<b>13-CH<sub>3</sub><sup>+</sup>_024</b>	-961.2789835	-960.837451	-958.9947902	-958.5532577
<b>13-CH<sub>3</sub><sup>+</sup>_027</b>	-961.2694122	-960.828039	-958.9851935	-958.5438204
<b>13-CH<sub>3</sub><sup>+</sup>_028</b>	-961.269041	-960.82791	-958.9851956	-958.5440646
<b>13-CH<sub>3</sub><sup>+</sup>_032</b>	-961.2676998	-960.826777	-958.9842658	-958.543343
<b>13-CH<sub>3</sub><sup>+</sup>_035</b>	-961.2697891	-960.827968	-958.9863528	-958.5445318
<b>13-CH<sub>3</sub><sup>+</sup>_036</b>	-961.279245	-960.837851	-958.994624	-958.55323

**Table A8.** Continued

<b>13-CH<sub>3</sub><sup>+</sup>_037</b>	-961.2752159	-960.833642	-958.9897649	-958.548191
<b>13-CH<sub>3</sub><sup>+</sup>_041</b>	-961.2680194	-960.826839	-958.984245	-958.5430645
<b>13-CH<sub>3</sub><sup>+</sup>_042</b>	-961.2777295	-960.836122	-958.9935499	-958.5519424
	B98/6-31G(d)		MP2/6-31+G(2d,p)// B98/6-31G(d)	
	E <sub>tot</sub>	H <sub>298</sub>	E <sub>tot</sub>	"H <sub>298</sub> "
<b>13-H<sup>+</sup>_001</b>	-921.9854970	-921.573439	-919.8021426	-919.3900846
<b>13-H<sup>+</sup>_003</b>	-921.9820369	-921.569711	-919.7970468	-919.3847208
<b>13-H<sup>+</sup>_005</b>	-921.9874302	-921.575058	-919.8049399	-919.3925677
<b>13-H<sup>+</sup>_009</b>	-921.9846153	-921.572554	-919.8024302	-919.3903690
<b>13-H<sup>+</sup>_010</b>	-921.9859751	-921.573740	-919.8009993	-919.3887642
<b>13-H<sup>+</sup>_014</b>	-921.9867974	-921.574325	-919.8055074	-919.3930351
<b>13-H<sup>+</sup>_017</b>	-921.9833559	-921.571260	-919.8004486	-919.3883527
<b>13-H<sup>+</sup>_019</b>	-921.9844475	-921.572097	-919.8010013	-919.3886508
<b>13-H<sup>+</sup>_020</b>	-921.9851451	-921.572429	-919.8027178	-919.3900017
<b>13-H<sup>+</sup>_021</b>	-921.9834898	-921.571202	-919.8011979	-919.3889101
<b>13-H<sup>+</sup>_024</b>	-921.9848182	-921.572276	-919.8000823	-919.3875402
<b>13-H<sup>+</sup>_027</b>	-921.9847166	-921.572549	-919.8010722	-919.3889045
<b>13-H<sup>+</sup>_028</b>	-921.9835273	-921.571602	-919.8009379	-919.3890126
<b>13-H<sup>+</sup>_032</b>	-921.9826975	-921.570484	-919.8005513	-919.3883378
<b>13-H<sup>+</sup>_035</b>	-921.9864892	-921.573954	-919.8027721	-919.3902370
<b>13-H<sup>+</sup>_036</b>	-921.9852688	-921.573068	-919.7998936	-919.3876928
<b>13-H<sup>+</sup>_037</b>	-921.9813243	-921.568993	-919.7955719	-919.3832406
	B98/6-31G(d)		MP2/6-31+G(2d,p)// B98/6-31G(d)	
	E <sub>tot</sub>	H <sub>298</sub>	E <sub>tot</sub>	"H <sub>298</sub> "
<b>13-MOSCre<sup>+</sup>_02</b>	-1643.604216	-1643.033721	-1639.997386	-1639.426891
<b>13-MOSCre<sup>+</sup>_01</b>	-1643.604003	-1643.033450	-1639.991993	-1639.421440
<b>13-MOSCre<sup>+</sup>_04</b>	-1643.603302	-1643.032845	-1639.991861	-1639.421403
<b>13-MOSCre<sup>+</sup>_07</b>	-1643.596255	-1643.026383	-1639.989422	-1639.419550
<b>13-MOSCre<sup>+</sup>_03</b>	-1643.598123	-1643.027715	-1639.988594	-1639.418186
<b>13-MOSCre<sup>+</sup>_05</b>	-1643.597636	-1643.027356	-1639.985511	-1639.415231
<b>13-MOSCsi<sup>+</sup>_01</b>	-1643.604578	-1643.033928	-1639.994649	-1639.423999
<b>13-MOSCsi<sup>+</sup>_02</b>	-1643.601806	-1643.031755	-1639.992958	-1639.422907
<b>13-MOSCsi<sup>+</sup>_03</b>	-1643.598395	-1643.028319	-1639.991055	-1639.420979
<b>13-MOSCsi<sup>+</sup>_07</b>	-1643.593332	-1643.023306	-1639.984099	-1639.414073
<b>13-MOSCsi<sup>+</sup>_08</b>	-1643.597859	-1643.027121	-1639.990434	-1639.419696
<b>13-MOSCsi<sup>+</sup>_09</b>	-1643.592418	-1643.022222	-1639.985238	-1639.415042
	B98/6-31G(d)		MP2/6-31+G(2d,p)// B98/6-31G(d)	
	E <sub>tot</sub>	H <sub>298</sub>	E <sub>tot</sub>	"H <sub>298</sub> "
<b>42_011</b>	-921.5937026	-921.196290	-919.415943	-919.0185304
<b>42_008</b>	-921.5931012	-921.195636	-919.416186	-919.0187208
<b>42_004</b>	-921.5905881	-921.193172	-919.412842	-919.0154259
<b>42_001</b>	-921.5859910	-921.189057	-919.409452	-919.0125180
<b>42_003</b>	-921.5843123	-921.186952	-919.4099995	-919.0126392
<b>42_002</b>	-921.5841879	-921.187245	-919.407321	-919.0103781
<b>42_005</b>	-921.5831981	-921.186264	-919.407092	-919.0101579
<b>42_007</b>	-921.583059	-921.185963	-919.4068056	-919.0097096

**Table A8.** Continued

<b>42_010</b>	-921.5816597	-921.184822	-919.4022503	-919.0054126
<b>42_009</b>	-921.5813917	-921.184215	-919.4077828	-919.0106061
<b>42_006</b>	-921.5813376	-921.183983	-919.4060963	-919.0087416
<b>42_012</b>	-921.5782126	-921.181049	-919.4035414	-919.0063778
	B98/6-31G(d)		MP2/6-31+G(2d,p)// B98/6-31G(d)	
	$E_{\text{tot}}$	$H_{298}$	$E_{\text{tot}}$	" $H_{298}$ "
<b>42-CH<sub>3</sub><sup>+</sup>_005</b>	-961.275600	-960.834365	-958.9908784	-958.5496434
<b>42-CH<sub>3</sub><sup>+</sup>_001</b>	-961.275128	-960.833347	-958.9911647	-958.5493837
<b>42-CH<sub>3</sub><sup>+</sup>_002</b>	-961.274996	-960.833715	-958.9912316	-958.5499506
<b>42-CH<sub>3</sub><sup>+</sup>_004</b>	-961.274761	-960.833666	-958.9907128	-958.5496178
<b>42-CH<sub>3</sub><sup>+</sup>_007</b>	-961.2706736	-960.829269	-958.9849794	-958.5435748
<b>42-CH<sub>3</sub><sup>+</sup>_010</b>	-961.267876	-960.826077	-958.9812340	-958.5394350
<b>42-CH<sub>3</sub><sup>+</sup>_003</b>	-961.266441	-960.824839	-958.9837564	-958.5421544
<b>42-CH<sub>3</sub><sup>+</sup>_006</b>	-961.265867	-960.824347	-958.9820648	-958.5405448
	B98/6-31G(d)		MP2/6-31+G(2d,p)// B98/6-31G(d)	
	$E_{\text{tot}}$	$H_{298}$	$E_{\text{tot}}$	" $H_{298}$ "
<b>42-H<sup>+</sup>_001</b>	-921.9897650	-921.577438	-919.8057554	-919.3934284
<b>42-H<sup>+</sup>_002</b>	-921.9908158	-921.578439	-919.8058960	-919.3935192
<b>42-H<sup>+</sup>_003</b>	-921.9787661	-921.566525	-919.7984950	-919.3862539
<b>42-H<sup>+</sup>_005</b>	-921.9904078	-921.578058	-919.8053782	-919.3930285
<b>42-H<sup>+</sup>_007</b>	-921.9865441	-921.574114	-919.8033243	-919.3908942
<b>42-H<sup>+</sup>_010</b>	-921.9765757	-921.564280	-919.7897948	-919.3774991
<b>42-H<sup>+</sup>_012</b>	-921.9754354	-921.563082	-919.7936851	-919.3813317
	B98/6-31G(d)		MP2/6-31+G(2d,p)// B98/6-31G(d)	
	$E_{\text{tot}}$	$H_{298}$	$E_{\text{tot}}$	" $H_{298}$ "
<b>42-MOSCre<sup>+</sup>_01</b>	-1643.599907	-1643.029913	-1639.990878	-1639.420884
<b>42-MOSCre<sup>+</sup>_08</b>	-1643.595862	-1643.025974	-1639.986129	-1639.416241
<b>42-MOSCre<sup>+</sup>_04</b>	-1643.595263	-1643.024818	-1639.985763	-1639.415318
<b>42-MOSCre<sup>+</sup>_02</b>	-1643.590038	-1643.019695	-1639.978220	-1639.407877
<b>42-MOSCre<sup>+</sup>_06</b>	-1643.585004	-1643.015109	-1639.973756	-1639.403861
<b>42-MOSCsi<sup>+</sup>_07</b>	-1643.598134	-1643.028139	-1639.987531	-1639.417536
<b>42-MOSCsi<sup>+</sup>_03</b>	-1643.592530	-1643.022426	-1639.984422	-1639.414318
<b>42-MOSCsi<sup>+</sup>_06</b>	-1643.595868	-1643.025713	-1639.984386	-1639.414231
<b>42-MOSCsi<sup>+</sup>_08</b>	-1643.589326	-1643.019343	-1639.980353	-1639.410370
<b>42-MOSCsi<sup>+</sup>_01</b>	-1643.587537	-1643.017702	-1639.976301	-1639.406466
	B98/6-31G(d)		MP2/6-31+G(2d,p)// B98/6-31G(d)	
	$E_{\text{tot}}$	$H_{298}$	$E_{\text{tot}}$	" $H_{298}$ "
<b>43_001</b>	-921.586855	-921.189962	-919.4101597	-919.0132666
<b>43_002</b>	-921.5851539	-921.187849	-919.4118147	-919.0145098
<b>43_003</b>	-921.5843472	-921.187457	-919.4078311	-919.0109410
<b>43_004</b>	-921.5909415	-921.193734	-919.4132823	-919.0160748
<b>43_005</b>	-921.5792106	-921.182199	-919.4062212	-919.0092096
<b>43_006</b>	-921.5837651	-921.187079	-919.4083575	-919.0116714
<b>43_008</b>	-921.5822106	-921.185048	-919.4084876	-919.0113250

**Table A8.** Continued

<b>43_009</b>	-921.5858902	-921.188566	-919.4066186	-919.0092944
<b>43_010</b>	-921.5823639	-921.185137	-919.4097914	-919.0125644
<b>43_011</b>	-921.5934826	-921.196198	-919.4169003	-919.0196157
<b>43_012</b>	-921.5939487	-921.196641	-919.4160391	-919.0187313
	B98/6-31G(d)		MP2/6-31+G(2d,p)// B98/6-31G(d)	
	$E_{\text{tot}}$	$H_{298}$	$E_{\text{tot}}$	" $H_{298}$ "
<b>43-CH<sub>3</sub><sup>+</sup>_001</b>	-961.2761820	-960.834570	-958.9915791	-958.5499671
<b>43-CH<sub>3</sub><sup>+</sup>_002</b>	-961.2675148	-960.826028	-958.9856333	-958.5441465
<b>43-CH<sub>3</sub><sup>+</sup>_003</b>	-961.2760041	-960.834664	-958.9920441	-958.5507040
<b>43-CH<sub>3</sub><sup>+</sup>_005</b>	-961.2670684	-960.825412	-958.9846029	-958.5429465
<b>43-CH<sub>3</sub><sup>+</sup>_006</b>	-961.2758561	-960.834986	-958.9924532	-958.5515831
<b>43-CH<sub>3</sub><sup>+</sup>_007</b>	-961.2714869	-960.829997	-958.9857173	-958.5442274
<b>43-CH<sub>3</sub><sup>+</sup>_009</b>	-961.2689803	-960.827495	-958.9820880	-958.5406027
	B98/6-31G(d)		MP2/6-31+G(2d,p)// B98/6-31G(d)	
	$E_{\text{tot}}$	$H_{298}$	$E_{\text{tot}}$	" $H_{298}$ "
<b>43-H<sup>+</sup>_001</b>	-921.9907576	-921.578573	-919.8067045	-919.394520
<b>43-H<sup>+</sup>_002</b>	-921.9801851	-921.567909	-919.8004411	-919.388165
<b>43-H<sup>+</sup>_003</b>	-921.9912899	-921.579292	-919.8065833	-919.3945854
<b>43-H<sup>+</sup>_005</b>	-921.9771038	-921.564715	-919.7965835	-919.3841947
<b>43-H<sup>+</sup>_006</b>	-921.9909514	-921.578831	-919.8064695	-919.394349
<b>43-H<sup>+</sup>_007</b>	-921.9878322	-921.575494	-919.8049421	-919.3926039
<b>43-H<sup>+</sup>_009</b>	-921.9812792	-921.569042	-919.7959612	-919.383724
	B98/6-31G(d)		MP2/6-31+G(2d,p)// B98/6-31G(d)	
	$E_{\text{tot}}$	$H_{298}$	$E_{\text{tot}}$	" $H_{298}$ "
<b>43-MOSCre<sup>+</sup>_01</b>	-1643.591739	-1643.022052	-1639.979353	-1639.409666
<b>43-MOSCre<sup>+</sup>_02</b>	-1643.594035	-1643.023841	-1639.986786	-1639.416591
<b>43-MOSCre<sup>+</sup>_02f</b>	-1643.594301	-1643.024413	-1639.985853	-1639.415965
<b>43-MOSCre<sup>+</sup>_03</b>	-1643.588318	-1643.018546	-1639.975928	-1639.406156
<b>43-MOSCre<sup>+</sup>_05</b>	-1643.590052	-1643.020011	-1639.976994	-1639.406953
<b>43-MOSCre<sup>+</sup>_07</b>	-1643.591980	-1643.021690	-1639.984500	-1639.414211
<b>43-MOSCre<sup>+</sup>-2</b>	-1643.592183	-1643.021895	-1639.980660	-1639.410372
<b>43-MOSCSi<sup>+</sup>_01</b>	-1643.591871	-1643.022034	-1639.980474	-1639.410638
<b>43-MOSCSi<sup>+</sup>_02</b>	-1643.593294	-1643.023359	-1639.985145	-1639.415210
<b>43-MOSCSi<sup>+</sup>_02f</b>	-1643.593394	-1643.023408	-1639.984166	-1639.414180
<b>43-MOSCSi<sup>+</sup>_03</b>	-1643.592200	-1643.022403	-1639.981519	-1639.411722
<b>43-MOSCSi<sup>+</sup>_05</b>	-1643.588134	-1643.017814	-1639.975150	-1639.404830
<b>43-MOSCSi<sup>+</sup>_07</b>	-1643.583921	-1643.014272	-1639.976940	-1639.407291
<b>43-MOSCSi<sup>+</sup>_09</b>	-1643.588586	-1643.018810	-1639.979200	-1639.409425
<b>43-MOSCSi<sup>+</sup>-2</b>	-1643.593438	-1643.023461	-1639.983880	-1639.413903
	B98/6-31G(d)		MP2/6-31+G(2d,p)// B98/6-31G(d)	
	$E_{\text{tot}}$	$H_{298}$	$E_{\text{tot}}$	" $H_{298}$ "
<b>22_001</b>	-1036.064045	-1035.63162	-1033.649626	-1033.217202
<b>22_002</b>	-1036.063271	-1035.63078	-1033.648677	-1033.216186
<b>22_003</b>	-1036.060307	-1035.628085	-1033.65003	-1033.217808

**Table A8. Continued**

22_004	-1036.065746	-1035.633292	-1033.653124	-1033.22067
22_005	-1036.068588	-1035.635811	-1033.654762	-1033.221985
22_006	-1036.063743	-1035.631425	-1033.650633	-1033.218315
22_007	-1036.060095	-1035.627863	-1033.64983	-1033.217598
22_008	-1036.067788	-1035.634853	-1033.655591	-1033.222656
22_009	-1036.058178	-1035.624878	-1033.643194	-1033.209894
22_010	-1036.064900	-1035.632649	-1033.653097	-1033.220846
22_011	-1036.065123	-1035.632846	-1033.65054	-1033.218263
22_012	-1036.064006	-1035.631081	-1033.651085	-1033.21816
		B98/6-31G(d)	MP2/6-31+G(2d,p)//	
			B98/6-31G(d)	
	$E_{\text{tot}}$	$H_{298}$	$E_{\text{tot}}$	" $H_{298}$ "
22-CH <sub>3</sub> <sup>+</sup> _001	-1075.758261	-1075.281138	-1073.236200	-1072.759077
22-CH <sub>3</sub> <sup>+</sup> _002	-1075.756332	-1075.279571	-1073.233120	-1072.756359
22-CH <sub>3</sub> <sup>+</sup> _003	-1075.750382	-1075.273443	-1073.229677	-1072.752738
22-CH <sub>3</sub> <sup>+</sup> _004	-1075.754008	-1075.277398	-1073.234446	-1072.757836
22-CH <sub>3</sub> <sup>+</sup> _005	-1075.762849	-1075.286009	-1073.242374	-1072.765534
22-CH <sub>3</sub> <sup>+</sup> _006	-1075.753359	-1075.277042	-1073.233924	-1072.757607
22-CH <sub>3</sub> <sup>+</sup> _007	-1075.752695	-1075.275749	-1073.232492	-1072.755546
22-CH <sub>3</sub> <sup>+</sup> _008	-1075.752904	-1075.276163	-1073.233009	-1072.756268
22-CH <sub>3</sub> <sup>+</sup> _009	-1075.741733	-1075.264618	-1073.218161	-1072.741045
22-CH <sub>3</sub> <sup>+</sup> _010	-1075.752606	-1075.276149	-1073.232304	-1072.755847
		B98/6-31G(d)	MP2/6-31+G(2d,p)//	
			B98/6-31G(d)	
	$E_{\text{tot}}$	$H_{298}$	$E_{\text{tot}}$	" $H_{298}$ "
22-H <sup>+</sup> _001	-1036.464439	-1036.016537	-1034.042318	-1033.594416
22-H <sup>+</sup> _002	-1036.464216	-1036.016273	-1034.040968	-1033.593025
22-H <sup>+</sup> _003	-1036.467315	-1036.019342	-1034.047485	-1033.599513
22-H <sup>+</sup> _004	-1036.467954	-1036.020606	-1034.048352	-1033.601004
22-H <sup>+</sup> _005	-1036.469061	-1036.021498	-1034.047347	-1033.599784
22-H <sup>+</sup> _006	-1036.467674	-1036.020218	-1034.049005	-1033.601549
22-H <sup>+</sup> _008	-1036.469727	-1036.021733	-1034.049578	-1033.601584
22-H <sup>+</sup> _009	-1036.460096	-1036.011861	-1034.037043	-1033.588808
		B98/6-31G(d)	MP2/6-31+G(2d,p)//	
			B98/6-31G(d)	
	$E_{\text{tot}}$	$H_{298}$	$E_{\text{tot}}$	" $H_{298}$ "
22-MOSCre <sup>+</sup> _01	-1758.087101	-1757.481402	-1754.241803	-1753.636104
22-MOSCre <sup>+</sup> _02	-1758.085724	-1757.479891	-1754.240389	-1753.634556
22-MOSCre <sup>+</sup> _06	-1758.083252	-1757.478000	-1754.238964	-1753.633711
22-MOSCre <sup>+</sup> _03	-1758.083808	-1757.478011	-1754.238272	-1753.632475
22-MOSCre <sup>+</sup> _05	-1758.079826	-1757.474023	-1754.234721	-1753.628918
22-MOSCre <sup>+</sup> _07	-1758.078561	-1757.472803	-1754.233430	-1753.627672
22-MOSCre <sup>+</sup> _09	-1758.075877	-1757.470431	-1754.229819	-1753.624372
22-MOSCsi <sup>+</sup> _01	-1758.086887	-1757.480574	-1754.241563	-1753.635250
22-MOSCsi <sup>+</sup> _02	-1758.088386	-1757.482683	-1754.239736	-1753.634033
22-MOSCsi <sup>+</sup> _03	-1758.085827	-1757.479999	-1754.238113	-1753.632285
22-MOSCsi <sup>+</sup> _04	-1758.081582	-1757.475894	-1754.235634	-1753.629947
22-MOSCsi <sup>+</sup> _05	-1758.079735	-1757.473733	-1754.234196	-1753.628194
22-MOSCsi <sup>+</sup> _06	-1758.082237	-1757.476455	-1754.233498	-1753.627717

**Table A8.** Continued

<b>22-MOSCsi<sup>+</sup></b> 07				
	-1758.074409	-1757.469048	-1754.230301	-1753.624940
	B98/6-31G(d)		MP2/6-31+G(2d,p)// B98/6-31G(d)	
	E <sub>tot</sub>	H <sub>298</sub>	E <sub>tot</sub>	“H <sub>298</sub> ”
<b>18_001</b>	-1036.066186	-1035.634125	-1033.653432	-1033.221371
<b>18_002</b>	-1036.061212	-1035.629042	-1033.651730	-1033.219561
<b>18_003</b>	-1036.064705	-1035.632445	-1033.650406	-1033.218146
<b>18_004</b>	-1036.061250	-1035.628863	-1033.652231	-1033.219843
<b>18_006</b>	-1036.069264	-1035.636554	-1033.655331	-1033.222621
<b>18_007</b>	-1036.065653	-1035.633417	-1033.654082	-1033.221846
<b>18_010</b>	-1036.067474	-1035.634889	-1033.657729	-1033.225144
<b>18_011</b>	-1036.064603	-1035.632424	-1033.651622	-1033.219442
<b>18_014</b>	-1036.066460	-1035.633434	-1033.655512	-1033.222486
<b>18_015</b>	-1036.064188	-1035.631910	-1033.652476	-1033.220198
<b>18_017</b>	-1036.066821	-1035.634217	-1033.653496	-1033.220892
<b>18_019</b>	-1036.065566	-1035.632922	-1033.651049	-1033.218404
<b>18_020</b>	-1036.063982	-1035.631807	-1033.652401	-1033.220226
<b>18_022</b>	-1036.059757	-1035.627553	-1033.651898	-1033.219694
<b>18_024</b>	-1036.059489	-1035.627123	-1033.650057	-1033.217691
<b>18_027</b>	-1036.066226	-1035.633741	-1033.652803	-1033.220317
<b>18_028</b>	-1036.064312	-1035.632147	-1033.651568	-1033.219403
<b>18_029</b>	-1036.059138	-1035.626945	-1033.65042	-1033.218227
<b>18_030</b>	-1036.062031	-1035.629745	-1033.648411	-1033.216124
	B98/6-31G(d)		MP2/6-31+G(2d,p)// B98/6-31G(d)	
	E <sub>tot</sub>	H <sub>298</sub>	E <sub>tot</sub>	“H <sub>298</sub> ”
<b>18-CH<sub>3</sub><sup>+</sup>_001</b>	-1075.753524	-1075.276884	-1073.233256	-1072.756616
<b>18-CH<sub>3</sub><sup>+</sup>_003</b>	-1075.759363	-1075.282498	-1073.238107	-1072.761242
<b>18-CH<sub>3</sub><sup>+</sup>_004</b>	-1075.754225	-1075.277182	-1073.235703	-1072.758660
<b>18-CH<sub>3</sub><sup>+</sup>_006</b>	-1075.763966	-1075.286973	-1073.243065	-1072.766072
<b>18-CH<sub>3</sub><sup>+</sup>_007</b>	-1075.753568	-1075.277100	-1073.233414	-1072.756946
<b>18-CH<sub>3</sub><sup>+</sup>_010</b>	-1075.753090	-1075.276204	-1073.236009	-1072.759123
<b>18-CH<sub>3</sub><sup>+</sup>_011</b>	-1075.752147	-1075.275488	-1073.231864	-1072.755205
<b>18-CH<sub>3</sub><sup>+</sup>_015</b>	-1075.752244	-1075.275869	-1073.232142	-1072.755767
<b>18-CH<sub>3</sub><sup>+</sup>_017</b>	-1075.762838	-1075.285569	-1073.242047	-1072.764778
<b>18-CH<sub>3</sub><sup>+</sup>_019</b>	-1075.755076	-1075.278025	-1073.233332	-1072.756281
<b>18-CH<sub>3</sub><sup>+</sup>_020</b>	-1075.751413	-1075.275020	-1073.231334	-1072.754941
<b>18-CH<sub>3</sub><sup>+</sup>_024</b>	-1075.749003	-1075.272002	-1073.229421	-1072.752420
<b>18-CH<sub>3</sub><sup>+</sup>_027</b>	-1075.761463	-1075.284388	-1073.240701	-1072.763627
<b>18-CH<sub>3</sub><sup>+</sup>_028</b>	-1075.751363	-1075.274728	-1073.231127	-1072.754492
<b>18-CH<sub>3</sub><sup>+</sup>_029</b>	-1075.751456	-1075.274779	-1073.233447	-1072.756770
<b>18-CH<sub>3</sub><sup>+</sup>_030</b>	-1075.756970	-1075.279975	-1073.235998	-1072.759002
	B98/6-31G(d)		MP2/6-31+G(2d,p)// B98/6-31G(d)	
	E <sub>tot</sub>	H <sub>298</sub>	E <sub>tot</sub>	“H <sub>298</sub> ”
<b>18-H<sup>+</sup>_001</b>	-1036.468900	-1036.021425	-1034.049063	-1033.601588
<b>18-H<sup>+</sup>_003</b>	-1036.465251	-1036.017590	-1034.043965	-1033.596304
<b>18-H<sup>+</sup>_004</b>	-1036.471033	-1036.023001	-1034.051905	-1033.603873
<b>18-H<sup>+</sup>_006</b>	-1036.469922	-1036.022067	-1034.048284	-1033.600429

**Table A8.** Continued

<b>18-H<sup>+</sup></b> _007	-1036.468966	-1036.021373	-1034.050215	-1033.602623
<b>18-H<sup>+</sup></b> _010	-1036.470314	-1036.022375	-1034.052590	-1033.604651
<b>18-H<sup>+</sup></b> _011	-1036.467820	-1036.020295	-1034.047881	-1033.600357
<b>18-H<sup>+</sup></b> _014	-1036.468427	-1036.020786	-1034.049680	-1033.602039
<b>18-H<sup>+</sup></b> _015	-1036.467903	-1036.020274	-1034.049280	-1033.601651
<b>18-H<sup>+</sup></b> _017	-1036.468656	-1036.020765	-1034.047237	-1033.599346
<b>18-H<sup>+</sup></b> _019	-1036.461187	-1036.013311	-1034.038792	-1033.590916
<b>18-H<sup>+</sup></b> _020	-1036.466996	-1036.019450	-1034.048423	-1033.600878
<b>18-H<sup>+</sup></b> _024	-1036.466047	-1036.018239	-1034.048998	-1033.601190
<b>18-H<sup>+</sup></b> _027	-1036.467320	-1036.019542	-1034.045863	-1033.598085
<b>18-H<sup>+</sup></b> _029	-1036.468475	-1036.020693	-1034.049488	-1033.601706
<b>18-H<sup>+</sup></b> _030	-1036.462827	-1036.015211	-1034.041877	-1033.594261
	B98/6-31G(d)		MP2/6-31+G(2d,p)// B98/6-31G(d)	
	$E_{\text{tot}}$	$H_{298}$	$E_{\text{tot}}$	" $H_{298}$ "
<b>18-MOSCre<sup>+</sup></b> _01	-1758.089079	-1757.482983	-1754.245720	-1753.639625
<b>18-MOSCre<sup>+</sup></b> _02	-1758.086967	-1757.481117	-1754.238695	-1753.632844
<b>18-MOSCre<sup>+</sup></b> _03	-1758.081215	-1757.475679	-1754.235692	-1753.630157
<b>18-MOSCre<sup>+</sup></b> _06	-1758.086117	-1757.480192	-1754.238379	-1753.632454
<b>18-MOSCre<sup>+</sup></b> _07	-1758.080637	-1757.474930	-1754.232354	-1753.626647
<b>18-MOSCre<sup>+</sup></b> _09	-1758.073677	-1757.468394	-1754.229712	-1753.624429
<b>18-MOSCsi<sup>+</sup></b> _01	-1758.088831	-1757.482880	-1754.242752	-1753.636801
<b>18-MOSCsi<sup>+</sup></b> _02	-1758.080947	-1757.475539	-1754.238234	-1753.632826
<b>18-MOSCsi<sup>+</sup></b> _03	-1758.085017	-1757.479075	-1754.239741	-1753.633799
<b>18-MOSCsi<sup>+</sup></b> _06	-1758.080731	-1757.474890	-1754.238224	-1753.632382
<b>18-MOSCsi<sup>+</sup></b> _07	-1758.075108	-1757.469477	-1754.232627	-1753.626996
<b>18-MOSCsi<sup>+</sup></b> _09	-1758.076332	-1757.471045	-1754.230981	-1753.625694
	B98/6-31G(d)		MP2/6-31+G(2d,p)// B98/6-31G(d)	
	$E_{\text{tot}}$	$H_{298}$	$E_{\text{tot}}$	" $H_{298}$ "
<b>44_001</b>	-1036.069980	-1035.637348	-1033.655999	-1033.223368
<b>44_002</b>	-1036.060772	-1035.628432	-1033.651101	-1033.218761
<b>44_003</b>	-1036.061379	-1035.629225	-1033.645507	-1033.213353
<b>44_004</b>	-1036.073096	-1035.640465	-1033.659264	-1033.226632
<b>44_005</b>	-1036.072849	-1035.640180	-1033.659619	-1033.226950
<b>44_006</b>	-1036.057383	-1035.625117	-1033.646699	-1033.214433
<b>44_007</b>	-1036.065999	-1035.633384	-1033.653150	-1033.220535
<b>44_008</b>	-1036.063713	-1035.631218	-1033.653399	-1033.220904
<b>44_009</b>	-1036.062208	-1035.629989	-1033.650035	-1033.217815
<b>44_010</b>	-1036.064545	-1035.632063	-1033.648819	-1033.216336
<b>44_011</b>	-1036.063588	-1035.631520	-1033.654862	-1033.222794
<b>44_012</b>	-1036.063071	-1035.630915	-1033.650758	-1033.218603
<b>44_013</b>	-1036.060730	-1035.628410	-1033.649180	-1033.216859
	B98/6-31G(d)		MP2/6-31+G(2d,p)// B98/6-31G(d)	
	$E_{\text{tot}}$	$H_{298}$	$E_{\text{tot}}$	" $H_{298}$ "
<b>44-CH<sub>3</sub><sup>+</sup></b> _001	-1075.758208	-1075.281675	-1073.237548	-1072.761015
<b>44-CH<sub>3</sub><sup>+</sup></b> _002	-1075.750370	-1075.273370	-1073.231407	-1072.754406
<b>44-CH<sub>3</sub><sup>+</sup></b> _003	-1075.758599	-1075.281679	-1073.236661	-1072.759740

**Table A8. Continued**

<b>44-CH<sub>3</sub><sup>+</sup></b> _004	-1075.751593	-1075.274793	-1073.228145	-1072.751344
<b>44-CH<sub>3</sub><sup>+</sup></b> _005	-1075.758893	-1075.282147	-1073.238368	-1072.761622
<b>44-CH<sub>3</sub><sup>+</sup></b> _006	-1075.754349	-1075.277519	-1073.232202	-1072.755373
<b>44-CH<sub>3</sub><sup>+</sup></b> _007	-1075.748924	-1075.272049	-1073.228549	-1072.751675
<b>44-CH<sub>3</sub><sup>+</sup></b> _008	-1075.758310	-1075.281794	-1073.238198	-1072.761683
	B98/6-31G(d)		MP2/6-31+G(2d,p)// B98/6-31G(d)	
	E <sub>tot</sub>	H <sub>298</sub>	E <sub>tot</sub>	"H <sub>298</sub> "
<b>44-H<sup>+</sup></b> _001	-1036.47379	-1036.026008	-1034.052194	-1033.604412
<b>44-H<sup>+</sup></b> _002	-1036.463488	-1036.015641	-1034.046685	-1033.598839
<b>44-H<sup>+</sup></b> _004	-1036.464182	-1036.016571	-1034.042085	-1033.594474
<b>44-H<sup>+</sup></b> _005	-1036.47352	-1036.025752	-1034.053123	-1033.605355
<b>44-H<sup>+</sup></b> _006	-1036.471088	-1036.023347	-1034.051572	-1033.603831
<b>44-H<sup>+</sup></b> _007	-1036.458393	-1036.010889	-1034.038478	-1033.590974
<b>44-H<sup>+</sup></b> _008	-1036.474456	-1036.026842	-1034.052981	-1033.605367
	B98/6-31G(d)		MP2/6-31+G(2d,p)// B98/6-31G(d)	
	E <sub>tot</sub>	H <sub>298</sub>	E <sub>tot</sub>	"H <sub>298</sub> "
<b>44-MOSCre<sup>+</sup></b> _01	-1758.082768	-1757.477270	-1754.237604	-1753.632106
<b>44-MOSCre<sup>+</sup></b> _02	-1758.078549	-1757.473387	-1754.232529	-1753.627367
<b>44-MOSCre<sup>+</sup></b> _03	-1758.072636	-1757.467147	-1754.224494	-1753.619006
<b>44-MOSCre<sup>+</sup></b> _04	-1758.077853	-1757.472186	-1754.232257	-1753.626591
<b>44-MOSCre<sup>+</sup></b> _08	-1758.067127	-1757.462117	-1754.219701	-1753.614691
<b>44-MOSCsi<sup>+</sup></b> _07	-1758.080712	-1757.475250	-1754.233964	-1753.628502
<b>44-MOSCsi<sup>+</sup></b> _01	-1758.074077	-1757.46862	-1754.226609	-1753.621152
<b>44-MOSCsi<sup>+</sup></b> _02	-1758.075044	-1757.469844	-1754.229000	-1753.623800
<b>44-MOSCsi<sup>+</sup></b> _06	-1758.068479	-1757.462669	-1754.221523	-1753.615712
<b>44-MOSCsi<sup>+</sup></b> _09	-1758.078083	-1757.472529	-1754.23062	-1753.625065
	B98/6-31G(d)		MP2/6-31+G(2d,p)// B98/6-31G(d)	
	E <sub>tot</sub>	H <sub>298</sub>	E <sub>tot</sub>	"H <sub>298</sub> "
<b>45_001</b>	-1036.066757	-1035.634453	-1033.653665	-1033.221362
<b>45_002</b>	-1036.064613	-1035.632176	-1033.655313	-1033.222875
<b>45_003</b>	-1036.063787	-1035.631846	-1033.651134	-1033.219193
<b>45_004</b>	-1036.073255	-1035.640778	-1033.66053	-1033.228052
<b>45_006</b>	-1036.058509	-1035.626247	-1033.649403	-1033.217141
<b>45_007</b>	-1036.063209	-1035.630900	-1033.650992	-1033.218684
<b>45_008</b>	-1036.061724	-1035.629189	-1033.651763	-1033.219228
<b>45_009</b>	-1036.073426	-1035.640779	-1033.659562	-1033.226915
<b>45_010</b>	-1036.061778	-1035.629425	-1033.653193	-1033.22084
<b>45_011</b>	-1036.060798	-1035.628276	-1033.651248	-1033.218726
<b>45_013</b>	-1036.06548	-1035.632868	-1033.649409	-1033.216797
	B98/6-31G(d)		MP2/6-31+G(2d,p)// B98/6-31G(d)	
	E <sub>tot</sub>	H <sub>298</sub>	E <sub>tot</sub>	"H <sub>298</sub> "
<b>45-CH<sub>3</sub><sup>+</sup></b> _001	-1075.759890	-1075.282709	-1073.238806	-1072.761625
<b>45-CH<sub>3</sub><sup>+</sup></b> _002	-1075.751348	-1075.274404	-1073.233069	-1072.756125
<b>45-CH<sub>3</sub><sup>+</sup></b> _003	-1075.759227	-1075.282477	-1073.238871	-1072.762121

**Table A8.** Continued

<b>45-CH<sub>3</sub><sup>+</sup></b> _004	-1075.759484	-1075.282844	-1073.239723	-1072.763083
<b>45-CH<sub>3</sub><sup>+</sup></b> _006	-1075.750040	-1075.273217	-1073.231028	-1072.754205
<b>45-CH<sub>3</sub><sup>+</sup></b> _007	-1075.754991	-1075.278206	-1073.232573	-1072.755788
<b>45-CH<sub>3</sub><sup>+</sup></b> _013	-1075.752728	-1075.275879	-1073.229197	-1072.752348
	B98/6-31G(d)		MP2/6-31+G(2d,p)// B98/6-31G(d)	
	$E_{\text{tot}}$	$H_{298}$	$E_{\text{tot}}$	" $H_{298}$ "
<b>45-H<sup>+</sup></b> _001	-1036.474576	-1036.026716	-1034.053847	-1033.605988
<b>45-H<sup>+</sup></b> _002	-1036.464880	-1036.017131	-1034.048621	-1033.600872
<b>45-H<sup>+</sup></b> _003	-1036.474995	-1036.027336	-1034.053486	-1033.605827
<b>45-H<sup>+</sup></b> _004	-1036.474442	-1036.027046	-1034.053450	-1033.606054
<b>45-H<sup>+</sup></b> _006	-1036.460176	-1036.012420	-1034.043405	-1033.595649
<b>45-H<sup>+</sup></b> _007	-1036.472390	-1036.024645	-1034.052974	-1033.605228
<b>45-H<sup>+</sup></b> _013	-1036.465316	-1036.017551	-1034.043134	-1033.595369
	B98/6-31G(d)		MP2/6-31+G(2d,p)// B98/6-31G(d)	
	$E_{\text{tot}}$	$H_{298}$	$E_{\text{tot}}$	" $H_{298}$ "
<b>45-MOSCre<sup>+</sup></b> _01	-1758.071703	-1757.466694	-1754.225036	-1753.620027
<b>45-MOSCre<sup>+</sup></b> _02	-1758.071484	-1757.466074	-1754.222728	-1753.617318
<b>45-MOSCre<sup>+</sup></b> _03	-1758.077001	-1757.471537	-1754.233897	-1753.628433
<b>45-MOSCre<sup>+</sup></b> _04	-1758.074804	-1757.469711	-1754.226469	-1753.621376
<b>45-MOSCre<sup>+</sup></b> _05	-1758.072838	-1757.467284	-1754.223426	-1753.617872
<b>45-MOSCre<sup>+</sup></b> _09	-1758.074977	-1757.468885	-1754.231469	-1753.625377
<b>45-MOSCre<sup>+</sup></b> -2	-1758.074917	-1757.469920	-1754.227396	-1753.622399
<b>45-MOSCsi<sup>+</sup></b> _01	-1758.074895	-1757.469573	-1754.227608	-1753.622286
<b>45-MOSCsi<sup>+</sup></b> _02	-1758.076414	-1757.471179	-1754.232221	-1753.626986
<b>45-MOSCsi<sup>+</sup></b> _03	-1758.075342	-1757.470189	-1754.228495	-1753.623341
<b>45-MOSCsi<sup>+</sup></b> _05	-1758.071021	-1757.465588	-1754.222066	-1753.616632
<b>45-MOSCsi<sup>+</sup></b> _09	-1758.071545	-1757.466157	-1754.226083	-1753.620695
<b>45-MOSCsi<sup>+</sup></b> -2	-1758.076534	-1757.470870	-1754.231179	-1753.625515
	B98/6-31G(d)		MP2/6-31+G(2d,p)// B98/6-31G(d)	
	$E_{\text{tot}}$	$H_{298}$	$E_{\text{tot}}$	" $H_{298}$ "
<b>23</b> _1	-654.7492304	-654.414312	-653.1329555	-652.7980371
<b>23</b> _2	-654.7479671	-654.413103	-653.1320615	-652.7971974
<b>23</b> _3	-654.7532243	-654.418531	-653.1369481	-652.8022548
<b>23</b> _4	-654.7443606	-654.409563	-653.1299122	-652.7951146
	B98/6-31G(d)		MP2/6-31+G(2d,p)// B98/6-31G(d)	
	$E_{\text{tot}}$	$H_{298}$	$E_{\text{tot}}$	" $H_{298}$ "
<b>23-CH<sub>3</sub><sup>+</sup></b> _1	-694.4348506	-694.054790	-692.7107562	-692.3306956
<b>23-CH<sub>3</sub><sup>+</sup></b> _2	-694.4415762	-694.061442	-692.718195	-692.3380608
	B98/6-31G(d)		MP2/6-31+G(2d,p)// B98/6-31G(d)	
	$E_{\text{tot}}$	$H_{298}$	$E_{\text{tot}}$	" $H_{298}$ "
<b>23-H<sup>+</sup></b> _1	-655.141367	-654.790594	-653.5186232	-653.1678502
<b>23-H<sup>+</sup></b> _2	-655.1441714	-654.793312	-653.5217463	-653.1708869
<b>23-H<sup>+</sup></b> _3	-655.1440534	-654.793600	-653.5206657	-653.1702123

<b>Table A8. Continued</b>				
<b>23-H<sup>+</sup></b> 4	-655.15792	-654.807365	-653.5349398	-653.1843848
	B98/6-31G(d)		MP2/6-31+G(2d,p)// B98/6-31G(d)	
	E <sub>tot</sub>	H <sub>298</sub>	E <sub>tot</sub>	"H <sub>298</sub> "
<b>23-MOSCre<sup>+</sup></b> 1	-1376.775325	-1376.266609	-1373.723672	-1373.214955
<b>23-MOSCre<sup>+</sup></b> 2	-1376.773697	-1376.264624	-1373.720932	-1373.211859
<b>23-MOSCre<sup>+</sup></b> 3	-1376.769370	-1376.260250	-1373.715651	-1373.206531
<b>23-MOSCsi<sup>+</sup></b> 3	-1376.775878	-1376.267013	-1373.721319	-1373.212454
<b>23-MOSCsi<sup>+</sup></b> 2	-1376.772857	-1376.264142	-1373.720307	-1373.211592
<b>23-MOSCsi<sup>+</sup></b> 1	-1376.772932	-1376.264167	-1373.719996	-1373.211230
	B98/6-31G(d)		MP2/6-31+G(2d,p)// B98/6-31G(d)	
	E <sub>tot</sub>	H <sub>298</sub>	E <sub>tot</sub>	"H <sub>298</sub> "
<b>46</b> 1	-654.7492304	-654.414312	-653.1329555	-652.7980371
<b>46</b> 2	-654.7479671	-654.413103	-653.1320615	-652.7971974
	B98/6-31G(d)		MP2/6-31+G(2d,p)// B98/6-31G(d)	
	E <sub>tot</sub>	H <sub>298</sub>	E <sub>tot</sub>	"H <sub>298</sub> "
<b>46-CH<sub>3</sub><sup>+</sup></b> 1	-736.1670902	-735.706313	-734.3148393	-733.8540621
<b>46-CH<sub>3</sub><sup>+</sup></b> 2	-736.1682069	-735.707928	-734.3129545	-733.8526756
<b>46-CH<sub>3</sub><sup>+</sup></b> 3	-736.1674464	-735.706487	-734.3148327	-733.8538733
	B98/6-31G(d)		MP2/6-31+G(2d,p)// B98/6-31G(d)	
	E <sub>tot</sub>	H <sub>298</sub>	E <sub>tot</sub>	"H <sub>298</sub> "
<b>46-H<sup>+</sup></b> 1	-696.8893978	-696.458337	-695.1368098	-694.705749
<b>46-H<sup>+</sup></b> 2	-696.9042990	-696.473310	-695.1519640	-694.720975
	B98/6-31G(d)		MP2/6-31+G(2d,p)// B98/6-31G(d)	
	E <sub>tot</sub>	H <sub>298</sub>	E <sub>tot</sub>	"H <sub>298</sub> "
<b>46-MOSCre<sup>+</sup></b> 1	-1418.478383	-1417.888939	-1415.302406	-1414.712962
<b>46-MOSCre<sup>+</sup></b> 2	-1418.474201	-1417.884423	-1415.293339	-1414.703561
<b>46-MOSCre<sup>+</sup></b> 3	-1418.467735	-1417.878659	-1415.289952	-1414.700877
<b>46-MOSCsi<sup>+</sup></b> 1	-1418.479207	-1417.889898	-1415.301225	-1414.711916
<b>46-MOSCsi<sup>+</sup></b> 2	-1418.469595	-1417.880386	-1415.290017	-1414.700808
<b>46-MOSCsi<sup>+</sup></b> 3	-1418.478015	-1417.888451	-1415.301781	-1414.712216

**Table A9.** Total Energies and Enthalpies of NMe<sub>3</sub> (**9**), PMe<sub>3</sub> (**34**), MVK (**47**) and Their Adducts and Complexes (in Hartree).

	HF/6-31G(d)		HF/6-31+G(d)		HF/6-31+G(2d)	
	E <sub>tot</sub>	H <sub>298</sub>	E <sub>tot</sub>	H <sub>298</sub>	E <sub>tot</sub>	H <sub>298</sub>
<b>47</b>	-229.806306	-229.703424	-229.813430	-229.710750	-229.820729	-229.719123
<b>9</b>	-173.269299	-173.133640	-173.272906	-173.137545	-173.274999	-173.141287
<b>48</b>	-403.032495	-402.789337	-403.045799	-402.802829	-403.052234	-402.812029
<b>34</b>	-459.567374	-459.439280	-459.569796	-459.441993	-459.572141	-459.446060
<b>49</b>	-689.337018	-689.103886	-689.352294	-689.119548	-689.363825	-689.134090
<b>50</b>	-689.353963	-689.119521	-689.363054	-689.129147	-689.375077	-689.144041
<b>9*47</b>	-403.079773	-402.838987	-403.089161	-402.848994	-403.097733	-402.860494
<b>34*47</b>	-689.377139	-689.144064	-689.385966	-689.153411	-689.394906	-689.165357
	HF/6-31+G(2d,p)		HF/6-311+G(2d,p)			
	E <sub>tot</sub>	H <sub>298</sub>	E <sub>tot</sub>	H <sub>298</sub>		
<b>47</b>	-229.834145	-229.732131	-229.877813	-229.776010		
<b>9</b>	-173.292332	-173.158308	-173.322146	-173.188433		
<b>48</b>	-403.083306	-402.842431	-403.156696	-402.916290		
<b>34</b>	-459.591526	-459.465063	-459.630786	-459.504652		
<b>49</b>	-689.396869	-689.166399	-689.480871	-689.250790		
<b>50</b>	-689.407422	-689.175630	-689.490944	-689.259589		
<b>9*47</b>	-403.128477	-402.890520	-403.201918	-402.964479		
<b>34*47</b>	-689.427696	-689.197356	-689.510696	-689.280892		
	B3LYP/6-31G(d)		B3LYP /6-31+G(d)		B3LYP /6-31+G(2d)	
	E <sub>tot</sub>	H <sub>298</sub>	E <sub>tot</sub>	H <sub>298</sub>	E <sub>tot</sub>	H <sub>298</sub>
<b>47</b>	-231.235183	-231.138593	-231.247553	-231.151066	-231.252087	-231.156248
<b>9</b>	-174.474415	-174.346923	-174.481766	-174.354635	-174.480914	-174.354713
<b>48</b>	-	-	-	-	-	-
<b>34</b>	-461.098422	-460.977318	-461.104538	-460.983820	-461.103674	-460.983983
<b>49</b>	-692.310644	-692.091071	-692.332828	-692.113626	-692.338648	-692.121211
<b>50</b>	-692.330843	-692.110022	-692.347273	-692.127052	-692.353641	-692.135061
<b>9*47</b>	-405.715763	-405.489282	-405.732249	-405.506553	-405.735581	-405.511487
<b>34*47</b>	-692.338286	-692.118449	-692.354674	-692.135510	-692.358059	-692.140630
	B3LYP /6-31+G(2d,p)		B3LYP /6-311+G(2d,p)		B3LYP /6-31G(2df,p)	
	E <sub>tot</sub>	H <sub>298</sub>	E <sub>tot</sub>	H <sub>298</sub>	E <sub>tot</sub>	H <sub>298</sub>
<b>47</b>	-231.262648	-231.166627	-231.313286	-231.217422	-231.253479	-231.157475
<b>9</b>	-174.494600	-174.368354	-174.531297	-174.405237	-174.489614	-174.363241
<b>48</b>	-	-	-	-	-	-
<b>34</b>	-461.119470	-460.999663	-461.170061	-461.050350	-461.117011	-460.997056
<b>49</b>	-692.365560	-692.147842	-692.466791	-692.249276	-692.350853	-692.13329
<b>50</b>	-692.380092	-692.161242	-692.481381	-692.262765	-692.372412	-692.153466
<b>9*47</b>	-405.759874	-405.535558	-405.846988	-405.623009	-405.749746	-405.524939
<b>34*47</b>	-692.384445	-692.166694	-692.485402	-692.267930	-692.375277	-692.157210
B3LYP /cc-pVTZ+d						
	E <sub>tot</sub>	H <sub>298</sub>				
<b>47</b>	-231.326094	-231.230100				
<b>9</b>	-174.542137	-174.416062				
<b>48</b>	-	-				
<b>34</b>	-461.186237	-461.066489				
<b>49</b>	-692.496069	-692.278608				
<b>50</b>	-692.514248	-692.295442				
<b>9*47</b>	-405.872195	-405.648005				
<b>34*47</b>	-692.515298	-692.297652				
	mPW1K /6-31G(d)		mPW1K /6-31+G(d)		mPW1K /6-31+G(2d)	
	E <sub>tot</sub>	H <sub>298</sub>	E <sub>tot</sub>	H <sub>298</sub>	E <sub>tot</sub>	H <sub>298</sub>
<b>47</b>	-231.1595826	-231.060288	-231.1677200	-231.068480	-231.174176	-231.075795

**Table A9.** Continued

<b>9</b>	-174.4287667	-174.297700	-174.4333788	-174.302578	-174.434669	-174.305052
<b>48</b>	-405.5713636	-405.336825	-405.5858077	-405.351422	-405.591021	-405.358617
<b>34</b>	-461.0730236	-460.948758	-461.0763315	-460.952349	-461.078027	-460.955317
<b>49</b>	-692.2231393	-691.997633	-692.2384318	-692.013290	-692.248911	-692.026004
<b>50</b>	-692.2463790	-692.020840	-692.2579971	-692.031679	-692.269076	-692.044845
<b>9*47</b>	-405.5942742	-405.361583	-405.6047015	-405.372614	-405.611750	-405.381738
<b>34*47</b>	-692.2371435	-692.011491	-692.2471850	-692.022047	-692.254815	-692.031873
	mPW1K /6-31+G(2d,p)		mPW1K /6-311+G(2d,p)		mPW1K/G3large// mPW1K/6-31+G(d)	
	$E_{tot}$	$H_{298}$	$E_{tot}$	$H_{298}$	$E_{tot}$	" $H_{298}$ "
<b>47</b>	-231.1848716	-231.086265	-231.2301345	-231.131754	-231.239052	-231.139812
<b>9</b>	-174.4482869	-174.318588	-174.4801497	-174.350777	-174.487966	-174.357166
<b>48</b>	-405.6158462	-405.383175	-405.6929462	-405.460814	-405.709615	-405.475230
<b>34</b>	-461.0938734	-460.971003	-461.1366978	-461.014151	-461.147186	-461.023204
<b>49</b>	-692.2760684	-692.052815	-692.3650754	-692.142276	-692.386651	-692.161509
<b>50</b>	-692.2955251	-692.070928	-692.3844590	-692.160335	-692.408192	-692.181874
<b>9*47</b>	-405.6362065	-405.405876	-405.7133765	-405.483570	-405.729921	-405.497834
<b>34*47</b>	-692.2814541	-692.058105	-692.3696406	-692.146817	-692.389027	-692.163889
	mPW1K/6-311+G(3df,2pd)// mPW1K/6-31+G(d)					
	$E_{tot}$	" $H_{298}$ "				
<b>47</b>	-231.2392279	-231.139988				
<b>9</b>	-174.4881315	-174.357331				
<b>48</b>	-405.7101920	-405.475806				
<b>34</b>	-461.1454675	-461.021485				
<b>49</b>	-692.3847810	-692.159640				
<b>50</b>	-692.4061228	-692.179805				
<b>9*47</b>	-405.7301285	-405.498041				
<b>34*47</b>	-692.3873394	-692.162201				
	MP2(FC) /6-31G(d)		MP2(FULL) /6-31G(d)		MP2(FC) /6-31+G(d)	
	$E_{tot}$	$H_{298}$	$E_{tot}$	$H_{298}$	$E_{tot}$	$H_{298}$
<b>47</b>	-230.4866670	-230.388763	-230.5085951	-230.410599	-230.502459	-230.404967
<b>9</b>	-173.8285982	-173.698370	-173.8464634	-173.716146	-173.839519	-173.709890
<b>48</b>	-	-	-	-	-404.333065	-404.101733
<b>34</b>	-460.0686967	-459.944835	-460.0948309	-459.970921	-460.076783	-459.953758
<b>49</b>	-	-	-	-	-690.575811	-690.352789
<b>50</b>	-690.5683612	-690.343253	-690.6184788	-690.393254	-690.595241	-690.371618
<b>9*47</b>	-404.3246498	-404.094162	-404.3646623	-404.133972	-404.349792	-404.120835
<b>34*47</b>	-690.5627738	-690.338843	-690.6112444	-690.387151	-690.586676	-690.364153
	MP2(FULL) /6-31+G(d)		MP2(FC) /6-31+G(2d)		MP2(FC) /6-31+G(2d,p)	
	$E_{tot}$	$H_{298}$	$E_{tot}$	$H_{298}$	$E_{tot}$	$H_{298}$
<b>47</b>	-230.5249747	-230.427390	-230.5618313	-230.465568	-230.607307	-230.509992
<b>9</b>	-173.8577726	-173.728070	-173.8794972	-173.752097	-173.949129	-173.820021
<b>48</b>	-404.3749606	-404.143447	-404.4327570	-404.205102	-404.547671	-404.317322
<b>34</b>	-460.1036288	-459.980571	-460.1194620	-459.998871	-460.191422	-460.068947
<b>49</b>	-690.6269323	-690.403816	-690.6809060	-690.462156	-690.797920	-690.576195
<b>50</b>	-690.6468862	-690.423171	-690.7019660	-690.482374	-690.819853	-690.597224
<b>9*47</b>	-404.3910523	-404.161899	-404.4488044	-404.223213	-404.563500	-404.335199
<b>34*47</b>	-690.6367417	-690.414081	-690.6879778	-690.469212	-690.805122	-690.583445
	MP2(FC) /6-311+G(2d,p)		MP2(FC)/G3MP2large// mPW1K/6-31+G(d)		MP2(Full)/G3large// mPW1K/6-31+G(d)	
	$E_{tot}$	$H_{298}$	$E_{tot}$	" $H_{298}$ "	$E_{tot}$	" $H_{298}$ "
<b>47</b>	-230.6775889	-230.581079	-230.7553794	-230.656139	-230.974264	-230.875024
<b>9</b>	-174.0019530	-173.873765	-174.0673161	-173.936515	-174.241264	-174.110463
<b>48</b>	-404.6717383	-404.442865	-404.8165040	-404.582119	-405.209674	-404.975288
<b>34</b>	-460.2527375	-460.131142	-460.3254119	-460.201429	-460.746824	-460.622841
<b>49</b>	-690.9308342	-690.710577	-691.0863870	-690.861246	-691.727859	-691.502717
<b>50</b>	-690.9524103	-690.731249	-691.1100547	-690.883737	-691.751499	-691.525181

**Table A9.** Continued

<b>9*47</b>	-404.6865713	-404.459925	-404.8294561	-404.597369	-405.222383	-404.990296
<b>34*47</b>	-690.9364906	-690.716461	-691.0867530	-690.861615	-691.727242	-691.502104
QCISD/6-31+G(d)		QCISD/6-31+G(2d)				
	$E_{\text{tot}}$	"H <sub>298</sub> "	$E_{\text{tot}}$	"H <sub>298</sub> "		
<b>47</b>	-230.5443916	-230.446900	-230.600729	-230.504466		
<b>9</b>	-173.8906110	-173.760999	-173.928651	-173.801251		
<b>48</b>	-404.4162350	-404.184903	-404.509748	-404.282093		
<b>34</b>	-460.1364251	-460.013399	-460.178096	-460.057505		
<b>49</b>	-690.6657602	-690.442738	-690.765512	-690.546762		
<b>50</b>	-690.6844817	-690.460859	-690.785731	-690.566139		
<b>9*47</b>	-404.4422113	-404.213254	-404.536027	-404.310436		
<b>34*47</b>	-690.6875248	-690.465003	-690.784593	-690.565827		
B2PLYP/6-31+G(2d)// mPW1K/6-31+G(d)		B2PLYP/G3Large// mPW1K/6-31+G(d)		B2PLYP-M1/6-31+G(2d)// mPW1K/6-31+G(d)		
	$E_{\text{tot}}$	"H <sub>298</sub> "	$E_{\text{tot}}$	"H <sub>298</sub> "	$E_{\text{tot}}$	"H <sub>298</sub> "
<b>47</b>	-231.0230511	-230.9238108	-231.1814226	-231.082182	-231.147263	-231.048022
<b>9</b>	-174.2733549	-174.1425541	-174.4101402	-174.279339	-174.374061	-174.243261
<b>48</b>	-405.2777379	-405.0433522	-405.5712343	-405.336849	-405.509618	-405.275232
<b>34</b>	-460.7997445	-460.6757620	-461.0221397	-460.898157	-460.894007	-460.770024
<b>49</b>	-691.8132016	-691.5880598	-692.1965015	-691.971360	-692.037145	-691.812003
<b>50</b>	-691.8310847	-691.6047666	-692.2157035	-691.989385	-692.056638	-691.830320
<b>9*47</b>	-405.3017288	-405.0696413	-405.5957785	-405.363691	-405.528138	-405.296050
<b>34*47</b>	-691.8273834	-691.6022454	-692.2073196	-691.982182	-692.047010	-691.821872
B2PLYP-M2/6-31+G(2d)// mPW1K/6-31+G(d)		B2PLYP-M2/G3Large// mPW1K/6-31+G(d)		B2PLYP-M3/6-31+G(2d)// mPW1K/6-31+G(d)		
	$E_{\text{tot}}$	"H <sub>298</sub> "	$E_{\text{tot}}$	"H <sub>298</sub> "	$E_{\text{tot}}$	"H <sub>298</sub> "
<b>47</b>	-231.1759268	-231.0766865	-231.3877052	-231.288465	-230.973626	-230.874385
<b>9</b>	-174.3973012	-174.2665004	-174.5816361	-174.450835	-174.222338	-174.091537
<b>48</b>	-405.5631286	-405.3287429	-405.9566487	-405.722263	-405.181646	-404.947260
<b>34</b>	-460.9157596	-460.7917771	-461.2266240	-461.102642	-460.683479	-460.559496
<b>49</b>	-692.0888239	-691.8636821	-692.6135074	-692.388366	-691.649840	-691.424698
<b>50</b>	-692.1086887	-691.8823706	-692.6345310	-692.408213	-691.668195	-691.441877
<b>9*47</b>	-405.5803861	-405.3482986	-405.9748005	-405.742713	-405.202329	-404.970241
<b>34*47</b>	-692.0976935	-691.8725555	-692.6190274	-692.393889	-691.662514	-691.437376
B2K-PLYP/6-31+G(2d)// mPW1K/6-31+G(d)						
	$E_{\text{tot}}$	"H <sub>298</sub> "				
<b>47</b>	-230.9313821	-230.8321418				
<b>9</b>	-174.2012820	-174.0704812				
<b>48</b>	-405.1191156	-404.8847299				
<b>34</b>	-460.6746595	-460.5506770				
<b>49</b>	-691.6017120	-691.3765702				
<b>50</b>	-691.6215806	-691.3952625				
<b>9*47</b>	-405.1394265	-404.9073390				
<b>34*47</b>	-691.6118368	-691.3866988				

**Table A10.** Total Energies and Enthalpies of NMe<sub>3</sub> (**9**), PMe<sub>3</sub> (**34**), MVK (**47**) and Their Adducts and Complexes (in Hartree) at G3(+) Level Based on Different Geometries and Thermal Corrections.

G3(+)	Geometry	Thermal correction	Geometry	Thermal correction
	MP2/6-31+G(d)	HF/6-31+G(d)	MP2/6-31+G(d)	MP2/6-31+G(d)
	G3 <sub>tot</sub>	H <sub>298</sub> (G3)	G3 <sub>tot</sub>	H <sub>298</sub> (G3)
<b>47</b>	-231.052427	-230.9599255	-231.052427	-230.954935
<b>9</b>	-174.320151	-174.1986275	-174.320151	-174.190539
<b>48</b>	-405.359832	-405.1416653	-405.359832	-405.128500
<b>34</b>	-460.834535	-460.7196379	-460.834535	-460.711509
<b>49</b>	-691.884474	-691.6752445	-691.884474	-691.661452
<b>50</b>	-691.908227	-691.6980522	-691.908227	-691.684604
<b>9*47</b>	-405.379355	-405.1634160	-405.379355	-405.150398
<b>34*47</b>	-691.893255	-691.6839760	-691.893255	-691.670733
G3(+)	Geometry	Thermal correction	Geometry	Thermal correction
	QCISD/6-31+G(d)	MP2/6-31+G(d)	mPW1K/6-31+G(d)	mPW1K/6-31+G(d)
	G3 <sub>tot</sub>	H <sub>298</sub> (G3)	G3 <sub>tot</sub>	H <sub>298</sub> (G3)
<b>47</b>	-231.052508	-230.955016	-231.052728	-230.953487
<b>9</b>	-174.319879	-174.190267	-174.319895	-174.189095
<b>48</b>	-405.359445	-405.128113	-405.359996	-405.125610
<b>34</b>	-460.834111	-460.711085	-460.834713	-460.710731
<b>49</b>	-691.883772	-691.660750	-691.884693	-691.659551
<b>50</b>	-691.907797	-691.684174	-691.908781	-691.682463
<b>9*47</b>	-405.379115	-405.150158	-405.379352	-405.147264
<b>34*47</b>	-691.907797	-691.670310	-691.893417	-691.668279
G3(+)	Geometry	Thermal correction	Geometry	Thermal correction
	MP2/6-31+G(2d)	HF/6-31+G(2d)	MP2/6-31+G(2d)	MP2/6-31+G(2d)
	G3 <sub>tot</sub>	H <sub>298</sub> (G3)	G3 <sub>tot</sub>	H <sub>298</sub> (G3)
<b>47</b>	-231.052631	-230.9612144	-231.0526306	-230.956368
<b>9</b>	-174.319993	-174.1999408	-174.3199927	-174.192593
<b>48</b>	-405.359719	-405.1440210	-405.3597189	-405.132064
<b>34</b>	-460.834321	-460.7209593	-460.8343212	-460.713730
<b>49</b>	-691.884559	-691.6780153	-691.8845591	-691.665809
<b>50</b>	-691.908204	-691.7005887	-691.9082035	-691.688612
<b>9*47</b>	-405.379380	-405.1660505	-405.3793801	-405.153789
<b>34*47</b>	-691.893246	-691.7005887	-691.8932460	-691.674480
G3(+)	Geometry	Thermal correction	Geometry	Thermal correction
	QCISD/6-31+G(2d)	MP2/6-31+G(2d)	mPW1K/6-31+G(2d)	mPW1K/6-31+G(2d)
	G3 <sub>tot</sub>	H <sub>298</sub> (G3)	G3 <sub>tot</sub>	H <sub>298</sub> (G3)
<b>47</b>	-231.052501	-230.956238	-231.052439	-230.954058
<b>9</b>	-174.319628	-174.192228	-174.319825	-174.190208
<b>48</b>	-405.359218	-405.131563	-405.359667	-405.127263
<b>34</b>	-460.833742	-460.713151	-460.834773	-460.712064
<b>49</b>	-691.883713	-691.664963	-691.884784	-691.661877
<b>50</b>	-691.907532	-691.687940	-691.908729	-691.684498
<b>9*47</b>	-405.378854	-405.153263	-405.378853	-405.148842
<b>34*47</b>	-691.892451	-691.673685	-691.893113	-691.670170

**Table A11.** Total Energies and Enthalpies of NMe<sub>3</sub> (**9**), PMe<sub>3</sub> (**34**), MVK (**47**) and Their Adducts and Complexes (in Hartree) at G3+ and G3(MP2)(+) Levels Based on Different Geometries and Thermal Corrections.

G3+	Geometry	Thermal correction	G3+	Geometry	Thermal correction
	G3 <sub>tot</sub>	H <sub>298</sub> (G3)		G3 <sub>tot</sub>	H <sub>298</sub> (G3)
<b>47</b>	-231.0518908	-230.9543988	<b>47</b>	-231.051904	-230.955641
<b>9</b>	-174.3198365	-174.1902245	<b>9</b>	-174.319586	-174.192186
<b>48</b>	-405.3586973	-405.1273653	<b>48</b>	-405.358484	-405.130829
<b>34</b>	-460.8341880	-460.7111620	<b>34</b>	-460.833817	-460.713226
<b>49</b>	-691.8830347	-691.6600127	<b>49</b>	-691.882991	-691.664241
<b>50</b>	-691.9070560	-691.6834330	<b>50</b>	-691.906815	-691.687223
<b>9*47</b>	-405.3785920	-405.1496350	<b>9*47</b>	-405.378347	-405.152756
<b>34*47</b>	-691.8924289	-691.6699069	<b>34*47</b>	-691.892057	-691.673291

G3(MP2)(+)	Geometry	Thermal correction
	G3 <sub>tot</sub>	H <sub>298</sub> (G3)
<b>47</b>	-230.8223126	-230.723072
<b>9</b>	-174.1340983	-174.003298
<b>48</b>	-404.9431349	-404.708749
<b>34</b>	-460.4000774	-460.276095
<b>49</b>	-691.2181926	-690.993051
<b>50</b>	-691.2422597	-691.015942
<b>9*47</b>	-404.9628639	-404.730776
<b>34*47</b>	-691.2279559	-691.002818

**Table A12.** Total Energies and Enthalpies (in Hartree) for Selected Nucleophiles, Electrophiles, Their Zwitterionic Adducts.

System	mPW1K/6-31+G(d)		B2PLYP-M2/6-31+G(2d)// mPW1K/6-31+G(d)	
	E <sub>tot</sub>	H <sub>298</sub>	E <sub>tot</sub>	"H <sub>298</sub> "
<b>51</b>	-170.7722837	-170.714693	-170.800470	-170.7428793
<b>52</b>	-548.1779580	-548.108884	-548.074252	-548.0051780
<b>53</b>	-283.1056817	-283.041928	-283.165399	-283.1016454
<b>54</b>	-627.0714233	-627.000858	-627.0193259	-626.9487606
<b>11</b>	-265.4567244	-265.347809	-265.4698923	-265.3609769
<b>27</b>	-382.1580634	-381.981125	-382.1614305	-381.9844921
<b>35</b>	-652.7608826	-652.578509	-652.6236039	-652.4412303
<b>39</b>	-1036.132093	-1035.833005	-1036.048669	-1035.749581
<b>47+11</b>	-496.6113098	-496.399939	-496.6336465	-496.4222757
<b>47+27</b>	-813.5983671	-813.417249	-813.5092635	-813.3281454
<b>47+35</b>	-883.9210272	-883.637389	-883.7964567	-883.5128185
<b>47+39</b>	-1267.285189	-1266.884678	-1267.218098	-1266.817587
<b>51+34</b>	-631.8277473	-631.644817	-631.6949270	-631.5119967
<b>51+35</b>	-823.5119169	-823.270362	-823.4052821	-823.1637272
<b>51+39</b>	-1206.874591	-1206.516277	-1206.827278	-1206.468964
<b>52+34</b>	-1009.232446	-1009.037341	-1008.972889	-1008.777784
<b>52+11</b>	-813.5983671	-813.417249	-813.5092635	-813.3281454
<b>52+27</b>	-930.3056019	-930.056004	-930.2091718	-929.9595739
<b>52+35</b>	-1200.916207	-1200.661933	-1200.682163	-1200.427889
<b>52+39</b>	-1584.277537	-1583.906571	-1584.102613	-1583.731647

**Table A12.** Continued

<b>53+9</b>	-457.5488234	-457.34894	-457.5743236	-457.3744402
<b>53+34</b>	-744.1966177	-744.006245	-744.0962614	-743.9058887
<b>53+11</b>	-548.5654424	-548.388897	-548.6339861	-548.4574407
<b>53+27</b>	-665.2754581	-665.030253	-665.3391675	-665.0939624
<b>53+35</b>	-935.8807409	-935.631693	-935.8048482	-935.5558003
<b>53+39</b>	-1319.246422	-1318.880824	-1319.225983	-1318.860385
<b>54+34</b>	-1088.145714	-1087.949129	-1087.930845	-1087.734259
<b>54+11</b>	-892.5184908	-892.335494	-892.4761114	-892.2931146
<b>54+27</b>	-1009.221629	-1008.970446	-1009.172429	-1008.921246
<b>54+35</b>	-1279.829254	-1279.574167	-1279.639343	-1279.384256
<b>54+39</b>	-1663.189548	-1662.817756	-1663.058366	-1662.686574
	G3(MP2)(+)		G3	
	$E_{\text{tot}}$	“H <sub>298</sub> ”	$E_{\text{tot}}$	“H <sub>298</sub> ”
<b>51</b>	-170.5204646	-170.4628746	-170.7010533	-170.6434633
<b>52</b>	-547.5066504	-547.4375764	-547.9530360	-547.8839620
<b>53</b>	-282.7665891	-282.7028351	-283.0049137	-282.9411597
<b>54</b>	-626.3729731	-626.3024081	-626.8715327	-626.8009677
<b>11</b>	-265.0431588	-264.9342438	-265.3171267	-265.2082117
<b>27</b>	-381.5367315	-381.3597925	-380.9455964	-380.7686574
<b>35</b>	-651.7645020	-651.582128	-652.4192921	-652.2369181
<b>39</b>	/	/	/	/
<b>47+11</b>	-495.8482847	-495.6369137	-496.354138	-496.142767
<b>47+27</b>	-612.3467952	-612.0670162	/	/
<b>47+35</b>	-882.584014	-882.300376	/	/
<b>47+39</b>	/	/	/	/
<b>51+34</b>	-630.8971922	-630.7142622	-631.513229	-631.330299
<b>51+35</b>	-822.2648286	-822.0232736	/	/
<b>51+39</b>	/	/	/	/
<b>52+34</b>	-1007.895710	-1007.700605	-1008.777492	-1008.582387
<b>52+11</b>	-812.5175724	-812.3364544	-813.2387445	-813.0576265
<b>52+27</b>	-929.0208683	-928.7712703	/	/
<b>52+35</b>	-1199.261303	-1199.007029	/	/
<b>52+39</b>	/	/	/	/
<b>53+9</b>	-456.9118744	-456.7119914	-457.3368824	-457.1369994
<b>53+34</b>	-743.1815296	-742.9911566	-743.8562019	-743.6658289
<b>53+11</b>	-547.8051479	-547.6286029	-548.3187730	-548.1422280
<b>53+27</b>	-664.3117066	-664.0665006	/	/
<b>53+35</b>	-934.5459438	-934.2968958	/	/
<b>53+39</b>	/	/	/	/
<b>54+34</b>	-1086.771924	-1086.575338	-1087.706663	-1087.510077
<b>54+11</b>	-891.4017745	-891.2187785	-892.1756020	-891.9926060
<b>54+27</b>	-1007.898537	-1007.647354	/	/
<b>54+35</b>	-1278.136356	-1277.88127	/	/
<b>54+39</b>	/	/	/	/

**Table A13.** Total Energies and Enthalpies (in Hartree) as Calculated at the RHF/3-21G, RHF/MIDI!, B3LYP/6-31G(d), and MP2(FC)/6-31G(d) Level of Theory for Pyridine Derivatives. Enthalpies Represent Boltzmann-Averaged Values over all Conformers at 298.15 K.

system	RHF/3-21G		RHF/MIDI!		B3LYP/6-31G(d)		MP2(FC)/6-31G(d)	
	$E_{\text{tot}}$	$H_{298}$	$E_{\text{tot}}$	$H_{298}$	$E_{\text{tot}}$	$H_{298}$	$E_{\text{tot}}$	$H_{298}$
<b>1</b> (pyridine)								
neutral	-245.312006	-245.210873	-245.239861	-245.138871	-248.2849730	-248.190715	-247.482532	-247.381399
cationic	-396.611964	-396.453100	-396.502142	-396.343739	-401.2995391	-401.151170	-400.047896	-399.889032
<b>27</b> (DMAP)								
neutral	-377.662675	-377.478683	-377.549433	-377.365951	-382.2573045	-382.085088	-380.995265	-380.811273
cationic	-528.997389	-528.754901	-528.845015	-528.603374	-535.3039587	-535.076979	-533.590978	-533.34849
<b>29</b> (PPY)								
neutral	-454.150742	-453.926606	-453.994262	-453.771056	-459.6842867	-459.474417	-458.165699	-457.941563
cationic	-605.489443	-605.206794	-605.293543	-605.012166	-612.7351191	-612.470454	-610.766062	-610.483413
<b>32</b> (TCAP)								
neutral	-530.641930	-530.378134	-530.451331	-530.188070	-537.120287	-536.872902	-535.350370	-535.086379
cationic	-681.985246	-681.662480	-681.753326	-681.431814	-690.176536	-689.874134	-687.955445	-687.632677
<b>25</b> (hassner)								
neutral	-602.383832	-602.092424	-602.223406	-601.932562	-609.6827138	-609.409084	-607.694519	-607.403111
cationic	-753.730110	-753.379503	-753.527572	-753.177979	-762.742090	-762.413064	-760.299073	-759.948535
<b>55</b> (Fuji)								
neutral	-1062.779108	-1062.299958	-1062.386677	-1061.906916	-1075.637970	-1075.189326	-1072.172053	-1071.694251
cationic	-1214.126219	-1213.586451	-1213.689635	-1213.151531	-1228.694660	-1228.191998	-1224.783758	-1224.247268
<b>56</b> (camp. 1)								
neutral	-737.456443	-737.105080	-	-	-	-	-743.917660	-743.566306
cationic	-888.791029	-888.380658	-	-	-	-	-896.515880	-896.106163
<b>57</b> (camp. 2)								
neutral	-1077.818934	-1077.361609	-	-	-	-	-1087.252421	-1086.795387
cationic	-1229.163093	-1228.646988	-	-	-	-	-1239.859269	-1239.343424
<b>58</b> (yamada)								
neutral	-1605.228930	-1604.834070	-	-	-	-	-1616.334113	-1615.940289
cationic	-1756.560014	-1756.106872	-	-	-	-	-1768.927544	-1768.474493
<b>59</b> (spivey)								
neutral	-1063.622982	-1063.139172	-	-	-1076.627385	-1076.174102	-1073.1186586	-1072.634876
cationic	-1214.966385	-1214.422984	-	-	-1229.682430	-1229.173746	-1225.7209592	-1225.177906

**Table A14.** Total Energies and Enthalpies (in Hartree) as Calculated at the MP2(FC)/6-31G(d)//RHF/3-21G, MP2(FC)/6-31G(d)//RHF/MIDI!, B3LYP/6-311+G(d,p)//B3LYP/6-31G(d), and MP2(FC)/6-311+G(d,p)//MP2(FC)/6-31G(d) Level of Theory for Pyridine Derivatives. Enthalpies Represent Boltzmann-Averaged Values over all Conformers at 298.15 K.

system	MP2(FC)/6-31G(d)// RHF/3-21G		MP2(FC)/6-31G(d)// RHF/MIDI!		B3LYP/6-311+G(d,p)// B3LYP/6-31G(d)		MP2(FC)/6-311+G(d,p)// MP2(FC)/6-31G(d)	
	E <sub>tot</sub>	H <sub>298</sub>	E <sub>tot</sub>	H <sub>298</sub>	E <sub>tot</sub>	H <sub>298</sub>	E <sub>tot</sub>	H <sub>298</sub>
<b>1</b> (pyridine)								
neutral	-247.480304	-247.379171	-247.480857	-247.379867	-248.3511637	-248.2569057	-247.608924	-247.507791
cationic	-400.044798	-399.885934	-400.044747	-399.886344	-401.4019729	-401.2536038	-400.251941	-400.093077
<b>27</b> (DMAP)								
neutral	-380.991642	-380.807650	-380.993441	-380.809959	-382.3599769	-382.1877604	-381.213684	-381.029692
cationic	-533.586980	-533.344492	-533.587477	-533.345836	-535.4427011	-535.2157214	-533.886472	-533.643984
<b>29</b> (PPY)								
neutral	-458.162244	-457.938108	-458.163261	-457.940055	-459.8042135	-459.5943438	-458.425954	-458.201818
cationic	-610.761224	-610.478575	-610.761889	-610.480512	-612.8911759	-612.6265108	-611.102583	-610.819934
<b>32</b> (TCAP)								
neutral	-535.345874	-535.081962	-535.347705	-535.084678	-537.254445	-537.0070597	-535.651626	-535.387643
cationic	-687.950248	-687.627479	-687.951018	-687.629470	-690.347629	-690.0452261	-688.333589	-688.010819
<b>25</b> (hassner)								
neutral	-607.687554	-607.396146	-607.690260	-607.399416	-609.845803	-609.5721731	-608.050009	-607.758601
cationic	-760.291530	-759.940989	-760.294290	-759.944809	-762.940980	-762.611971	-760.730507	-760.379970
<b>55</b> (Fuji)								
neutral	-1072.160959	-1071.682893	-1072.163484	-1071.685718	-1075.915101	-1075.467624	-1072.764316	-1072.286499
cationic	-1224.768436	-1224.231467	-1224.770119	-1224.234057	-1229.007589	-1228.506292	-1225.457641	-1224.921420
<b>56</b> (camp. 1)								
neutral	-743.911902	-743.560388	-	-	-	-	-744.357643	-744.006246
cationic	-896.508466	-896.098366	-	-	-	-	-897.032430	-896.622801
<b>57</b> (camp. 2)								
neutral	-1087.238575	-1086.780666	-	-	-	-	-1087.859053	-1087.401980
cationic	-1087.847005	-1239.331018	-	-	-	-	-1240.544747	-1240.029325
<b>58</b> (yamada)								
neutral	-1616.326463	-1615.932519	-	-	-	-	-1616.891340	-1616.497581
cationic	-1768.918946	-1768.465745	-	-	-	-	-1769.562782	-1769.109634
<b>59</b> (spivey)								
neutral	-1073.106046	-1072.621996	-	-	-1076.892420	-1076.439019	-1073.691705	-1073.208010
cationic	-1225.707404	-1225.163917	-	-	-1229.984546	-1229.475804	-1226.370998	-1225.827967

**Table A15.** Total Energies and Enthalpies (in Hartree) as Calculated at the SCS-MP2(FC)/6-311+G(d,p)//MP2(FC)/6-31G(d) Level of Theory for Pyridine Derivatives. Enthalpies Represent Boltzmann-Averaged Values over all Conformers at 298.15 K.

system	SCS-MP2(FC)/6-311+G(d,p)// MP2(FC)/6-31G(d)	
	$E_{\text{tot}}$	$H_{298}$
<b>1</b> (pyridine)		
neutral	-247.583611	-247.482478
cationic	-400.215941	-400.057077
<b>27</b> (DMAP)		
neutral	-381.181350	-380.997358
cationic	-533.844447	-533.601959
<b>29</b> (PPY)		
neutral	-458.386137	-458.162000
cationic	-611.053190	-610.770541
<b>32</b> (TCAP)		
neutral	-535.602550	-535.338577
cationic	-688.274568	-687.951801
<b>25</b> (hassner)		
neutral	-607.997488	-607.706080
cationic	-760.668735	-760.318195
<b>55</b> (Fuji)		
neutral	-535.602550	-1072.168817
cationic	-688.274568	-1224.789477
<b>56</b> (camp. 1)		
neutral	-744.292015	-743.940629
cationic	-896.957388	-896.547743
<b>57</b> (camp. 2)		
neutral	-1087.744456	-1087.287380
cationic	-1240.417955	-1239.902269
<b>58</b> (yamada)		
neutral	-1616.802534	-1616.408729
cationic	-1769.464658	-1769.011525
<b>59</b> (spivey)		
neutral	-1073.565565	-1073.0818010
cationic	-1226.234859	-1225.6918564

**Table A16.** Total Energies and Enthalpies (in Hartree) as Calculated at the RHF/6-311+G(d,p)//MP2(FC)/6-31G(d) Level of Theory for Pyridine Derivatives. Enthalpies Represent Boltzmann-Averaged Values over all Conformers at 298.15 K.

system	RHF/6-311+G(d,p)// MP2(FC)/6-31G(d)	
	$E_{\text{tot}}$	$H_{298}$
<b>1</b> (pyridine)		
neutral	-246.7509029	-246.6497699
cationic	-398.9237915	-398.7649275
<b>27</b> (DMAP)		
neutral	-379.8691959	-379.6852039
cationic	-532.0743842	-531.8318962
<b>29</b> (PPY)		
neutral	-456.7987245	-456.5745885
cationic	-609.0083452	-608.7256962
<b>32</b> (TCAP)		
neutral	-533.731066	-533.4670918
cationic	-685.9458719	-685.6231073
<b>25</b> (hassner)		
neutral	-605.9001196	-605.6087116
cationic	-758.1184977	-757.7679479
<b>55</b> (Fuji)		
neutral	-1068.955233	-1068.477411
cationic	-1221.163428	-1220.627081
<b>56</b> (camp. 1)		
neutral	-741.750892	-741.399740
cationic	-893.958842	-893.549178
<b>57</b> (camp. 2)		
neutral	-1084.0820908	-1083.624969
cationic	-1236.297955	-1235.782026
<b>58</b> (yamada)		
neutral	-1613.693426	-1613.299462
cationic	-1765.896857	-1765.443668
<b>59</b> (spivey)		
neutral	-1069.8038777	-1069.3203059
cationic	-1222.0151850	-1221.4721568

**Table A17.** Enthalpies for all Stationary Points Located on the Potential Energy Surface along Nucleophilic and Basis Catalysis Pathways of Acylation Reaction at Different Levels of Theory.<sup>a</sup>

	B3LYP/6-311+G(d,p)// B3LYP/6-31G(d)		MP2(FC)/6-31G(d)// B3LYP/6-31G(d)	
	H <sub>298</sub> (gas) hartree	ΔH <sub>298</sub> (gas) kJ/mol	H <sub>298</sub> (gas) <sup>b</sup> hartree	ΔH <sub>298</sub> (gas) <sup>c</sup> kJ/mol
<b>59a+60+61</b>	-2155.015976	0.00	-	-
<b>(R)-64</b> (reactant complex)	-2155.024727	-22.98	-2147.511223	0.0
<b>(S)-64</b> (reactant complex)	-2155.024562	-22.54	-	-
<b>(R)-65</b> (first TS)	-2155.005768	26.80	-2147.508455	7.23
<b>(S)-65</b> (first TS)	-2155.002914	34.29	-	-
<b>(R)-66</b> (intermediate)	-2155.013093	7.56	-	-
<b>(S)-66</b> (intermediate)	-2155.011512	11.72	-	-
<b>(R)-67</b> (second TS)	-2155.010620	14.06	-2147.506622	12.08
<b>(S)-67</b> (second TS)	-2155.008320	20.10	-	-
<b>(R)-68</b> (product complex)	-2155.049246	-87.35	-	-
<b>(S)-68</b> (product complex)	-2155.049064	-86.87	-	-
<b>59a+(R)-62+63</b>	-2155.024206	-21.61	-	-
<b>(R)-69</b> (TS along basis catalysis pathway)	-2154.990370	67.23	-2147.494859	42.96
<b>(S)-69</b> (TS along basis catalysis pathway)	-2154.986461	77.49	-	-

<sup>a</sup> using the best conformer at the B3LYP/6-311+G(d,p)//B3LYP/6-31G(d) level of theory and thermal correction is taken at B3LYP/6-31G(d) level; <sup>b</sup> Relative to the reactant complex .

**Table A18.** Total Energies, Enthalpies and Free Energies (in Hartree) for Catalysts **59a** – **59c**.

Results for <b>59a</b>						
	B3LYP/ 6-31G(d) E(total, E <sub>h</sub> )	B3LYP/ 6-31G(d) H <sub>298</sub>	B3LYP/6-311+G(d, p)// B3LYP/6-31G(d) E(total, E <sub>h</sub> )	B3LYP/6-311+G(d, p)// B3LYP/6-31G(d) “H <sub>298</sub> ”	B3LYP/ 6-31G(d) G <sub>298</sub>	B3LYP/6-311+G(d, p)// B3LYP//6-31G(d) “G <sub>298</sub> ”
<b>59a</b> _1	-1076.617372	-1076.165093	-1076.882415	-1076.430136	-1076.242895	-1076.804613
<b>59a</b> _2	-1076.616695	-1076.164422	-1076.881229	-1076.428956	-1076.242598	-1076.803053
<b>59a</b> _3	-1076.622467	-1076.169867	-1076.888051	-1076.435451	-1076.247545	-1076.810373
<b>59a</b> _4	-1076.624664	-1076.171772	-1076.890347	-1076.437455	-1076.248673	-1076.813446
<b>59a</b> _5	-1076.625219	-1076.172667	-1076.890947	-1076.438395	-1076.248774	-1076.814840
<b>59a</b> _6	-1076.627273	-1076.174584	-1076.892261	-1076.439572	-1076.250986	-1076.815859
<b>59a</b> _7	-1076.624492	-1076.171763	-1076.889913	-1076.437184	-1076.248199	-1076.813477
<b>59a</b> _8	-1076.625219	-1076.171272	-1076.889051	-1076.435104	-1076.248202	-1076.812121
<b>59a</b> _9	-1076.621758	-1076.168955	-1076.887178	-1076.434375	-1076.246555	-1076.809578
<b>59a</b> _10	-1076.622976	-1076.170216	-1076.888867	-1076.436107	-1076.247354	-1076.811729
<b>59a</b> _11	-1076.622845	-1076.170012	-1076.888279	-1076.435446	-1076.247164	-1076.811127
Results for <b>59b</b>						
<b>59b</b> _1	-997.995219	-997.602391	-998.2401073	-997.8472798	-997.674305	-997.9191938
<b>59b</b> _2	-997.996809	-997.603984	-998.2416124	-997.8487873	-997.674747	-997.9195503
<b>59b</b> _3	-997.997611	-997.604899	-998.2424727	-997.8497607	-997.675193	-997.9200547
<b>59b</b> _4	-997.999226	-997.606587	-998.2439669	-997.8513278	-997.677662	-997.9224028
Results for <b>59c</b>						
<b>59c</b> _1	-1075.425687	-1074.995072	-1075.687764	-1075.257149	-1075.068174	-1075.330251
<b>59c</b> _2	-1075.424153	-1074.993443	-1075.686247	-1075.255536	-1075.066421	-1075.328514
<b>59c</b> _3	-1075.423581	-1074.99283	-1075.685874	-1075.255124	-1075.066881	-1075.329175
<b>59c</b> _4	-1075.424341	-1074.99368	-1075.686608	-1075.255947	-1075.066507	-1075.328774

**Table A19.** Total Energies, Enthalpies and Free Energies (in Hartree) for *sec*-alcohol **60**.

	B3LYP/ 6-31G(d) E(total, E <sub>h</sub> )	B3LYP/ 6-31G(d) H <sub>298</sub>	B3LYP/6-311+G(d,p)// B3LYP/6-31G(d) E(total, E <sub>h</sub> )	B3LYP/6-311+G(d,p)// B3LYP/6-31G(d) “H <sub>298</sub> ”	B3LYP/ 6-31G(d) G <sub>298</sub>	B3LYP/6-311+G(d,p)// B3LYP/6-31G(d) “G <sub>298</sub> ”
<b>60_1</b>	-539.728903	-539.508024	-539.877522	-539.656643	-539.555797	-539.704416
<b>60_2</b>	-539.729933	-539.509145	-539.878222	-539.657434	-539.556961	-539.705250
<b>60_3</b>	-539.730441	-539.509667	-539.878932	-539.658158	-539.557622	-539.706113
<b>60_4</b>	-539.728042	-539.507362	-539.877255	-539.656575	-539.55524	-539.704453
<b>60_5</b>	-539.726038	-539.505299	-539.875044	-539.654305	-539.553025	-539.702031
<b>60_6</b>	-539.726776	-539.506103	-539.875370	-539.654697	-539.553900	-539.702494

**Table A20.** Total Energies, Enthalpies and Free Energies (in Hartree) for Isobutyric Anhydride **61**.

	B3LYP/ 6-31G(d) E(total, E <sub>h</sub> )	B3LYP/ 6-31G(d) H <sub>298</sub>	B3LYP/6-311+G(d, p)// B3LYP/6-31G(d) E(total, E <sub>h</sub> )	B3LYP/6-311+G(d, p)// B3LYP/6-31G(d) “H <sub>298</sub> ”	B3LYP/ 6-31G(d) G <sub>298</sub>	B3LYP/6-311+G(d, p)// B3LYP//6-31G(d) “G <sub>298</sub> ”
<b>61_1</b>	-538.985402	-538.757851	-539.145797	-538.9182460	-538.812546	-538.972941
<b>61_2</b>	-538.985018	-538.757446	-539.145246	-538.9176740	-538.811257	-538.970977
<b>61_3</b>	-538.984625	-538.757043	-539.144695	-538.9171130	-538.812367	-538.972884
<b>61_4</b>	-538.984149	-538.756488	-539.144666	-538.9170050	-538.810579	-538.971155
<b>61_5</b>	-538.983751	-538.756076	-539.144074	-538.9163990	-538.811761	-538.972171
<b>61_6</b>	-538.983219	-538.755487	-539.143629	-538.9158970	-538.807372	-538.967261
<b>61_7</b>	-538.984043	-538.756147	-539.143768	-538.9158715	-538.813111	-538.973339
<b>61_8</b>	-538.983872	-538.756134	-539.143592	-538.9158540	-538.811503	-538.971826
<b>61_9</b>	-538.982916	-538.755129	-539.143492	-538.9157045	-538.812335	-538.972405
<b>61_10</b>	-538.980569	-538.752754	-539.140458	-538.9126430	-538.810824	-538.970549

**Table A21.** Total Energies, Enthalpies and Free Energies (in Hartree) for Ester **(R)-62** and Carboxylic Acid **63**.

	B3LYP/ 6-31G(d) E(total, E <sub>h</sub> )	B3LYP/ 6-31G(d) H <sub>298</sub>	B3LYP/6-311+G(d,p)// B3LYP/6-31G(d) E(total, E <sub>h</sub> )	B3LYP/6-311+G(d,p)// B3LYP/6-31G(d) “H <sub>298</sub> ”	B3LYP/ 6-31G(d) G <sub>298</sub>	B3LYP/6-311+G(d,p)// B3LYP/6-31G(d) “G <sub>298</sub> ”
<b>(R)-62_1</b>	-771.0145362	-770.692440	-771.2194450	-770.8973488	-770.755317	-770.960226
<b>(R)-62_2</b>	-771.0155590	-770.693467	-771.2209689	-770.8988769	-770.756502	-770.961912
<b>63_1</b>	-307.7006200	-307.573522	-307.8127947	-307.6856967	-307.612541	-307.724716
<b>63_2</b>	-307.7102187	-307.582823	-307.8131525	-307.6857568	-307.621989	-307.724923

**Table A22.** Total Energies, Enthalpies and Free Energies (in Hartree) for Reactant Complex **64**.

	B3LYP/ 6-31G(d) E(total, E <sub>h</sub> )	B3LYP/ 6-31G(d) H <sub>298</sub>	B3LYP/6-311+G(d,p)// B3LYP/6-31G(d) E(total, E <sub>h</sub> )	B3LYP/6-311+G(d,p)// B3LYP/6-31G(d) “H <sub>298</sub> ”	B3LYP/ 6-31G(d) G <sub>298</sub>	B3LYP/6-311+G(d,p)// B3LYP/6-31G(d) “G <sub>298</sub> ”
<b>(R)-64_1</b>	-2155.365249	-2154.459047	-2155.930929	-2155.024727	-2154.607011	-2155.172691
<b>(R)-64_2</b>	-2155.364774	-2154.458518	-2155.930003	-2155.023747	-2154.604174	-2155.169403
<b>(R)-64_3</b>	-2155.363769	-2154.457713	-2155.929197	-2155.023142	-2154.604532	-2155.169961
<b>(R)-64_4</b>	-2155.363227	-2154.457232	-2155.928842	-2155.022847	-2154.603071	-2155.168686
<b>(R)-64_5</b>	-2155.363653	-2154.457713	-2155.927447	-2155.021507	-2154.604432	-2155.168226
<b>(R)-64_6</b>	-2155.365131	-2154.459152	-2155.930257	-2155.024278	-2154.604732	-2155.169858
<b>(S)-64_1</b>	-2155.365316	-2154.458968	-2155.930910	-2155.024562	-2154.605361	-2155.170955
<b>(S)-64_2</b>	-2155.360083	-2154.454087	-2155.925710	-2155.019714	-2154.601892	-2155.167519
<b>(S)-64_3</b>	-2155.362907	-2154.456808	-2155.928018	-2155.021919	-2154.606040	-2155.169151

**Table A23.** Total Energies, Enthalpies and Free Energies (in Hartree) for TS **65**.

	B3LYP/ 6-31G(d) E(total, E <sub>h</sub> )	B3LYP/ 6-31G(d) H <sub>298</sub>	B3LYP/6-311+G(d,p)// B3LYP/6-31G(d) E(total, E <sub>h</sub> )	B3LYP/6-311+G(d,p)// B3LYP/6-31G(d) “H <sub>298</sub> ”	B3LYP/ 6-31G(d) G <sub>298</sub>	B3LYP/6-311+G(d,p)// B3LYP/6-31G(d) “G <sub>298</sub> ”
(R)-65_1	-2155.340783	-2154.435565	-2155.908441	-2155.003224	-2154.577014	-2155.144673
(R)-65_2	-2155.339899	-2154.434727	-2155.906840	-2155.001668	-2154.576738	-2155.143679
(R)-65_3	-2155.341224	-2154.435724	-2155.907925	-2155.002425	-2154.574346	-2155.141047
(R)-65_4	-2155.342802	-2154.437454	-2155.909107	-2155.003759	-2154.576873	-2155.143276
(R)-65_5	-2155.343035	-2154.437600	-2155.909267	-2155.003832	-2154.577653	-2155.143885
(R)-65_6	-2155.345655	-2154.439971	-2155.910742	-2155.005059	-2154.575853	-2155.140941
(R)-65_7	-2155.346414	-2154.441054	-2155.911128	-2155.005768	-2154.577227	-2155.141941
(R)-65_8	-2155.344817	-2154.439462	-2155.909934	-2155.004579	-2154.576176	-2155.141293
(R)-65_9	-2155.346432	-2154.441140	-2155.910865	-2155.005573	-2154.577497	-2155.141930
(R)-65_10	-2155.340783	-2154.435565	-2155.908441	-2155.003224	-2154.577014	-2155.144673
(S)-65_1	-2155.339242	-2154.433995	-2155.906604	-2155.001357	-2154.576959	-2155.144321
(S)-65_2	-2155.341562	-2154.436543	-2155.907933	-2155.002914	-2154.577244	-2155.143586
(S)-65_3	-2155.340662	-2154.435537	-2155.906652	-2155.001527	-2154.575015	-2155.141005
(S)-65_4	-2155.340467	-2154.435192	-2155.906289	-2155.001014	-2154.572733	-2155.138555
(S)-65_5	-2155.342546	-2154.437188	-2155.907604	-2155.002246	-2154.574389	-2155.139447
(S)-65_6	-2155.342609	-2154.437014	-2155.907545	-2155.001950	-2154.574802	-2155.139738

**Table A24.** Total Energies, Enthalpies and Free Energies (in Hartree) for Intermediate **66**.

	B3LYP/ 6-31G(d) E(total, E <sub>h</sub> )	B3LYP/ 6-31G(d) H <sub>298</sub>	B3LYP/6-311+G(d,p)// B3LYP/6-31G(d) E(total, E <sub>h</sub> )	B3LYP/6-311+G(d,p)// B3LYP/6-31G(d) “H <sub>298</sub> ”	B3LYP/ 6-31G(d) G <sub>298</sub>	B3LYP/6-311+G(d,p)// B3LYP/6-31G(d) “G <sub>298</sub> ”
(R)-66_1	-2155.350527	-2154.443986	-2155.919634	-2155.013093	-2154.584531	-2155.153638
(R)-66_2	-2155.347856	-2154.441049	-2155.917593	-2155.010787	-2154.585213	-2155.154951
(R)-66_3	-2155.346503	-2154.439940	-2155.912236	-2155.005674	-2154.578171	-2155.143905
(S)-66_1	-2155.348148	-2154.441549	-2155.918111	-2155.011512	-2154.583161	-2155.153124
(S)-66_2	-2155.349541	-2154.442418	-2155.917472	-2155.010349	-2154.601892	-2155.169823

**Table A25.** Total Energies, Enthalpies and Free Energies (in Hartree) for TS **(R)-67**.

	B3LYP/ 6-31G(d) E(total, E <sub>h</sub> )	B3LYP/ 6-31G(d) H <sub>298</sub>	B3LYP/6-311+G(d,p)// B3LYP/6-31G(d) E(total, E <sub>h</sub> )	B3LYP/6-311+G(d,p)// B3LYP/6-31G(d) “H <sub>298</sub> ”	B3LYP/ 6-31G(d) G <sub>298</sub>	B3LYP/6-311+G(d,p)// B3LYP/6-31G(d) “G <sub>298</sub> ”
<b>(R)-67_1</b>	-2155.344683	-2154.443571	-2155.911732	-2155.010620	-2154.580979	-2155.148028
<b>(R)-67_2</b>	-2155.343760	-2154.442678	-2155.911154	-2155.010072	-2154.580810	-2155.148204
<b>(R)-67_3</b>	-2155.343428	-2154.442335	-2155.910464	-2155.009371	-2154.579421	-2155.146457
<b>(R)-67_4</b>	-2155.343057	-2154.441900	-2155.910546	-2155.009389	-2154.580041	-2155.147530
<b>(R)-67_5</b>	-2155.342699	-2154.441355	-2155.910441	-2155.009097	-2154.580290	-2155.148032
<b>(R)-67_6</b>	-2155.342674	-2154.441389	-2155.910113	-2155.008828	-2154.579088	-2155.146527
<b>(R)-67_7</b>	-2155.341445	-2154.439934	-2155.907835	-2155.006324	-2154.576641	-2155.143031
<b>(R)-67_8</b>	-2155.341746	-2154.440135	-2155.907567	-2155.005956	-2154.576314	-2155.142135
<b>(R)-67_9</b>	-2155.340416	-2154.438778	-2155.906460	-2155.004822	-2154.574798	-2155.140842
<b>(R)-67_10</b>	-2155.339775	-2154.438508	-2155.905842	-2155.004575	-2154.574810	-2155.140877
<b>(R)-67_11</b>	-2155.338918	-2154.437749	-2155.905937	-2155.004768	-2154.576906	-2155.143925
<b>(R)-67_12</b>	-2155.338247	-2154.437146	-2155.905303	-2155.004202	-2154.574954	-2155.142010
<b>(R)-67_13</b>	-2155.338823	-2154.437818	-2155.904680	-2155.003675	-2154.575385	-2155.141242
<b>(R)-67_14</b>	-2155.336647	-2154.435712	-2155.903655	-2155.002720	-2154.573821	-2155.140829
<b>(R)-67_15</b>	-2155.336776	-2154.435920	-2155.903414	-2155.002558	-2154.574180	-2155.140818
<b>(R)-67_16</b>	-2155.337598	-2154.436601	-2155.903525	-2155.002528	-2154.574916	-2155.140843
<b>(R)-67_17</b>	-2155.337835	-2154.436396	-2155.903653	-2155.002214	-2154.571846	-2155.137664
<b>(R)-67_18</b>	-2155.334291	-2154.433469	-2155.899712	-2154.998890	-2154.570692	-2155.136113
<b>(R)-67_19</b>	-2155.334459	-2154.433330	-2155.899931	-2154.998802	-2154.570202	-2155.135674
<b>(R)-67_21</b>	-2155.333691	-2154.432543	-2155.899534	-2154.998386	-2154.570127	-2155.135970
<b>(R)-67_22</b>	-2155.331799	-2154.430131	-2155.898531	-2154.996863	-2154.565357	-2155.132089

**Table A26.** Total Energies, Enthalpies and Free Energies (in Hartree) for (S)-67.

	B3LYP/ 6-31G(d) E(total, E <sub>h</sub> )	B3LYP/ 6-31G(d) H <sub>298</sub>	B3LYP/6-311+G(d,p)// B3LYP/6-31G(d) E(total, E <sub>h</sub> )	B3LYP/6-311+G(d,p)// B3LYP/6-31G(d) “H <sub>298</sub> ”	B3LYP/ 6-31G(d) G <sub>298</sub>	B3LYP/6-311+G(d,p)// B3LYP/6-31G(d) “G <sub>298</sub> ”
(S)-67_1	-2155.342717	-2154.441441	-2155.909596	-2155.008320	-2154.577125	-2155.143086
(S)-67_2	-2155.342022	-2154.440900	-2155.908998	-2155.007876	-2154.575289	-2155.142450
(S)-67_3	-2155.342041	-2154.440720	-2155.908002	-2155.006681	-2154.577328	-2155.143174
(S)-67_4	-2155.340842	-2154.439345	-2155.908003	-2155.006506	-2154.574659	-2155.141592
(S)-67_5	-2155.341761	-2154.440580	-2155.907607	-2155.006426	-2154.575337	-2155.140753
(S)-67_6	-2155.340193	-2154.438875	-2155.907126	-2155.005808	-2154.575646	-2155.140676
(S)-67_7	-2155.339563	-2154.438047	-2155.906702	-2155.005186	-2154.574881	-2155.140107
(S)-67_8	-2155.340634	-2154.439187	-2155.906050	-2155.004603	-2154.573646	-2155.138875
(S)-67_9	-2155.340504	-2154.439377	-2155.905534	-2155.004407	-2154.572929	-2155.139690
(S)-67_10	-2155.340147	-2154.438775	-2155.905373	-2155.004001	-2154.571433	-2155.137342
(S)-67_11	-2155.339876	-2154.438630	-2155.905105	-2155.003859	-2154.559338	-2155.126726
(S)-67_12	-2155.335532	-2154.434280	-2155.902293	-2155.001041	-2154.571553	-2155.138344
(S)-67_13	-2155.335911	-2154.434703	-2155.901820	-2155.000612	-2154.568813	-2155.134793
(S)-67_14	-2155.334642	-2154.433101	-2155.902030	-2155.000489	-2154.579385	-2155.146264
(S)-67_15	-2155.334803	-2154.433639	-2155.901594	-2155.000430	-2154.577727	-2155.144703
(S)-67_16	-2155.333616	-2154.432189	-2155.900947	-2154.999520	-2154.570153	-2155.137484
(S)-67_17	-2155.333675	-2154.432194	-2155.899655	-2154.998174	-2154.575634	-2155.142773

**Table A27.** Total Energies, Enthalpies and Free Energies (in Hartree) for Product Complex **68**.

	B3LYP/ 6-31G(d) E(total, E <sub>h</sub> )	B3LYP/ 6-31G(d) H <sub>298</sub>	B3LYP/6-311+G(d,p)// B3LYP/6-31G(d) E(total, E <sub>h</sub> )	B3LYP/6-311+G(d,p)// B3LYP/6-31G(d) “H <sub>298</sub> ”	B3LYP/ 6-31G(d) G <sub>298</sub>	B3LYP/6-311+G(d,p)// B3LYP/6-31G(d) “G <sub>298</sub> ”
<b>(R)-68_1</b>	-2155.384261	-2154.477427	-2155.9477203	-2155.0408863	-2154.622758	-2155.1862173
<b>(R)-68_2</b>	-2155.391142	-2154.483991	-2155.956396	-2155.0492456	-2154.630448	-2155.1957026
<b>(S)-68_1</b>	-2155.382773	-2154.476182	-2155.946588	-2155.0399971	-2154.622695	-2155.1865101
<b>(S)-68_2</b>	-2155.390166	-2154.483392	-2155.955838	-2155.0490642	-2154.631541	-2155.1972132

**Table A28.** Total Energies, Enthalpies and Free Energies (in Hartree) for TS **69**.

	B3LYP/ 6-31G(d) E(total, E <sub>h</sub> )	B3LYP/ 6-31G(d) H <sub>298</sub>	B3LYP/6-311+G(d,p)// B3LYP/6-31G(d) E(total, E <sub>h</sub> )	B3LYP/6-311+G(d,p)// B3LYP/6-31G(d) “H <sub>298</sub> ”	B3LYP/ 6-31G(d) G <sub>298</sub>	B3LYP/6-311+G(d,p)// B3LYP/6-31G(d) “G <sub>298</sub> ”
<b>(R)-69_1</b>	-2155.330578	-2154.428852	-2155.892096	-2154.990370	-2154.566639	-2155.128157
<b>(R)-69_2</b>	-2155.330844	-2154.426787	-2155.891114	-2154.987057	-2154.561806	-2155.122076
<b>(R)-69_3</b>	-2155.324617	-2154.421188	-2155.887880	-2154.984452	-2154.559232	-2155.122496
<b>(R)-69_4</b>	-2155.329594	-2154.426106	-2155.893304	-2154.989815	-2154.564939	-2155.128648
<b>(S)-69_1</b>	-2155.327559	-2154.424366	-2155.889653	-2154.986461	-2154.562589	-2155.124684
<b>(S)-69_2</b>	-2155.326889	-2154.422945	-2155.889172	-2154.985228	-2154.559380	-2155.121663

**Table A29.** Total Energies, Enthalpies and Free Energies (in Hartree) for TS **67** with Catalyst **59b**.

	B3LYP/ 6-31G(d) E(total, E <sub>h</sub> )	B3LYP/ 6-31G(d) H <sub>298</sub>	B3LYP/6-311+G(d,p)// B3LYP/6-31G(d) E(total, E <sub>h</sub> )	B3LYP/6-311+G(d,p)// B3LYP/6-31G(d) “H <sub>298</sub> ”	B3LYP/ 6-31G(d) G <sub>298</sub>	B3LYP/6-311+G(d,p)// B3LYP/6-31G(d) “G <sub>298</sub> ”
59btsr1	-2076.716129	-2075.874884	-2077.262935	-2076.421690	-2076.006359	-2076.553165
59btsr2	-2076.713069	-2075.871793	-2077.260449	-2076.419172	-2076.004977	-2076.552356
59btsr3	-2076.712340	-2075.87108	-2077.258523	-2076.417263	-2076.003002	-2076.549185
59btsr4	-2076.716058	-2075.87482	-2077.262873	-2076.421635	-2076.006170	-2076.552985
59btsr5	-2076.713050	-2075.871836	-2077.260376	-2076.419161	-2076.005520	-2076.552845
59btsr6	-2076.712296	-2075.870999	-2077.257780	-2076.416483	-2076.001521	-2076.547005
59btsr7	-2076.710690	-2075.869403	-2077.255577	-2076.414290	-2075.998743	-2076.543630
59btss1	-2076.714456	-2075.873226	-2077.260691	-2076.419461	-2076.004963	-2076.551198
59btss2	-2076.712305	-2075.871028	-2077.258664	-2076.417387	-2076.001713	-2076.548072
59btss3	-2076.714447	-2075.873120	-2077.260686	-2076.419359	-2076.004232	-2076.550471
59btss4	-2076.705444	-2075.864360	-2077.251910	-2076.410826	-2075.995275	-2076.541741
59btss5	-2076.713839	-2075.872730	-2077.259256	-2076.418147	-2076.003607	-2076.549024
59btss6	-2076.712396	-2075.871203	-2077.257247	-2076.416054	-2076.001160	-2076.546011

**Table A30.** Total Energies, Enthalpies and Free Energies (in Hartree) for TS **67** with Catalyst **59c**.

	B3LYP/ 6-31G(d) E(total, E <sub>h</sub> )	B3LYP/ 6-31G(d) H <sub>298</sub>	B3LYP/6-311+G(d,p)// B3LYP/6-31G(d) E(total, E <sub>h</sub> )	B3LYP/6-311+G(d,p)// B3LYP/6-31G(d) “H <sub>298</sub> ”	B3LYP/ 6-31G(d) G <sub>298</sub>	B3LYP/6-311+G(d,p)// B3LYP/6-31G(d) “G <sub>298</sub> ”
59ctsr1	-2154.144501	-2153.265439	-2154.70852	-2153.829458	-2153.399735	-2153.963754
59ctsr2	-2154.142919	-2153.263907	-2154.707312	-2153.8283	-2153.398012	-2153.962405
59ctsr3	-2154.144418	-2153.265388	-2154.708707	-2153.829677	-2153.399573	-2153.963862
59ctsr4	-2154.142821	-2153.263846	-2154.707101	-2153.828126	-2153.398454	-2153.962734
59ctsr5	-2154.142842	-2153.263855	-2154.707137	-2153.82815	-2153.398493	-2153.962788
59ctsr6	-2154.141846	-2153.262782	-2154.7047998	-2153.825736	-2153.395792	-2153.958746
59ctsr7	-2154.140627	-2153.261536	-2154.703487	-2153.824396	-2153.394392	-2153.957252
59ctsr8	-2154.138947	-2153.259612	-2154.701439	-2153.822104	-2153.39103	-2153.953522
59ctss1	-2154.142882	-2153.263762	-2154.706432	-2153.827312	-2153.396108	-2153.9596580
59ctss2	-2154.140006	-2153.260935	-2154.702061	-2153.82299	-2153.393611	-2153.955666
59ctss3	-2154.141178	-2153.261986	-2154.703323	-2153.824131	-2153.39349	-2153.955635
59ctss4	-2154.142808	-2153.263626	-2154.70639	-2153.827208	-2153.396468	-2153.960050
59ctss5	-2154.142508	-2153.263597	-2154.705203	-2153.826292	-2153.396601	-2153.959296

**Table A31.** Total Energies, Enthalpies and Free Energies (in Hartree) for TS **67** Including Catalyst **59a** and Different Substrates.

substrate	type		B3LYP/	B3LYP/	B3LYP/	B3LYP/	B3LYP/	B3LYP/
			6-31G(d)	6-31G(d)	6-311+G(d,p)// B3LYP/6-31G(d)	6-311+G(d,p)// B3LYP/6-31G(d)	6-31G(d)	6-311+G(d,p)// B3LYP/6-31G(d)
			E(total, E <sub>h</sub> )	H <sub>298</sub>	E(total, E <sub>h</sub> )	“H <sub>298</sub> ”	G <sub>298</sub>	“G <sub>298</sub> ”
<b>60</b>	TS-R	<b>I</b>	-2155.344683	-2154.443571	-2155.911732	-2155.010620	-2154.580979	-2155.148028
	TS-S	<b>III</b>	-2155.342717	-2154.441441	-2155.909596	-2155.008320	-2154.577125	-2155.143086
<b>70</b>	TS-R	<b>I</b>	-2001.702504	-2000.851189	-2002.235634	-2001.384320	-2000.985550	-2001.518681
	TS-S	<b>III</b>	-2001.702102	-2000.850245	-2002.234888	-2001.383030	-2000.981370	-2001.514155
<b>71</b>	TS-R	<b>I</b>	-2080.330158	-2079.419060	-2080.880932	-2079.969834	-2079.555752	-2080.106526
	TS-S	<b>III</b>	-2080.328509	-2079.417252	-2080.878994	-2079.967737	-2079.554038	-2080.104523
<b>72</b>	TS-R	<b>I</b>	-2005.326490	-2004.403071	-2005.862821	-2004.939402	-2004.538066	-2005.074397
	TS-S	<b>III</b>	-2005.326259	-2004.402575	-2005.861977	-2004.938294	-2004.537860	-2005.073579

**Table A32.** Total Energies, Enthalpies and Free Energies (in Hartree) for TS **67** Including Catalyst **59d** and Substrate **60**.

catalyst	type		B3LYP/6-	B3LYP/	B3LYP/	B3LYP/	B3LYP/	B3LYP/
			31G(d)	6-31G(d)	6-311+G(d,p)// B3LYP/6-31G(d)	6-311+G(d,p)// B3LYP/6-31G(d)	6-31G(d)	6-311+G(d,p)// B3LYP/6-31G(d)
			E(total, E <sub>h</sub> )	H <sub>298</sub>	E(total, E <sub>h</sub> )	“H <sub>298</sub> ”	G <sub>298</sub>	“G <sub>298</sub> ”
<b>59d</b>	TS-R	<b>I</b>	-2233.980833	-2233.020723	-2234.566646	-2233.606535	-2233.166649	-2233.752461
	TS-S	<b>II</b>	-2233.978138	-2233.017829	-2234.562985	-2233.602676	-2233.162576	-2233.747423
	TS-S	<b>III</b>	-2233.976674	-2233.016333	-2234.562153	-2233.601812	-2233.161501	-2233.746980

**Table A33.** RHF/6-31G(d) Results of Tautomers of Compound **73**.

tautomer	$E_{\text{tot}}$	$H_{298}$	$G_{298}$	$\Delta G_{\text{solv}}^{[\text{a}]}$ (kJ/mol)	$\Delta G_{\text{solv}}^{[\text{b}]}$ (kJ/mol)
I_01	-450.7944679	-450.603457	-450.650149	-76.93	-77.61
I_02	-450.7926100	-450.601635	-450.647715	-78.81	-78.99
I_03	-450.7907700	-450.599969	-450.646885	-81.92	-82.72
I_04	-450.7937385	-450.602769	-450.649696	-78.78	-79.45
I_05	-450.7908436	-450.600005	-450.646820	-82.01	-82.68
I_06	-450.7938009	-450.602823	-450.648998	-77.41	-78.20
I_07	-450.7924861	-450.601545	-450.647778	-78.77	-78.99
I_08	-450.7946231	-450.603622	-450.649984	-76.91	-77.66
I_09	-450.7939644	-450.602996	-450.649454	-78.74	-79.45
I_10	-450.7964789	-450.605459	-450.651338	-77.80	-78.66
I_11	-450.7960074	-450.604931	-450.650540	-76.16	-76.53
I_12	-450.7936637	-450.602756	-450.649066	-80.54	-81.13
I_13	-450.7967861	-450.605722	-450.651701	-77.17	-78.12
I_14	-450.7937522	-450.602837	-450.649132	-80.25	-81.04
I_15	-450.7963409	-450.605322	-450.650910	-77.03	-77.95
I_16	-450.7959584	-450.604886	-450.650500	-76.22	-76.53
I_17	-450.7964646	-450.605445	-450.651329	-77.86	-78.70
I_18	-450.7968166	-450.605748	-450.651724	-77.19	-78.16
tautomer	$E_{\text{tot}}$	$H_{298}$	$G_{298}$	$\Delta G_{\text{solv}}^{[\text{a}]}$ (kJ/mol)	$\Delta G_{\text{solv}}^{[\text{b}]}$ (kJ/mol)
V_19	-450.7928364	-450.601494	-450.647945	-72.18	-72.38
V_22	-450.7933581	-450.601835	-450.647282	-66.51	-67.78
V_23	-450.7927888	-450.601441	-450.647885	-72.29	-72.30
V_25	-450.7934380	-450.601912	-450.647355	-66.34	-67.82
V_26	-450.7925349	-450.601189	-450.647789	-73.08	-73.01
V_28	-450.7914039	-450.600009	-450.645170	-71.06	-70.00
V_29	-450.7897333	-450.598443	-450.644671	-76.25	-75.56
V_30	-450.7915010	-450.600312	-450.646248	-76.88	-77.15
V_31	-450.7903609	-450.598971	-450.645309	-74.62	-70.12
V_32	-450.7897794	-450.598479	-450.644679	-76.13	-75.48
V_33	-450.7913471	-450.599959	-450.645136	-71.25	-70.37
V_34	-450.7902722	-450.598892	-450.645230	-72.96	-72.72
V_35	-450.7913683	-450.600197	-450.646271	-77.04	-77.15
V_36	-450.7915206	-450.600339	-450.646280	-76.81	-77.15
tautomer	$E_{\text{tot}}$	$H_{298}$	$G_{298}$	$\Delta G_{\text{solv}}^{[\text{a}]}$ (kJ/mol)	$\Delta G_{\text{solv}}^{[\text{b}]}$ (kJ/mol)
II_01	-450.7943873	-450.603620	-450.649522	-65.85	-69.04
II_02	-450.794725	-450.603924	-450.649761	-65.13	-68.37
II_03	-450.7893238	-450.598403	-450.643568	-65.73	-68.99
II_04	-450.7947035	-450.603909	-450.649758	-65.20	-68.45
II_05	-450.7940284	-450.603356	-450.649215	-67.75	-71.00
II_06	-450.7944502	-450.603664	-450.649545	-65.70	-68.91
II_07	-450.7940106	-450.603341	-450.649201	-67.81	-71.04
II_08	-450.7889458	-450.598116	-450.64331	-67.06	-70.37
II_09	-450.7892768	-450.598369	-450.643545	-65.86	-69.08

**Table A33.** Continued

tautomer	$E_{\text{tot}}$	$H_{298}$	$G_{298}$	$\Delta G_{\text{solv}}^{[a]}$ (kJ/mol)	$\Delta G_{\text{solv}}^{[b]}$ (kJ/mol)
VI_10	-450.7978043	-450.606949	-450.653075	-63.05	-65.56
VI_11	-450.7968818	-450.606143	-450.652307	-65.25	-68.28
VI_12	-450.7946715	-450.603914	-450.649724	-60.28	-63.14
VI_13	-450.7968946	-450.606145	-450.652315	-65.37	-68.16
VI_14	-450.7975994	-450.606860	-450.653006	-64.06	-66.94
VI_15	-450.7977173	-450.606893	-450.653060	-63.17	-65.86
VI_16	-450.7976086	-450.606867	-450.653018	-64.23	-67.07
VI_17	-450.7936732	-450.603077	-450.649233	-63.29	-66.27
VI_18	-450.7947299	-450.603954	-450.649745	-60.14	-63.01
tautomer	$E_{\text{tot}}$	$H_{298}$	$G_{298}$	$\Delta G_{\text{solv}}^{[a]}$ (kJ/mol)	$\Delta G_{\text{solv}}^{[b]}$ (kJ/mol)
III_01	-450.7935643	-450.602443	-450.649079	-78.09	-79.24
III_02	-450.7937954	-450.602588	-450.648538	-76.06	-76.44
III_03	-450.7908844	-450.599894	-450.646683	-82.03	-82.80
III_04	-450.7932735	-450.602157	-450.648916	-79.12	-80.21
III_05	-450.7903265	-450.599339	-450.646481	-80.82	-81.80
III_06	-450.7927963	-450.601718	-450.647898	-79.25	-80.29
III_07	-450.7934333	-450.602252	-450.648418	-76.65	-77.03
III_08	-450.7937332	-450.602636	-450.649084	-78.74	-79.54
III_09	-450.7933749	-450.602293	-450.648906	-79.38	-80.25
III_10	-450.7969917	-450.605787	-450.651806	-75.69	-76.99
III_11	-450.7954993	-450.604283	-450.650146	-76.48	-76.90
III_12	-450.7930700	-450.602026	-450.648660	-80.95	-81.92
III_13	-450.7958861	-450.604730	-450.650908	-78.51	-79.41
III_14	-450.7930267	-450.601999	-450.648723	-80.93	-82.09
III_15	-450.7955535	-450.604397	-450.650242	-77.94	-79.16
III_16	-450.7954823	-450.604263	-450.650106	-76.48	-76.86
III_17	-450.7969987	-450.605791	-450.651811	-75.73	-77.07
III_18	-450.7958456	-450.604696	-450.650934	-78.69	-79.79
tautomer	$E_{\text{tot}}$	$H_{298}$	$G_{298}$	$\Delta G_{\text{solv}}^{[a]}$ (kJ/mol)	$\Delta G_{\text{solv}}^{[b]}$ (kJ/mol)
VII_19	-450.7986654	-450.606726	-450.651140	-60.94	-65.06
VII_20	-450.7902411	-450.598703	-450.645138	-75.53	-76.02
VII_21	-450.7908911	-450.599481	-450.645872	-75.54	-76.02
VII_23	-450.7914448	-450.599991	-450.646088	-74.25	-74.94
VII_24	-450.7991974	-450.607244	-450.651565	-59.93	-63.68
VII_26	-450.7913861	-450.599954	-450.646189	-74.27	-74.81
VII_28	-450.7897437	-450.598359	-450.643944	-75.06	-75.35
VII_29	-450.7911703	-450.599668	-450.645828	-73.49	-73.89
VII_30	-450.7921660	-450.600824	-450.646812	-75.99	-76.82
VII_31	-450.7902311	-450.598796	-450.645134	-75.77	-75.90
VII_32	-450.7907004	-450.599217	-450.645489	-74.61	-74.94
VII_33	-450.7902896	-450.598868	-450.644339	-73.87	-73.81
VII_34	-450.7906363	-450.599188	-450.645393	-75.07	-75.10
VII_35	-450.7912077	-450.599959	-450.646097	-78.29	-78.91
VII_36	-450.7926792	-450.601305	-450.647174	-74.76	-75.56

**Table A33.** Continued

tautomer	E <sub>tot</sub>	H <sub>298</sub>	G <sub>298</sub>	$\Delta G_{\text{solv}}$ <sup>[a]</sup> (kJ/mol)	$\Delta G_{\text{solv}}$ <sup>[b]</sup> (kJ/mol)
IV_01	-450.7963451	-450.605700	-450.651396	-78.76	-83.47
IV_02	-450.7953482	-450.604759	-450.650197	-80.94	-85.56
IV_03	-450.7930685	-450.602591	-450.648753	-82.89	-87.86
IV_04	-450.7952355	-450.604657	-450.650491	-81.62	-86.11
IV_05	-450.7929764	-450.602520	-450.648706	-83.09	-88.03
IV_06	-450.7958282	-450.605285	-450.650648	-80.93	-85.69
IV_07	-450.7954362	-450.604828	-450.650242	-80.69	-85.31
IV_08	-450.7963320	-450.605689	-450.651388	-78.84	-83.60
IV_09	-450.7952044	-450.604634	-450.650473	-81.67	-86.23
IV_10	-450.7943987	-450.603925	-450.649996	-79.04	-83.72
IV_11	-450.7947958	-450.604287	-450.649990	-78.26	-82.72
IV_12	-450.7917416	-450.601393	-450.647795	-81.76	-86.48
IV_13	-450.7941328	-450.603657	-450.649811	-79.96	-84.39
IV_14	-450.7918424	-450.601474	-450.647873	-81.50	-86.19
IV_15	-450.7944501	-450.604064	-450.649730	-80.26	-84.98
IV_16	-450.7947580	-450.604260	-450.649961	-78.11	-82.72
IV_17	-450.7943889	-450.603924	-450.650003	-79.14	-83.81
IV_18	-450.7941842	-450.603695	-450.649831	-79.84	-84.31
tautomer	E <sub>tot</sub>	H <sub>298</sub>	G <sub>298</sub>	$\Delta G_{\text{solv}}$ <sup>[a]</sup> (kJ/mol)	$\Delta G_{\text{solv}}$ <sup>[b]</sup> (kJ/mol)
VIII_19	-450.7919619	-450.601396	-450.647623	-73.42	-76.40
VIII_22	-450.7909689	-450.600103	-450.645407	-69.44	-73.26
VIII_23	-450.7917128	-450.601218	-450.647572	-74.08	-77.36
VIII_25	-450.7911846	-450.600271	-450.645463	-68.87	-72.68
VIII_26	-450.7904524	-450.600071	-450.647704	-77.83	-79.29
VIII_28	-450.7876756	-450.596663	-450.642039	-74.51	-76.94
VIII_29	-450.7898317	-450.598907	-450.644712	-78.37	-82.68
VIII_31	-450.7890219	-450.598099	-450.643956	-80.46	-83.55
VIII_32	-450.7898725	-450.598945	-450.644746	-78.20	-82.59
VIII_33	-450.7877928	-450.596752	-450.642097	-74.09	-76.86
VIII_34	-450.7889899	-450.598075	-450.643941	-80.53	-83.60

<sup>[a]</sup>  $\Delta G_{\text{solv}}$  calculated at PCM/UAHF/RHF/6-31G(d)//PCM/UAHF//B98/6-31G(d) level;<sup>[b]</sup>  $\Delta G_{\text{solv}}$  calculated at PCM/UAHF/RHF/6-31G(d)//B98/6-31G(d) level.

**Table A34.** B98/6-31G(d) Results of Tautomers of Compound **73**

tautomer	$E_{\text{tot}}$	$H_{298}$	$G_{298}$	$\Delta G_{\text{solv}}^{[\text{a}]}$ (kJ/mol)	$\Delta G_{\text{solv}}^{[\text{b}]}$ (kJ/mol)
I_01	-453.4532556	-453.274704	-453.322371	-75.34	-71.67
I_02	-453.4517287	-453.273323	-453.320916	-77.35	-73.39
I_03	-453.4495243	-453.271150	-453.319398	-79.73	-76.07
I_04	-453.4537971	-453.275125	-453.322790	-76.49	-72.93
I_05	-453.4494548	-453.271093	-453.319425	-79.84	-76.02
I_06	-453.4539805	-453.275438	-453.322911	-75.29	-71.84
I_07	-453.4517853	-453.273405	-453.321184	-77.19	-73.35
I_08	-453.4532632	-453.274719	-453.322373	-75.40	-71.71
I_09	-453.4537839	-453.275122	-453.322814	-76.57	-72.97
I_10	-453.4550960	-453.276494	-453.323524	-76.59	-72.80
I_11	-453.4551092	-453.276382	-453.322988	-75.24	-71.38
I_12	-453.4523185	-453.273823	-453.321370	-78.81	-74.85
I_13	-453.4565513	-453.277759	-453.324808	-75.46	-71.96
I_14	-453.4523991	-453.273896	-453.321435	-78.49	-74.77
I_15	-453.4563545	-453.277681	-453.324306	-75.42	-71.96
I_16	-453.4550580	-453.276338	-453.322964	-75.31	-71.38
I_17	-453.4550802	-453.276485	-453.323517	-76.64	-72.89
I_18	-453.4565789	-453.277782	-453.324817	-75.47	-72.01
tautomer	$E_{\text{tot}}$	$H_{298}$	$G_{298}$	$\Delta G_{\text{solv}}^{[\text{a}]}$ (kJ/mol)	$\Delta G_{\text{solv}}^{[\text{b}]}$ (kJ/mol)
V_19	-453.4527022	-453.273871	-453.321170	-71.32	-67.74
V_22	-453.4550314	-453.275834	-453.321856	-66.11	-62.80
V_23	-453.4527076	-453.273890	-453.321190	-71.37	-67.66
V_25	-453.4550751	-453.275944	-453.322211	-66.12	-62.84
V_26	-453.4536796	-453.274737	-453.322142	-71.29	-67.40
V_28	-453.4517986	-453.273009	-453.319249	-68.65	-64.73
V_29	-453.4492133	-453.270328	-453.316997	-73.27	-69.41
V_30	-453.4510647	-453.272420	-453.319304	-75.64	-71.42
V_31	-453.4514444	-453.272466	-453.319335	-70.66	-64.31
V_32	-453.4492453	-453.270356	-453.317081	-73.18	-69.33
V_33	-453.4517338	-453.272961	-453.319212	-68.86	-65.06
V_34	-453.4513358	-453.272353	-453.319198	-69.11	-66.90
V_35	-453.4517842	-453.273077	-453.320219	-74.78	-70.92
V_36	-453.4511014	-453.272498	-453.319420	-75.60	-71.42
tautomer	$E_{\text{tot}}$	$H_{298}$	$G_{298}$	$\Delta G_{\text{solv}}^{[\text{a}]}$ (kJ/mol)	$\Delta G_{\text{solv}}^{[\text{b}]}$ (kJ/mol)
II_01	-453.4511964	-453.272845	-453.319929	-62.67	-61.59
II_02	-453.4513391	-453.272967	-453.319993	-62.48	-61.30
II_03	-453.4475806	-453.269223	-453.315492	-62.91	-61.84
II_04	-453.4513191	-453.272959	-453.320000	-62.52	-61.38
II_05	-453.4520364	-453.273660	-453.320690	-64.39	-63.22
II_06	-453.4512504	-453.272878	-453.319930	-62.55	-61.46
II_07	-453.4520246	-453.273649	-453.320678	-64.43	-63.26

**Table A34.** Continued

tautomer	$E_{\text{tot}}$	$H_{298}$	$G_{298}$	$\Delta G_{\text{solv}}^{[\text{a}]}$ (kJ/mol)	$\Delta G_{\text{solv}}^{[\text{b}]}$ (kJ/mol)
II_08	-453.4479507	-453.269630	-453.315940	-64.33	-63.22
II_09	-453.4475426	-453.269202	-453.315491	-63.00	-61.92
VI_10	-453.4541742	-453.275705	-453.323107	-60.25	-58.79
VI_11	-453.4533161	-453.274956	-453.322275	-62.30	-61.17
VI_12	-453.4516861	-453.273361	-453.320300	-58.11	-57.03
VI_13	-453.4533165	-453.274950	-453.322343	-62.45	-61.04
VI_14	-453.4551999	-453.276718	-453.324020	-61.15	-59.96
VI_15	-453.4541020	-453.275650	-453.323066	-60.34	-59.08
VI_16	-453.4552079	-453.276718	-453.323986	-61.28	-60.08
VI_17	-453.4516359	-453.273325	-453.320419	-60.55	-59.45
VI_18	-453.4517383	-453.273461	-453.320824	-57.99	-56.90
III_01	-453.4537723	-453.275098	-453.322690	-75.72	-72.13
III_02	-453.4539240	-453.275159	-453.322336	-73.97	-70.17
III_03	-453.4506117	-453.272051	-453.320688	-78.61	-75.02
III_04	-453.4546985	-453.275886	-453.323669	-75.95	-72.55
III_05	-453.4507518	-453.272174	-453.320087	-78.19	-74.18
III_06	-453.4542364	-453.275561	-453.323237	-76.19	-72.76
III_07	-453.4538327	-453.275082	-453.322939	-74.14	-70.63
III_08	-453.4536714	-453.275004	-453.323060	-76.02	-72.34
III_09	-453.4546397	-453.275847	-453.323770	-76.11	-72.59
III_10	-453.4568871	-453.278137	-453.325240	-73.16	-70.08
III_11	-453.4558900	-453.277076	-453.323909	-74.30	-70.71
III_12	-453.4529337	-453.274336	-453.322135	-77.99	-74.43
III_13	-453.4570045	-453.278158	-453.325327	-75.33	-72.01
III_14	-453.4529479	-453.274361	-453.322239	-77.90	-74.56
III_15	-453.4569552	-453.278226	-453.325108	-74.80	-71.67
III_16	-453.4558479	-453.277031	-453.323815	-74.34	-70.67
III_17	-453.4568862	-453.278110	-453.325217	-73.25	-70.12
III_18	-453.4570107	-453.278158	-453.325359	-75.40	-72.30
VII_19	-453.4637683	-453.284434	-453.329487	-62.15	-59.54
VII_20	-453.4523217	-453.273469	-453.320586	-72.66	-69.12
VII_21	-453.4523216	-453.273473	-453.320596	-72.66	-69.16
VII_23	-453.4525790	-453.273679	-453.320688	-72.03	-68.32
VII_24	-453.4643174	-453.284974	-453.329925	-61.02	-58.45
VII_26	-453.4534305	-453.274323	-453.321439	-71.46	-67.78
VII_28	-453.4509329	-453.272017	-453.318339	-72.13	-68.74
VII_29	-453.4513222	-453.272227	-453.319362	-70.70	-67.24
VII_30	-453.4526406	-453.273905	-453.320931	-74.13	-70.33
VII_31	-453.4520679	-453.272966	-453.32007	-71.98	-68.66

**Table A34.** Continued

VII_32	-453.4509867	-453.271913	-453.318691	-71.50	-68.12
VII_33	-453.4514346	-453.272452	-453.318574	-70.96	-67.45
VII_34	-453.4523043	-453.273226	-453.320218	-71.36	-67.99
VII_35	-453.4526499	-453.273846	-453.321026	-75.32	-71.50
VII_36	-453.4530355	-453.274213	-453.321036	-73.21	-69.25
tautomer	E <sub>tot</sub>	H <sub>298</sub>	G <sub>298</sub>	$\Delta G_{\text{solv}}^{[a]}$ (kJ/mol)	$\Delta G_{\text{solv}}^{[b]}$ (kJ/mol)
IV_01	-453.4493521	-453.271323	-453.318010	-76.15	-74.77
IV_02	-453.4490732	-453.271093	-453.317486	-78.64	-77.15
IV_03	-453.4459374	-453.268070	-453.315349	-79.79	-78.45
IV_04	-453.4497091	-453.271611	-453.318433	-77.89	-76.53
IV_05	-453.4458578	-453.268009	-453.315325	-79.93	-78.62
IV_06	-453.4504230	-453.272406	-453.318711	-77.69	-76.36
IV_07	-453.4491554	-453.271165	-453.317537	-78.43	-76.94
IV_08	-453.4493437	-453.271298	-453.317970	-76.26	-74.89
IV_09	-453.4496803	-453.271576	-453.318391	-78.02	-76.69
IV_10	-453.4474232	-453.269587	-453.316652	-76.71	-75.27
IV_11	-453.4484728	-453.270506	-453.317007	-76.43	-74.85
IV_12	-453.4446232	-453.266917	-453.314435	-78.92	-77.45
IV_13	-453.4485929	-453.27058	-453.317623	-76.65	-75.31
IV_14	-453.4447220	-453.266974	-453.314428	-78.66	-77.19
IV_15	-453.4489782	-453.271146	-453.317697	-77.50	-76.15
IV_16	-453.4484308	-453.270471	-453.316982	-76.49	-74.89
IV_17	-453.4474193	-453.269602	-453.316684	-76.75	-75.35
IV_18	-453.4486496	-453.270636	-453.317666	-76.55	-75.19
tautomer	E <sub>tot</sub>	H <sub>298</sub>	G <sub>298</sub>	$\Delta G_{\text{solv}}^{[a]}$ (kJ/mol)	$\Delta G_{\text{solv}}^{[b]}$ (kJ/mol)
VIII_19	-453.4465922	-453.268735	-453.315673	-71.12	-69.2
VIII_22	-453.4477273	-453.269475	-453.315381	-65.79	-64.73
VIII_23	-453.4463751	-453.268571	-453.315595	-71.72	-70.04
VIII_25	-453.4479523	-453.269676	-453.315541	-65.24	-64.18
VIII_26	-453.4462903	-453.268247	-453.315627	-73.02	-70.54
VIII_28	-453.4433377	-453.265115	-453.311013	-69.95	-67.91
VIII_29	-453.4447844	-453.266687	-453.313391	-76.57	-74.10
VIII_31	-453.4450675	-453.266779	-453.313655	-77.17	-74.10
VIII_32	-453.4448261	-453.266735	-453.313431	-76.48	-74.01
VIII_33	-453.4434167	-453.265206	-453.311152	-69.71	-67.82
VIII_34	-453.4450375	-453.266747	-453.313599	-77.24	-74.14

<sup>[a]</sup>  $\Delta G_{\text{solv}}$  calculated at PCM/UAHF/B98/6-31G(d)//PCM/UAHF//B98/6-31G(d) level; <sup>[b]</sup>  $\Delta G_{\text{solv}}$  calculated at PCM/UAHF/B98/6-31G(d)//B98/6-31G(d) level.

**Table A35.** MP2/6-31+G(2d, p)//B98/6-31G(d) Results<sup>[a]</sup> of Tautomers of Compound **73**.

	E <sub>tot</sub>	"H <sub>298</sub> "	"G <sub>298</sub> "
I_01	-452.4267255	-452.2481740	-452.2958410
I_02	-452.4246776	-452.2462720	-452.2938650
I_03	-452.4232865	-452.2449122	-452.2931602
I_04	-452.4262642	-452.2475921	-452.2952571
I_05	-452.4232408	-452.2448790	-452.2932110
I_06	-452.4255795	-452.2470370	-452.2945100
I_07	-452.4246895	-452.2463092	-452.2940882
I_08	-452.4267513	-452.2482071	-452.2958611
I_09	-452.4262642	-452.2476023	-452.2952943
I_10	-452.4284069	-452.2498049	-452.2968349
I_11	-452.4279538	-452.2492266	-452.2958326
I_12	-452.4260408	-452.2475453	-452.2950923
I_13	-452.4289031	-452.2501108	-452.2971598
I_14	-452.4261016	-452.2475985	-452.2951375
I_15	-452.4279053	-452.2492318	-452.2958568
I_16	-452.4279058	-452.2491858	-452.2958118
I_17	-452.4283911	-452.2497959	-452.2968279
I_18	-452.4289194	-452.2501225	-452.2971575
	E <sub>tot</sub>	"H <sub>298</sub> "	"G <sub>298</sub> "
V_25	-452.4283922	-452.2492611	-452.2955281
V_22	-452.4284144	-452.2492169	-452.2952389
V_33	-452.4269173	-452.2481445	-452.2943955
V_28	-452.4269320	-452.2481424	-452.2943824
V_26	-452.4260736	-452.2471310	-452.2945360
V_23	-452.4259328	-452.2471152	-452.2944152
V_19	-452.4259292	-452.2470980	-452.2943970
V_31	-452.4257681	-452.2467897	-452.2936587
V_34	-452.4257057	-452.2467228	-452.2935678
V_36	-452.4251998	-452.2465963	-452.2935183
V_30	-452.4250900	-452.2464452	-452.2933292
V_35	-452.4250307	-452.2463235	-452.2934655
V_29	-452.4240889	-452.2452037	-452.2918727
V_32	-452.4240866	-452.2451973	-452.2919223
	E <sub>tot</sub>	"H <sub>298</sub> "	"G <sub>298</sub> "
II_02	-452.4185242	-452.2401521	-452.2871781
II_04	-452.4185053	-452.2401452	-452.2871862
II_06	-452.4184561	-452.2400837	-452.2871357
II_01	-452.4184092	-452.2400578	-452.2871418
II_05	-452.4182780	-452.2399016	-452.2869316
II_07	-452.4182597	-452.2398841	-452.2869131
II_03	-452.4144155	-452.2360580	-452.2823270
II_09	-452.4143734	-452.2360328	-452.2823218
II_08	-452.4138657	-452.2355450	-452.2818550
	E <sub>tot</sub>	"H <sub>298</sub> "	"G <sub>298</sub> "
VI_10	-452.4216527	-452.2431835	-452.2905855
VI_14	-452.4216641	-452.2431822	-452.2904842
VI_16	-452.4216639	-452.2431740	-452.2904420
VI_15	-452.4215748	-452.2431228	-452.2905388

**Table A35.** Continued

VI_13	-452.4206149	-452.2422484	-452.2896414
VI_11	-452.4205808	-452.2422207	-452.2895397
VI_18	-452.4185356	-452.2402583	-452.2876213
VI_12	-452.4184771	-452.2401520	-452.2870910
VI_17	-452.4175321	-452.2392212	-452.2863152
	$E_{\text{tot}}$	"H <sub>298</sub> "	"G <sub>298</sub> "
III_10	-452.4294012	-452.2506511	-451.4019153
III_17	-452.4294136	-452.2506374	-451.4019410
III_18	-452.4285599	-452.2497072	-451.4001091
III_13	-452.4285462	-452.2496997	-451.4000880
III_11	-452.4278657	-452.2490517	-451.3998414
III_16	-452.4278151	-452.2489982	-451.3997823
III_15	-452.4276642	-452.2489350	-451.3983733
III_01	-452.4260560	-452.2473817	-451.3983396
III_08	-452.4259466	-452.2472792	-451.3982218
III_14	-452.4258608	-452.2472739	-451.3987737
III_12	-452.4258306	-452.2472329	-451.3987276
III_04	-452.4259694	-452.2471569	-451.3972403
III_09	-452.4259286	-452.2471359	-451.3972174
III_02	-452.4258435	-452.2470785	-451.3977630
III_07	-452.4257215	-452.2469708	-451.3976103
III_06	-452.4248928	-452.2462174	-451.3955492
III_05	-452.4235024	-452.2449246	-451.3962529
III_03	-452.4232842	-452.2447235	-451.3959567
	$E_{\text{tot}}$	"H <sub>298</sub> "	"G <sub>298</sub> "
VII_24	-452.4358393	-452.2564959	-451.4073612
VII_19	-452.4355508	-452.2562165	-451.4073333
VII_36	-452.4260850	-452.2472625	-451.3991345
VII_30	-452.4257991	-452.2470635	-451.3989576
VII_33	-452.4253631	-452.2463806	-451.3992917
VII_34	-452.4252735	-452.2461952	-451.3982427
VII_35	-452.4249966	-452.2461927	-451.3973433
VII_23	-452.4250588	-452.2461587	-451.3975385
VII_28	-452.4249774	-452.2460615	-451.3990219
VII_31	-452.4251329	-452.2460311	-451.3981980
VII_29	-452.4250617	-452.2460096	-451.3988013
VII_21	-452.4247366	-452.2458879	-451.3971515
VII_20	-452.4247399	-452.2458872	-451.3971582
VII_26	-452.4249861	-452.2458785	-451.3965416
VII_32	-452.4248379	-452.2457642	-451.3986892
	$E_{\text{tot}}$	"H <sub>298</sub> "	"G <sub>298</sub> "
IV_01	-452.4161600	-452.2381309	-452.2848179
IV_08	-452.4161503	-452.2381047	-452.2847767
IV_04	-452.4156994	-452.2376013	-452.2844233
IV_06	-452.4156024	-452.2375854	-452.2838904
IV_09	-452.4156695	-452.2375652	-452.2843802
IV_07	-452.4155551	-452.2375647	-452.2839367
IV_02	-452.4154810	-452.2375008	-452.2838938
IV_11	-452.4138883	-452.2359215	-452.2824225

**Table A35.** Continued

IV_16	-452.4138628	-452.2359029	-452.2824139
IV_18	-452.4135284	-452.2355148	-452.2825448
IV_13	-452.4134968	-452.2354838	-452.2825268
IV_15	-452.4131556	-452.2353234	-452.2818744
IV_10	-452.4131269	-452.2352907	-452.2823557
IV_17	-452.4131058	-452.2352885	-452.2823705
IV_03	-452.4131307	-452.2352633	-452.2825423
IV_05	-452.4130560	-452.2352072	-452.2825232
IV_14	-452.4108678	-452.2331198	-452.2805738
IV_12	-452.4108078	-452.2331017	-452.2806197
	$E_{\text{tot}}$	“H <sub>298</sub> ”	“G <sub>298</sub> ”
VIII_25	-452.4138673	-452.2355911	-452.2814561
VIII_22	-452.4136579	-452.2354056	-452.2813116
VIII_19	-452.4123681	-452.2345109	-452.2814489
VIII_23	-452.4121154	-452.2343113	-452.2813353
VIII_32	-452.4115070	-452.2334159	-452.2801119
VIII_29	-452.4114625	-452.2333651	-452.2800691
VIII_26	-452.4111830	-452.2331397	-452.2805197
VIII_33	-452.4112615	-452.2330507	-452.2789967
VIII_31	-452.4112752	-452.2329867	-452.2798627
VIII_34	-452.4112442	-452.2329536	-452.2798056
VIII_28	-452.4111721	-452.2329494	-452.2788474

<sup>[a]</sup> Thermal correction calculated at B98/6-31G(d) level.

**Table A36.** G3MP2B3 Results of Tautomers of Compound **73**.

	$E_{\text{tot}}$	$H_{298}$	$G_{298}$
I_18	-452.9527548	-452.941324	-452.988908
I_13	-452.9527524	-452.941317	-452.988913
I_17	-452.9523196	-452.940892	-452.988480
I_10	-452.9522629	-452.940832	-452.988424
II_02	-452.9443331	-452.933061	-452.980577
II_04	-452.9443435	-452.933062	-452.980602
II_05	-452.9439796	-452.932735	-452.980230
II_06	-452.9441816	-452.932908	-452.980434
II_01	-452.9441799	-452.932891	-452.980450
III_10	-452.9527834	-452.941369	-452.989022
III_17	-452.9527820	-452.941366	-452.989038
III_18	-452.9521313	-452.940684	-452.988429
III_13	-452.9521282	-452.940686	-452.988408
IV_01	-452.9437006	-452.932452	-452.979735
IV_08	-452.9436883	-452.932440	-452.979723
IV_09	-452.9432680	-452.931983	-452.979416
IV_04	-452.9432857	-452.932003	-452.979432
IV_06	-452.9438292	-452.932662	-452.979611
IV_11	-452.9420976	-452.930886	-452.977973
V_25	-452.9515826	-452.940415	-452.987200
V_22	-452.9515495	-452.940386	-452.987162
V_36	-452.9491132	-452.937794	-452.985272
V_33	-452.9496247	-452.938456	-452.985025
V_28	-452.9496490	-452.938493	-452.985036
VI_10	-452.9470747	-452.935792	-452.983678
VI_14	-452.9470297	-452.935763	-452.983618
VI_16	-452.9470273	-452.935762	-452.983597
VI_15	-452.9470548	-452.935750	-452.983669
VII_24	-452.9567476	-452.946055	-452.991563
VII_19	-452.9567476	-452.945760	-452.991379
VII_36	-452.9493367	-452.938072	-452.985389
VII_30	-452.9491743	-452.937863	-452.985337
VIII_25	-452.9410216	-452.930069	-452.976394
VIII_22	-452.9408866	-452.929912	-452.976277
VIII_32	-452.9393930	-452.928241	-452.975455
VIII_19	-452.9404838	-452.929297	-452.976759
VIII_23	-452.9403418	-452.929132	-452.976672

**Table A37.** B98/6-31G(d) Results of Tautomers of **73-H<sup>+</sup>**

	$E_{\text{tot}}$	$H_{298}$	$G_{298}$	$\Delta G_{\text{solv}}^{[a]}$ (kJ/mol)	$\Delta G_{\text{solv}}^{[b]}$ (kJ/mol)
I-3H <sup>+</sup> _01	-453.8477855	-453.655964	-453.704526	-277.91	-274.26
I-3H <sup>+</sup> _02	-453.8513008	-453.659435	-453.707650	-269.88	-265.56
I-3H <sup>+</sup> _03	-453.8448373	-453.653120	-453.702267	-280.06	-275.68
I-3H <sup>+</sup> _04	-453.8459807	-453.655080	-453.701215	-285.14	-281.63
I-3H <sup>+</sup> _05	-453.8465915	-453.655007	-453.703196	-284.31	-280.12
I-3H <sup>+</sup> _06	-453.8500542	-453.658132	-453.706531	-276.21	-272.55
I-3H <sup>+</sup> _07	-453.8520217	-453.660145	-453.708076	-272.22	-267.94
I-3H <sup>+</sup> _08	-453.8482902	-453.656633	-453.704499	-284.33	-280.41
I-3H <sup>+</sup> _09	-453.8472836	-453.655433	-453.703919	-286.01	-282.29
	$E_{\text{tot}}$	$H_{298}$	$G_{298}$	$\Delta G_{\text{solv}}^{[a]}$ (kJ/mol)	$\Delta G_{\text{solv}}^{[b]}$ (kJ/mol)
IV-1H <sup>+</sup> _01	-453.8510767	-453.659550	-453.706906	-280.69	-277.02
IV-1H <sup>+</sup> _02	-453.8533841	-453.661972	-453.708997	-278.49	-274.43
IV-1H <sup>+</sup> _03	-453.8488795	-453.657308	-453.704659	-288.98	-284.47
IV-1H <sup>+</sup> _04	-453.8498040	-453.658621	-453.705572	-289.21	-285.14
IV-1H <sup>+</sup> _05	-453.8548977	-453.663580	-453.710662	-272.56	-268.11
IV-1H <sup>+</sup> _06	-453.8507355	-453.659347	-453.706797	-278.83	-275.01
IV-1H <sup>+</sup> _07	-453.8498854	-453.658339	-453.705797	-284.05	-279.37
IV-1H <sup>+</sup> _08	-453.8502027	-453.659047	-453.705910	-285.99	-281.54
	$E_{\text{tot}}$	$H_{298}$	$G_{298}$	$\Delta G_{\text{solv}}^{[a]}$ (kJ/mol)	$\Delta G_{\text{solv}}^{[b]}$ (kJ/mol)
IV-3H <sup>+</sup> _01	-453.8264195	-453.635725	-453.683098	-287.90	-282.84
IV-3H <sup>+</sup> _02	-453.8250236	-453.634163	-453.681373	-294.11	-288.32
IV-3H <sup>+</sup> _03	-453.8249985	-453.634782	-453.681837	-297.50	-291.21
IV-3H <sup>+</sup> _04	-453.8311661	-453.640522	-453.687644	-281.43	-276.23
IV-3H <sup>+</sup> _05	-453.8273765	-453.636912	-453.684250	-284.47	-278.74
IV-3H <sup>+</sup> _06	-453.8236862	-453.633171	-453.680897	-288.32	-283.42
IV-3H <sup>+</sup> _07	-453.8214575	-453.630827	-453.678384	-296.86	-290.33
IV-3H <sup>+</sup> _08	-453.8218814	-453.631774	-453.678940	-299.15	-292.92
IV-3H <sup>+</sup> _09	-453.8215640	-453.630941	-453.678456	-296.63	-290.29
	$E_{\text{tot}}$	$H_{298}$	$G_{298}$	$\Delta G_{\text{solv}}^{[a]}$ (kJ/mol)	$\Delta G_{\text{solv}}^{[b]}$ (kJ/mol)
<b>74</b>	-281.4608308	-281.366415	-281.400796	-55.23	-51.88
<b>74-H<sup>+</sup></b>	-281.8496537	-281.741921	-281.777392	-272.38	-270.29

<sup>[a]</sup>  $\Delta G_{\text{solv}}$  calculated at PCM/UAHF/B98/6-31G(d)//PCM/UAHF/B98/6-31G(d) level; <sup>[b]</sup>  $\Delta G_{\text{solv}}$  calculated at PCM/UAHF/B98/6-31G(d)//B98/6-31G(d) level.

**Table A38.** MP2/6-31+G(2d,p) Results of Tautomers of **73-H<sup>+</sup>**

	$E_{\text{tot}}$	“H <sub>298</sub> ”	“G <sub>298</sub> ”	$\Delta G_{\text{solv}}^{[\text{a}]}$ (kJ/mol)	$\Delta G_{\text{solv}}^{[\text{b}]}$ (kJ/mol)
I-3H <sup>+</sup> _01	-452.8045233	-452.6127018	-452.661264	-276.41	-278.95
I-3H <sup>+</sup> _02	-452.8077022	-452.6158364	-452.664051	-269.47	-270.12
I-3H <sup>+</sup> _03	-452.8023975	-452.6106802	-452.659827	-277.45	-280.45
I-3H <sup>+</sup> _04	-452.8017795	-452.6108788	-452.657014	-286.44	-288.70
I-3H <sup>+</sup> _05	-452.8023026	-452.6107182	-452.658907	-283.66	-286.31
I-3H <sup>+</sup> _06	-452.8069918	-452.6150696	-452.663469	-275.88	-277.48
I-3H <sup>+</sup> _07	-452.8085140	-452.6166373	-452.664568	-272.90	-273.01
I-3H <sup>+</sup> _08	-452.8038880	-452.6122308	-452.660097	-285.28	-287.15
I-3H <sup>+</sup> _09	-452.8036967	-452.6118460	-452.660332	-287.52	-289.53
	$E_{\text{tot}}$	“H <sub>298</sub> ”	“G <sub>298</sub> ”	$\Delta G_{\text{solv}}^{[\text{a}]}$ (kJ/mol)	$\Delta G_{\text{solv}}^{[\text{b}]}$ (kJ/mol)
IV-1H <sup>+</sup> _01	-452.7994076	-452.6078809	-452.655237	-280.45	-281.96
IV-1H <sup>+</sup> _02	-452.8014767	-452.6100646	-452.657090	-279.26	-280.04
IV-1H <sup>+</sup> _03	-452.7963791	-452.6048076	-452.652150	-293.59	-293.67
IV-1H <sup>+</sup> _04	-452.7972750	-452.6060921	-452.653043	-290.26	-291.88
IV-1H <sup>+</sup> _05	-452.8014588	-452.6101411	-452.657223	-271.52	-271.58
IV-1H <sup>+</sup> _06	-452.7974587	-452.6060702	-452.653520	-277.35	-278.53
IV-1H <sup>+</sup> _07	-452.7956242	-452.6040778	-452.651536	-287.84	-287.02
IV-1H <sup>+</sup> _08	-452.7961767	-452.6050210	-452.651884	-285.40	-286.39
	$E_{\text{tot}}$	“H <sub>298</sub> ”	“G <sub>298</sub> ”	$\Delta G_{\text{solv}}^{[\text{a}]}$ (kJ/mol)	$\Delta G_{\text{solv}}^{[\text{b}]}$ (kJ/mol)
IV-3H <sup>+</sup> _01	-452.7749296	-452.5842351	-452.631608	-291.00	-291.96
IV-3H <sup>+</sup> _02	-452.7722341	-452.5813735	-452.628584	-304.53	-302.75
IV-3H <sup>+</sup> _03	-452.7731042	-452.5828878	-452.629943	-302.13	-302.08
IV-3H <sup>+</sup> _04	-452.7797500	-452.5891059	-452.636228	-285.50	-285.31
IV-3H <sup>+</sup> _05	-452.7752568	-452.5847923	-452.632130	-289.46	-288.78
IV-3H <sup>+</sup> _06	-452.7717580	-452.5812428	-452.628969	-292.19	-293.42
IV-3H <sup>+</sup> _07	-452.7682959	-452.5776654	-452.625222	-308.05	-305.68
IV-3H <sup>+</sup> _08	-452.7692436	-452.5791362	-452.626302	-304.95	-304.93
IV-3H <sup>+</sup> _09	-452.7683836	-452.5777605	-452.625276	-308.12	-305.72
	$E_{\text{tot}}$	H <sub>298</sub>	G <sub>298</sub>	$\Delta G_{\text{solv}}^{[\text{a}]}$ (kJ/mol)	$\Delta G_{\text{solv}}^{[\text{b}]}$ (kJ/mol)
<b>74</b>	-280.8425657	-280.7481499	-280.782531	-58.53	-57.07
<b>74-H<sup>+</sup></b>	-281.2160103	-281.1082776	-281.143749	-271.35	-272.46

<sup>[a]</sup>  $\Delta G_{\text{solv}}$  calculated at PCM/UAHF/RHF/6-31G(d)//PCM/UAHF/B98/6-31G(d) level; <sup>[b]</sup>  $\Delta G_{\text{solv}}$  calculated at PCM/UAHF/RHF/6-31G(d)//B98/6-31G(d) level.

**Table A39.** G3MP2B3 Results of Tautomers of **73-H<sup>+</sup>**.

	E <sub>tot</sub>	H <sub>298</sub>	G <sub>298</sub>
I-3H <sup>+</sup> <sub>-07</sub>	-453.314216	-453.313272	-453.361800
I-3H <sup>+</sup> <sub>-02</sub>	-453.313032	-453.312088	-453.360942
I-3H <sup>+</sup> <sub>-09</sub>	-453.309462	-453.308518	-453.357550
IV-1H <sup>+</sup> <sub>-05</sub>	-453.309113	-453.308169	-453.355797
IV-1H <sup>+</sup> <sub>-02</sub>	-453.308867	-453.307922	-453.355565
IV-1H <sup>+</sup> <sub>-04</sub>	-453.305509	-453.304564	-453.352191
IV-3H <sup>+</sup> <sub>-04</sub>	-453.288243	-453.287299	-453.334963
IV-3H <sup>+</sup> <sub>-05</sub>	-453.284329	-453.283384	-453.331291
IV-3H <sup>+</sup> <sub>-03</sub>	-453.282788	-453.281844	-453.329549
<b>74</b>	-281.161830	-281.160886	-281.195512
<b>74-H<sup>+</sup></b>	-281.527356	-281.526412	-281.562160

## Bibliography

- (1) Berkessel, A.; Groeger, H. *Asymmetric Organocatalysis*; Wiley-VCH Verlag GmbH & Co.: Weinheim, **2005**.
- (2) Muller, P. *Pure Appl. Chem.* **1994**, *66*, 1077-1184.
- (3) Denmark, S. E.; Beutner, G. L. *Angew. Chem. Int. Ed.* **2008**, *47*, 1560-1638.
- (4) Litinenko, L. M.; Kirichenko, A. I. *Dokl. Akad. Nauk. SSSR* **1967**, *176*, 97.
- (5) Hoefle, G.; Steglich, W. *Synthesis* **1972**, 619-621; Steglich, W.; Hoefle, G. *Angew. Chem. Int. Ed.* **1969**, *8*, 981.
- (6) Spivey, A. C.; Arseniyadis, S. *Angew. Chem. Int. Ed.* **2004**, *43*, 5436-5441.
- (7) Hoefle, G.; Steglich, W.; Vorbrueggen, H. *Angew. Chem. Int. Ed.* **1978**, *90*, 569-583.
- (8) Fu, G. C. *Acc. Chem. Res.* **2004**, *37*, 542-547.
- (9) Fischer, C. B.; Xu, S.; Zipse, H. *Chem. Eur. J.* **2006**, *12*, 5779-5784.
- (10) Xu, S.; Held, I.; Kempf, B.; Mayr, H.; Steglich, W.; Zipse, H. *Chem. Eur. J.* **2005**, *11*, 4751-4757.
- (11) Held, I.; Xu, S.; Zipse, H. *Synthesis* **2007**, 1185-1196.
- (12) Vedejs, E.; Daugulis, O.; Diver, S. T. *J. Org. Chem.* **1996**, *61*, 430-431.
- (13) Vedejs, E.; Daugulis, O. *J. Am. Chem. Soc.* **2003**, *125*, 4166-4173; Vedejs, E.; Daugulis, O. *J. Am. Chem. Soc.* **1999**, *121*, 5813-5814.
- (14) Vedejs, E.; Daugulis, O.; Harper, L. A.; MacKay, J. A.; Powell, D. R. *J. Org. Chem.* **2003**, *68*, 5020-5027.
- (15) Sano, T.; Imai, K.; Ohashi, K.; Oriyama, T. *Chem. Lett.* **1999**, 265-266.
- (16) Kawabata, T.; Stragies, R.; Fukaya, T.; Fuji, K. *Chirality* **2003**, *15*, 71-76; Kawabata, T.; Stragies, R.; Fukaya, T.; Nagaoka, Y.; Schedel, H.; Fuji, K. *Tetrahedron Lett.* **2003**, *44*, 1545-1548; Kawabata, T.; Yamamoto, K.; Momose, Y.; Yoshida, H.; Nagaoka, Y.; Fuji, K. *Chem. Commun.* **2001**, 2700-2701.
- (17) Kawabata, T.; Nagato, M.; Takasu, K.; Fuji, K. *J. Am. Chem. Soc.* **1997**, *119*, 3169-3170.
- (18) Pelotier, B.; Priem, G.; Macdonald, S. J. F.; Anson, M. S.; Upton, R. J.; Campbell, I. B. *Tetrahedron Lett.* **2005**, *46*, 9005-9007; Priem, G.; Pelotier, B.; Macdonald, S. J. F.; Anson, M. S.; Campbell, I. B. *J. Org. Chem.* **2003**, *68*, 3844-3848.
- (19) Yamada, S.; Misono, T.; Iwai, Y.; Masumizu, A.; Akiyama, Y. *J. Org. Chem.* **2006**, *71*, 6872-6880.
- (20) Yamada, S.; Misono, T.; Iwai, Y. *Tetrahedron Lett.* **2005**, *46*, 2239-2242.
- (21) Dalaigh, C. O.; Hynes, S. J.; O'Brien, J. E.; McCabe, T.; Maher, D. J.; Watson, G. W.; Connon, S. J. *Org. Biomol. Chem.* **2006**, *4*, 2785-2793; Dalaigh, C. O.; Hynes, S. J.; Maher, D. J.; Connon, S. J. *Org. Biomol. Chem.* **2005**, *3*, 981-984.
- (22) Spivey, A. C.; Fekner, T.; Spey, S. E. *J. Org. Chem.* **2000**, *65*, 3154-3159; Spivey, A. C.; Fekner, T.; Adams, H. *Tetrahedron Lett.* **1998**, *39*, 8919-8922; Spivey, A. C.; Zhu, F.; Mitchell, M. B.; Davey, S. G.; Jarvest, R. L. *J. Org. Chem.* **2003**, *68*, 7379-7385.
- (23) Spivey, A. C.; Fekner, T.; Spey, S. E.; Adams, H. *J. Org. Chem.* **1999**, *64*, 9430-9443.
- (24) Fu, G. C. *Pure Appl. Chem.* **2001**, *73*, 1113-1116; Fu, G. C. *Pure Appl. Chem.* **2001**, *73*, 347-349.
- (25) Birman, V. B.; Jiang, H.; Li, X.; Guo, L.; Uffman, E. W. *J. Am. Chem. Soc.* **2006**, *128*, 6536-6537; Birman, V. B.; Li, X. *Org. Lett.* **2006**, *8*, 1351-1354; Birman, V. B.; Uffman, E. W.; Jiang, H.; Li, X.; Kilbane, C. J. *J. Am. Chem. Soc.* **2004**, *126*, 12226-12227.
- (26) Baylis, A. B.; Hillman, M. E. D.; Offenlegungsschrift 2155113; Germany, 1972; Morita, K.; Suzuki, Z.; Hirose, H. *Bull. Chem. Soc. Jpn.* **1968**, *41*, 2815-2820.

- (27) Krafft, M. E.; Haxell, T. F. N.; Seibert, K. A.; Abboud, K. A. *J. Am. Chem. Soc.* **2006**, *128*, 4174-4175.
- (28) Shi, M.; Chen, L.-H.; Li, C.-Q. *J. Am. Chem. Soc.* **2005**, *127*, 3790-3800.
- (29) Santos, L. G.; Pavam, C. H.; Almeida, W. P.; Coehlo, F.; Eberlin, M. N. *Angew. Chem. Int. Ed.* **2004**, *43*, 4330-4333.
- (30) Price, K. E.; Broadwater, S. J.; Jung, H. M.; McQuade, D. T. *Org. Lett.* **2005**, *7*, 147-150; Price, K. E.; Broadwater, S. J.; Walker, B. J.; McQuade, D. T. *J. Org. Chem.* **2005**, *70*, 3980-3987.
- (31) Robiette, R.; Aggarwal, V. K.; Harvey, J. N. *J. Am. Chem. Soc.* **2007**, *129*, 15513-15525.
- (32) Roy, D.; Sunoj, R. B. *Org. Lett.* **2007**, *9*, 4873-4876.
- (33) Xu, J. *J. Mol. Struct. (THEOCHEM)* **2006**, *767*, 61-66.
- (34) Masson, G.; Housseman, C.; Zhu, J. *Angew. Chem. Int. Ed.* **2007**, *46*, 4614-4628.
- (35) Uggerud, E. *Chem. Eur. J.* **2006**, *12*, 1127-1136.
- (36) Brauman, J. I.; Han, C.-C. *J. Am. Chem. Soc.* **1989**, *111*, 3485.
- (37) Brauman, J. I.; Han, C.-C. *J. Am. Chem. Soc.* **1988**, *110*, 5611-5613.
- (38) McMahan, T. B.; Heinis, T.; Nicol, G.; Hovey, J. K.; Kebarke, P. *J. Am. Chem. Soc.* **1988**, *110*, 7591-7598.
- (39) Curtiss, L. A.; Carpenter, J. E.; Raghavachari, K.; Pople, J. A. *J. Chem. Phys.* **1992**, *96*, 9030-9034; Curtiss, L. A.; Raghavachari, K.; Trucks, G. W.; Pople, J. A. *J. Chem. Phys.* **1991**, *94*, 7221-7230.
- (40) Baboul, A. G.; Curtiss, L. A.; Redfern, P. C.; Raghavachari, K. *J. Chem. Phys.* **1999**, *110*, 7650-7657.
- (41) Curtiss, L. A.; Raghavachari, K.; Redfern, P. C.; Rassolov, V.; Pople, J. A. *J. Chem. Phys.* **1998**, *109*, 7764-7776.
- (42) Martin, J. M. L.; de Oliveria, G. *J. Chem. Phys.* **1999**, *111*, 1843-1856.
- (43) Parthiban, S.; Martin, J. M. L. *J. Chem. Phys.* **2001**, *114*, 6014-6029.
- (44) Perdew, J. P.; Burke, K.; Ernzerhof, M. *Phys. Rev. Lett.* **1997**, *78*, 1396; Perdew, J. P.; Burke, K.; Ernzerhof, M. *Phys. Rev. Lett.* **1996**, *77*, 3865-3868.
- (45) Adamo, C.; Barone, V. *J. Chem. Phys.* **1998**, *108*, 664-675.
- (46) Becke, A. D. *J. Chem. Phys.* **1996**, *104*, 1040-1046.
- (47) Becke, A. D. *J. Chem. Phys.* **1993**, *98*, 5648-5652.
- (48) Lee, C.; Yang, W.; Parr, R. G. *Phys. Rev. B* **1988**, *37*, 785.
- (49) Stephens, P. J.; Devlin, F. J.; Chabalowski, C. F.; Frisch, M. J. *J. Phys. Chem.* **1994**, *98*, 11623-11627.
- (50) Schmider, H. L.; Becke, A. D. *J. Chem. Phys.* **1998**, *108*, 9624-9631.
- (51) Becke, A. D. *J. Chem. Phys.* **1997**, *107*, 8554-8560.
- (52) Bienati, M.; Adamo, C.; Barone, V. *Chem. Phys. Lett.* **1999**, *311*, 69-76.
- (53) Defrees, D. J.; Levi, B. A.; Pollack, S. K.; Hehre, W. J.; Binkley, J. S.; Pople, J. A. *J. Am. Chem. Soc.* **1979**, *101*, 4085-4089.
- (54) Hariharan, P. C.; Pople, J. A. *Theor. Chim. Acta.* **1973**, *28*, 213.
- (55) Dunning, T. H., Jr. *J. Chem. Phys.* **1989**, *90*, 1007-1023.
- (56) Kendall, R. A.; Dunning, T. H., Jr.; Harrison, R. J. *J. Chem. Phys.* **1992**, *96*, 6796-6806.
- (57) Wilson, A. K.; van Mourik, T.; Dunning, T. H., Jr. *J. Mol. Struct.* **1997**, *388*, 339-349.
- (58) NIST Chemistry WebBook; June 2005 ed.; NIST Standard Reference Database Nr. 69.
- (59) Hunter, E. P.; Lias, S. G. *J. Phys. Chem. Ref. Data* **1998**, *27*, 413-656.
- (60) Del Bene, J. E. *J. Phys. Chem.* **1993**, *97*, 107-110.
- (61) Smith, B. J.; Radom, L. *Chem. Phys. Lett.* **1994**, *231*, 345-351.

- (62) Dinadayalane, T. C.; Sastry, G. N.; Leszczynski, J. *Int. J. Quant. Chem.* **2006**, *106*, 2920-2933; Hwang, S.; Jang, Y. H.; Chung, D. S. *Bull. Korean Chem. Soc.* **2005**, *26*, 585-588; Peterson, K. A.; Yantheas, S. S.; Dixon, D. A.; Dunning, T. H., Jr. *J. Phys. Chem. A* **1998**, *102*, 2449-2554; Kallies, B.; Mitzner, R. *J. Phys. Chem. B* **1997**, *101*, 2959-2967.
- (63) Grimme, S. *J. Chem. Phys.* **2003**, *118*, 9095-9102.
- (64) Herzberg, G. *Electronic Spectra and Electronic Structure of Polyatomic Molecules*; Van Nostrand: New York, **1966**.
- (65) Chan, B.; Del Bene, J. E.; Elguero, J.; Radom, L. *J. Phys. Chem. A* **2005**, *109*, 5509-5517.
- (66) Pham-Tran, N.-N.; Bouchoux, G.; Delaere, D.; Nguyen, M. T. *J. Phys. Chem. A* **2005**, *109*, 2957-2963.
- (67) Swart, M.; Rösler, E.; Bickelhaupt, F. M. *J. Comput. Chem.* **2006**, *27*, 1486-1493.
- (68) Curtiss, L. A.; Redfern, P. C.; Raghavachari, K. *J. Chem. Phys.* **2005**, *123*, 124107.
- (69) Schreiner, P. R.; Fokin, A. A.; Pascal, R. A., Jr.; de Meijere, A. *Org. Lett.* **2006**, *8*, 3635-3638; Wodrich, M. D.; Corminiboeuf, C.; von Rague Schleyer, P. *Org. Lett.* **2006**, *8*, 3631-3634; Check, C. E.; Gilbert, T. M. *J. Org. Chem.* **2005**, *70*, 9828-9834.
- (70) Wei, Y.; Held, I.; Zipse, H. *Org. Biomol. Chem.* **2006**, *4*, 4223-4230.
- (71) Held, I.; Villinger, A.; Zipse, H. *Synthesis* **2005**, 1425-1430.
- (72) Brotzel, F.; Kempf, B.; Singer, T.; Zipse, H.; Mayr, H. *Chem. Eur. J.* **2007**, *13*, 336-345; Kempf, B.; Mayr, H. *Chem. Eur. J.* **2005**, *11*, 917-927.
- (73) Millers, S. *J. Acc. Chem. Res.* **2004**, *37*, 601-610.
- (74) Kolb, H. C.; Andersson, P. G.; Sharpless, K. B. *J. Am. Chem. Soc.* **1994**, *116*, 1278-1291.
- (75) Birman, V. B.; Li, X.; Han, Z. *Org. Lett.* **2007**, *9*, 37-40.
- (76) MacKay, J. A.; Vedejs, E. *J. Org. Chem.* **2006**, *71*, 498-503; Vedejs, E.; Daugulis, O.; Tuttle, N. *J. Org. Chem.* **2004**, *69*, 1389-1392.
- (77) Lias, S. G.; Liebman, J. F.; Levine, R. D. *J. Phys. Chem. Ref. Data* **1984**, *13*, 695-808.
- (78) Mezzache, S.; Bruneleua, N.; Vekey, K.; Alfonso, C.; Karoyan, P.; Fournier, F.; Tabet, J.-C. *J. Mass. Spectrom.* **2005**, *40*, 1300-1308.
- (79) Decouzon, M.; Gal, J.-F.; Maria, P.-C.; Raczynska, E. D. *Rapid Commun. Mass Spectrom.* **1993**, *7*, 599-602.
- (80) Faltin, C.; Fleming, E. M.; Connon, S. J. *J. Org. Chem.* **2004**, *69*, 6496-6499.
- (81) Aggarwal, V. K.; Emme, I.; Fulford, S. Y. *J. Org. Chem.* **2003**, *68*, 692-700.
- (82) Aggarwal, V. K.; Mereu, A. *Chem. Commun.* **1999**, 2311 - 2312.
- (83) Heinrich, M. R.; Klisa, H. S.; Mayr, H.; Steglich, W.; Zipse, H. *Angew. Chem. Int. Ed.* **2003**, *42*, 4826-4828.
- (84) Keck, G. E.; Welch, D. S. *Org. Lett.* **2002**, *4*, 3687-3690.
- (85) Luo, S.; Mi, X.; Xu, H.; Wang, P. G.; Cheng, J.-P. *J. Org. Chem.* **2004**, *69*, 8413-8422.
- (86) Murtagh, J. E.; McCooley, S. H.; Connon, S. J. *Chem. Commun.* **2005**, 227-229.
- (87) Vedejs, E.; Diver, S. T. *J. Am. Chem. Soc.* **1993**, *115*, 3358-3359.
- (88) Jencks, W. P. *Catalysis in Chemistry and Enzymology*; Dover: Mineola, NY, **1987**.
- (89) Castro, E. A.; Aliaga, M.; Campodonico, P. R.; Leis, J. R.; Garcia-Rio, L.; Santos, J. G. *J. Phys. Org. Chem.* **2006**, *19*, 683-688; Castro, E. A.; Campodonico, P. R.; Contreras, R.; Fuentealba, P.; Santos, J. G.; Leis, J. R.; Garcia-Rio, L.; Saez, J. A.; Domingo, L. R. *Tetrahedron* **2006**, *62*, 2555-2562; Castro, E. A.; Aliaga, M.; Campodonico, P.; Santos, J. G. *J. Org. Chem.* **2002**, *67*, 8911-8916.
- (90) France, S.; Guerin, D. J.; Miller, S. J.; Leckta, T. *Chem. Rev.* **2003**, *103*, 2985-3012.
- (91) Carey, F. A.; Sundberg, R. J. *Advanced Organic Chemistry, Part B: Reactions and Synthesis*; 4th ed.; Kluwer Academic/Plenum: Dordrecht, The Netherlands, **2001**.

- (92) Marcelli, T.; van Maarseveen, J. H.; Hiemstra, H. *Angew. Chem. Int. Ed.* **2006**, *45*, 7496-7504; Hoffmann, H. M. R.; Frackenpohl, J. *Eur. J. Org. Chem.* **2004**, 4293-4312; Kacprzak, K.; Gawronski, J. *Synthesis* **2001**, 961-998.
- (93) Yoon, T. P.; Jacobsen, E. N. *Science* **2003**, *299*, 1691-1693.
- (94) Sano, T.; Miyata, H.; Oriyama, T. *Enantiomer* **2000**, *5*, 119; Oriyama, T.; Hori, Y.; Imai, K.; Sasaki, R. *Tetrahedron Lett.* **1996**, *37*, 8543.
- (95) Dale, J. A.; Mosher, H. S. *J. Am. Chem. Soc.* **1973**, *95*, 512-519; Sullivan, G. R.; Dale, J. A.; Mosher, H. S. *J. Org. Chem.* **1973**, *38*, 2143-2147; Dale, J. A.; Dull, D. L.; Mosher, H. S. *J. Org. Chem.* **1969**, *34*, 2543-2549.
- (96) Seco, J. M.; Quinoa, E.; Riguera, R. *Chem. Rev.* **2004**, *104*, 17-118.
- (97) Hiratake, J.; Inagaki, M.; Yamanoto, Y.; Oda, J. *J. Chem. Soc., Perkin Trans. 1* **1987**, *1*, 1053-1058; Hiratake, J.; Yamanoto, Y.; Oda, J. *J. Chem. Soc., Chem. Commun.* **1985**, 1717-1719.
- (98) Aitken, R. A.; Gopal, J. *Tetrahedron: Asymmetry* **1990**, *1*, 517-520; Aitken, R. A.; Gopal, J.; Hirst, J. A. *J. Chem. Soc., Chem. Commun.* **1988**, 632-634.
- (99) Bolm, C.; Atodiresei, I.; Schiffrers, I. *Org. Synth.* **2005**, *82*, 120; Bolm, C.; Schiffrers, I.; Atodiresei, I.; Hackenberger, C. P. R. *Tetrahedron: Asymmetry* **2003**, *14*, 3455-3467; Bolm, C.; Schiffrers, I.; Atodiresei, I.; Ozcubukcu, S.; Raabe, G. *New J. Chem.* **2003**, *27*, 14-17; Bolm, C.; Schiffrers, I.; Dinter, C. L.; Gerlach, A. *J. Org. Chem.* **2000**, *65*, 6984-6991; Bolm, C.; Gerlach, A.; Dinter, C. L. *Synlett* **1999**, 195-196.
- (100) Dijkstra, G. D.; Kellogg, R. M.; Wynberg, H. *Trav. Chim. Pays-Bas* **1989**, *108*, 195-204.
- (101) Dijkstra, G. D.; Kellogg, R. M.; Wynberg, H.; Svendsen, J. S.; Marko, I.; Sharpless, K. B. *J. Am. Chem. Soc.* **1989**, *21*, 8069-8076.
- (102) Caner, H.; Biedermann, P. U.; Agranat, I. *Chirality* **2003**, *15*, 637-645.
- (103) Olsen, R. A.; Borchardt, D.; Mink, L.; Agarwal, A.; Mueller, L. J.; F., Z. *J. Am. Chem. Soc.* **2006**, *128*, 15594-15595.
- (104) Buergi, T.; Baiker, A. *J. Am. Chem. Soc.* **1998**, *120*, 12920-12926.
- (105) Alvarez, S.; Alemany, P.; Avnir, D. *Chem. Soc. Rev.* **2005**, *34*, 313-326; Zabrodsky, H.; Avnir, D. *J. Am. Chem. Soc.* **1995**, *117*, 462-473.
- (106) Curtiss, L. A.; Redfern, P. C.; Raghavachari, K. *J. Chem. Phys.* **2007**, *126*, 84108.
- (107) Lynch, B. J.; Fast, P. L.; Harris, M.; Truhlar, D. G. *J. Phys. Chem. A* **2000**, *104*, 4811-4815.
- (108) Gronert, S. A. *J. Am. Chem. Soc.* **1993**, *115*, 10258-10266.
- (109) Glukhovtsev, M. N.; Pross, A.; Radom, L. *J. Am. Chem. Soc.* **1995**, *117*, 2024-2032.
- (110) Neese, F.; Schwabe, T.; Grimme, S. *J. Chem. Phys.* **2007**, *126*, 124115.
- (111) Grimme, S. *J. Chem. Phys.* **2006**, *124*, 034108.
- (112) Tarnopolsky, A.; Karton, A.; Sertchook, R.; Vuzman, D.; Martin, R. L. *J. Phys. Chem. A* **2008**, *112*, 3-8.
- (113) Fast, P. L.; Corchado, J.; Sanchez, M. L.; Truhlar, D. G. *J. Phys. Chem. A* **1999**, *103*, 3139-3143; Gordon, M. S.; Truhlar, D. G. *J. Am. Chem. Soc.* **1986**, *108*, 5412-5419.
- (114) Siegbahn, P. E. M.; Blomberg, M. R. A.; M., S. *Chem. Phys. Lett.* **1994**, *223*, 35-45.
- (115) Vedejs, E.; Jure, M. *Angew. Chem. Int. Ed.* **2005**, *44*, 3974-4001.
- (116) Fu, G. C. *Acc. Chem. Res.* **2000**, *33*, 412-420.
- (117) Jorgensen, W. L.; Tirado-Rives, J. *J. Comput. Chem.* **2005**, *26*, 1689-1700.
- (118) Jorgensen, W. L.; Maxwell, D. A.; Tirado-Rives, J. *J. Am. Chem. Soc.* **1996**, *118*, 11225-11236.
- (119) Cornell, W. D.; Cieplak, P.; Bayly, C. I.; Gould, I. R.; Kenneth M. Merz, J.; Ferguson, D. M.; Spellmeyer, D. C.; Fox, T.; Caldwell, J. W.; Kollman, P. A. *J. Am. Chem. Soc.* **1995**, *117*, 5179-5197.

- (120) Jurecka, P.; Sponer, J.; Cerny, J.; Hobza, P. *Phys. Chem. Chem. Phys.* **2006**, *8*, 1985-1993; Hobza, P.; Sponer, J. *J. Am. Chem. Soc.* **2002**, *124*, 11802-11808; Hobza, P.; Sponer, J. *Chem. Rev.* **1999**, *99*, 3247-3276; Allen, M. J.; Tozer, D. J. *J. Chem. Phys.* **2002**, *117*, 11113-11120.
- (121) Grimme, S.; Diedrich, C.; Korth, M. *Angew. Chem. Int. Ed.* **2006**, *45*, 625-629.
- (122) Piacenza, M.; Grimme, S. *J. Am. Chem. Soc.* **2005**, *127*, 14841-14848.
- (123) Sinnokrot, M. O.; Sherrill, C. D. *J. Phys. Chem. A* **2004**, *108*, 10200-10207; Sinnokrot, M. O.; Valeev, E. F.; Sherrill, C. D. *J. Am. Chem. Soc.* **2002**, *124*, 10887-10893.
- (124) Binkley, J. S.; Pople, J. A.; Hehre, W. J. *J. Am. Chem. Soc.* **1980**, *102*, 939-947.
- (125) Easton, R. E.; Giesen, D. J.; Cramer, C. J.; Truhlar, D. G. *Theor. Chem. Acc.* **1996**, *93*, 281-301.
- (126) Spivey, A. C.; Maddaford, A.; Leese, D. P.; Redgrave, A. J. *J. Chem. Soc., Perkin Trans. I* **2001**, 1785-1794.
- (127) Hassner, A. *Encyclopedia of Reagents for Organic Synthesis*; Wiley: Chichester, **1995**.
- (128) Vedejs, E.; Chen, X. *J. Am. Chem. Soc.* **1996**, *118*, 1809-1810.
- (129) Hills, I. D.; Fu, G. C. *Angew. Chem. Int. Ed.* **2003**, *42*, 3921-3924; Mermerian, A. H.; Fu, G. C. **2003**, *125*, 4050-4051; Hodous, B. L.; Fu, G. C. *J. Am. Chem. Soc.* **2002**, *124*, 10006-10007; Hodous, B. L.; Fu, G. C. *J. Am. Chem. Soc.* **2002**, *124*, 1578-1579; Ruble, J. C.; Latham, A.; Fu, G. C. *J. Am. Chem. Soc.* **1997**, *119*, 1492-1493.
- (130) Spivey, A. C.; Arseniyadis, S.; Fekner, T.; Maddaford, A.; Leese, D. P. *Tetrahedron* **2006**, *62*, 295-301; Spivey, A. C.; Leese, D. P.; Zhu, F.; Davey, S. G.; Jarvest, R. L. *Tetrahedron* **2004**, *60*, 4513-4525.
- (131) Al-Mourabit, A.; Potier, P. *Eur. J. Org. Chem.* **2001**, 237-243.
- (132) Abou-Jneid, R.; Ghoullami, S.; Martin, M.-T.; E. T. H. Dau; N. Travert; Al-Mourabit, A. *Org. Lett.* **2004**, *6*, 3933-3936.
- (133) Hoffmann, H.; Lindel, T. *Synthesis* **2003**, 1753-1783.
- (134) Baran, P. S.; O'Malley, D. P.; Zografos, A. L. *Angew. Chem. Int. Ed.* **2004**, *43*, 2674-2677; Köck, M.; Grube, A.; Seiple, I. B.; Baran, P. S. *Angew. Chem. Int. Ed.* **2007**, *46*, 6586-6594.
- (135) Jacquot, D. E. N.; Lindel, T. *Curr. Org. Chem.* **2005**, *9*, 1551-1565.
- (136) Wei, Y.; Sastry, G. N.; Zipse, H. *J. Am. Chem. Soc.* **2008**, *130*, 3473-3477.
- (137) Wei, Y.; Singer, T.; Mayr, H.; Sastry, G. N.; Zipse, H. *J. Comput. Chem.* **2008**, *29*, 291-297.
- (138) Paine, S. W.; Kresge, A. J.; Salam, A. *J. Phys. Chem. A* **2005**, *109*, 4149-4153.
- (139) Cossi, M.; Scalmani, G.; Rega, N.; Barone, V. *J. Chem. Phys.* **2002**, *117*, 43-54.
- (140) Amovilli, C.; Barone, V.; Cammi, R.; Cance, E.; Cossi, M.; Mennucci, B.; Pomelli, C.; Tomasi, J. *Adv. Quantum Chem.* **1998**, *32*, 227-261.
- (141) Cance, E.; Mennucci, B.; Tomasi, J. *J. Chem. Phys.* **1997**, *107*, 3032-3041.
- (142) Ganellin, C. R. In *Molecular and Quantum Pharmacology, Proceedings of the 7th Jerusalem Symposium on Quantum and Biochemistry*; D. Reidel Publishing Co.: **1974**, p 43-55.
- (143) Brownstein, S.; Stillman, A. E. *J. Phy. Chem.* **1959**, *63*, 2061-2062.
- (144) Frisch, M. J.; Trucks, G. W.; Schlegel, H. B.; Scuseria, G. E.; Robb, M. A.; Cheeseman, J. R.; Zakrzewski, V. G.; Montgomery, J. A. J.; Stratmann, R. E.; Burant, J. C. D. S.; Millam, J. M.; Daniels, A. D.; Kudin, K. N.; Strain, M. C.; Farkas, O.; Tomasi, J.; Barone, V.; Cossi, M.; Cammi, R.; Mennucci, B.; Pomelli, C.; Adamo, C.; Clifford, S.; Ochterski, J.; Petersson, G. A.; Ayala, P. Y.; Cui, Q.; Morokuma, K.; Malick, D. K.; Rabuck, A. D.; Raghavachari, K.; Foresman, J. B.; Cioslowski, J.; Ortiz, J. V.; Stefanov, B. B.; Liu, G.; Liashenko, A.; Piskorz, P.; Komaromin, I.; Gomperts, R.; Martin, R. L.; Fox, D. J.; Keith,

- T.; Al-Laham, M. A.; Peng, C. Y.; Nanayakkara, A.; Gonzalez, C.; Challacombe, M.; Gill, P. M. W.; Johnson, B. G.; Chen, W.; Wong, M. W.; Andres, J. L.; Head-Gordon, M.; Replogle, E. S.; Pople, J.; Gaussian 03, B.03 ed.; Gaussian, Inc.: Pittsburgh, PA, **2003**.
- (145) Werner, H. J.; Knowles, P. J.; Lindh, R.; Manby, F. R.; Shuetz, M.; MOLPRO, 2002.6 ed.
- (146) Ponder, J. W. *TINKER*; 4.2 ed., **2004**.
- (147) Wiberg, K. B.; Bailey, W. F. *J. Mol. Struct.* **2000**, *556*, 239-244.
- (148) Frisch, M. J.; Trucks, G. W.; Schlegel, H. B.; Scuseria, G. E.; Robb, M. A.; Cheeseman, J. R.; Zakrzewski, V. G.; Montgomery, J. A. J.; Stratmann, R. E.; Burant, J. C. D. S.; Millam, J. M.; Daniels, A. D.; Kudin, K. N.; Strain, M. C.; Farkas, O.; Tomasi, J.; Barone, V.; Cossi, M.; Cammi, R.; Mennucci, B.; Pomelli, C.; Adamo, C.; Clifford, S.; Ochterski, J.; Petersson, G. A.; Ayala, P. Y.; Cui, Q.; Morokuma, K.; Malick, D. K.; Rabuck, A. D.; Raghavachari, K.; Foresman, J. B.; Cioslowski, J.; Ortiz, J. V.; Stefanov, B. B.; Liu, G.; Liashenko, A.; Piskorz, P.; Komaromin, I.; Gomperts, R.; Martin, R. L.; Fox, D. J.; Keith, T.; Al-Laham, M. A.; Peng, C. Y.; Nanayakkara, A.; Gonzalez, C.; Challacombe, M.; Gill, P. M. W.; Johnson, B. G.; Chen, W.; Wong, M. W.; Andres, J. L.; Head-Gordon, M.; Replogle, E. S.; Pople, J.; Gaussian 03, D.01 ed.; Gaussian, Inc.: Pittsburgh, PA, **2003**.
- (149) Damm, W.; Frontera, A.; Tirado-Rives, J.; Jorgensen, W. L. *J. Comput. Chem.* **1997**, *18*, 1955-1970; Jorgensen, W. L.; McDonald, N. A. *Theochem.* **1998**, *424*, 145-155; Jorgensen, W. L.; McDonald, N. A. *J. Phys. Chem. B* **1998**, *102*, 8049-8059; Rizzo, R. C.; Jorgensen, W. L. *J. Am. Chem. Soc.* **1999**, *121*, 4827-4836; Watkins, E. K.; Jorgensen, W. L. *J. Phys. Chem. A* **2001**, *105*, 4118-4125.
- (150) Grimme, S. *J. Comput. Chem.* **2006**, *27*, 1787-1799; Grimme, S. *J. Comput. Chem.* **2004**, *25*, 1463-1473.
- (151) Neese, F. ORCA 2.6.4, an ab initio density functional and semiempirical program package, **2007**.
- (152) Cossi, M.; Barone, V.; Mennucci, B.; Tomasi, J. *Chem. Phys. Lett.* **1998**, *286*, 253-260; Mennucci, B.; Tomasi, J. *J. Chem. Phys.* **1997**, *106*, 5151-5158.

## Curriculum Vitae

Name: Yin Wei

Date of birth: 12<sup>th</sup>, July, 1977

Place of birth: Xinxiang, P. R. China

Nationality: Chinese

Marital status: Married

## Education

2005.4 - now Ludwig-Maximilians-Universität München, Germany

Ph.D Program in Chemistry

2008.7 – 2008.9 Visiting Ph. D student as part of DST-DAAD program (Indo-German cooperated) in IICT, Hyderabad, India

2002.9 - 2005.2 Concordia University, Montreal, Canada

Master of Science (Chemistry)

2001.9 - 2002.6 Dalian Institute of Chemical Physics, Chinese Academy of Sciences, Dalian, P. R. China

Ph.D Program in Chemistry

1998.9 - 2001.7 Zhengzhou University, Zhengzhou, P. R. China

Master of Science (Chemistry)

2000.1 - 2001.6 Dalian Institute of Chemical Physics, Chinese Academy of Sciences, Dalian, P. R. China

Exchange Student, Proceeding Master's thesis

1994.9 - 1998.7 Zhengzhou University, Zhengzhou, P. R. China

Bachelor of Science (Chemistry)

## Work Experience

2005.10 - now Ludwig-Maximilians-Universität München

Department Chemistry und Biochemistry

Teaching Assistant (T.A.)

2002.9 - 2005.2 Concordia University, Montreal, Canada

Department of Chemistry and Biochemistry

Teaching Assistant (T.A.)

1999.1 - 2000.1 Zhengzhou University, Zhengzhou, P. R. China

Department of Chemistry

Teaching Assistant (T.A.)

## Publications

1. Estimating the Stereoinductive Potential of Cinchona Alkaloids with a Prochiral Probe Approach

Yin Wei, G. N. Sastry, Hendrik Zipse, *Org. Lett.* **2008**, *23*, 5413-5416.

2. Tautomeric Equilibria in 3-Amino-1-(2-aminoimidazol-4-yl)-prop-1-ene, a Central Building Block of Marine Alkaloids

Yin Wei, Hendrik Zipse, *Eur. J. Org. Chem.* **2008**, 3811-3816.

3. Methyl Cation Affinities of Commonly Used Organocatalysts

Yin Wei, G. N. Sastry, Hendrik Zipse, *J. Am. Chem. Soc.* **2008**, *130*, 3473-3477.

4. Assessment of Theoretical Methods for the Calculation of Methyl Cation Affinities

Yin Wei, Thomas Singer, Herbert Mayr, G. N. Sastry, Hendrik Zipse, *J. Comput. Chem.* **2008**, *29*, 291-297.

5. Stacking Interactions as the Principal Design Element in Acyl-Transfer Catalysts.

- Yin Wei, Ingmar Held, Hendrik Zipse, *Org. Biomol. Chem.* **2006**, *4*, 4223-4230.
6. Effect of surface modification of support on properties of Cu-Co-Fe/Al<sub>2</sub>O<sub>3</sub> catalyst for alcohol synthesis.
- Jie Xu, Yin Wei, Lin Zheng, Huanwen Zhou, Baoshi Du, *Cuihua Xuebao* **2001**, *22*, 419-422.
7. Progress in hydroformylation of ethene to propanal by catalytic synthesis.
- Yin Wei, Huanwen Zhou, Jie Xu, Baoshi Du, Wei Zhang, *Xiandai Huagong* **2001**, *21*, 27-30.
8. Thermodynamic calculation and analysis for low carbon alcohol synthesis from CO and H<sub>2</sub>
- Yin Wei, Jie Xu, Baoshi Du, Qin Xin, Can Li, *Zhengzhou Daxue Xuebao* **2000**, *32*, 70-73.
9. The Performance of Computational Techniques in Locating the Charge Separated Intermediates in Organocatalytic Transformations
- Yin Wei, B. Sateesh, Boris Maryasin, G. N. Sastry, Hendrik Zipse, *J. Comput. Chem.* Submitted.
10. Optimal Selectivity of Chiral Analogues of 4-DMAP for Non-enzymatic Enantioselective Acylations: a Theoretical Investigation.
- Yin Wei, Hendrik Zipse, *in preparation*.

### **Presentation in Conference**

1. SPP 1179 Organokatalyse Workshop Immobilisierung (Nov. 7- 8, 2008, Regensburg, Germany)  
Theoretical benchmarking in organocatalytic processes (Talk)  
Y. Wei, H. Zipse
2. GDCh-Wissenschaftsforums Chemie 2007 (Sep. 16-19, 2007, Ulm, Germany)  
Stacking interactions as the principal design element in acyl-transfer catalysts (Poster)  
Y. Wei, I. Held, H. Zipse
3. 86<sup>th</sup> CSC and 39<sup>th</sup> IUPAC (August 10-15, 2003, Ottawa, Canada)  
Theoretical Studies of Cluster Dissociation Following Mode-Specific Excitation (Poster)  
Y. Wei, P. Larrégaray and G. H. Peslherbe,
4. 6<sup>th</sup> Annual Chemistry and Biochemistry Graduate Research Conference (Nov. 14-15, Montreal, Canada)  
Computational Studies of the Structure of Vanadium Oxide Clusters and their Reactivity towards Halocarbons (Poster)  
Y. Wei and G. H. Peslherbe

### **Languages**

Chinese- Native language  
English- Fluent writing, reading, speaking  
German- Basic writing, reading, speaking

### **Honors and Awards**

- 2007.6-2007.12 STIBET scholarship supported by DAAD
- 2002-2003 a) Concordia University International Tuition Fee Remission Award b) J. W. Burns Graduate Award, Concordia University
- 2001 "Excellent Graduate Student" of Zhengzhou University
- 1997-1998 The third grade scholarship of People's Government, Zhengzhou University
- 1994-1995, 1996-1997, 1996-1997 The first grade scholarship of People's Government, Zhengzhou University